

INTRODUCTION TO
**Hypersonic
Flow**

BY

G. G. CHERNYI

Moscow State University, Moscow

TRANSLATED AND EDITED BY

RONALD F. PROBSTEIN

Brown University, Providence, Rhode Island

1961

ACADEMIC PRESS New York and London



COPYRIGHT © 1961, BY ACADEMIC PRESS INC.

ALL RIGHTS RESERVED

NO PART OF THIS BOOK MAY BE REPRODUCED IN ANY FORM
BY PHOTOSTAT, MICROFILM, OR ANY OTHER MEANS,
WITHOUT WRITTEN PERMISSION FROM THE PUBLISHERS

ACADEMIC PRESS INC.

111 FIFTH AVENUE

NEW YORK 3, N. Y.

United Kingdom Edition

Published by

ACADEMIC PRESS INC. (LONDON) LTD.
17 OLD QUEEN STREET, LONDON S.W. 1

Library of Congress Catalog Card Number 61-16624

PRINTED IN THE UNITED STATES OF AMERICA

Originally published under the title:

Течения Газа с Большой Сверхзвуковой Скоростью
(Gas Flows at High Supersonic Speed)

by

Gosudarstvennoe Izdatel'stvo, Fiziko-Matematicheskoi Literatury, Moscow, 1959

Translator's and Editor's Preface

Although other books in the field of hypersonic flow are now published in English, it was felt that this book should be made available to the English speaking reader because of its usefulness for those individuals desirous of obtaining an introduction to the subject. Except for a general introductory chapter the book concentrates on the inviscid, perfect fluid aspects of hypersonic flow, with emphasis on the fundamental concepts and rational methods of calculation. The book is directed to students of aerodynamics and gasdynamics, as well as to scientists and engineers interested in problems of hypersonic flight. The level of approach is such that it should prove particularly useful as an undergraduate and introductory graduate text.

Written by an internationally acknowledged expert in the field of hypersonic flow, the book makes available heretofore unpublished Soviet work, as well as published work little known outside the Soviet Union. The author has however made every effort to include, where appropriate, Western references for the work he discusses. Indeed, approximately two-thirds of the cited references have their origin outside of the Soviet Union. Since the book is intended for the English speaking reader, an attempt has been made to supply a source of an English translation for each of the cited Russian references. A brief discussion of these sources, along with the transliteration system employed, may be found at the end of the book in the Cited References section.

Most of the editorial changes were made in an effort either to clarify the text or to correct inaccuracies that inevitably arise in a technical book of this kind. In most cases these changes were incorporated directly into the text with the agreement and approval of the author. In those instances where it was thought helpful to insert new references or clarify old ones, to explain changes in terminology, to indicate the editor's point of view, or simply to amplify statements in a way best done in a note, an editor's footnote was added and clearly indicated as such. As with all other editorial changes, these footnotes were checked by the author himself. In addition an author index has been added and the subject index substantially enlarged and revised.

Every effort has been made to eliminate errors appearing in the original Russian edition. In this task we are grateful to the author for his assistance and help. It is inevitable, however, that not all of the miscellaneous errors and inaccuracies have been uncovered, and further that

new ones have been introduced in the process of translating, editing, and publishing.

In spite of the fact that an attempt has been made to retain the original style of the author, it is natural that the present text reflects to some extent the style of the translator. A more literal translation was employed in those instances where it was felt that excessive alteration of style from the original for purposes of "smooth" English might tend to alter the author's intent. It should be mentioned that both the terminology and notation have been changed to be consistent with commonly accepted usage in the English aeronautical literature. Where this could lead to confusion for those readers wishing to avail themselves of the original Russian references, a footnote regarding the change has been added.

A debt of gratitude is due Professor Michal Lunc of the Polish Academy of Sciences, with whom the translation was originally undertaken as a joint effort. Due to unforeseen circumstances, it was necessary for the translator to carry out the project alone. Much credit is however due Professor Lunc for his patience, particularly at the beginning, in helping one unaccustomed to foreign tongues through the intricacies of the Russian language. We also wish to thank Dr. G. D. Waldman and Dr. H. T. Ho for their editorial assistance in various phases of the work.

We gratefully acknowledge the John Simon Guggenheim Foundation for their support through a Guggenheim Fellowship during the period when much of the work on the book was carried out. Grateful acknowledgment is also due for the indirect support supplied by the Aeronautical Research Laboratory of the Wright Air Development Division through a contract with Brown University.

Finally, the translator wishes to express his sincere thanks to Professor G. G. Chernyi himself for his cooperation and assistance in all phases of preparation of the book.

RONALD F. PROBSTEIN

July, 1961

Author's Preface to Russian Edition

Solutions to a number of important scientific and technical problems that have arisen in recent years have been linked to studies of the motion of bodies through gases at hypersonic speeds.

The flight of a body in the atmosphere at speeds of the order of several kilometers per second gives rise to phenomena whose effects are of interest in connection with practical applications of the interaction characteristics of a body with its surrounding medium. At moderate supersonic flight speeds, one can usually neglect these effects. In regions near a body moving with hypersonic speed a significant increase in the temperature of the air can take place, and this increase results in physical-chemical processes which no longer allow the air to be treated as a perfect gas with constant specific heats. We may mention, as examples, excitation of the vibrational degrees of freedom of the molecules, dissociation of the molecular components of the air, chemical reactions between the components, and ionization of the atoms. Owing to the large speed, these processes may not proceed in thermodynamic equilibrium.

For hypersonic flight speeds it is necessary to determine the heat flux from the hot air to the surface of the body, as well as to find the forces acting on the body. One must then consider the physical-chemical processes which take place in the flow. Moreover, melting and sublimation of the surface layer of the body may take place because it is not always possible to transfer into the interior of the body the large amount of heat which is generated in the air near the surface.

In order to estimate these effects on flows past bodies, theoretical studies and extensive experimental investigations are now being carried out (mainly in wind tunnels, shock tubes, and other special facilities, and also under free flight conditions); approximate methods of calculation are also being developed.

Parallel with this work there has been an intensive development in the course of the last ten years of the theory of flow of an ideal gas with constant specific heats. This theory is a necessary step in the study of hypersonic flows past bodies and provides many important results by simple means. Since certain aspects of the theory are now well established, their study is a necessary part of the preparation of aerodynamicists for work on very high speed flight.

Many papers have been devoted to the theory of ideal gas flows at

hypersonic speeds, although at present there are no specific books on this subject either in the USSR or abroad. However, almost all of the textbooks on aerodynamics which have appeared in recent years devote some space to the theory of hypersonic gas flows and, in particular, to the hypersonic similarity law.

In view of the ever increasing number of scientists and engineers drawn to problems of flight at very high speeds, and also because of the need to acquaint undergraduate and graduate students specializing in the field of aerodynamics with the theory of hypersonic flow, it seems advisable to present in a systematic form the fundamentals of the theory and the most important methods for calculating ideal gas flows at very high speeds.

The present book is based on material from special courses which the author gave between 1954 and 1956 at the Mechanical-Mathematical Faculty of Moscow State University and is supplemented by more recent research on the subject.

The book does not pretend to provide an exhaustive presentation of all the important problems of hypersonic ideal gas flows. The first two chapters contain general information on supersonic flow and, in particular, an account is given of the already widely disseminated theory of hypersonic flow past slender bodies. The remainder of the book (Chapters III to V) includes only those parts of the theory of hypersonic ideal gas flows in the development of which the author took part in one way or another. For this reason, the interesting and important problem of flow near the blunt nose of a body with the presence of a local subsonic zone was not covered in the book. A review of the work on this problem can be found in an article by Van Dyke, "The supersonic blunt-body problem—review and extension," *J. Aero/Space Sci.* **25**, 485–496 (1958).

The author has not included in the book a treatment of the effects due to the departure of air properties from those of a perfect gas with constant specific heats, mainly because the calculation of these effects do not in principle present any difficulty. The methods of calculating hypersonic flows which are given in Chapter III and in Chapter IV can easily be generalized to the case in which the gas properties differ from those of a perfect gas with constant specific heats. However, in this case the calculations become significantly more unwieldy and the results difficult to analyze.

As was already mentioned, the effect of viscosity on hypersonic flows is not considered at all in the book. The effects of viscosity and heat transfer are fundamental to the fluid dynamics of very high speeds and

these problems are now being intensively studied. In this area there are still many unsolved problems. One can become acquainted with the present state of development in this field through the survey article of L. Lees, "Recent developments in hypersonic flow," *Jet Propulsion* **27**, 1162-1178 (1957).*

The author expresses his gratitude to L. I. Sedov for fruitful discussions of many problems considered in this book; to K. M. Bam-Zelikovich for reading the manuscript and for making valuable comments; to G. I. Barenblatt for useful discussions of Section 2 of Chapter I; and to A. L. Gonor and V. I. Shul'gin for placing experimental material at the author's disposal.

G. G. CHERNYI

* *Author's note:* A detailed account of the theory of hypersonic flow is contained in the recently published book of W. D. Hayes and R. F. Probstein, *Hypersonic Flow Theory*, Academic Press, New York, 1959.

Author's Preface to English Edition

The period which has passed since the completion of the manuscript of the original edition of this book several years ago has been one of intensive theoretical and experimental study in the field of hypersonic aerodynamics. These studies have considerably increased our previous knowledge of the general properties of hypersonic flows and brought about substantial improvements in earlier methods of calculation. In addition, because the status of hypersonic flows up to 1959 was fully expressed in the monograph "Hypersonic Flow Theory" by W. D. Hayes and R. F. Probstein, the author had initially intended, in preparing the English translation, to revise substantially the book in comparison with the Russian edition. It had been planned to add a chapter on flows past bodies with detached shock waves, in addition to new theoretical results related principally to Newton-Busemann flows, to thin shock layers, and to flows past bodies with small leading edge blunting. Because of lack of time, however, the author was unable to carry out this plan and had to limit the revisions to minor editorial changes in various parts of the book and to the correction of errors and inaccurate statements.

The author is grateful to Academic Press for agreeing to publish the English translation of the book. The author also wishes to express his sincere gratitude to the editor and translator Professor Ronald F. Probstein of Brown University, without whose collaboration it would not have been possible to realize so successful a translation.

G. G. CHERNYI

Moscow, May 1961

INTRODUCTION

1. Historical remarks and characteristic features of hypersonic aerodynamics

The foundations for the theoretical study of supersonic gas flows past bodies were laid down during the decade 1925–1935 (see References [1–6]).* In these works, and in many others which followed them, an examination was made of the steady flow of an ideal gas past slender airfoils and bodies of revolution with sharp leading and trailing edges and at small angles of attack. These bodies produce only a small disturbance of the free stream, so that the flow could be studied by an approximate method based on the linearization of the flow equations. By this method, the distribution of velocity, density, and pressure in the flow could be found and, in particular, simple expressions for the forces and moments acting on slender airfoils and bodies of revolution moving at supersonic speeds could be obtained.

When the thickness of the body or its angle of attack is increased sufficiently the assumptions used in the linearization of the flow equations are no longer valid. These assumptions also break down for slender bodies at hypersonic speeds, where the velocity perturbations are small with respect to the flow velocity but not small with respect to the sound velocity. In order to evaluate the limits of the linear theory, it is necessary to compare its results with those of more exact theories and with experiments. Such a comparison was made possible a short time after the appearance of the linear theory when solutions of the exact nonlinear equations were obtained for several important flow problems.

In [7] it was shown, for airfoils having a straight line segment at the leading edge, that the pressure distribution could be calculated exactly using the well-known shock [8, 9] and simple wave [10, 11] relations. An exact solution of the nonlinear equations was also ob-

* Here, and in what follows, the numbers in square brackets refer to the numbers in the reference list at the end of the book.

tained for axisymmetric supersonic flow past the simplest body of revolution, the circular cone [12]. For the calculation of supersonic flows past sharp-edged airfoils and bodies of revolution, having thickness ratios for which the linear theory was not valid, the numerical or numerical-graphical method of characteristics was developed [13–17]. Although effective in its application, the method requires a rather large expenditure of effort. In the case of flows at moderate supersonic speeds past slender airfoils with sharp leading edges, simple and convenient expressions were obtained for calculating surface pressures, aerodynamics forces, and moments. In these expressions, which improved the linear theory results, terms of second and third order [18] and of fourth order [19] in the flow deflection angle were retained.

During the Thirties, works appeared which took into account the effect of viscosity on supersonic flows past bodies. In these works the classical boundary layer idea for fluids with small viscosity was applied to calculate the frictional drag, surface temperature, and heat transfer for compressible flows. Most of these investigations were concerned with laminar boundary layers [20–25] but some attempts were also made to obtain results for the turbulent boundary layer [5, 26].

Thus, at the beginning of the Forties many important results in supersonic flow theory had already been obtained. The theoretical methods which had been developed permitted the determination of the basic aerodynamic characteristics of wing sections and axisymmetric fuselages. However, these theoretical results had been checked by experiment to only a very limited extent. In this regard we may mention the confirmation of the theory of supersonic flows past slender airfoils [18, 27] and the good agreement with experiment of the exact solution for the circular cone [12].

Up to this time most of the experimental material had been obtained by ballisticians, who were the first to accelerate bodies—artillery projectiles and rockets—to supersonic speeds. This experimental material consisted primarily of information about the flow pattern and total drag of projectiles of various shapes. In addition some data on aerodynamic stability had been obtained. Experimental data for lifting bodies was very meager, in spite of the fact that in the middle Thirties some wind tunnels had already been built which were specifically intended for the study of supersonic air flow [28, 29].

The rapid expansion of theoretical and experimental supersonic aerodynamics began in the Forties, when it became clear that jet and rocket propulsion made it possible to build supersonic aircraft and missiles. In this connection a great number of effective theoretical methods were developed which permitted the determination of the aerodynamic characteristics of finite span wings [30-42] and wing-body combinations [43, 44, etc.] within the limits of linearized theory. Methods for calculating compressible laminar [45-50] and turbulent [48, 51] boundary layers were also developed rapidly. Construction of wind tunnels began on a broad scale, and experimental studies of the aerodynamics of flight vehicles took on a systematic character.

As with the theoretical work, the experimental studies carried out through the middle Forties were concerned with flight velocities not more than three to five times the velocity of sound. There were only isolated attempts to study the specific properties of gas flows for velocities many times greater than the velocity of sound. In the paper of Epstein [7], which has been mentioned previously, the first estimate was made of the drag of bodies at very high supersonic speeds by employing the methods of supersonic aerodynamics. In the same paper attention was drawn to the fact that the flow pattern around a body moving at these speeds closely resembles the model considered by Newton [52] for motion through a resisting medium composed of individual particles which do not interact with each other. From Newton's arguments it follows that the pressure acting on a forward-facing element of a moving body is proportional to the square of the sine of the angle between the surface element and the particles of the medium. An improvement on the Newtonian formula was made in [53] where an approximate relation was obtained for calculating surface pressures on the forward portion of airfoils and bodies of revolution at very high supersonic speeds.

At the time, these attempts at considering flows with very high supersonic speeds were far removed from practical application. Only meteorites moved with velocities considerably in excess of the velocities of ballistic projectiles. The development of vehicles moving at speeds comparable with those of meteorites seemed to be a very distant one and to have little real prospect. For these reasons the study of phenomena accompanying the flight of meteorites in the

atmosphere, apart from its use as one of the principal methods for the investigation of the upper layers of the atmosphere, was of interest mainly to astronomers and geophysicists.

The situation began to change in the middle Forties. Extensive theoretical investigations and experiments in wind tunnels and on free flight models led to the successive solution of many basic problems related to the accomplishment of flight at supersonic velocity. By the end of the Forties flights of aircraft and guided missiles at speeds greater than the speed of sound had been achieved. Somewhat earlier, at the end of the Second World War, ballistic vehicles had been developed with a range of several hundred kilometers and with speeds five to six times the speed of sound.

In recent years the scope of technical and scientific problems arising from the study of phenomena connected with vehicle flight in the earth's atmosphere at speeds from 3 to 10 km/sec and more has been broadened considerably. The acceleration of vehicles to these high speeds has been brought about by an increase in the power of rockets and by the successful development of automatic guidance and control. Through the use of rocket propulsion, long-range ballistic vehicles and earth satellites with velocities from 6 to 8 km/sec have been developed. The time is near at hand when lifting vehicles will also attain these velocities.

For this reason, parallel with the further development of the theoretical and experimental aerodynamics of flight at moderate supersonic speeds, i.e., speeds not greater than four to five times the speed of sound, an intensive development of the aerodynamics of hypersonic flow was begun. The basis for systematic investigations in the regime of hypersonic aerodynamics can be traced to the work of [54] and also to the works which followed it [55-57]. Let us briefly look into some of the specific features of this new branch of aerodynamics.

As was already pointed out, for hypersonic flows past slender bodies the velocity perturbations are small compared with the free stream velocity, but are not small compared with the free stream sound velocity. Under these conditions many of the results of linearized theory, which are so useful for studying flows past slender bodies at moderate supersonic speeds, can no longer be applied. As a

result it becomes necessary in any theoretical analysis to retain nonlinear terms in the flow equations. This feature materially complicates the methods of calculating flows at hypersonic speeds compared to moderate supersonic speeds.

This is not the only difficulty in the theoretical study of hypersonic flow, however. The gas temperature near the surface of the body increases to very high values at hypersonic flight speeds. The increase in temperature is caused by the strong compression of the gas ahead of the nose of the body and by the generation of heat due to viscous shear in the gas carried along by the body. Theoretical estimates and observations of the luminosity of meteorites show that for atmospheric flight at speeds corresponding, for example, to the speed of re-entry of a long-range ballistic vehicle into the dense layers of the atmosphere, temperatures are developed which can reach those existing at the surface of the sun.

In this connection it is necessary to take into account, in the theory of ideal gas flows at hypersonic speeds, the changes in air properties resulting from the high temperatures. Among these are the excitation of the internal degrees of freedom of the molecules; the dissociation of the components of air; chemical reactions, as for example the formation of nitric oxides; and electronic excitation and ionization. For adiabatic equilibrium flows, these factors influence the dependence on the temperature and pressure of the enthalpy and entropy of the gas. In problems in which transport phenomena are important, as for example in the calculation of skin friction or surface temperature of a body, one must take into consideration the large changes in the viscosity and heat conductivity of the air. In some cases it is also necessary to consider the diffusion and thermal diffusion of the air components, as well as other transport phenomena.

It can also happen that under some circumstances the thermodynamic processes cannot be assumed to be in equilibrium, so that consideration of nonequilibrium conditions may be necessary in theoretical investigations. The distinguishing feature of hypersonic aerodynamics, a feature which relates it to physics, is this need to consider phenomena which occur in high temperature gases.

In experimental investigations of hypersonic flows, difficulties arise which are connected, first of all, with the need to heat the air enter-

ing a wind tunnel to high temperatures, in order to prevent its condensation as a result of the expansions required to develop high speeds. In a number of cases, in order to reproduce flight conditions in the wind tunnel, it is necessary to consider the changes in air properties associated with the high temperatures which accompany hypersonic flight. It is therefore insufficient only to try to prevent air condensation and to simulate the Mach and Reynolds number: the actual temperature conditions must also be simulated. This requirement makes the techniques used for experimental investigations at hypersonic speeds essentially different from those used at moderate supersonic speeds. In particular, it has been necessary to develop totally new types of test equipment for these investigations, such as shock tubes, piston driven tubes ("adiabatic tubes"), and so forth.

2. Basic aerodynamic problems connected with flight at hypersonic speeds

We shall briefly describe some of the basic aerodynamic problems connected with flight in the atmosphere at very high velocities.

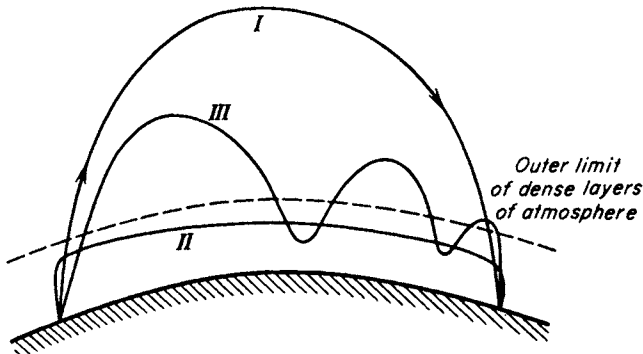


FIG. I.1. Trajectories for long-range vehicles: I—ballistic; II—glide; III—skip.

In Fig. I.1 are shown [58] various possible trajectories for long-range hypervelocity vehicles. (For clarity, the vertical scale on Fig. I.1 has been greatly enlarged.) For a ballistic vehicle (curve I), the ascent through the dense layers of the atmosphere takes place at a steep angle to the horizontal and at relatively low velocity. In the less dense layers of the atmosphere the vehicle gradually increases

its velocity and takes on the specified flight direction. After the propulsive thrust is cut off, the vehicle moves outside the atmosphere in the gravitational field of the earth, describing a ballistic trajectory. In the descent phase the vehicle re-enters the dense layers of the atmosphere like a meteorite with high velocity and at a steep angle.

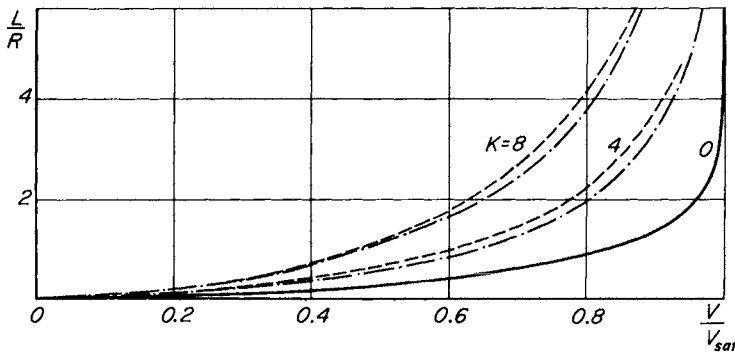


FIG. I.2. Flight range for hypervelocity vehicles.

In Fig. I.2, the attainable range of a ballistic vehicle (in earth radii) is shown by the solid line as a function of its velocity at the beginning of the inertial part of its flight (the velocity is expressed as a fraction of the velocity necessary to make the vehicle an earth satellite). Only a small portion of the powered phase of the trajectory of a long-range ballistic vehicle takes place in the dense layers of the atmosphere, and its velocity during the ascent in these layers is relatively low. Therefore the shape of the vehicle, which determines its aerodynamic drag, has only a very minor influence on the flight range.

On the other hand, the factors which determine the possibility of the vehicle reaching the earth's surface without being destroyed by the high temperatures during the descent in the dense layers of the atmosphere depend, to a large extent, on the nose shape. These factors are the total amount of heat absorbed by the vehicle during the descent and the intensity of the local heat fluxes from the very hot air to the vehicle. Therefore the basic aerodynamic problem for a long-range ballistic vehicle consists in selecting that shape which lends itself most readily to the cooling of the surface as it decelerates

in the dense layers of the atmosphere, and which at the same time ensures its aerodynamic stability.

Another possible type of trajectory for a long-range vehicle which flies at hypersonic speeds is a glide trajectory (curve II in Fig. I.1). As in the case of the ballistic vehicle, the initial ascent takes place at a steep angle with a progressively increasing velocity. The difference lies in the fact that at the end of the powered phase, the glide vehicle is directed horizontally or at a small angle to the horizontal. Thereafter it glides in the earth's atmosphere, gradually descending in such a way that its weight is almost in equilibrium with the aerodynamic lift and centrifugal force.

Finally one may combine both types of trajectories into the so-called skip trajectory (curve III in Fig. I.1), in which ballistic flight alternates with lifting flight [59].

For the same initial velocity, the flight range of a glide or skip vehicle can be greater than that of a ballistic vehicle, as a result of the use of aerodynamic lift. Obviously, the larger the aerodynamic lift-drag ratio, the greater will be the possible advantage in range. In Fig. I.2 are shown the attainable flight ranges for a glide vehicle (dashed-dotted line) and for a skip vehicle (dashed line) for two values of the lift-drag ratio K . (For $K > 4$, the ranges of these two types of vehicles differ very little from each other.)

In gliding or skipping flight all of the trajectory, or at least a significant part of it, is in the relatively dense layers of the atmosphere, so that the vehicle will spend an appreciable length of time in contact with very hot air. From what has been said, it follows that the basic aerodynamic problem for the long-range glide or skip vehicle is to find those shapes which possess a high lift-drag ratio for flight at very high velocity and high altitude, and which at the same time provide the possibility of effectively dispersing the heat produced in the layer of air close to the surface.

To obtain a sufficiently high lift-drag ratio, the drag of the vehicle must not be large—i.e., its fuselage must be slender and elongated in the flight direction, and the lifting and stabilizing surfaces must also be slender. However, in order to conduct away large amounts of heat from the nose and wing leading edges, the nose and leading edges must be blunted. If the choice of shape of the blunt nose is correct,

then the body drag need not be greater than the drag of a sharp-nosed body. On the other hand, blunting of the wing edges sharply increases their drag and consequently decreases the lift-drag ratio. This increase

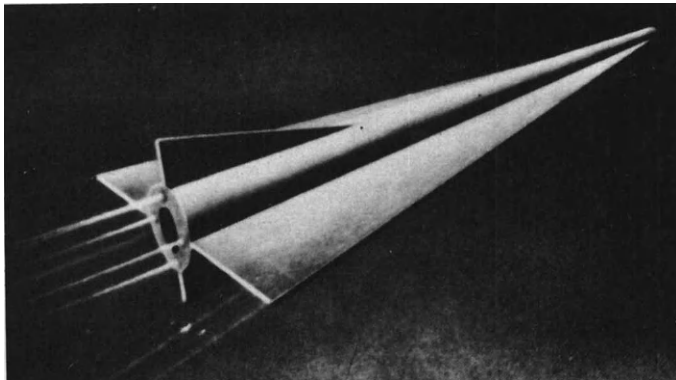


FIG. I.3. Envisaged form of a hypervelocity glide vehicle.

in drag can be reduced by using swept wings. The presence of a sweep angle also reduces the heat flux. A theoretically feasible hypervelocity glide vehicle is shown in Fig. I.3.

3. Some information on the properties of air at high temperatures

In order to solve aerodynamic problems connected with atmospheric hypersonic flight, it is necessary to take into account the fact that the air near the moving body is heated to very high temperatures. Thus for a long-range ballistic vehicle re-entering the dense layers of the atmosphere, or for a long-range winged vehicle during any portion of its flight, the temperature of the gas behind the strongest part of the bow shock wave can reach 6000 to 8000 °K. At such high temperatures the properties of air differ considerably from the properties of a perfect gas with constant specific heats. Already at temperatures of the order of 1500 °K the excitation of the vibrational degrees of freedom of the nitrogen and oxygen molecules begins to play an important role. For temperatures of the order of 3000 °K the oxygen molecules dissociate, decomposing into individual atoms. In addition, chemical reactions take place in the air, with the result

that a certain amount of nitric oxide appears. This nitric oxide also dissociates into atoms of oxygen and nitrogen when the temperature is increased still further. At a temperature of between 5000 and 6000 °K the oxygen molecules are almost completely dissociated and a portion of the nitrogen molecules are also dissociated. Ionization of the components of air (atomic oxygen and nitrogen, and nitrogen and nitric oxide molecules) begins at these temperatures. As a result of the ionization, there is an appreciable concentration of free electrons.

In order to excite the internal degrees of freedom of the molecules, to dissociate the molecular components of air, and to produce ionization, the heat which is transported to the air must go not only into increasing the energy of the translational and rotational motion of the molecules, but also into increasing the energy of vibrational motion of the atoms in the molecules, into overcoming the interaction force between the atoms in the molecules when dissociation occurs, and into expelling electrons from the atoms when ionization takes place. As a result, the specific heat per unit mass of air is considerably increased at high temperatures. As an example, the dependence of the specific heat of air on temperature is shown in Fig. I.4, for a density equal to one-tenth of the atmospheric density at standard

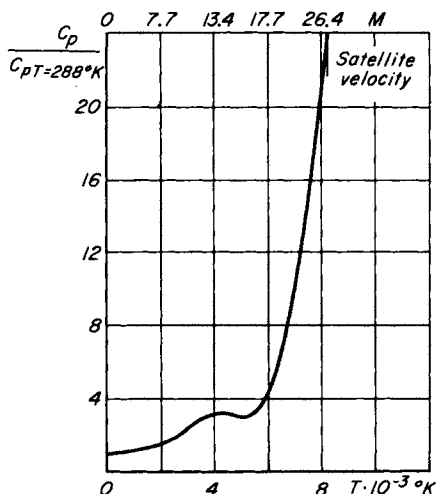


FIG. I.4. Dependence of the specific heat of air upon temperature.

conditions [60]. (Standard conditions are a pressure of 1 atm and a temperature of 288 °K.) A Mach number scale is also given on this figure; the temperature corresponds to the conditions behind a normal shock wave for the given Mach number. At high temperatures the specific heat increases sharply, so that at 7000 °K it is twelve times the specific heat at standard conditions.

The high temperature processes described above change the composition of the gas and the total number of particles per unit mass and, as a result, the molecular weight of the gas. Figure I.5 presents

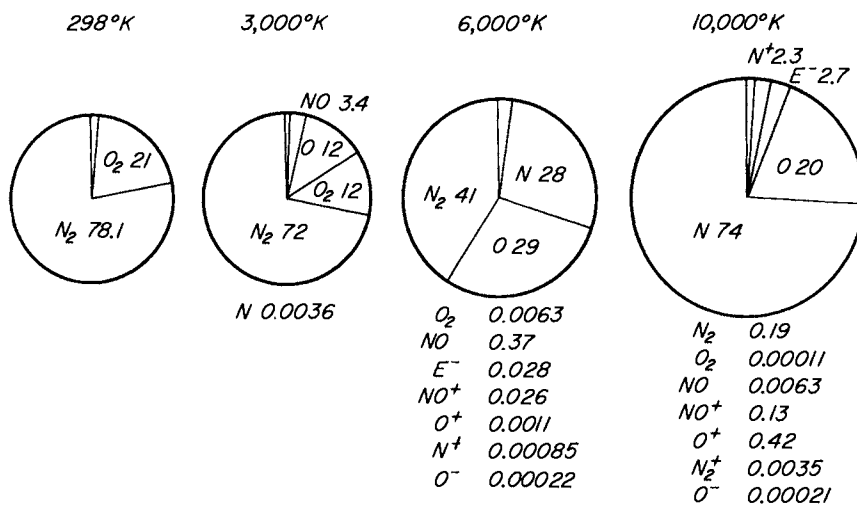


FIG. I.5. Composition of air as a function of temperature.

pictorially the change in the composition of air as a function of temperature for a density equal to atmospheric density at standard conditions [61]. The total number of particles per unit mass is illustrated in this figure by the area of the circular diagrams.

The changes in the properties of air at high temperatures can produce a difference between an equilibrium flow outside a boundary layer and the flow of a perfect gas of constant specific heat under the same conditions. This difference is not present for air at moderate temperatures. The change in air properties does not in principle, however, introduce any difficulty either in the theory or in the methods of calculation of equilibrium ideal gas flows. The theoretical

methods developed for a perfect gas with constant molecular weight and constant specific heats can, as a rule, be easily generalized to the case of air flows at high temperatures. The possibility of such a generalization justifies the large amount of attention which has been given, and is still being given, to the development of methods of calculating perfect gas flows with constant specific heats for hypersonic speeds. Of course, for air at high temperatures the expressions for the entropy and enthalpy of the gas, which enter into the equations of motion and the shock wave relations, are not simple functions of the pressure and density. The calculations employing these functions, therefore, become more unwieldy than those for a perfect gas with constant molecular weight and constant specific heats. Besides this, for flows which are not hypersonic, the only parameter on which the steady flow of an ideal gas past a body of given shape depends is the Mach number. On the other hand, for hypersonic flows it is necessary to introduce one more parameter which characterizes the free stream stagnation temperature, as, for example, the ratio of this temperature to the characteristic temperature for oxygen dissociation. This factor increases the amount of calculation required to analyze hypersonic air flows past bodies, and complicates the presentation of the results.

In contrast to the theory of ideal gas flows, the change in air composition with temperature (i.e., the change in concentration of the individual components) can play an important role in the theoretical study of phenomena connected with molecular transport processes. The study of these phenomena is important for determining surface skin friction and heat transfer, as well as for determining body surface temperatures. The presence of concentration and temperature gradients in the moving gas gives rise to diffusive flows of matter and of heat. These diffusive flows can lead to departures in the concentrations of the individual components of the air from their equilibrium values, and can also have an important effect on the heat transfer. Let us examine, for example, a cooled surface in a flow of high temperature air which contains dissociated oxygen. As a result of the decrease in the temperature of the air, the concentration of the dissociated particles of oxygen near the wall is decreased. This concentration difference produces a diffusive flow of dissociated

oxygen towards the wall, and the heat released due to the recombination of the oxygen atoms in the region of low temperature near the wall increases the heat flux in comparison to the case where diffusion is not taken into account. The need to consider such diffusion phenomena in order to determine the surface skin friction and heat transfer distinguishes the aerodynamics of hypersonic flows from the aerodynamics of moderate supersonic flows.

Another important feature of the aerodynamics of hypersonic flows is that the establishment of thermodynamic equilibrium in the moving gas does not take place instantaneously, but requires a finite time. Hence the pressure, temperature, the concentration of each component of the gas (even when diffusion phenomena are not considered), and its specific heat depend not only on the instantaneous value of the internal energy and particle density, but also on the preceding history of the gas (approximately on the rate of change of the internal energy and particle density). Departures from thermodynamic equilibrium can have a significant effect on the structure of shock waves, on the propagation of small disturbances, and on other phenomena connected with the flow of air [62-64]. The characteristic time necessary to reach thermodynamic equilibrium—the so-called relaxation time—is different for different processes. Thus to establish the equilibrium value for the energy of translational motion of the molecules, it is sufficient on average to have one molecular collision; for the energy of rotational motion, from 10 to 100 collisions; for the energy of vibrational motion of the atoms inside a molecule, 500,000 collisions in the case of oxygen. In some cases the relaxation times can be estimated by theoretical means; experimental methods, however, are more important for determining the effects of relaxation phenomena in hypersonic gas flows. In Fig. I.6 are shown [65] the altitude and flight velocity regions in which relaxation phenomena connected with dissociation can be present to an appreciable extent. The calculations on the basis of which Fig. I.6 was drawn assume that the body has a blunt nose and that the air after passing through the shock wave is in thermodynamic equilibrium in the region of the stagnation point. In the shaded region the flow can be considered to be in equilibrium since the relaxation time is one-tenth the time necessary for a particle to move along the sur-

face of the body a distance of 0.3 meters. (Naturally, the effect of the relaxation time is smaller when the body is larger. For example, if the distance along the surface of the body were 3 meters, the limit of the shaded region would be displaced upward as shown on the

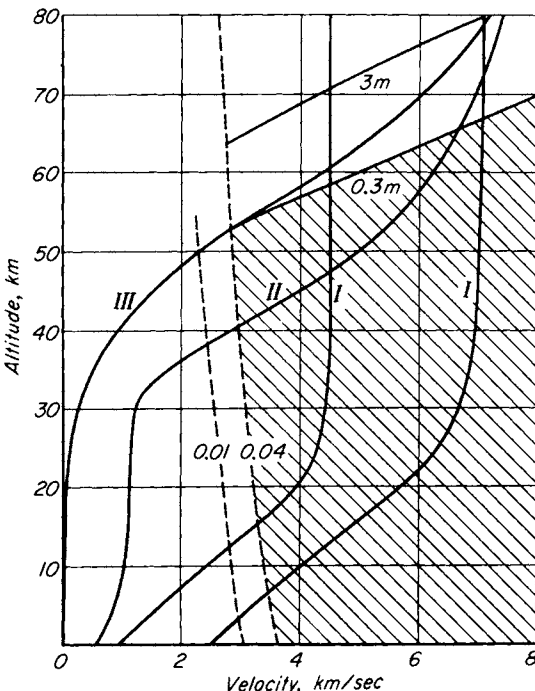


FIG. I.6. Flight conditions for which relaxation phenomena connected with dissociation can be important: I—ballistic; II—glide; III—satellite.

figure.) To the left of the dashed lines the degree of air dissociation at the stagnation point is less than 0.01 and 0.04, respectively, so that if relaxation phenomena connected with dissociation take place in this region, they cannot have a significant effect on the flow.

In Fig. I.6 are also drawn some typical trajectories for long-range vehicles re-entering the dense layers of the atmosphere at different speeds. Curves I are for long-range ballistic vehicles, curve II is for a glide vehicle, and curve III is for the re-entry of an earth satellite.

As is evident, the flow produced by a re-entering earth satellite may not be in thermodynamic equilibrium.

Apart from calculations of hypersonic flows past bodies, it is necessary to take into account possible departures from thermodynamic equilibrium when designing wind tunnel nozzles intended to produce hypersonic flows. For purposes of aerodynamic investigations, the undisturbed air in the test section of the tunnel must be in an equilibrium state.

As was already pointed out, free electrons are present in air at very high temperatures, and the air becomes a good conductor of electricity. In Fig. I.7 are presented some experimentally determined

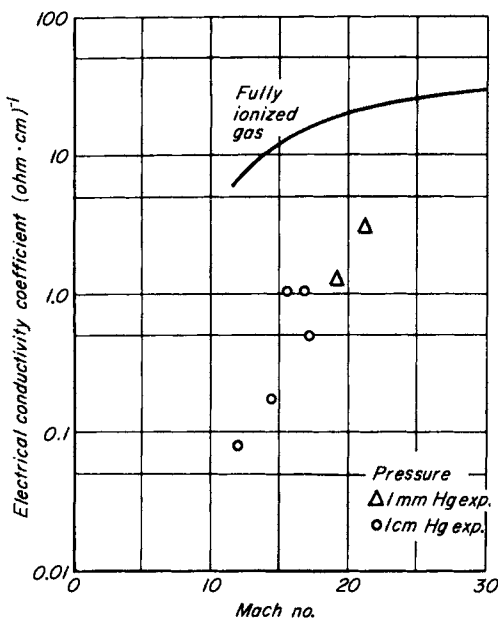


Fig. I.7. Electrical conductivity of air at high temperatures.

values [60] of the electrical conductivity coefficient of air at high temperatures. (The abscissa is expressed in terms of the Mach number ahead of a normal shock wave, behind which the corresponding temperature is reached. The pressures ahead of the shock are 1 and 10 mm Hg.) The good electrical conductivity of air near a body moving at hypersonic speeds presents the possibility of utilizing electric

and magnetic fields to alter the flow [66]. It can also make the solution of radio communication problems with the vehicle difficult, however.

Finally, we note that the heating of the air as a result of the compression at the nose of a body moving at hypersonic speeds can give rise to an intense flux of radiation which is partly transmitted to the body surface but which for the most part is scattered in the surrounding layers of air. These effects must also be taken into account when studying hypersonic flows.

Thus, as we have seen, the motion of bodies at hypersonic speeds takes place in quite a different medium than the air which scientists and engineers deal with when solving flight problems at moderate supersonic speeds.

4. Experimental methods for studying high speed gas flows

In the present section a short description is given of the methods of laboratory simulation and modeling of phenomena which arise from the motion of bodies in air at hypersonic speeds. We shall not discuss the methods of carrying out free flight aerodynamic investigations of aircraft and missiles, and we shall not touch on problems of measurement of various physical quantities for hypersonic flows and for the high temperatures which accompany such flows.

In aerodynamics and ballistics, experimental investigations of models of aircraft, rockets, projectiles, and their components have always had great importance, along with investigations of a general character which have been carried out for the purpose of establishing the basic properties of gas flows and verifying theoretical results. For these investigations, wind tunnels and ballistic ranges have been employed. In the wind tunnel the model is at rest in an artificially generated air stream, while in the ballistic range the model is accelerated by one of a number of methods and then flies freely in a gas medium which is at rest. The earlier investigations were concerned with flight problems at moderate supersonic speeds where the air temperatures near the body were not high. The modeling rules for the solution of aerodynamic problems in steady flow required only that the Mach and Reynolds numbers correspond to the actual flight conditions. (The necessary condition of the equality of the specific

heat ratio was automatically ensured when the models were tested in air.)

The transition to hypersonic speeds significantly complicates the modeling problems, mainly because a series of new similarity criteria must be introduced in place of the specific heat ratio in order to take into account the changes in air properties at high temperatures. In addition, at hypersonic speeds where heat transfer phenomena are important it is necessary to ensure the similarity of those phenomena. The large number of similarity criteria at hypersonic speeds makes it impossible to realize complete similarity between the phenomena in flight and in the laboratory. As in classical aerodynamics, however, when studying a certain class of phenomena, not all the quantities which define the flow have an equal effect on the phenomena. For this reason a partial modeling of the flight conditions acquires meaning—i.e., conserving only those similarity criteria which are most important for studying the phenomena being considered. For the purpose of partially reproducing the actual conditions of hypersonic flows past bodies, one can use wind tunnels which operate in the usual manner, ballistic ranges, and in addition special experimental equipment having no application in classical aerodynamics.

An increase in the test section Mach number in a wind tunnel is associated with an increase in the required ratio of the stagnation pressure to the test section pressure. This increase results in two features which are distinctive of hypersonic wind tunnels. First, since as a rule wind tunnel dimensions only allow one to test models which are many times smaller than the actual vehicle, the air entering the nozzle must be highly compressed, usually to pressures from 50 to 150 atm, in order that the Reynolds number in the test section be not too low. Secondly, since the expansion of the air in the nozzle is nearly adiabatic, the air temperature in the nozzle is sharply reduced for a high pressure ratio. Therefore the entering air must be heated to a high temperature to prevent condensation. This temperature rapidly increases for an increase in the test section Mach number M : for $M = 10$ it is between 800 and 1100 °K (depending on the pressure), and for $M = 12$ it is between 1100 and 1400 °K. To reduce the difficulties connected with a still further increase in the temperature with a further increase in the Mach number, one can replace the air

by helium, which has a much lower condensation temperature. By such means Mach numbers up to 20 are attained in wind tunnels. Of course, for wind tunnels having temperatures in the test section close to the condensation temperature of air (and more so with helium), one can study only those phenomena related to atmospheric hypersonic flight for which the fundamental parameter is the Mach number (and sometimes also the Reynolds number), and upon which the thermodynamic properties of the air have only a small effect.

For flight speeds which are no greater than seven to eight times the speed of sound, the effect of departures in the air properties from the properties of a perfect gas with constant specific heats is not great.

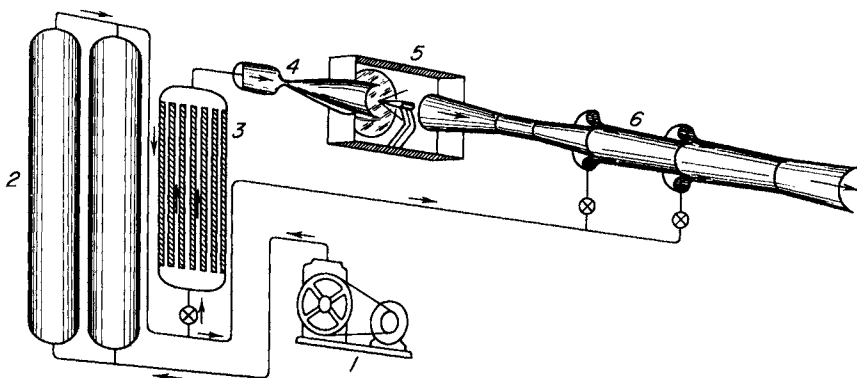


FIG. I.8. Schematic picture of a wind tunnel for obtaining hypersonic flows: 1—compressor; 2—high pressure tanks; 3—air heater; 4—nozzle; 5—test section; 6—ejector and downstream diffuser.

In a number of such cases, to approximate the similarity conditions for free flight in a wind tunnel it is sufficient to ensure the equality of the respective Mach and Reynolds numbers and the absence of air condensation in the flow. For higher flight speeds the satisfaction of these similarity criteria alone is insufficient to model the flight conditions. Let us cite an example which illustrates the necessary values of the stagnation pressure and temperature of the air in a wind tunnel designed for hypersonic speeds. (A schematic picture of one possible version of such a wind tunnel is depicted in Fig. I.8.) Suppose a study is required, by means of a model, of the characteristics of a vehicle

which has a length of 6 meters, flying at an altitude of 40 km with a speed of 3 km/sec. The model length is assumed equal to 0.4 meters (i.e., a rather large wind tunnel is involved). To retain the same values of Mach and Reynolds numbers as in flight and to avoid air condensation, the entering air is compressed to 150 atm and has a temperature of 820 °K. Under these conditions, however, complete similarity between the phenomena in the wind tunnel and flight conditions will not be ensured. Actually, if the full-scale vehicle flies at a velocity of 3 km/sec, the air temperatures near the nose of the body will be above 3000 °K. For such high temperatures the internal degrees of freedom of the molecules will be fully excited and dissociation will play an important role. In the tunnel, for the above conditions, the temperatures near the surface of the model will only excite the internal degrees of freedom to a small extent. Therefore many phenomena (in particular, heat transfer phenomena), will take place under conditions which do not correspond to flight conditions when investigated in wind tunnels of the type described. In the example considered, in order to ensure similarity of the thermal phenomena, the stagnation temperature of the air must be raised to 3000 °K.

It is difficult by ordinary means (i.e., by means of contact of the air with hot surfaces or even by means of combustion in the flow) to heat the entering air to the required temperature. The problem of cooling the wind tunnel for long running times also becomes a very complicated one. One method of heating the air to 3000 °K and higher is to use an arc discharge. By this means one can obtain gas jets with temperatures of 10,000 °K and even higher. Another possible method of obtaining gas streams at very high speeds involves flows of very short duration, of the order of one ten-thousandth of a second. Such flows are set up in so-called shock tubes and in piston driven tubes ("adiabatic tubes") and are based on a variety of different operating schemes. The simplest kind of shock tube is a channel closed at both ends and divided into two parts by a partition (diaphragm) (Fig. I.9). On one side of the diaphragm the gas is at a high pressure (the "working" gas); on the other side there is a vacuum. After rupture of the diaphragm a shock wave propagates into the low pressure side, followed by a column of gas at constant

velocity which has been heated by compression through the wave. The higher the pressure ratio across the diaphragm, the higher the gas velocity and the higher its stagnation temperature. By such means speeds of 5 km/sec and more can be obtained without excep-

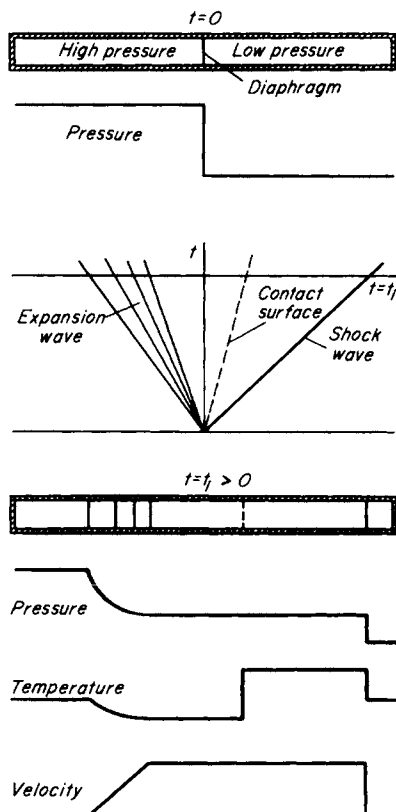


FIG. I.9. Schematic picture of a simple shock tube and the flow in it after rupture of the diaphragm.

tional difficulty, with the required values of stagnation temperatures.

In this scheme, however, the Mach number remains low, of the order of Mach 2. In order to increase the Mach number in the flow behind the shock wave, the gas can be expanded through a nozzle connected to the end of the tube (Fig. I.10,a). In other shock tube configurations the entrance to the nozzle has a considerably smaller

diameter than the diameter of the tube (Fig. I.10,b). After the shock wave reflects from the end of the tube, a region of gas at high temperature and pressure is formed between the entrance to the nozzle and the reflected wave. From this region the gas flows through the nozzle into a chamber, with a drop in its pressure. Such a shock tube

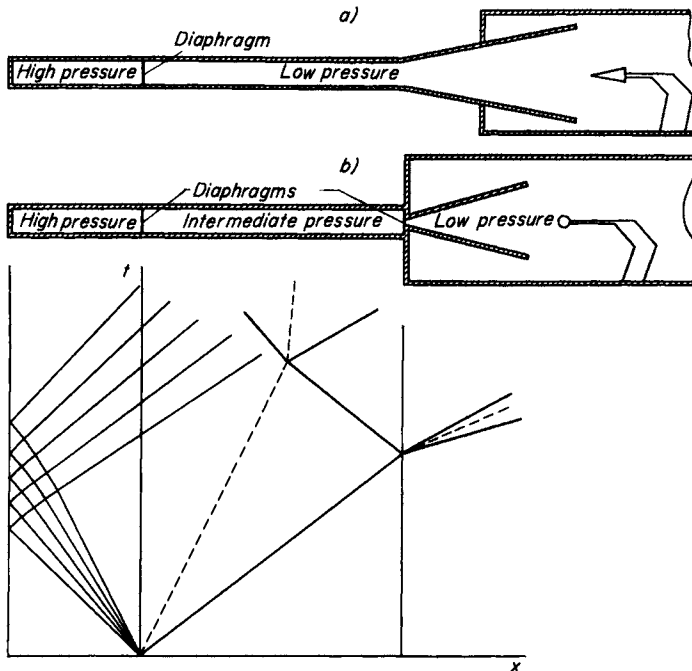


FIG. I.10. Some shock tube schemes: — shock wave; — — contact surface; — — — expansion wave.

is similar to the so-called adiabatic tube (piston driven tube) in which the gas ahead of the nozzle is compressed by means of a very rapidly moving piston. The higher pressures and temperatures of the working gas required to increase the velocity and temperature of the air column in shock tubes can be obtained by passing a strong electric discharge through it, or if the working gas is a combustible mixture, by exploding it.

The principal shortcoming of shock tubes and adiabatic tubes is their very short running time, as a result of which many difficulties

arise in measuring the flow parameters. Besides this, the heat exchange between the hot gas and the model in the tube changes rapidly with time. Methods have nevertheless been worked out which permit one to observe the flow under these conditions and to determine the surface pressures and the heat flow between the gas and the surface of the model.

Shock tubes are used mainly for investigating the fundamental physical and chemical processes which take place in the flow of air and other gases at high speeds and high temperatures, and not for determining the aerodynamic characteristics of a model. With the aid of shock tubes, studies have been made of the heat conductivity [67] and electrical conductivity [60] of air at high temperatures, the dissociation and formation of nitric oxide [68], relaxation phenomena accompanying dissociation [65], and so forth.

Ballistic ranges afford another means of obtaining conditions which correspond to very high flight speeds. In the past they were used mainly by ballisticians for determining the drag of projectiles and their stability in flight. In recent times, however, they have received

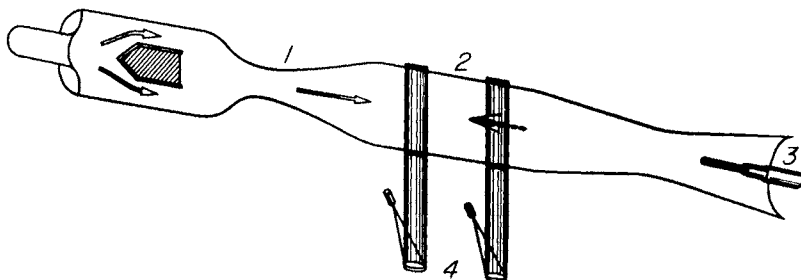


FIG. I.11. Schematic picture of a ballistic range with counterflow of air: 1- nozzle; 2- tunnel; 3- gun; 4- optical system.

widespread use as a means of studying phenomena connected with hypersonic flows. In ballistic ranges one can obtain the actual flight Mach numbers and temperatures when the flight speed of the model is equal to the actual flight speed. The required values of Reynolds number can also be achieved by firing the model into a pressurized chamber whose pressure can be regulated. At the present time model velocities in ballistic ranges approach 3 to 4 km/sec.

To attain such velocities it was necessary to develop special guns for firing the models which use compressed light gases instead of the products of powder combustion. In order to increase the relative velocity between the model and the air, a combination of a wind tunnel and a ballistic range is used in which the model is fired upstream into the flow (Fig. I.11). In ballistic ranges, as in shock tubes, gases other than air can be used for studying the physical processes connected with high stagnation temperature flows. For example, the effect of dissociation and relaxation processes on flows past bodies has been studied by such means [67].

CHAPTER I

GENERAL CONSIDERATIONS ON HYPERSONIC FLOWS OF AN IDEAL GAS

1. Formulation of the problem of supersonic flow of an ideal gas past a body

When a body moves at supersonic speed in an ideal gas, the region of influence of the disturbances produced by the body is separated from the gas at rest by a surface moving with the body called the bow wave. If the bow wave has a common point or common line with the surface of the body, it is termed attached (Fig. 1.1,a). If it does not, it is termed detached (Fig. 1.1,b). The detached bow wave always represents a surface of strong discontinuity—that is, a shock wave. When the gas crosses the shock wave it is suddenly set in motion and acquires a density and pressure different from its initial values. The attached bow wave is usually also a surface of strong discontinuity. In some cases, however (for example, for a body with an infinitely thin, sharp leading edge, or for a wing at a sufficiently large angle of attack), part of the attached bow wave may be a weak discontinuity surface—that is, a Mach wave whose velocity of propagation (along the normal to the wave) is the velocity of sound. Across such a wave the values of the flow parameters are continuous, and only some of the derivatives are discontinuous.

Behind an attached bow wave the gas velocity with respect to the body may be all supersonic, or it may be subsonic in some parts of the disturbed region. Behind a detached shock wave near the nose of the body there is always a region in which the gas velocity with respect to the body is less than the velocity of sound.

When a body is moving with supersonic speed, discontinuity surfaces other than the bow wave may be present within the disturbed region. Examples of these are shock waves, vortex (or contact) surfaces, and weak discontinuity surfaces (Fig. 1.1,a). The theoretical analysis of supersonic flows is made extremely difficult by the complicated character of the flow (i.e., the presence of discontinuity surfaces whose positions

and even configurations are unknown beforehand as well as possible regions of subsonic velocity with respect to the body). At the present time effective methods of calculation for many of these cases are lacking.

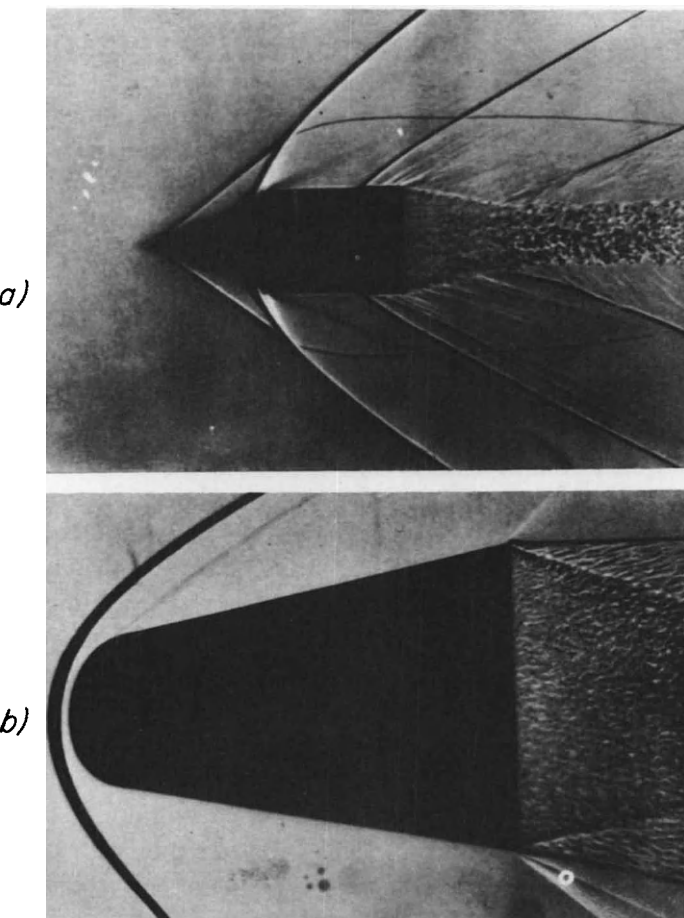


FIG. 1.1. Supersonic motion of a body in a gas: (a) attached bow wave, (b) detached bow wave.

Let us turn to the mathematical formulation of the problem of flow past a body moving at supersonic speed in an ideal gas. The motion of the gas will be considered in a system of coordinates fixed with respect to the body. We choose the x -axis in a direction opposite to the direction

of the velocity of the body, and we take the y and z axes in the plane normal to this direction with the axes orthogonal to each other. We shall denote by u , v , and w , respectively, the components of the disturbance velocity, and by p and ρ the pressure and density of the gas. If the velocity of the body is constant and equal to V , then the gas motion in the chosen system of coordinates will be steady, and the basic equations which describe the flow can be expressed in the following form [1]. (In these equations the body forces are not taken into account, since in supersonic flow problems their effect can usually be neglected.)

Equations of motion:

$$\begin{aligned} (V + u) \frac{\partial u}{\partial x} + v \frac{\partial u}{\partial y} + w \frac{\partial u}{\partial z} &= - \frac{1}{\rho} \frac{\partial p}{\partial x}, \\ (V + u) \frac{\partial v}{\partial x} + v \frac{\partial v}{\partial y} + w \frac{\partial v}{\partial z} &= - \frac{1}{\rho} \frac{\partial p}{\partial y}, \\ (V + u) \frac{\partial w}{\partial x} + v \frac{\partial w}{\partial y} + w \frac{\partial w}{\partial z} &= - \frac{1}{\rho} \frac{\partial p}{\partial z}, \end{aligned} \quad (1.1)$$

Continuity equation:

$$\frac{\partial \rho(V + u)}{\partial x} + \frac{\partial \rho v}{\partial y} + \frac{\partial \rho w}{\partial z} = 0, \quad (1.2)$$

Entropy equation (S is the entropy per unit mass):

$$(V + u) \frac{\partial S}{\partial x} + v \frac{\partial S}{\partial y} + w \frac{\partial S}{\partial z} = 0. \quad (1.3)$$

For a perfect gas with constant specific heats, the entropy is related to the pressure and density by the equation

$$\frac{p}{\rho^\gamma} = \text{const } e^{S/c_v}, \quad (1.4)$$

where c_v is the specific heat at constant volume, and γ is the ratio of the specific heat at constant pressure to the specific heat at constant volume.

Equations (1.1) to (1.4) serve to describe the continuous flow in each of the regions separated by strong discontinuity surfaces. In these regions the derivatives of the hydrodynamic quantities can be discontinuous across characteristic surfaces, which in a steady flow have the property

that the velocity component of the gas particles normal to them is either zero (stream surfaces) or equal to the velocity of sound (Mach waves).

The values of the flow parameters across the surfaces of strong discontinuity are related by the following conditions which derive from the laws of conservation of mass, momentum, and energy:

$$\begin{aligned}\rho_1(D - v_{1n}) &= \rho_2(D - v_{2n}), \\ \rho_1(D - v_{1n})\mathbf{v}_1 - p_1\mathbf{n} &= \rho_2(D - v_{2n})\mathbf{v}_2 - p_2\mathbf{n}, \\ \rho_1(D - v_{1n}) \left(\frac{\mathbf{v}_1^2}{2} + e_1 \right) - p_1 v_{1n} &= \rho_2(D - v_{2n}) \left(\frac{\mathbf{v}_2^2}{2} + e_2 \right) - p_2 v_{2n}.\end{aligned}\quad (1.5)$$

Here D is the velocity of propagation of the discontinuity surface in space:

$$D = -V \cos(n, x),$$

where (n, x) is the angle between the normal \mathbf{n} to the discontinuity surface and the x -axis, \mathbf{v} is the vector velocity of the gas particles ($\mathbf{v}^2 = \mathbf{v} \cdot \mathbf{v}$), v_n is the component of this velocity in the direction of the unit vector \mathbf{n} , e is the internal energy per unit mass, and the subscripts 1 and 2 correspond respectively to the conditions in front of and behind the discontinuity surface.

If the mass flow through the discontinuity surface is zero, then the conditions (1.5) take the simpler form

$$\begin{aligned}v_{1n} - D &= 0, & v_{2n} - D &= 0, \\ p_2 &= p_1.\end{aligned}\quad (1.6)$$

In this case the discontinuity surface is called a vortex or contact surface.

When the mass flow through the discontinuity surface is different from zero, then the pressure undergoes a jump across the surface. The density of the gas also changes, and this change in density and pressure is accompanied by a change in the entropy of the gas. On the basis of the second law of thermodynamics, when the gas passes adiabatically through a discontinuity surface its entropy can only increase. As is well known, it follows* from this that the pressure and density of the gas increase across surfaces of strong discontinuity, as a result of which such surfaces are called shock waves.

* Concerning mediums for which exceptions are possible see, for example, [2].

On the surface of the body it is necessary to satisfy the condition of equality of the normal velocity component of the gas particles and the normal velocity component of points on the surface of the body, i.e., the condition

$$v_{1n} = -V \cos(n_b, x), \quad (1.7)$$

where (n_b, x) is the angle between the normal to the body surface and the direction of the x -axis. Finally, at upstream infinity the flow parameters must take on the given values:

$$u = v = w = 0, \quad p = p_1, \quad \rho = \rho_1. \quad (1.8)$$

Thus the problem of flow past a body at constant supersonic velocity in an ideal gas is reduced to the determination of the solution of equations (1.1) to (1.4) which is continuous in every region separated by strong discontinuity surfaces, and which must satisfy equations (1.5) across shock waves, equations (1.6) across vortex surfaces, condition (1.7) on the body surface, and conditions (1.8) at upstream infinity.

We note that since the gas is undisturbed until its passage through the bow wave, the conditions (1.8) at upstream infinity can be replaced by the conditions across the bow wave, which in this case according to (1.5) take the form:

$$\begin{aligned} \rho_1 D &= \rho_2(D - v_{2n}), \\ -p_1 &= \rho_1 D v_{2n} - p_2, \quad \mathbf{v}_{2t} = 0, \\ \rho_1 D e_1 &= \rho_1 D \left(\frac{v_{2n}^2}{2} + e_2 \right) - p_2 v_{2n}. \end{aligned} \quad (1.9)$$

Here \mathbf{v}_t is the vector component of the gas velocity in the plane tangent to the bow wave. For a perfect gas with constant specific heats, the internal energy of the gas is expressed in terms of the pressure and density by the formula

$$e = \frac{1}{\gamma - 1} \frac{p}{\rho}.$$

Solving the system of equations (1.9) for v_{2n} , p_2 , and ρ_2 ($v_{2n} = |\mathbf{v}_2|$, since $\mathbf{v}_{2t} = 0$), we obtain

$$\begin{aligned} |\mathbf{v}_2| &= \left(1 - \frac{\rho_1}{\rho_2}\right) D = \frac{2}{\gamma + 1} D \left(1 - \frac{a_1^2}{D^2}\right), \\ p_2 - p_1 &= \rho_1 D |\mathbf{v}_2| = \frac{2}{\gamma + 1} \rho_1 D^2 \left(1 - \frac{a_1^2}{D^2}\right), \quad (1.10) \\ \rho_2 &= \frac{\frac{\gamma + 1}{\gamma - 1} \rho_1}{1 + \frac{2}{\gamma - 1} \frac{a_1^2}{D^2}}. \end{aligned}$$

Here

$$a_1 = \sqrt{\frac{\gamma p_1}{\rho_1}}$$

is the velocity of sound in the undisturbed gas.

Little is known in general about the question of the existence of a solution to the formulated mathematical problem of the motion of a body in an ideal gas and about the question of the uniqueness of this solution. Some considerations pertaining to these questions will be given in the following section.

2. Additional remarks on the formulation of the problem of supersonic flows past bodies

Consideration of the simplest cases of two-dimensional flow shows that attempts to describe a steady supersonic flow of an ideal gas past a body in an infinite uniform stream by means of a continuous solution of the differential equations (1.1) to (1.4) leads to a physically nonsensical result. The solution is not single-valued [3], at least at some distance from the body. The solution can be made single-valued if appropriate discontinuity surfaces are introduced. In this case uniqueness of the solution is not guaranteed, however, since the discontinuity surfaces can be chosen differently. But the solution of a correctly formulated physical problem must be unique and correspond exactly to the phenomena which result from the given physical conditions. Moreover, it is not possible to satisfy the conditions of conservation of mass, momentum, and energy on an arbitrary discontinuity surface which is introduced.

Therefore, having seen that in general continuous solutions of the equations have no physical sense for ideal supersonic gas flows, it is

natural to take into account from the start the possibility of the presence of discontinuities. In order to do this, the basic physical laws of conservation of mass, momentum, and energy are applied to a finite volume—that is, the flow equations are written in the form of integrals which are taken over an arbitrary finite portion of the region occupied by the moving gas (see, for example, [1]). At those points of the flow region in which the functions satisfying these equations are continuous and have continuous first derivatives, they satisfy the system of differential equations (1.1) to (1.4). On the discontinuity surfaces the limiting values of these functions are related by equations (1.5). Discontinuous solutions of the equations in integral form can, in a certain sense, be considered as generalizations of the solutions of the differential equations (1.1) to (1.4). Having such solutions, it follows that they should be used in the problem of supersonic flow past a body. (The construction of the generalized solutions can be carried out in accordance with the statement of the problem given in the previous section. There are methods, primarily numerical, of finding the generalized solutions directly, however, which avoid the use of equations (1.5) across the discontinuity surfaces which are unknown beforehand; see below.) But such generalized solutions of the problem of steady supersonic flow past a body are still not unique even if we also require, in accordance with the second law of thermodynamics, that the entropy of the gas particles should not decrease when crossing discontinuity surfaces.

Let us consider, for example, the axisymmetric supersonic flow past a body of revolution in the form of a cylinder with a conical nose (a cone-cylinder) illustrated in Fig. 1.2,a. Characteristic of such a flow is the fact that the pressure is constant on the cone surface. But this flow is not unique. It is clear that one can represent many other flows around this same body to which correspond other generalized solutions. For instance, a conical region can be formed in front of the body which is filled with gas at rest at constant pressure, as in Fig. 1.2,b. That such a flow can be realized under certain conditions is shown by the schlieren photograph in Fig. 1.3.

The question of the conditions which uniquely determine the solution of the problem of steady supersonic flow past a body has not been answered up to the present time. Strictly speaking, the steady unbounded flow past a body should be considered as the limiting state which is

reached asymptotically from a given initial state by a body moving in a gas which is at rest at infinity, after the velocity of the body has become constant. (See [3, 4] for a discussion of this question.) The existence of

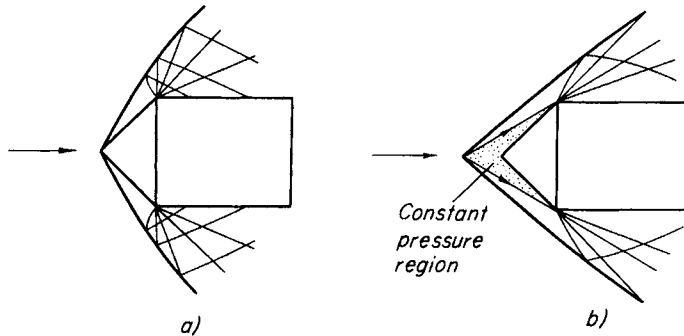


FIG. 1.2. Supersonic flow past a cone-cylinder: (a) normal flow, (b) flow with the formation of a stagnation zone in front of the body.

such steady-state limits is not obvious.* In those cases where such a steady flow limit exists, it can depend on the manner of approach to the limit state, even for the same conditions at upstream infinity.

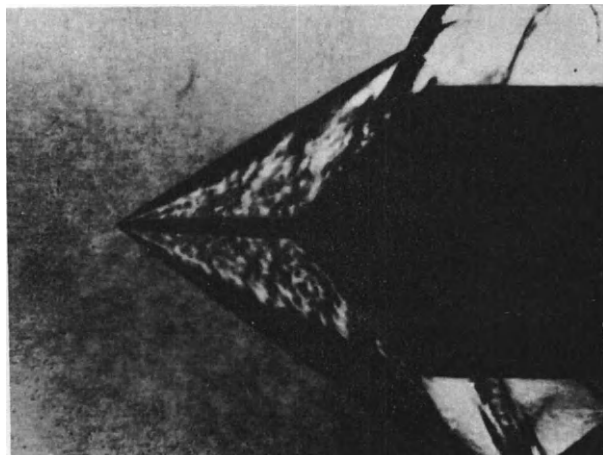


FIG. 1.3. Supersonic flow past a cone-cylinder with a spike.

* Experiments show that for flows which are steady at large distances from the body, the flow near the body can have an unsteady (sometimes a periodical) character.

A well known example which can serve to illustrate this is the flow past a body with a duct whose cross section between the entrance and the exit first decreases and then increases (Fig. 1.4). For a certain range

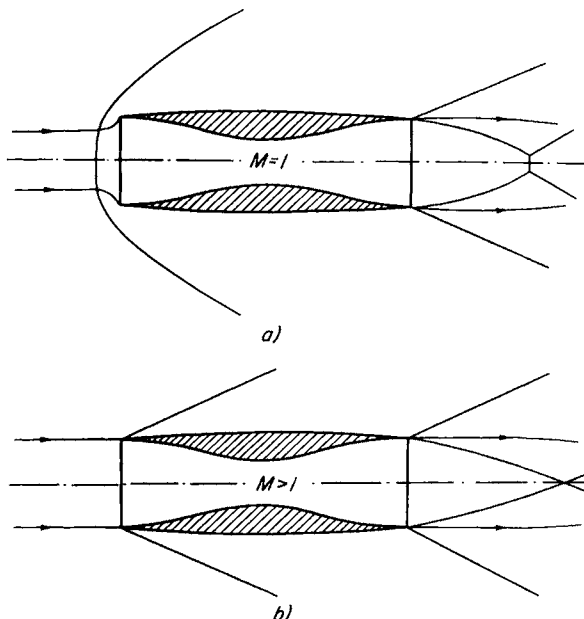


FIG. 1.4. Two possible types of supersonic flows past a ducted body, with the same velocity: (a) with a detached bow wave, (b) with an attached bow wave.

of supersonic velocities, two types of steady flow past such a body are possible. The first exhibits a detached shock wave and a region of subsonic velocity between the central part of the wave and the throat section of the duct (Fig. 1.4,a). The second exhibits an attached bow wave and supersonic flow everywhere (Fig. 1.4,b). The first type of flow is realized by approaching the steady-state regime gradually from low values of the velocity. The second type can be realized if the body is first brought rapidly up to high velocity and then the velocity is gradually decreased. This phenomenon can be characterized as a kind of hysteresis for supersonic flow past a body.

The example which was presented shows that in some cases it is necessary when selecting the solution of a steady flow problem to consider it as

the limit of an unsteady flow. It has been asserted (see, for example, [5]), that this consideration is sufficient to ensure the uniqueness of the generalized solution of the problem of steady supersonic flow past a body. The correctness of this assertion remains unproven.

From physical considerations it is apparent that the necessary condition which the solution of a flow problem satisfies is its stability with respect to small disturbances. The opinion has been expressed that this condition can ensure the uniqueness of the solution. This criterion does not appear to be sufficient, however, for those cases in which several discrete regimes of steady flow past a body are possible with the same velocity, as in the example above of the ducted body. Stability with respect to small disturbances is possible for more than one type of flow. When a continuous sequence of flows is possible around the same body, as in the example of the body with a conical stagnation region, the stability criterion can provide one or more solutions which are stable with respect to small disturbances. It is obvious that in those cases for which the generalized solution of the steady flow problem is the limit of a nonsteady flow for all possible ways of approaching the steady state, the criterion of flow stability is automatically satisfied.

Finally, the opinion has been expressed that the condition which ensures uniqueness of the generalized solution of a flow problem is the requirement that the generalized solution of the equations of motion for an ideal gas should be the limit of continuous solutions of the equations of motion for a viscous gas when the viscosity coefficient tends to zero (the "vanishing viscosity" theory). It is highly probable that this requirement does in fact guarantee the existence and uniqueness of the generalized solution of the problem with given initial conditions and with a prescribed body motion. The uniqueness of the solution of steady flow problems, in general, is apparently ensured only if one considers them as the limit of problems with given initial conditions.

One may assume that in some cases no other conditions can replace the vanishing viscosity requirement for selecting the solution which corresponds to the actual flow. The flow pattern past some bodies, and in particular the pattern which arises in flows with strong discontinuities, is essentially connected with the presence of vortex discontinuities which originate at the surface of the body. (An example is the flow past a body with a spike in front; see Fig. 1.3.) Discontinuities of this type can appear

in the solution only after one has taken the limit of the solution of the viscous equations.

The fact that a generalized solution of the equations of motion of an ideal gas has physical sense when it represents the limit of a continuous solution of the differential equations of motion of a viscous gas, is of fundamental importance not only in selecting the required solution from all possible generalized solutions. In practice this fact can also serve as the basis for developing methods of calculating ideal gas flows which are not complicated by the need to satisfy equations (1.5) on discontinuity surfaces which are unknown beforehand. Such methods possess definite advantages when carrying out computations with the aid of high speed computing machines. In a scheme of this type, dissipative terms containing a small parameter are added to the differential equations for the flow of an ideal gas. The presence of these dissipative terms allows one to obtain continuous solutions of the equations for flows past bodies of arbitrary shape. Moreover the dissipative terms which are introduced need not describe the actual viscous and heat conductive processes. It is only important that in the limit, when the small parameter tends to zero, the solution should tend to the generalized solution obtained if viscosity and heat conduction were correctly taken into account.

The differential equations modified in this manner can be solved by the method of finite differences. The strong discontinuity surfaces will appear in the form of layers of finite thickness within which large gradients of the flow quantities occur. This method of artificially introducing dissipative terms in order to solve the equations of motion of an ideal gas by finite differences was proposed by von Neumann and Richtmeyer [6]. A finite difference scheme for the solution of the differential equations of one-dimensional unsteady motion of an ideal gas, which ensures obtaining generalized solutions, has also been proposed by Lax [7] and Godunov [8].

What has been said above in relation to the system of gasdynamic equations involves assumptions which are more or less physically justified. A rigorous theory of generalized solutions* has been developed at the present time only for the "model" equation

$$\frac{\partial u}{\partial t} + \frac{\partial \varphi(t, x, u)}{\partial x} + \psi(t, x, u) = 0.$$

* Generalized solutions of equations of hyperbolic type were introduced and systematically applied by Sobolev [9].

A large number of publications [7, 10, 11, etc.] are devoted to the study of the generalized solutions of this equation. The most complete treatment of the problem, together with a bibliography of related papers, is contained in the work of Oleinik [12], which may be consulted by the interested reader.

3. Characteristic properties of hypersonic flows

The kinetic energy of the gas particles in a hypersonic flow is large compared to their thermal energy. For fixed values of the state parameters, the ratio of the kinetic to the internal energy in the free stream increases in proportion to the square of the Mach number M . This ratio is equal to $\frac{1}{2}\gamma(\gamma - 1)M^2$ for a perfect gas with constant specific heats. With $\gamma = 1.40$ and a velocity five times the velocity of sound, the kinetic energy of a gas particle is seven times greater than its internal energy, while for $M = 10$ the kinetic energy is almost 30 times greater than the thermal energy. This fact leads to the appearance of some properties in steady hypersonic flows which are different from those in flows at moderate and low velocities, where the kinetic energy of the gas particles is of the same order as, or lower than, the thermal energy. Thus when a gas particle is decelerated adiabatically in a steady hypersonic flow, the conversion of its kinetic energy into heat results in a very considerable increase in the gas temperature. It is clear, then, that in such cases relatively small changes in the particle velocity (i.e., kinetic energy) must lead to relatively large changes in the enthalpy, and as a result, to relatively large changes in the other thermodynamic quantities. Indeed, for steady adiabatic flow along a streamline the thermodynamic parameters of the gas and its velocity V are connected by the two relations:

$$V dV + \frac{dp}{\rho} = 0,$$

$$dS = 0.$$

For a perfect gas with constant specific heats, using the equation of state $p = \rho RT$ (R is the gas constant) and the expressions for the entropy $S = c_v \ln p/\rho^\gamma$ and the speed of sound $a = (\gamma p/\rho)^{1/2}$, the following relations are easily found:

$$\frac{dp}{p} = \gamma \frac{d\rho}{\rho} = -\gamma M^2 \frac{dV}{V},$$

$$\frac{dT}{T} = 2 \frac{da}{a} = -(\gamma - 1)M^2 \frac{dV}{V}, \quad (1.11)$$

$$\frac{dM}{M} = - \left(1 + \frac{2}{(\gamma - 1)M^2} \right) \frac{da}{a} = \left(1 + \frac{\gamma - 1}{2} M^2 \right) \frac{dV}{V}.$$

From these relations it follows that for $M \gg 1$, relatively small perturbations in the velocity are connected with relatively large perturbations in the density, pressure, temperature, and speed of sound. Hence, in a hypersonic flow the Mach number changes principally as a result of the change in the speed of sound. These conclusions are in contrast to those made for the case of low subsonic speeds (i.e., for $M \ll 1$), where it is necessary to consider only the changes in velocity. In the latter case, the relative changes in the thermodynamic quantities are very small, and as a result changes in the Mach number are brought about principally by changes in the velocity.

Neglecting the first term in comparison with the second in the sum $1 + \frac{1}{2}(\gamma - 1)M^2$, and integrating equations (1.11), we find the following relations which are valid for $M \gg 1$:

$$\begin{aligned} \frac{p}{p_1} &= \left(\frac{M_1}{M} \right)^{2\gamma/(\gamma-1)}, & \frac{\rho}{\rho_1} &= \left(\frac{M_1}{M} \right)^{2/(\gamma-1)}, & \frac{T}{T_1} &= \left(\frac{M_1}{M} \right)^2, \\ \frac{a}{a_1} &= \frac{M_1}{M}, & \frac{V}{V_1} &= 1 + \frac{1}{\gamma - 1} \left(\frac{1}{M_1^2} - \frac{1}{M^2} \right). \end{aligned} \quad (1.12)$$

Here the subscript 1 denotes quantities which correspond to some characteristic state of the gas.

The above considerations on the relations between the relative changes in the flow parameters for steady hypersonic flows hold only in those regions of the flow where the *local* value of the Mach number is large. Near the body there can be regions with moderate supersonic velocities, and behind a detached bow wave there is always a region where the local value of the Mach number is actually less than 1. In such flow regions the conclusions which were drawn are naturally not applicable.

In order to illustrate some other characteristic properties of hypersonic flows let us consider the two-dimensional flow past a flat plate which makes an angle of attack α with the free stream (Fig. 1.5). If the angle of attack does not exceed some maximum value, then for suffi-

ciently large values of the free stream Mach number an expansion wave will emanate from the leading edge on one side of the flat plate and a shock wave will emanate on the other side [1]. The bow wave separating the disturbed flow region from the uniform free stream flow is an attached one, and consists of a weak discontinuity in one of the half planes and a shock wave in the other. A similar pattern will also occur in the flow

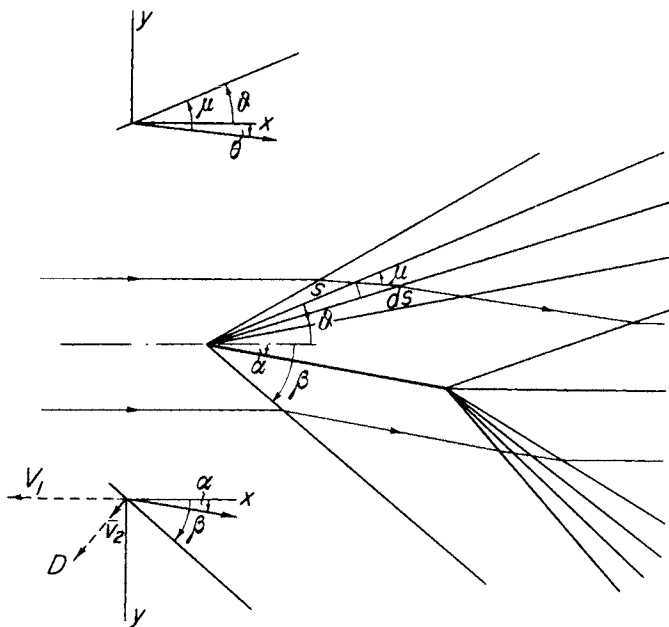


FIG. 1.5. Supersonic flow past a flat plate at angle of attack.

past the forward portion of a triangular airfoil, provided the angle of attack is sufficiently large.

Let us first consider the expansion flow. This flow represents a system of plane sound waves along which the values of the flow parameters remain constant. In a system of coordinates fixed in the plate each such sound wave remains stationary, since its propagation velocity is exactly balanced by the gas velocity (the component of the gas velocity normal to the wave is equal in magnitude and opposite in direction to the propagation velocity of the wave). The Mach angle μ between the direction of the relative velocity of the gas and the front of the wave is then expressed by the following formula:

$$\sin \mu = \frac{a}{V}.$$

If we denote by θ the angle between the direction of the velocity at a given point and the direction of the undisturbed flow, and by ϑ the angle between the front of the wave and the direction of the undisturbed flow, then it is evident that*

$$\vartheta = \mu + \theta. \quad (1.13)$$

The isentropic flow condition and the Bernoulli integral permit the pressure, density, flow velocity, local speed of sound, Mach number, and Mach angle to be expressed in terms of any one of the remaining quantities [see equations (1.11)]. In order to find the dependence of these quantities on the coordinates one can use, for example, the condition of conservation of mass. The condition of conservation of mass in an infinitesimal volume bounded by two stream surfaces and two adjacent sound waves (Fig. 1.5) can be written in the form

$$\frac{d}{d\vartheta} \rho a s = 0.$$

Since

$$\frac{ds}{sd\vartheta} = -\cot \mu,$$

we find

$$\frac{d\rho}{\rho} + \frac{da}{a} - \cot \mu d\vartheta = 0.$$

In the case of a perfect gas with constant specific heats we have according to equations (1.11)

$$\frac{d\rho}{\rho} = - \frac{M dM}{1 + \frac{\gamma - 1}{2} M^2},$$

and

$$\frac{da}{a} = - \frac{\gamma - 1}{2} \frac{M dM}{1 + \frac{\gamma - 1}{2} M^2}.$$

* The angles θ and ϑ are taken positive in a counterclockwise direction.

Substituting these quantities along with the value of $\cot \mu$ given by

$$\cot \mu = \sqrt{M^2 - 1}$$

into the continuity equation, we obtain the following differential relationship between the Mach number M and the coordinate angle ϑ in the plane of flow:

$$d\vartheta = -\frac{\gamma + 1}{2} \frac{M dM}{\sqrt{M^2 - 1} \left(1 + \frac{\gamma - 1}{2} M^2 \right)}.$$

Carrying out the quadrature and using equation (1.13) we find

$$\theta = -\sqrt{\frac{\gamma + 1}{\gamma - 1}} \tan^{-1} \left(\sqrt{\frac{\gamma - 1}{\gamma + 1}} \cot \mu \right) - \mu + \text{const.} \quad (1.14)$$

For hypersonic speeds

$$\begin{aligned} \frac{d\rho}{\rho} &= -\frac{2}{\gamma - 1} \frac{dM}{M}, \\ \frac{da}{a} &= -\frac{dM}{M}, \\ \cot \mu &= M, \end{aligned}$$

so that in this case the differential relationship between M and ϑ takes the simpler form

$$-\frac{dM}{M^2} = \frac{\gamma - 1}{\gamma + 1} d\vartheta.$$

Equation (1.13) is also simplified for hypersonic speeds and is

$$\vartheta = \theta + \frac{1}{M}.$$

After integrating the preceding differential relation and using the condition $M = M_1$ for $\theta = 0$, i.e., for $\vartheta = M_1^{-1}$ (M_1 is the free stream Mach number), we find

$$\frac{M_1}{M} = \frac{2}{\gamma + 1} + \frac{\gamma - 1}{\gamma + 1} M_1 \vartheta = 1 + \frac{\gamma - 1}{2} M_1 \theta. \quad (1.15)$$

The values of the other flow parameters are determined in this case by equations (1.12). In particular we obtain for the relation between the pressure and the angle θ which characterizes the direction of the velocity

$$\frac{p}{p_1} = \left(1 + \frac{\gamma - 1}{2} M_1 \theta \right)^{2\gamma/(\gamma-1)}$$

When the flow deflection angle is equal to $-2/(\gamma - 1)M_1$ the pressure in the expansion wave drops to zero. Thus when the angle of attack of the flat plate is greater than $2/(\gamma - 1)M_1$, the flow detaches from the leading edge, and a region of zero pressure is formed between the flow and the plate surface.

For the value of the pressure coefficient

$$C_p = \frac{p - p_1}{\frac{1}{2}\rho_1 V_1^2} = \frac{2}{\gamma M_1^2} \left(\frac{p}{p_1} - 1 \right)$$

we obtain the expression

$$C_p = \frac{2}{\gamma M_1^2} \left[\left(1 + \frac{\gamma - 1}{2} M_1 \theta \right)^{2\gamma/(\gamma-1)} - 1 \right]. \quad (1.16)$$

An important feature of this flow can be seen by transforming the relations $\vartheta = \theta + M^{-1}$ and (1.15) into the form

$$\bar{\vartheta} = \frac{1}{K} + \frac{\gamma + 1}{2} \bar{\theta}, \quad \frac{M_1}{M} = 1 + \frac{\gamma - 1}{2} K \bar{\theta},$$

where $K = M_1 \alpha$, $\bar{\vartheta} = \vartheta/\alpha$, and $\bar{\theta} = \theta/\alpha$. From these relations and from equations (1.12) it follows that if we vary the Mach number M_1 and the angle of attack α in such a way that the parameter K remains constant, then the dimensionless quantities p/p_1 , ρ/ρ_1 , and M/M_1 remain unchanged at corresponding points and the pressure coefficient C_p changes in proportion to α^2 . This result is a particular case of a general similarity law for hypersonic flows where the velocity perturbations are small. This similarity law will be considered in detail in Chapter II. The establishment of the flow similarity rests upon the fact that in the region occupied by the gas the angles θ and μ , and hence ϑ , are small, although the angle of attack need not be small. For large angles of attack, as already pointed out, a region of zero pressure is formed between the plate and the region

occupied by the gas, and the expansion flow no longer depends upon the angle of attack. Then the angle α in the expressions for K , $\bar{\vartheta}$, and $\bar{\theta}$ is understood to be the maximum flow deflection angle $2/(\gamma - 1)M_1$.

Let us turn now to a consideration of the flow behind the attached shock wave. Behind the shock the gas moves uniformly, and the flow quantities in terms of the disturbance velocity are given by equations (1.10). In order to use these equations, we take into account the two-dimensional character of the flow and put

$$D = V_1 \sin \beta, \quad u = -|\mathbf{v}_2| \sin \beta, \quad v = |\mathbf{v}_2| \cos \beta, \quad w = 0,$$

where β is the shock inclination angle with respect to the free stream direction. These relations are illustrated at the bottom of Fig. 1.5 by the dashed lines. After carrying out the above substitutions we obtain

$$\begin{aligned} \frac{u}{V_1} &= -\frac{2}{\gamma + 1} \left(\sin^2 \beta - \frac{1}{M_1^2} \right), \\ \frac{v}{V_1} &= \frac{2}{\gamma + 1} \cot \beta \left(\sin^2 \beta - \frac{1}{M_1^2} \right), \\ w &= 0, \\ \frac{p - p_1}{\rho_1 V_1^2} &= \frac{2}{\gamma + 1} \left(\sin^2 \beta - \frac{1}{M_1^2} \right), \\ \frac{\rho}{\rho_1} &= \frac{\frac{\gamma + 1}{\gamma - 1}}{1 + \frac{2}{\gamma - 1} \frac{1}{M_1^2 \sin^2 \beta}}. \end{aligned} \tag{1.17}$$

The relation between the angle of attack α and the shock angle β is easily determined from the condition

$$\frac{v}{V_1 + u} = \tan \alpha,$$

which expresses the fact that the relative velocity behind the shock is parallel to the plate surface. This gives

$$\tan \alpha = \frac{\frac{2}{\gamma + 1} \cot \beta \left(\sin^2 \beta - \frac{1}{M_1^2} \right)}{1 - \frac{2}{\gamma + 1} \left(\sin^2 \beta - \frac{1}{M_1^2} \right)}. \tag{1.18}$$

As is known, it follows from this relation that for angles α which are smaller than a certain limiting value (which depends upon M_1 and γ), two values of the shock angle β correspond to each angle α . If a flat plate of finite length is placed in an unbounded flow, then the shock wave which is obtained corresponds to the smaller of the two angles. For $M_1 \gg 1$ this smaller angle differs little from the angle α , and between the plate and the shock a thin layer of condensed gas is formed. As an example, the flow pattern around a flat plate for $M_1 = 10$ and $\gamma = 1.4$ is shown in Fig. 1.6,a.

At very high supersonic speeds and for a fixed angle of attack α , which can be as small as we like, we can neglect terms of order M_1^{-2} in comparison with $\sin^2 \beta$, since β is always greater than α . With this assumption, equations (1.17) and (1.18), which determine the values of the flow parameters behind the shock and the shock location, take the following form:

$$\begin{aligned} \frac{u}{V_1} &= -\frac{2}{\gamma + 1} \sin^2 \beta, \\ \frac{v}{V_1} &= \frac{2}{\gamma + 1} \sin \beta \cos \beta, \\ \frac{p - p_1}{\rho_1 V_1^2} &= \frac{2}{\gamma + 1} \sin^2 \beta, \\ \frac{\rho}{\rho_1} &= \frac{\gamma + 1}{\gamma - 1}, \\ \tan \alpha &= \frac{\frac{2}{\gamma + 1} \sin \beta \cos \beta}{1 - \frac{2}{\gamma + 1} \sin^2 \beta}. \end{aligned} \quad (1.19)$$

From these equations it follows that for a flow at very high supersonic speed through a concave angle, behind the shock the velocity component ratios u/V_1 and v/V_1 , the density ratio ρ/ρ_1 , the pressure coefficient $C_p = (p - p_1)/\frac{1}{2}\rho_1 V_1^2$, and the shock inclination angle β do not depend on the free stream Mach number M_1 . In addition the pressure and temperature ratios p/p_1 and T/T_1 vary in proportion to M_1^2 . This behavior is a particular example of a general property of flows behind strong bow shock waves at very high supersonic speeds, to be discussed in the next section.

An examination of the flow pattern past a flat plate at hypersonic speeds shows a close resemblance to the flow model considered by Newton (see Chapter III), in which the only gas particles affected by the body are those which undergo collision with the parts of the body facing the inci-

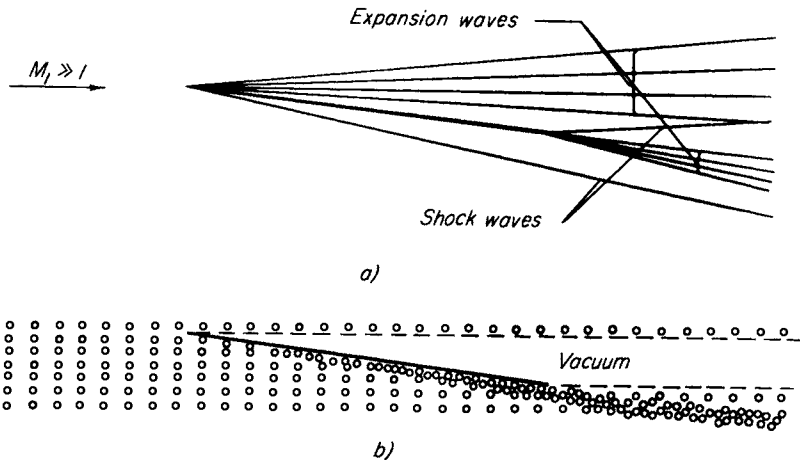


FIG. 1.6. Hypersonic flow past a flat plate at angle of attack: (a) gas flow, (b) flow of non-interacting particles (Newtonian model).

dent flow. On collision with the surface the particles lose their normal component of momentum and then slide along the surface conserving their tangential component of momentum. The particles have no effect on the portion of the body surface facing away from the flow (i.e., lying in the "aerodynamic shadow" of the body). The pressure on this part of the surface is equal to zero (Fig. 1.6,b).

Let us suppose now that the angle of attack α of the plate is small. Then for large Mach numbers M_1 the angle β will also be small. If in equations (1.17) and (1.18) we replace the sine of the angle by its argument and the cosine by unity, these equations become

$$\begin{aligned} \frac{u}{V_1 \alpha^2} &= - \frac{2}{\gamma + 1} \frac{K_s^2 - 1}{K^2}, \\ \frac{v}{V_1 \alpha} &= 1, \\ \frac{p}{p_1} &= 1 + \frac{2\gamma}{\gamma + 1} (K_s^2 - 1), \end{aligned} \quad (1.20)$$

$$\frac{\rho}{\rho_1} = \frac{\frac{\gamma+1}{\gamma-1}}{1 + \frac{2}{\gamma-1} \frac{1}{K_s^2}},$$

$$K_s = \frac{\gamma+1}{4} K + \sqrt{\left(\frac{\gamma+1}{4} K\right)^2 + 1},$$

where $K_s = M_1 \beta$ and, as before, $K = M_1 \alpha$. These relations show that for flow through a concave angle the flow remains similar for different values of M_1 if the parameter $K = M_1 \alpha$ is held constant. That is, with the parameter K held constant the quantities p/p_1 and ρ/ρ_1 remain unchanged as in the case of the expansion flow, and all angles (shock inclination angle, streamline inclination angle) vary in proportion to the angle α . The pressure coefficient varies in proportion to α^2 , and is given by

$$C_p = \frac{4}{\gamma+1} \frac{1}{M_1^2} (K_s^2 - 1) = \frac{4}{\gamma+1} \frac{K_s^2 - 1}{K^2} \alpha^2. \quad (1.21)$$

Consequently we have here found a further example of the general similarity law which was mentioned above.

Having obtained relations which permit the calculation of the flow on both sides of a flat plate at a small angle of attack in a hypersonic flow, we can apply them to the determination of the aerodynamic characteristics of the flat plate [13]. To the approximation considered, the drag coefficient C_D and the lift coefficient C_L of the plate are given by

$$C_D = \frac{p_l - p_u}{\frac{1}{2} \rho V^2} \alpha = (C_{p_l} - C_{p_u}) \alpha,$$

$$C_L = \frac{p_l - p_u}{\frac{1}{2} \rho V^2} = C_{p_l} - C_{p_u} = \frac{C_D}{\alpha}.$$

Here the subscripts l and u denote the values on the lower and upper surfaces of the plate, respectively. Replacing C_{p_l} and C_{p_u} by their values given by equations (1.16) and (1.21), we find

$$C_L = \frac{C_D}{\alpha} = \left\{ \frac{\gamma+1}{2} + \sqrt{\left(\frac{\gamma+1}{2}\right)^2 + \frac{4}{K^2}} \right. \\ \left. + \frac{2}{\gamma K^2} \left[1 - \left(1 - \frac{\gamma-1}{2} K\right)^{2\gamma/(\gamma-1)} \right] \right\} \alpha^2. \quad (1.22)$$

If $\frac{1}{2}(\gamma - 1)K \geq 1$, the quantity in square brackets is taken equal to unity. The pressure on the upper surface of the plate is then equal to zero.

The dependence of C_L on the angle of attack of the plate is shown by the solid lines in Fig. 1.7 for several values of the Mach number and with

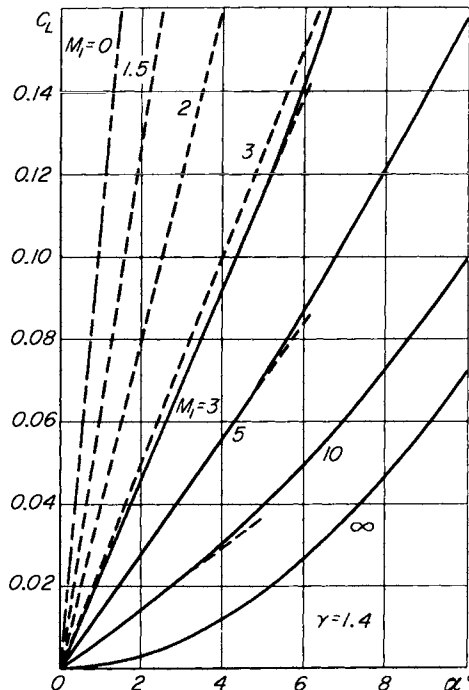


FIG. 1.7. Lift coefficient for a flat plate: —— equation (1.22);
- - - linear theory; - - - incompressible flow.

$\gamma = 1.4$. These curves have been calculated from equation (1.22). For finite values of the Mach number the dependence of C_L on α is nearly linear for small values of α . With increasing α this dependence becomes quadratic, while with increasing Mach number the linear portion of the dependence of C_L on α decreases, and for $M = \infty$ it vanishes altogether. For $M = \infty$ equation (1.22) takes the form

$$C_L = (\gamma + 1)\alpha^2.$$

The dashed lines in Fig. 1.7 are the values of C_L for a flat plate as obtained from the linear theory [1]. This result is given by

$$C_L = \frac{4\alpha}{\sqrt{M^2 - 1}}.$$

The dashed-dotted line in this same figure is the value of C_L for a flat plate in an incompressible flow (i.e., for $M = 0$):

$$C_L = 2\pi\alpha.$$

Figure 1.7 shows that for large values of the Mach number and for large angles of attack the linear theory underestimates the value of the lift coefficient and can no longer be applied. It must be emphasized that the flat plate lift coefficient decreases sharply with increasing Mach number, and is very low for hypersonic speeds.

We would like to point out still one other very interesting feature of hypersonic flows past a flat plate at small angles of attack α . For this case the first two expressions of (1.20) show that in the disturbed flow region behind the shock wave under the plate, the component of the disturbance velocity in the direction of motion of the plate is small, of higher order than the transverse component of the velocity. This also holds true for the expansion flow above the plate. This can be seen by substituting the value of V given by equation (1.12) in the relations

$$V_1 + u = V \cos \theta, \quad v = V \sin \theta,$$

using (1.15) for the relation between M and θ in the expansion flow, and taking $\sin \theta = \theta$ and $\cos \theta = 1 - \frac{1}{2}\theta^2$. After some simple calculations we obtain

$$\frac{u}{V_1 \alpha^2} = -\frac{\bar{\theta}}{K} - \frac{\gamma + 1}{4} \bar{\theta}^2, \quad \frac{v}{V_1 \alpha} = \bar{\theta} \quad (|\bar{\theta}| \leq 1).$$

Thus a slender body (in our case a flat plate at small angles of attack) flying in air which is at rest "pushes away" the air in a direction normal to the flight direction, without producing a displacement in the flight direction. This property is a particular example of the so-called equivalence principle to be considered in Chapter II. It follows that in the whole of the disturbed region the value of the component of relative velocity in the direction of flight can be considered constant to terms of second order in the small quantity α , and equal to the free stream velocity.

In conclusion, let us determine the value of the Mach number behind

the shock wave for later use (see Chapter IV, Section 2). Using equations (1.20) we obtain

$$M^2 = M_1^2 \frac{V^2}{V_1^2} \frac{p}{p_1} \frac{\rho}{\rho_1} = \frac{M_1^2}{\left(\frac{2\gamma}{\gamma+1} K_s^2 - \frac{\gamma-1}{\gamma+1} \right) \left(\frac{\gamma-1}{\gamma+1} + \frac{2}{\gamma+1} \frac{1}{K_s^2} \right)}. \quad (1.23)$$

The quantity K_s varies from 1 to ∞ with increasing shock strength. Thus for moderate shock strengths the Mach number behind the shock is of the same order as the free stream Mach number. For very strong shocks ($K_s \rightarrow \infty$), however, we find that

$$M \rightarrow \frac{1}{\alpha} \sqrt{\frac{2}{\gamma(\gamma-1)}}.$$

Thus, for small values of α the Mach number behind the shock is in this case also large.

4. Similarity law for limiting hypersonic flows past bodies of given shape

In the present section it will be shown that when $M \rightarrow \infty$, the flow in the neighborhood of a body of given shape tends to a certain limit state. We shall call the flow in this limit state a "limiting hypersonic flow."** Just as the ensemble of flows around a given body is bounded

* *Editor's note:* In conformity with Russian usage, Chernyi uses the term "high supersonic" throughout the book in place of "hypersonic" common outside Russia and used in the present translation. To define a hypersonic flow involving the limiting process $M \rightarrow \infty$, he introduces the expression "very high supersonic." To date, no term has been generally accepted to describe the flow state resulting from an application of the basic hypersonic limiting process $M \rightarrow \infty$. In the book by Hayes and Probstein ("Hypersonic Flow Theory," Academic Press, New York, 1959), reference was simply made to "the flow resulting from the limiting process," although in that book a "limiting perfect gas model" was defined for a Newtonian flow involving both the limit $M_1 \rightarrow \infty$ and $\gamma \rightarrow 1$. To keep as close as possible to the author's intent and still be consistent with usage outside Russia we replace the expression "very high supersonic" by "limiting hypersonic." Chernyi in his own footnote at this point in the text notes that Oswatitsch [14] defined hypersonic flow as the limit state of the flow for $M_1 \rightarrow \infty$. He also remarks that in the literature outside Russia the flow is called hypersonic when one deals with slender bodies with sharp leading edges moving "at high supersonic velocity," for which it becomes necessary to take nonlinear effects into account. The reader is then referred to Chapter II.

at the low Mach number end by the incompressible flow limit, so the limit flow for hypersonic speeds bounds the ensemble at the high Mach number end. The practical value of the study of limiting hypersonic flows goes beyond the determination of the aerodynamic characteristics of bodies at very large flight speeds which can be attained only rarely. Value also lies in the fact that from the study of such flows one can establish the asymptotic behavior of the flow when the velocity becomes indefinitely large. In some cases this makes it easier to predict flow properties at moderate supersonic speeds.

In practice the limit state is reached for some bodies at comparatively moderate values of the free stream Mach number M_1 . The exact solutions for supersonic flow past not too slender wedges and cones, as well as experimental results on the flows past these and other bodies, show that

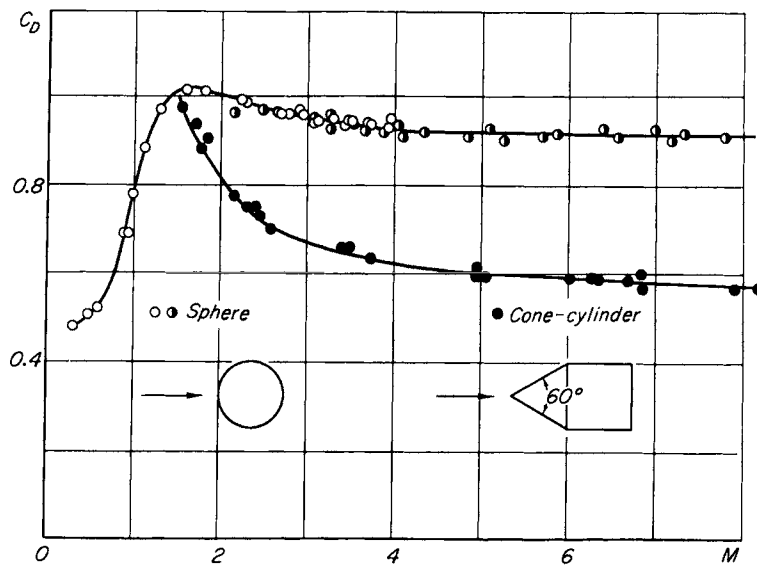


FIG. 1.8. Drag coefficients for a sphere and a cone-cylinder:
 ○-[15], ▲-[16], ●-[17].

the drag coefficients remain practically unchanged for free stream Mach numbers greater than 3 or 4. In addition, the flow pattern in the neighborhood of the body remains unchanged. As an example, experimental values of the drag coefficients for a sphere and a cone-cylinder obtained from ballistic tests are shown in Fig. 1.8 [15-17].

The proof of the existence of a limiting state of flow near a body for $M \rightarrow \infty$ was given by S. V. Vallander in 1949 and independently somewhat later in [14]. Basing our analysis on the first of these works, we shall rewrite all the relations of Section 1 of the present chapter in dimensionless form by setting

$$\begin{aligned} x &= Lx', & y &= Ly', & z &= Lz', \\ u &= V_1u', & v &= V_1v', & w &= V_1w', \\ p &= \rho_1V_1^2p', & \rho &= \rho_1\rho', & a &= V_1a', & D &= V_1D', \\ \frac{S}{c_v} &= S' + \ln \gamma M_1^2, \end{aligned}$$

where L is the characteristic dimension of the body, and where the primes denote dimensionless quantities. After transforming to the new variables, equations (1.1) to (1.4) take the form

$$\begin{aligned} (1+u') \frac{\partial u'}{\partial x'} + v' \frac{\partial u'}{\partial y'} + w' \frac{\partial u'}{\partial z'} &= -\frac{1}{\rho'} \frac{\partial p'}{\partial x'}, \\ (1+u') \frac{\partial v'}{\partial x'} + v' \frac{\partial v'}{\partial y'} + w' \frac{\partial v'}{\partial z'} &= -\frac{1}{\rho'} \frac{\partial p'}{\partial y'}, \\ (1+u') \frac{\partial w'}{\partial x'} + v' \frac{\partial w'}{\partial y'} + w' \frac{\partial w'}{\partial z'} &= -\frac{1}{\rho'} \frac{\partial p'}{\partial z'}, \\ \frac{\partial \rho'(1+u')}{\partial x'} + \frac{\partial \rho'v'}{\partial y'} + \frac{\partial \rho'w'}{\partial z'} &= 0, \\ (1+u') \frac{\partial S'}{\partial x'} + v' \frac{\partial S'}{\partial y'} + w' \frac{\partial S'}{\partial z'} &= 0, \\ \frac{p'}{\rho'^\gamma} &= e^{S'}. \end{aligned} \tag{1.24}$$

For a perfect gas with constant specific heats, the boundary conditions at the discontinuity surfaces (1.5) and at the surface of the body (1.7) become in terms of the new variables

$$\begin{aligned} \rho'_1(D' - v'_{1n}) &= \rho'_2(D' - v'_{2n}), \\ \rho'_1(D' - v'_{1n})\mathbf{v}'_1 - p'_1\mathbf{n} &= \rho'_2(D' - v'_{2n})\mathbf{v}'_2 - p'_2\mathbf{n}, \\ \rho'_1(D' - v'_{1n}) \left(\frac{\mathbf{v}'_1^2}{2} + \frac{1}{\gamma - 1} \frac{p'_1}{\rho'_1} \right) - p'_1 v'_{1n} &= \rho'_2(D' - v'_{2n}) \left(\frac{\mathbf{v}'_2^2}{2} + \frac{1}{\gamma - 1} \frac{p'_2}{\rho'_2} \right) - p'_2 v'_{2n} \end{aligned} \tag{1.25}$$

and

$$v'_{1n} = -\cos(n_b, x'), \quad (1.26)$$

respectively.

The relations (1.10) across the bow shock wave, which serve as the boundary conditions for the system of equations (1.24), take the form

$$\begin{aligned} |\mathbf{v}'_2| &= \frac{2}{\gamma + 1} D' \left(1 - \frac{1}{M_1^2 D'^2} \right), \\ p'_2 &= \frac{2}{\gamma + 1} D'^2 \left(1 - \frac{\gamma - 1}{2\gamma} \frac{1}{M_1^2 D'^2} \right), \\ \rho'_2 &= \frac{\frac{\gamma + 1}{\gamma - 1}}{1 + \frac{2}{\gamma - 1} \frac{1}{M_1^2 D'^2}}. \end{aligned} \quad (1.27)$$

In our new variables, the problem of supersonic flow past a body reduces to the problem of integrating the system of equations (1.24) subject to the conditions (1.26), (1.27), and (1.25) given respectively on the surface of the body, at the bow shock wave, and on the strong discontinuity surfaces located inside the disturbed region. For a given body shape the problem as formulated contains two dimensionless parameters, γ and M_1 . In general both these parameters are important.

For what follows, it is necessary to point out that, due to the nature of a supersonic flow, the shape of the shock wave at some distance from the body has no effect on the flow near the nose of the body. The flow near the body (Fig. 1.9) is affected only by a limited part of the shock

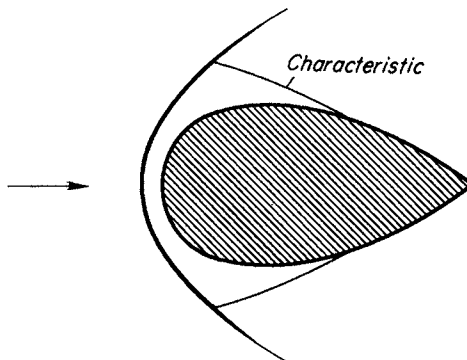


FIG. 1.9. Effect of the bow wave on the flow near a body.

wave which is also the stronger part. On this part of the bow wave the angle between the surface of the wave and the direction of the free stream flow does not become zero for any value of the free stream Mach number. Thus even at $M_1 = \infty$ the shock wave degenerates into a weak discontinuity surface—that is, a sound wave—only at infinity. Hence for $M_1 = \infty$ a flow state will always be reached in which $M_1^2 D'^2 = M_1^2 \cos^2(n_s, x') \gg 1$ on part of the bow shock wave. We shall now make more precise the definition given at the beginning of the present section: we term such a limit state a hypersonic flow.

If we neglect quantities of order $(M_1 D')^{-2}$ in comparison with unity for such flows, equations (1.27) at the bow shock wave become

$$\begin{aligned} |\mathbf{v}'_2| &= \frac{2}{\gamma + 1} D', \\ p'_2 &= \frac{2}{\gamma + 1} D'^2, \\ \rho'_2 &= \frac{\gamma + 1}{\gamma - 1}. \end{aligned} \quad (1.28)$$

In Fig. 1.10 the ratios of the exact to the approximate value of $|\mathbf{v}'_2|$ (the function f_1), p'_2 (the function f_2), and ρ'_2 (the function f_3) are given in terms of the pressure ratio across the shock (for $\gamma = 1.4$).

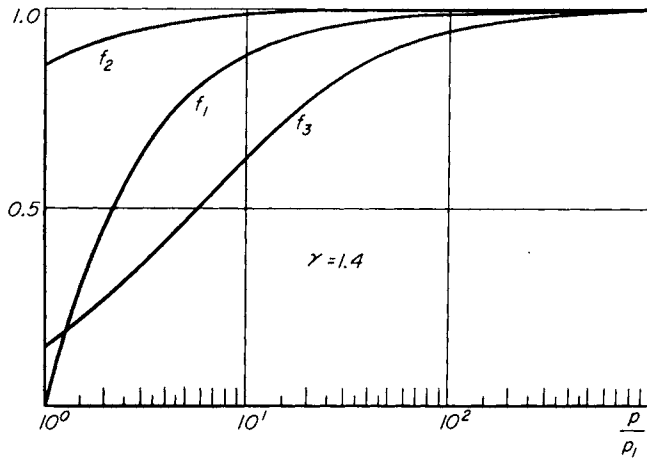


FIG. 1.10. Ratios of exact to approximate values of the flow parameters behind the shock as a function of the pressure ratio across the shock.

If the simplified conditions (1.28) are used instead of the boundary conditions (1.27), the system of equations which determines the flow about a body does not contain the free stream Mach number M_1 . Consequently the distribution of the quantities

$$\frac{u}{V_1}, \frac{v}{V_1}, \frac{w}{V_1}, \frac{p}{\rho_1 V_1^2}, \frac{\rho}{\rho_1}, S - c_v \ln \gamma M_1^2$$

does not depend on the free stream Mach number M_1 for a limiting hypersonic flow past a body of given shape. In addition the shape of the shock waves, vortex surfaces, stream surfaces, and Mach surfaces (in the regions where the velocity is greater than the velocity of sound), which are formed in the flow, also remain unchanged when the free stream Mach number is varied.

The above results can be stated in the form of the following similarity law: *Limiting hypersonic flows about geometrically similar bodies with the same value of γ but different values of p_1 , ρ_1 , and V_1 are similar to each other.* In other words, the ratios of the velocity components u , v , w to the free stream velocity V_1 , and the ratio of the density to the free stream density have the same values at corresponding points in such flows. Furthermore, at corresponding points, the ratios of pressure and temperature to the free stream values vary in proportion to M_1^2 , and the difference between the entropy rise is equal to the difference of $c_v \ln \gamma M_1^2$.

We remind the reader once again that these conclusions are not valid in the whole of the region occupied by the gas, but only in those parts which are affected by the stronger portion of the shock wave. At large distances from the nose of the body (and also near it when part of the bow wave is a weak discontinuity surface) the flow will still depend on the free stream Mach number M_1 for all values of M_1 , no matter how large.

We note, however, that for limiting hypersonic speeds the pressure on the forward part of the body is many times greater than the pressure in the undisturbed flow, while the pressure on the rearward part is of the same order of magnitude as, or lower than, the free stream pressure. Thus one can use the previously formulated similarity law to determine resultant aerodynamic forces and moments for limiting hypersonic speeds without introducing significant errors.

Since, according to the similarity law, the local values of the surface

pressure coefficient do not change when the Mach number is altered, the resultant aerodynamic force and moment coefficients do not depend on the Mach number for limiting hypersonic speeds. (This is similar to the situation for flows at low subsonic speeds, when the compressibility of the gas can be neglected.) The drag coefficient data for a sphere and a cone-cylinder shown in Fig. 1.8 illustrates this conclusion.

CHAPTER II

HYPersonic FLOWS PAST SLENDER BODIES WITH SHARP LEADING EDGES

1. Estimate of the disturbance produced by the supersonic motion of bodies in a gas

For the steady supersonic motion of a body in an ideal gas the Euler-d'Alembert paradox is in general not applicable and the body experiences a drag. The drag results from the irreversible entropy increase across the shock waves which are formed in the flow about the body. The larger the disturbance produced by the body, the stronger are the shock waves and the greater is the drag. Thus the drag experienced by a body at supersonic speeds depends essentially on its shape. Figure 2.1 serves

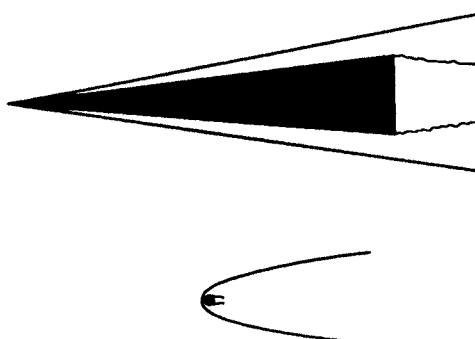


FIG. 2.1. Two bodies having the same drag at hypersonic speed.

graphically to illustrate this dependence; it shows two bodies, a cone and a sphere, having the same drag at hypersonic speed. A body of aerodynamically perfect shape (i.e., a shape with relatively low pressure drag at supersonic speeds) has the property that the normal to its surface makes a small angle to the plane normal to the direction of motion—i.e., it is slender, with sharp leading and trailing edges. (For the exceptions to this rule, see Chapter V.) We note that for supersonic flows past such bodies, the flow in any plane normal to the direction of motion depends

only on the shape of the part of the body located upstream of this plane. Therefore many results of the theory of flows past slender, sharp-edged bodies are directly applicable to bodies having, for example, a rear part which terminates in a flat base, as in the case of projectiles. The study of flows past such slender, sharp-edged bodies is of great practical significance because of their relatively low drag.

In flows past bodies which have aerodynamically perfect shapes, the velocity perturbations are small compared with the free stream velocity. At moderate supersonic speeds, where the free stream velocity is not more than a few times the speed of sound, the small velocity perturbations in a continuous adiabatic flow are connected with small perturbations of the pressure, density, speed of sound, and hence Mach number (see Chapter I, Section 3). The equations for the perturbed motion can then be linearized. Effective methods have been developed for solving these linearized equations which enable one to determine the aerodynamic characteristics of various bodies by numerical means [1-3].

If the free stream velocity is many times greater than the velocity of sound, then for small velocity perturbations in a continuous adiabatic flow the changes in the pressure, density, speed of sound, and hence Mach number will no longer be small. It will be shown below that this conclusion is also valid for flows with shock waves. If the perturbations of the flow parameters are not small, it is necessary to use nonlinear equations in order to study such flows. When hypersonic flows past slender bodies are spoken of in what follows, it will be implied that the range of free stream Mach numbers and body thickness ratios is such that the nonlinear effects are important.

The theory of gas flows with small velocity perturbations leads to the establishment of similarity laws which relate flows past affinely related bodies at different speeds. The similarity law for hypersonic velocities was first established for two-dimensional and axisymmetric flows by Tsien [4]. This law was deduced for two-dimensional flows by a different method in [5]. The authors of [4] and [5] assumed the flow to be a potential one, which narrowed the region of applicability of the similarity law as far as hypersonic speeds are concerned, since in many cases the irrotationality of the flow is an essential feature. In a brief note [6], Hayes removed the restrictions of irrotationality and two-dimensionality, and gave a simple physical interpretation of the hypersonic similarity law

(see Section 4 of this chapter). A detailed derivation of the equations for hypersonic flows past slender bodies and of the hypersonic similarity law, along with an error analysis and numerical examples, was given in [7], as well as in [8–11] and elsewhere.

Let us consider the steady flow past a slender, sharp-nosed body moving with a velocity V in an ideal gas. We locate the origin O of a moving system of coordinates at the nose of the body. The axis Ox is taken in the direction of the free stream flow, and the axes Oy and Oz orthogonal to each other in a plane normal to this direction (Fig. 2.2).

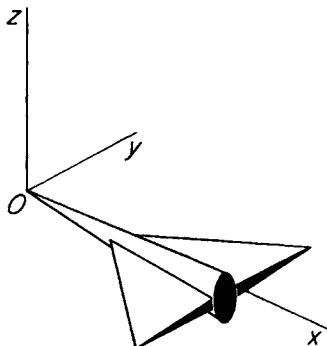


FIG. 2.2. Coordinate system.

According to the assumption made previously about the shape of the body, the angle between the normal to the surface \mathbf{n} and the direction of the free stream at points on the forward portion of the body is close to 90 deg, so that

$$\cos(n, x) \sim \tau.$$

Here τ is a small parameter—the thickness ratio of the body, or the maximum value of the angle between the surface of the forward portion of the body and the free stream direction, or the maximum value of $\cos(n, x)$, for example.

The dimensions of the body along the axes Oy and Oz will for the present be considered to be of the same order of magnitude (as, for example, in the case of a projectile or fuselage). That is, we assume that

$$\cos(n, y) \sim 1, \quad \cos(n, z) \sim 1.$$

If the components of the disturbance velocity are denoted by u, v, w , as before, then the boundary condition on the surface of the body (1.7) can be rewritten in the form

$$v \cos (n, y) + w \cos (n, z) = -(V + u) \cos (n, x).$$

From this relation we obtain the following estimates near the body for the orders of magnitude of the velocity components transverse to the flow direction:

$$v \sim w \sim \tau(V + u).$$

We shall make the natural assumption that in the whole flow region between the bow wave and the surface of the body, the velocity components v and w have the same order of magnitude as, or are smaller than, determined above.

To estimate the values of the velocity component u and the pressure and density of the gas in this region we use equations (1.10) across the bow wave. Solving the first of these relations with respect to the wave propagation velocity $D = -V \cos (n_s, x)$, we obtain

$$D = \frac{\gamma + 1}{4} |\mathbf{v}_2| + \sqrt{\left(\frac{\gamma + 1}{4}\right)^2 \mathbf{v}_2^2 + a_1^2}.$$

From this it follows that

$$D = -V \cos (n_s, x) \sim |\mathbf{v}_2| + a_1.$$

Since at the bow wave

$$u = |\mathbf{v}_2| \cos (n_s, x), \quad v = |\mathbf{v}_2| \cos (n_s, y), \quad w = |\mathbf{v}_2| \cos (n_s, z),$$

and

$$\cos (n_s, y) \sim 1, \quad \cos (n_s, z) \sim 1,$$

it is apparent that

$$|\mathbf{v}_2| \sim v \sim w.$$

Therefore,

$$\cos (n_s, x) \sim \frac{|\mathbf{v}_2| + a_1}{V} \sim \tau + \frac{1}{M}$$

and

$$u \sim V \left(\tau^2 + \frac{\tau}{M} \right).$$

From the last two of equations (1.10) we obtain the following estimates for the changes in pressure and density across the bow shock wave:

$$\Delta p = \rho_1 D |\mathbf{v}_2| \sim \rho_1 V^2 \tau^2 \left(1 + \frac{1}{M\tau} \right),$$

$$\Delta \rho = \rho_1 \frac{D^2 - a_1^2}{a_1^2 + \frac{1}{2}(\gamma - 1)D^2} \sim \rho_1 \frac{V\tau(V\tau + a_1)}{(V\tau + a_1)^2} \sim \rho_1 \frac{M\tau}{1 + M\tau}.$$

These estimates show that for flows past slender bodies ($\tau \ll 1$) at moderate supersonic speeds ($M = V/a_1$ of the order of unity), the perturbations of all gasdynamic parameters are small, and have the orders of magnitude given by

$$u \sim a_1 \tau, \quad v \sim w \sim V\tau, \quad \frac{\Delta p}{p_1} \sim M\tau, \quad \frac{\Delta \rho}{\rho_1} \sim M\tau.$$

Here the angle made by the forward portion of the body with the free stream direction is small compared to the angle between the bow wave and the free stream direction—that is,

$$\cos(n, x) \sim \tau \ll \frac{1}{M} \sim \cos(n_s, x).$$

Furthermore, the direction of the bow wave does not differ much from the direction of the characteristic surfaces (Mach waves) which are given by $\cos(n, x) = M^{-1}$. In accordance with these estimates, one can use the linearized method for calculating flows past slender bodies at moderate supersonic speeds ($M\tau \ll 1$).

In hypersonic flows past slender bodies (i.e., for $\tau \ll 1$, and $M\tau \sim 1$ or $M\tau \gg 1$) the velocity perturbations remain small, as before. In this case, however, the axial component of the disturbance velocity is a small quantity of higher order than the transverse components—that is,

$$u \sim V\tau^2, \quad v \sim w \sim V\tau.$$

On the other hand the pressure and density perturbations are no longer small, and the correct estimates for these quantities are

$$\frac{\Delta p}{p_1} \sim M^2 \tau^2, \quad \frac{\Delta \rho}{\rho_1} \sim 1.$$

It follows that the pressure increase behind a shock wave for flows past slender bodies can not only be of the same order as the free stream pressure, but for limiting hypersonic speeds can exceed this pressure many times. We note that the pressure coefficient

$$C_p = \frac{\Delta p}{\frac{1}{2} \rho_1 V^2} \sim \tau^2$$

is also small in this case.

The shock wave inclination angle with the free stream direction for $M_\tau \sim 1$ or $M_\tau \gg 1$ is of the same order as the inclination angle of the forward portion of the body with the free stream direction—i.e.,

$$\cos(n_s, x) \sim \tau.$$

Thus, for hypersonic speeds the disturbed region between the surface of the slender body and the bow shock wave is a thin layer of condensed gas. The angle between the forward portion of the body surface and the free stream direction has the same order of magnitude as the Mach angle for $M_\tau \sim 1$, while for $M_\tau \gg 1$ the former is considerably in excess of the latter. From these considerations it is clear that the method of linearizing the equations of motion for flows past slender bodies becomes invalid if $M_\tau \sim 1$ or $M_\tau \gg 1$.

2. Similarity law for hypersonic flows past slender bodies

Let a hypersonic flow be directed along the axis Ox past a slender body belonging to a family of affinely related bodies which are derived from each other by changing the lengths along the axes Oy and Oz in the same ratio. Let us take the length of the body in the direction of the free stream flow to be unity, and as before let τ be a small dimensionless quantity characterizing the maximum flow deflection angle. The equation defining the body surface can then be represented in the form

$$F\left(x, \frac{y}{\tau}, \frac{z}{\tau}\right) = 0.$$

The corresponding equations for the vortex surfaces and shock waves which arise in the flow, and which are determined by the solution of the problem, are

$$F_v(x, y, z, \tau, M) = 0,$$

$$F_s(x, y, z, \tau, M) = 0.$$

Here the functions F_s and F_s' depend on the shape of the body, i.e., the parameter τ , and on the free stream Mach number M as well as on the coordinates x, y, z .*

In accordance with the estimates for a hypersonic flow made in Section 1 of this chapter, we shall transform the system of equations (1.1) to (1.4) to new dimensionless variables by setting

$$\begin{aligned} u &= V\tau^2 u', \quad v = V\tau v', \quad w = V\tau w', \\ p &= \rho_1 V^2 \tau^2 p' = \gamma M^2 \tau^2 \rho_1 p', \quad \rho = \rho_1 \rho', \\ x &= x', \quad y = \tau y', \quad z = \tau z'. \end{aligned} \quad (2.1)$$

Upon substituting and neglecting terms of order τ^2 in comparison with unity, equations (1.1) to (1.4) reduce to the following:

$$\begin{aligned} \frac{\partial u'}{\partial x'} + v' \frac{\partial u'}{\partial y'} + w' \frac{\partial u'}{\partial z'} + \frac{1}{\rho'} \frac{\partial p'}{\partial x'} &= 0, \\ \frac{\partial v'}{\partial x'} + v' \frac{\partial v'}{\partial y'} + w' \frac{\partial v'}{\partial z'} + \frac{1}{\rho'} \frac{\partial p'}{\partial y'} &= 0, \\ \frac{\partial w'}{\partial x'} + v' \frac{\partial w'}{\partial y'} + w' \frac{\partial w'}{\partial z'} + \frac{1}{\rho'} \frac{\partial p'}{\partial z'} &= 0, \\ \frac{\partial \rho'}{\partial x'} + \frac{\partial \rho' v'}{\partial y'} + \frac{\partial \rho' w'}{\partial z'} &= 0, \\ \frac{\partial}{\partial x'} \frac{p'}{\rho'^\gamma} + v' \frac{\partial}{\partial y'} \frac{p'}{\rho'^\gamma} + w' \frac{\partial}{\partial z'} \frac{p'}{\rho'^\gamma} &= 0. \end{aligned} \quad (2.2)$$

We now transform the supplementary relations (1.5) to (1.8) which apply on discontinuity surfaces, on the body, and in the free stream, and neglect terms of order τ^2 in comparison with unity. The shock relations (1.5) become

$$\rho'_1 \left(\frac{\partial F_s}{\partial x'} + v'_1 \frac{\partial F_s}{\partial y'} + w'_1 \frac{\partial F_s}{\partial z'} \right) = \rho'_2 \left(\frac{\partial F_s}{\partial x'} + v'_2 \frac{\partial F_s}{\partial y'} + w'_2 \frac{\partial F_s}{\partial z'} \right),$$

* *Editor's note:* Here, as elsewhere in the discussion, the functional dependence on the equation of state, which for the perfect gas being considered is characterized by γ , is understood.

$$\begin{aligned}
& \rho'_1 \left(\frac{\partial F_s}{\partial x'} + v'_1 \frac{\partial F_s}{\partial y'} + w'_1 \frac{\partial F_s}{\partial z'} \right) u'_1 + p'_1 \frac{\partial F_s}{\partial x'} \\
& \quad = \rho'_2 \left(\frac{\partial F_s}{\partial x'} + v'_2 \frac{\partial F_s}{\partial y'} + w'_2 \frac{\partial F_s}{\partial z'} \right) u'_2 + p'_2 \frac{\partial F_s}{\partial x'}, \\
& \rho'_1 \left(\frac{\partial F_s}{\partial x'} + v'_1 \frac{\partial F_s}{\partial y'} + w'_1 \frac{\partial F_s}{\partial z'} \right) v'_1 + p'_1 \frac{\partial F_s}{\partial y'} \\
& \quad = \rho'_2 \left(\frac{\partial F_s}{\partial x'} + v'_2 \frac{\partial F_s}{\partial y'} + w'_2 \frac{\partial F_s}{\partial z'} \right) v'_2 + p'_2 \frac{\partial F_s}{\partial y'}, \\
& \rho'_1 \left(\frac{\partial F_s}{\partial x'} + v'_1 \frac{\partial F_s}{\partial y'} + w'_1 \frac{\partial F_s}{\partial z'} \right) w'_1 + p'_1 \frac{\partial F_s}{\partial z'} \\
& \quad = \rho'_2 \left(\frac{\partial F_s}{\partial x'} + v'_2 \frac{\partial F_s}{\partial y'} + w'_2 \frac{\partial F_s}{\partial z'} \right) w'_2 + p'_2 \frac{\partial F_s}{\partial z'}, \\
& \rho'_1 \left(\frac{\partial F_s}{\partial x'} + v'_1 \frac{\partial F_s}{\partial y'} + w'_1 \frac{\partial F_s}{\partial z'} \right) \left(\frac{v'^2_1 + w'^2_1}{2} + \frac{1}{\gamma - 1} \frac{p'_1}{\rho'_1} \right) \\
& \quad + p'_1 \left(v'_1 \frac{\partial F_s}{\partial y'} + w'_1 \frac{\partial F_s}{\partial z'} \right) \\
& = \rho'_2 \left(\frac{\partial F_s}{\partial x'} + v'_2 \frac{\partial F_s}{\partial y'} + w'_2 \frac{\partial F_s}{\partial z'} \right) \left(\frac{v'^2_2 + w'^2_2}{2} + \frac{1}{\gamma - 1} \frac{p'_2}{\rho'_2} \right) \\
& \quad + p'_2 \left(v'_2 \frac{\partial F_s}{\partial y'} + w'_2 \frac{\partial F_s}{\partial z'} \right)
\end{aligned} \tag{2.3}$$

The conditions (1.6) on the vortex surfaces yield

$$\begin{aligned}
& \frac{\partial F_v}{\partial x'} + v'_1 \frac{\partial F_v}{\partial y'} + w'_1 \frac{\partial F_v}{\partial z'} = 0, \\
& \frac{\partial F_v}{\partial x'} + v'_2 \frac{\partial F_v}{\partial y'} + w'_2 \frac{\partial F_v}{\partial z'} = 0, \quad p'_1 = p'_2.
\end{aligned} \tag{2.4}$$

The body condition (1.7) takes the form

$$\frac{\partial F}{\partial x'} + v' \frac{\partial F}{\partial y'} + w' \frac{\partial F}{\partial z'} = 0 \quad \text{for} \quad F(x', y', z') = 0. \tag{2.5}$$

Finally conditions (1.8) for the free stream (that is, for $x' \rightarrow -\infty$) give

$$u' = v' = w' = 0, \quad p' = \frac{1}{\gamma M^2 r^2}, \quad \rho' = 1. \tag{2.6}$$

The system of equations (2.2) to (2.6) describing hypersonic flows past affinely related bodies which differ from each other only in the value of the parameter τ , contains the two parameters τ and M only in the form of the product $M\tau$. This means that flows past affinely related bodies corresponding to different values of the parameter τ are similar for different values of the Mach number if the parameter $M\tau$ remains constant. In other words, if $M\tau$ is constant, the dimensionless quantities u' , v' , w' , p' , and ρ' are unchanged at corresponding points in the flow. The discontinuity surfaces, stream surfaces, and Mach surfaces are affinely related also, since according to relations (2.2) to (2.6) the equations of these surfaces must have the form

$$F_i \left(x, \frac{y}{\tau}, \frac{z}{\tau}, M\tau \right) = 0.$$

When the quantity τ is held constant and the velocity is increased to an indefinitely large value, the flow pattern tends to the limit state. In this limit state the pressure coefficient and the density no longer depend on the Mach number. The quantity $M\tau$ is called the hypersonic similarity parameter for flows past slender bodies, and it will be denoted by the symbol K .

Using the similarity law which has been developed, let us compute the resultant forces on a body. The drag force acting on the body in the direction of the free stream flow is

$$D = \int p dy dz = \rho_1 V^2 \tau^4 \int p' dy' dz' = \rho_1 V^2 \tau^4 \bar{D}(K).$$

(Here base pressure forces are not taken into account, since in the flow region at the base of the body we cannot apply the similarity law.) This expression shows that the hypersonic drag of the body depends very strongly on the maximum flow deflection angle, being proportional to the fourth power of this angle. The lift force acting on the body in the direction normal to the free stream velocity is

$$L = \int p dx dy = \rho_1 V^2 \tau^3 \int p' dx' dy' = \rho_1 V^2 \tau^3 \bar{L}(K).$$

Thus the drag coefficient C_D and the lift coefficient C_L based on an appropriate cross-sectional area of the body can be written in the form

$$C_D = \tau^2 F(K) = \frac{F_1(K)}{M^2}, \quad C_L = \tau \tilde{F}(K) = \frac{\tilde{F}_1(K)}{M}.$$

If $K \rightarrow \infty$, the ratios C_D/τ^2 and C_L/τ tend to constant values.

Let us now consider some particular cases. For flow past a projectile-like body at an angle of attack α , we take for the parameter τ the maximum thickness ratio of the body. For various values of the Mach number, angle of attack α , and body thickness ratio τ , the conditions of similarity for two flows will be met if the flows have not only the same parameter $M\tau$ but also the same ratio α/τ . (It is easy to satisfy oneself that with α/τ held constant, the bodies will be affinely related to changes in τ to the degree of approximation considered.) In this case we may express the drag and lift coefficients in the form

$$\frac{C_D}{\tau^2} = F\left(K, \frac{\alpha}{\tau}\right), \quad \frac{C_L}{\tau} = \tilde{F}\left(K, \frac{\alpha}{\tau}\right).$$

For flow past an infinite span wing (airfoil) with no side slip and at an angle of attack α , we shall similarly take for the parameter τ the maximum thickness ratio of the airfoil. Then for the coefficients C_D and C_L based on the force per unit span length of the wing and on the corresponding plan area of the wing we obtain the relations

$$\frac{C_D}{\tau^3} = F_1\left(K, \frac{\alpha}{\tau}\right), \quad \frac{C_L}{\tau^2} = \tilde{F}_1\left(K, \frac{\alpha}{\tau}\right).$$

For $K \rightarrow \infty$, i.e., for a limiting hypersonic flow, the functions F , \tilde{F} , F_1 , and \tilde{F}_1 become dependent only on the ratio α/τ .

The similarity law formulated above is of importance for high speed experiments. In particular one can use this law to obtain data on the aerodynamic characteristics of bodies at hypersonic speeds by means of lower speed wind tunnel tests of affinely related models. Let us suppose,

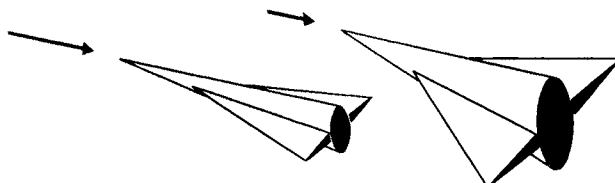


FIG. 2.3. Hypersonic similarity law.

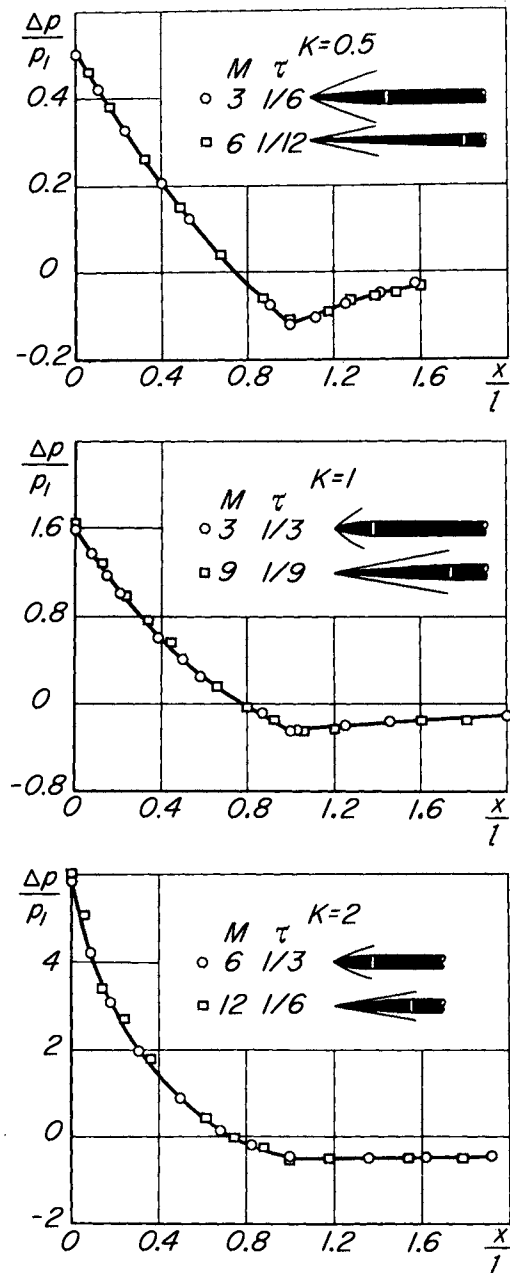


FIG. 2.4. Pressure distributions for hypersonic flows past affinely related bodies.

for example, that we want to determine the aerodynamic characteristics of the body depicted on the left side of Fig. 2.3 for a Mach number equal to 6. We can carry out the test at a Mach number equal to 3 with the transverse dimensions of the body doubled (right side of Fig. 2.3). The pressures at corresponding points in the flows past these two bodies are the same. (If the angle of attack is different from zero, then the angle of attack of the second body must be twice that of the first body.)

The hypersonic similarity law allows us to carry over the results of calculations or experiments determining the aerodynamic characteristics of a slender body at some hypersonic speed to an infinite set of affinely related bodies at corresponding speeds. Figure 2.4 shows calculations carried out by the method of characteristics for the pressure distributions along bodies of revolution having ogival noses and cylindrical after-bodies (ogive-cylinders) [12]. On each of the three graphs are given the pressure distributions on two bodies which have different thickness ratios but where the Mach numbers are such that the similarity parameters $K = M\tau$ are the same (in the upper graph, $K = 0.5$; in the middle, $K = 1$; and in the lower, $K = 2$). From Fig. 2.4 we see that pressure distributions for the same values of the similarity parameter agree within the accuracy of the calculations.* It is important to note that even for the relatively low Mach number of 3 and for a thickness ratio of $1/3$, the calculated results still agree well with the similarity law which was derived under the assumptions $M \gg 1$, $\tau \ll 1$. This provides some basis for believing that the hypersonic similarity law is valid over a considerably wider range of values of M and τ than would be expected on the basis of the assumptions made in its derivation.

Let us estimate the limits of applicability of the similarity law for bodies with an ogival nose [12]. To do this let us first refer to Fig. 2.5 which shows the pressure coefficients for $\gamma = 1.405$, according to [13], on circular cones with different apex angles α and at different Mach numbers plotted as a function of the hypersonic similarity parameter $K = M \tan \alpha$. (The curves shown in this figure will be discussed in Section 5 of this chapter and in Section 3 of Chapter III.) Let us assume that for practical purposes the similarity law can be used to determine

* Strictly speaking, ogival bodies with different thickness ratios are not affinely related. For small thickness ratios, however, the difference in the thickness ratio distribution is negligibly small from one body to another.

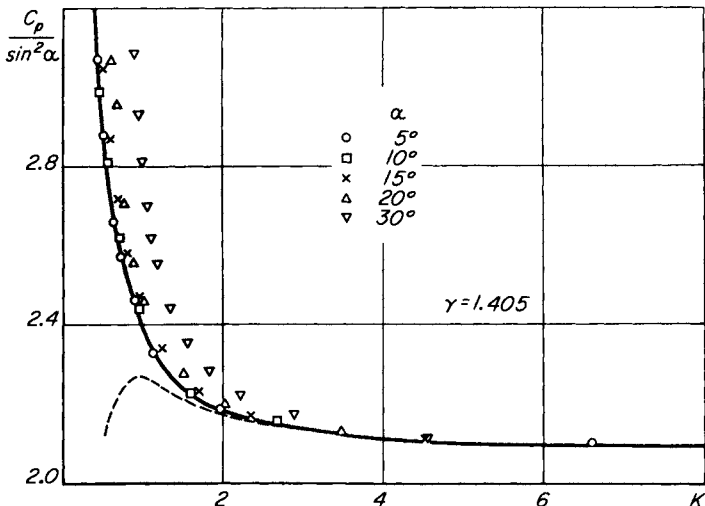


FIG. 2.5. Surface pressure on circular cones for supersonic speeds.

the pressure on a cone if the exact values of the pressure do not differ by more than 5 per cent from the values for the smallest apex angle cones with the same value of K . Then the similarity law can be used for evaluating cone pressures at hypersonic speeds with $\gamma \approx 1.4$ for values of M and τ indicated by the unhatched region of Fig. 2.6. If we assume that the applicability of the hypersonic similarity law for the evaluation

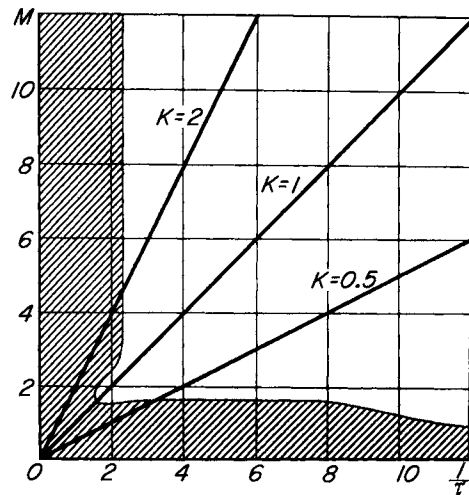


FIG. 2.6. Region of applicability of the hypersonic similarity law for cones.

of pressures on ogives is determined by its applicability in evaluating pressures at the noses of these bodies, then by a simple reinterpretation of the data presented in Fig. 2.6 one can find the region of validity of the hypersonic similarity law for ogives (Fig. 2.7). The cor-

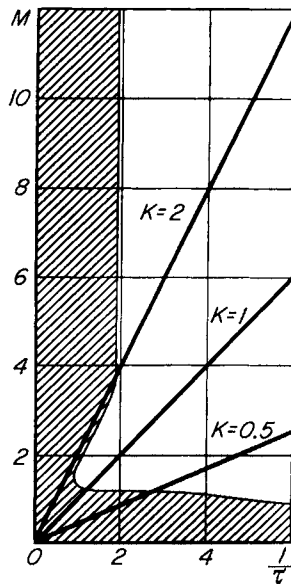


FIG. 2.7. Region of applicability of the hypersonic similarity law for ogives.

rectness of this assumption has been substantiated by additional method of characteristics calculations similar to those shown in Fig. 2.4.

We note that the region of applicability of the hypersonic similarity law is considerably extended for lower Mach numbers if we take the quantity $\sqrt{M^2 - 1} \tau$ for the similarity parameter, instead of $M\tau$ ([14], see also [9]).

To conclude this section, we present generalized curves (Fig. 2.8) which permit the determination of surface pressures on ogive-cylinders in the range of Mach numbers and thickness ratios for which the hypersonic similarity law is justified. These curves were constructed on the basis of a large number of calculations by the method of characteristics [15].

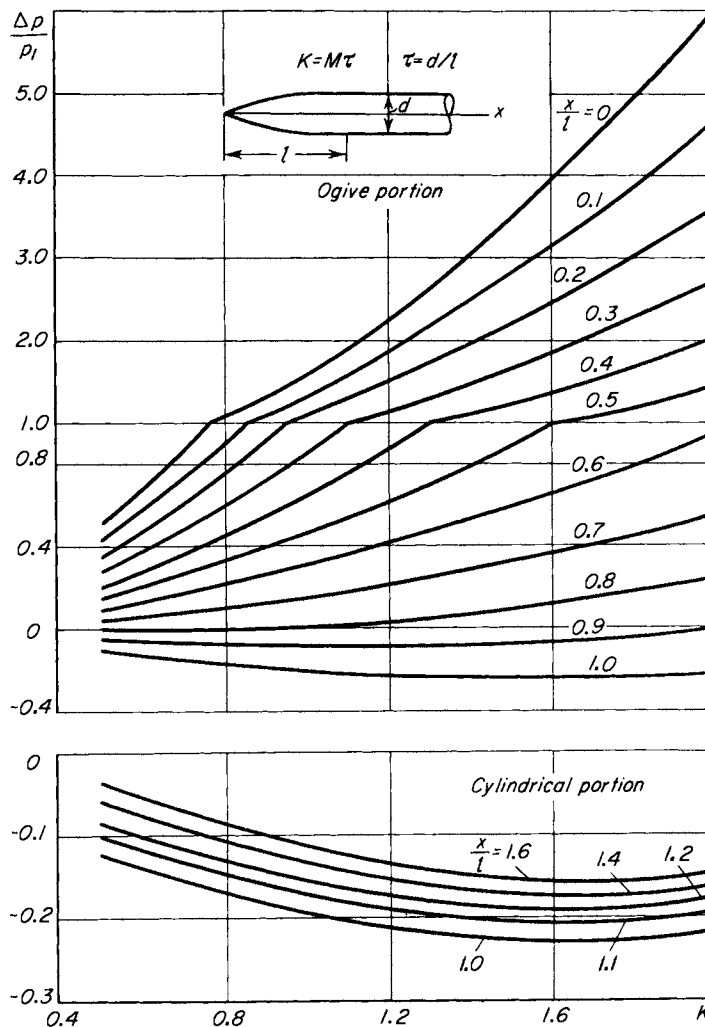


FIG. 2.8. Generalized curves for determining surface pressures on ogive-cylinders.

3. Simplification of the equations for hypersonic flows past slender bodies

The system of relations (2.2) to (2.6) obtained in the previous section is simpler than the original system (1.1) to (1.8). It is important to note that the system (2.2) to (2.6) is composed of two independent sets of

relations. Thus the last four equations of (2.2) do not contain the velocity component u , and this quantity does not appear in condition (2.5) at the surface of the body or in conditions (2.4) on the vortex surfaces. It is also not contained in four of the five conditions (2.3) at the shock wave surfaces and in four of the five conditions (2.6) in the free stream. This reduced number of supplementary conditions is just sufficient to determine the functions v , w , p , and ρ from the four equations of (2.2) which contain only these functions. After determining the unknown quantities v , w , p , and ρ , the velocity component u can be found from the first of equations (2.2) with the aid of the conditions at the shock surfaces and in the free stream which contain this component.

The velocity component u can be determined in a simpler manner: the x -momentum equation [the first equation of the system (2.2)] can be replaced by the Bernoulli integral. For adiabatic flow the Bernoulli integral is written in the form

$$\frac{(V + u)^2 + v^2 + w^2}{2} + \frac{\gamma}{\gamma - 1} \frac{p}{\rho} = \frac{V^2}{2} + \frac{\gamma}{\gamma - 1} \frac{p_1}{\rho_1}.$$

The free stream conditions and the shock conditions have already been utilized in this form. Substituting the dimensionless variables given by (2.1) into the Bernoulli integral and neglecting terms of order τ^2 in comparison with unity, we find

$$u' + \frac{v'^2 + w'^2}{2} + \frac{\gamma}{\gamma - 1} \frac{p'}{\rho'} = \frac{1}{(\gamma - 1) M^2 \tau^2}.$$

The velocity component u can be determined from this relation by using the known values of the other flow parameters. We note that a knowledge of the velocity component u is not necessary in a number of problems.

It is clear that the condition that the velocity perturbations remain small in hypersonic flow past a slender body, although the pressure and density perturbations may be large, leads to substantial mathematical simplifications.

We emphasize again, that when replacing the exact equations for hypersonic flows past slender bodies by the approximate relations, the neglected terms are of the order of τ^2 in comparison with the terms which are retained. On the other hand, the neglected terms are of the order of τ in the linearized theory of small disturbances for moderate supersonic

speeds. This circumstance enhances the value of the approximate theory of flows past slender bodies at high speeds.

In contrast to the case considered in Section 1 of this chapter, let us now suppose that the dimension of the body in the direction of one of the transverse axes, for example the axis Oy , is much larger than the dimension in the direction of the other axis (a winglike body). Then at all points on the forward portion of the body, excluding perhaps a small region in the neighborhood of its edges, the quantity $\cos(n, y)$ is small. Carrying out estimates of the orders of magnitude of the flow parameters in a manner completely analogous to that of Section 1, the velocity component v along the y -axis is found to be of higher order than w , as is the component u . Neglecting higher order quantities in the equations of motion (1.1) to (1.4), we reduce these equations to the form

$$V \frac{\partial u}{\partial x} + w \frac{\partial u}{\partial z} + \frac{1}{\rho} \frac{\partial p}{\partial x} = 0,$$

$$V \frac{\partial v}{\partial x} + w \frac{\partial v}{\partial z} + \frac{1}{\rho} \frac{\partial p}{\partial y} = 0,$$

$$V \frac{\partial w}{\partial x} + w \frac{\partial w}{\partial z} + \frac{1}{\rho} \frac{\partial p}{\partial z} = 0,$$

$$V \frac{\partial \rho}{\partial x} + \frac{\partial \rho w}{\partial z} = 0,$$

$$V \frac{\partial}{\partial x} \frac{p}{\rho^\gamma} + w \frac{\partial}{\partial z} \frac{p}{\rho^\gamma} = 0,$$

where we have kept dimensional variables.

The supplementary conditions at the body and on the discontinuity surfaces retain their previous form, but the quantities v_n and \mathbf{v}^2 which enter into them must be calculated in terms of the velocity component w only. The normals to the body and to the discontinuity surfaces in these relations can be replaced by a unit vector directed along the axis Oz . The quantity D is understood to be the propagation velocity of the discontinuity surfaces in this direction.

The last three equations written above do not contain the velocity components u and v , nor do these velocity components enter into the supplementary conditions at the body and on the vortex surfaces. In addition, they do not appear in three of the five shock conditions (the

continuity, z -momentum, and energy conditions) and in the free stream conditions. The three quantities w , p , and ρ can therefore be found independently, and then with the aid of the other two equations the two remaining quantities u and v can be determined. (The quantity u can alternatively be determined from the Bernoulli integral.)

4. The equivalence principle for hypersonic flows past slender bodies

Let us return to the use of dimensional variables in the last four equations of (2.2). If we interpret the quantity $x/V = t$ as the time variable, these equations will agree exactly with the system of equations for unsteady gas motion in a fixed plane normal to the direction of motion of the body. With such an interpretation the approximate relations (2.3) and (2.4) on the discontinuity surfaces also agree with the relations which must be satisfied in plane motion.* The approximate condition (2.5) at the body surface is

$$\frac{\partial F}{\partial t} + v \frac{\partial F}{\partial y} + w \frac{\partial F}{\partial z} = 0.$$

In the present interpretation this relation represents the condition governing gas displacement in the chosen plane due to the motion of an impermeable boundary (a piston). The piston path is determined by the shape of the moving body in accordance with the relation

$$F \left(Vt, \frac{y}{\tau}, \frac{z}{\tau} \right) = 0.$$

Thus, to terms of order τ^2 , the problem of steady hypersonic flow past a slender body is equivalent to the problem of unsteady gas motion in a plane.

This statement comprises the equivalence principle† [6]. The substance of this principle was already established in Section 1, when it was shown

* We note that to terms of order τ^2 ,

$$|\text{grad } F| = \sqrt{\left(\frac{\partial F}{\partial y}\right)^2 + \left(\frac{\partial F}{\partial z}\right)^2}.$$

† *Editor's note:* The original Russian edition, in common with the Russian literature, refers to the "equivalence principle" as the "law of plane sections."

that, to the approximation mentioned above, the hypersonic motion of a slender body through a gas produces only a transverse displacement of the gas. If we consider a layer of gas ahead of the body which is perpendicular to the direction of motion (Fig. 2.9), then when the body moves through this layer the gas will be set in motion without being displaced axially. The similarity law which was formulated in Section 2 of this chapter, and which is of fundamental significance in hypersonic

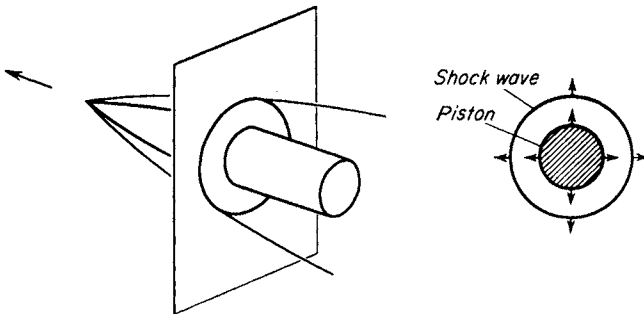


FIG. 2.9. Illustration of equivalence principle.

aerodynamics, follows directly from the equivalence principle. Thus the velocity of points on the moving boundary in the equivalent unsteady plane flow problem is the same for affinely related bodies if the product $V\tau$ is held constant. For the same product $V\tau$, therefore, unsteady flows with different values of V and τ differ only by a linear scale factor, and consequently the quantities v' , w' , p' , and ρ' are the same at corresponding points.

Let us determine how to compute the drag of a body using the equivalence principle. The drag experienced by the body is equal to the work done by the body over a path of unit length. In accordance with the equivalence principle, this work equals the work done by the equivalent piston on a layer of gas of unit width in a time equal to the time for the body to pass through this layer. Therefore the drag of the body D can be expressed by the relation

$$D = \int_0^T \int_l p v_n dl dt, \quad (2.7)$$

where the integration with respect to l is carried out along the contour of the piston. The shape of this contour at each instant of time, and its

normal velocity v_n , are determined by the shape of the body. The pressure p on the surface of the piston must be found from the solution of the corresponding unsteady problem. For flow past an airfoil or axisymmetric flow past a body of revolution, the quantity pv_n is the same on all points of the contour, and equation (2.7) takes the form

$$D = \int_0^T p v_n (2\pi R)^{\nu-1} dt = \int_0^R p (2\pi R)^{\nu-1} dR \quad (2.8)$$

(\tilde{R} is the distance of a point on the piston surface from the initial plane or axis of symmetry; $\nu = 1$ for an airfoil and $\nu = 2$ for a body of revolution; for an airfoil D is the drag of only one side of the airfoil).

In a similar manner we can calculate the transverse force (in particular the lift force) which acts on a moving body. The transverse force is equal to the impulse per unit time which the gas receives in a direction normal to the direction of motion of the body. It is also equal to the flight velocity multiplied by the impulse imparted by the body to the gas over a path of unit length. In accordance with the equivalence principle, the transverse force is then expressed by the following relation:

$$\mathbf{L} = V \int_0^T \int_l p \mathbf{n} dl dt.$$

According to this relation, for the flow past an airfoil the transverse force which acts on one of its sides is equal to

$$L = \int_0^T p V dt.$$

For axisymmetric flow past a body of revolution the resultant transverse force is obviously equal to zero. The transverse force acting on a section of such a body situated between two planes which are infinitely close together and which pass through the axis of the body is equal to

$$d\theta \int_0^T p R V dt$$

($d\theta$ is the angle between the planes). If we denote the force corresponding to the angle 2π by L , then for an airfoil and a body of revolution we can write the single relation:

$$L = \int_0^T pV(2\pi R)^{r-1} dt. \quad (2.9)$$

The equivalence principle shows that to a specified degree of approximation, a hypersonic flow past a slender body is equivalent to an unsteady plane flow of a gas displaced by a moving boundary (piston) of corresponding shape.

By way of example, let us consider the application of the equivalence principle to the calculation of some flows past slender airfoils, and some axisymmetric flows past slender bodies of revolution, for $M \gg 1$. The region of disturbed motion for a piston moving into a uniform gas at rest is contained between the shock wave which propagates in the gas and the surface of the piston. In the present section we shall discuss the gas motion from the Lagrangian point of view, since it is our intention in the following chapter to present an approximate method for calculating such flows by the use of Lagrangian variables. From the Lagrangian point of view the basic unknown functions used to characterize the gas motion in this region are the distance R of a particle from the initial plane or axis of symmetry, the pressure p , and the density ρ (the velocity v is expressed by the relation $v = \partial R / \partial t$). The parameters which define these quantities are the time t and the Lagrangian coordinate $m = \rho_1 r^\nu / v$ (r is the value of R at the initial instant of time, ρ_1 is the initial density, and as before, $\nu = 1$ or 2 for flows with planar or cylindrical symmetry respectively).

The equations of continuity, motion, and energy can be written in terms of these variables as follows:

$$\frac{\partial R}{\partial m} = \frac{1}{\rho R^{r-1}}, \quad \frac{\partial v}{\partial t} = -R^{r-1} \frac{\partial p}{\partial m}, \quad \frac{\partial}{\partial t} \frac{p}{\rho^\nu} = 0, \quad \left(v = \frac{\partial R}{\partial t} \right). \quad (2.10)$$

The solution of this system of equations must satisfy the conditions on the shock wave and on the piston surface. If the "path" of the shock wave is denoted by $R^*(t)$, then the conditions at the shock wave take the form [see equations (1.10)]:

$$m^* = \frac{\rho_1 R^{**}}{\nu}, \quad p^* = \frac{2}{\gamma + 1} \rho_1 D^2 - \frac{\gamma - 1}{\gamma + 1} p_1, \quad \rho^* = \frac{\frac{\gamma + 1}{\gamma - 1} \rho_1}{1 + \frac{2}{\gamma - 1} \frac{a_1^2}{D^2}}, \quad (2.11)$$

where $D = dR^*/dt$ is the shock wave propagation velocity. On the piston surface $m = 0$ [†], the condition

$$R = \bar{R}(t) \quad (2.12)$$

must be fulfilled.

In general, solutions of the partial differential equations (2.10) which satisfy conditions (2.11) for a given piston path $\bar{R}(t)$, or for a given shock wave path $R^*(t)$ can only be found by complicated numerical methods. For some gas motions, however, it turns out that these equations can be reduced to ordinary differential equations, and one can obtain exact solutions in closed form or approximate solutions through the use of comparatively simple numerical integration methods. Such motions are called self-similar.

In self-similar motions the quantities which characterize the state and motion of the gas vary in such a way that the distribution of each quantity in space remains similar to itself with changing time. The scales characterizing the numerical values of these quantities may also depend on time, depending on the specified law. In order to determine such self-similar motions we shall make use of some considerations from the theory of similarity and dimensional analysis [16].

Equations (2.10) do not contain dimensional constants, and the dimensions of the variables t and m which appear in these equations are independent. Consider the dimensional constants in equations (2.11) at the shock wave, and in the relation $R = \bar{R}(t)$ specifying the piston path or in the relation $R = R^*(t)$ specifying the shock wave path: if among these dimensional constants only two have independent dimensions which are not expressible in terms of the dimensions of t and m , then we can construct in dimensionless combination only one independent variable from all the defining parameters. In this case the partial differential equations (2.10) can be reduced to equations which depend on only one independent variable—that is, to ordinary differential equations—and the resulting

[†] For flows past annular bodies of revolution, $m = m_0 = \text{const.} \neq 0$ on the surface of the piston.

motion is self-similar. We note that for a given shock wave path the path of the other boundary of the disturbed region may be determined by additional dimensional constants, in which case the motion of this boundary may not be a self-similar one.

The dimensions of the constants ρ_1 and p_1 which enter into conditions (2.11) on the shock wave are independent and can be expressed by the formulas

$$[\rho_1] = ML^{-3}, \quad [p_1] = ML^{-1}T^{-2}.$$

If both these constants have importance in the problem the constant m_0 in condition (2.12) for flow past an annular body of revolution, and the kinematic constants in this condition (or in the case of a given shock wave path, the kinematic constants entering into the description of this path) must have dimensions which are expressed through the dimensions of ρ_1 and p_1 , in order that the motion be self-similar. Upon eliminating the mass from the formulas specifying the dimensions of ρ_1 and p_1 , we thus find that the kinematic constants must have the dimensions LT^{-1} . Hence the equation of the piston path (2.12) or the equation of the shock path must have the form

$$\bar{R} = Ut$$

and

$$R^* = Dt,$$

where U and D are constants. If the constant p_1 is important (that is, if the initial gas pressure has an appreciable effect on the motion), then the motion is self-similar only if the piston starts from rest and suddenly moves with a constant velocity into a gas at rest. This motion corresponds to the propagation of a shock wave with constant speed. If we apply the equivalence principle to such a motion, we find that it corresponds to flow past a slender wedge for $\nu = 1$, and to flow past a slender cone for $\nu = 2$.

If the pressure behind the shock wave is much greater than the initial pressure (i.e., if $D^2 \gg a_1^2$), one can neglect the effect of the parameter p_1 on the gas motion. The motion is then self-similar if the constant which enters into the equation of the piston path or into the equation of the shock path has the kinematic dimension $LT^{-(n+1)}$, that is, if

$$\bar{R} = \frac{C}{n+1} t^{n+1} \quad \text{or} \quad R^* = \frac{C_1}{n+1} t^{n+1}, \quad (2.13)$$

where n is any number other than -1 . For $\nu = 1$, such unsteady motions correspond to hypersonic flows past slender airfoils with power law contours, while for $\nu = 2$ they correspond to flows past bodies of revolution with power law contours and to certain annular bodies of revolution.

Let us now consider the unsteady self-similar flow produced by the motion of a piston or by the propagation of a shock wave described by equations (2.13). We recall that if $n = 0$, the flow is self-similar even if the initial gas pressure is taken into account. In place of the unknown functions R , p , ρ , and v we shall introduce new dimensionless quantities \mathfrak{R} , Φ , Ω , and V defined by the relations

$$R = R^* \mathfrak{R}, \quad p = p^* \Phi, \quad \rho = \rho^* \Omega, \quad v = \dot{R}^* V. \quad (2.14)$$

Here R^* , p^* , and ρ^* are the values of R , p , and ρ at the shock wave. They depend on t in a manner specified by equations (2.13) and (2.11), where in (2.11) we replace D by $C_1 t^n$. For $n \neq 0$ it is also necessary to set $p_1 = 0$ and $a_1 = 0$. As a consequence of the assumptions which have been made, the dimensionless functions \mathfrak{R} , Φ , Ω , and V depend only on the variable

$$\mu = \frac{m}{m^*} \quad \left(m^* = \frac{\rho_1 R^{*\nu}}{\nu} \right).$$

Substituting expressions (2.14) for R , p , ρ , and v into equations (2.10), we obtain the following system of ordinary differential equations to determine the functions \mathfrak{R} , Φ , Ω , and V :

$$\begin{aligned} \nu \frac{\rho^*}{\rho_1} \Omega \mathfrak{R}^{\nu-1} \mathfrak{R}' &= 1, \\ \frac{n}{n+1} V - \nu \mu \frac{dV}{d\mu} + \nu \frac{p^*}{\rho_1 \dot{R}^{*2}} \mathfrak{R}^{\nu-1} \Phi' &= 0, \\ \left(\frac{\Phi}{\Omega^\gamma \mu^{2n/\nu(n+1)}} \right)' &= 0, \quad V = \mathfrak{R} - \nu \mu \mathfrak{R}'. \end{aligned} \quad (2.15)$$

The quantities ρ^*/ρ_1 and $p^*/\rho_1 \dot{R}^{*2}$ which appear in these equations are constants. The first, third, and fourth equations of (2.15) allow us to express Ω , P , and V in terms of μ , \mathfrak{R} , and Φ' :

$$\begin{aligned}\Omega &= \left(\frac{\rho^*}{\rho_1} \nu R^{r-1} R' \right)^{-1}, \\ P &= A \gamma \Omega \mu^{2n/\nu(n+1)}, \\ V &= R - \nu \mu R'.\end{aligned}\quad (2.16)$$

Substituting these expressions into the second of equations (2.15), we obtain the following second order differential equation which determines the function R in terms of μ :

$$\begin{aligned}\frac{n}{n+1} (R - \nu \mu R') - \nu \mu \frac{d}{d\mu} (R - \nu \mu R') \\ + \frac{\nu p^* A}{\rho_1 R^{*2}} \left(\frac{\rho^*}{\rho_1} \right)^\gamma R^{r-1} \frac{d}{d\mu} [\mu^{2n/\nu(n+1)} (\nu R^{r-1} R')^{-\gamma}] = 0.\end{aligned}\quad (2.17)$$

The three conditions at the shock wave

$$R(1) = \mathcal{P}(1) = \Omega(1) = 1,$$

serve to determine the two constants of integration of this equation and the constant A which appears in the integral of the equation expressing the adiabatic condition. From these conditions we find

$$A = 1, \quad R'(1) = \frac{\rho_1}{\nu \rho^*}.$$

If the piston path $\bar{R}(t)$ is specified, then we may relate it to the shock path $R^*(t)$ by using the condition (2.12) on the piston. Thus, for $\mu = 0$,

$$\bar{R}(t) = R^*(t)R(0),$$

$$C = C_1 R(0).$$

This relation is required in order to apply the solution of (2.17).

5. Examples of the application of the equivalence principle

Flow past a wedge and cone. In these cases we have $n = 0$, and equation (2.17) takes the form

$$\nu \mu^2 R'' + (\nu - 1) \mu R' + B R^{r-1} \frac{d}{d\mu} (\nu R^{r-1} R')^{-\gamma} = 0,$$

where $B = (\rho^*/\rho_1)\gamma p^* A / \rho_1 \dot{R}^{*2}$. For wedge flow with $\nu = 1$, we obtain from this equation

$$(\mu^2 - \gamma B \mathfrak{R}'^{-(\gamma+1)}) \mathfrak{R}'' = 0.$$

The only solution of this equation which satisfies the conditions at the shock wave is the function

$$\mathfrak{R} = 1 - \frac{\rho_1}{\rho^*} (1 - \mu).$$

Substituting this solution into equations (2.16), we find

$$\Omega = 1, \quad \Phi = 1, \quad V = 1.$$

To determine the constant $C_1 \equiv D$ when the piston path $\bar{R} = Ut$ is given, we use the condition $U = D\mathfrak{R}(0)$, obtaining

$$U = D \left(1 - \frac{\rho_1}{\rho^*} \right) = \frac{2}{\gamma + 1} \left(D - \frac{a_1^2}{D} \right)$$

or

$$D = \frac{\gamma + 1}{4} U + \sqrt{\left(\frac{\gamma + 1}{4} U \right)^2 + a_1^2}.$$

Setting $U = V_1 \tan \alpha$, $D = V_1 \tan \beta$, and denoting $(V_1/a_1) \tan \alpha = K$, $(V_1/a_1) \tan \beta = K_s$, in accordance with the equivalence principle, we obtain the following relations:

$$K_s = \frac{\gamma + 1}{4} K + \sqrt{\left(\frac{\gamma + 1}{4} K \right)^2 + 1},$$

$$C_p M^2 = \frac{4}{\gamma + 1} (K_s^2 - 1).$$

These relations were derived previously when we considered the flow past a flat plate (Chapter I, Section 3). A comparison of these relations with exact calculations [7] is shown in Figs. 2.10 and 2.11.

Let us now consider the more interesting case of flow past a cone ($\nu = 2$). Equations (2.15) take the form

$$2 \frac{\rho^*}{\rho_1} \mathcal{R} \mathcal{R}' \Omega = 1, \quad \left(\frac{\Omega}{\Omega'} \right)' = 0,$$

$$2\mu^2 \mathcal{R}'' + \mu \mathcal{R}' + \mathcal{R}' \mathcal{R} \frac{\rho^*}{\rho_1 D^2} = 0.$$

As before, the boundary conditions at the shock wave and the condition (2.12) at the piston

$$\mathcal{R}(0) = \frac{U}{D}$$

serve to determine the constant D and the three arbitrary constants which appear in the solution.

The problem of the piston moving into a gas with constant velocity was solved for spherically symmetric flow in [17] and [18] by numerical integration of equations equivalent to equations (2.15) but expressed

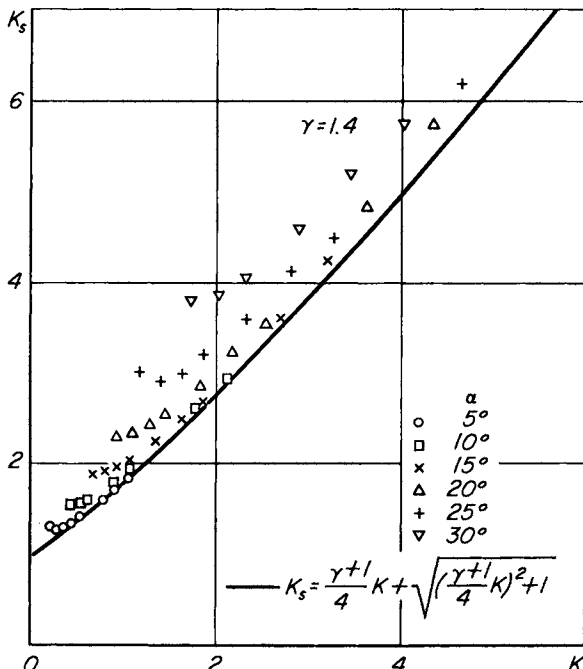


FIG. 2.10. Angle between bow shock wave and free stream direction for supersonic flow past a wedge.

in Eulerian variables. Results of calculations for a cylindrical piston were given in [7]. The dependence of the quantities $K_s = (V_1/a_1) \tan \beta$ and $C_p/\sin^2 \alpha$ on the parameter $K = (V_1/a_1) \tan \alpha$ from these calculations

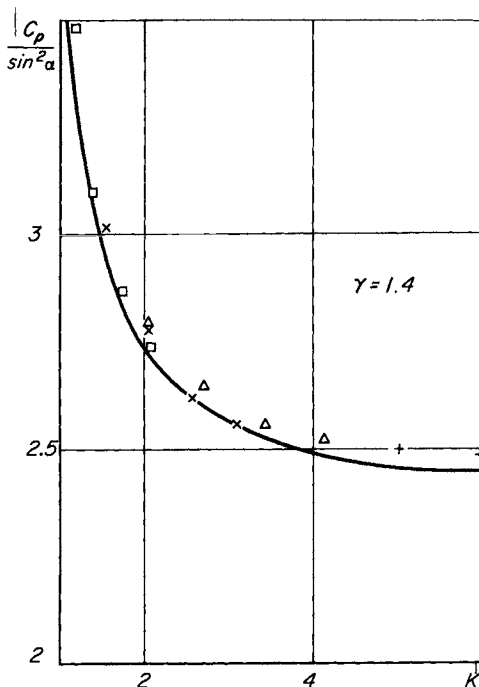


FIG. 2.11. Surface pressure on wedges for supersonic speeds.

is compared with the exact results for flow past a cone [13] in Figs. 2.12 and 2.5, respectively. The results of the numerical solution obtained using the equivalence principle are shown as the solid curves in Figs. 2.12 and 2.5. They are seen to be in good agreement with the results of the exact solutions for small values of the cone angle. (The methods of obtaining the dashed curves shown in these figures will be explained in Section 3 of Chapter III.)

Flows Past Power Law Bodies. The system of equations (2.15) was first studied (in Eulerian variables) in [19] for $n \neq 0$. By means of a qualitative analysis it was shown in this work that for a given piston path, the solution of the problem does not exist for all values of the exponent n in equation (2.13). A physical explanation of this fact was not

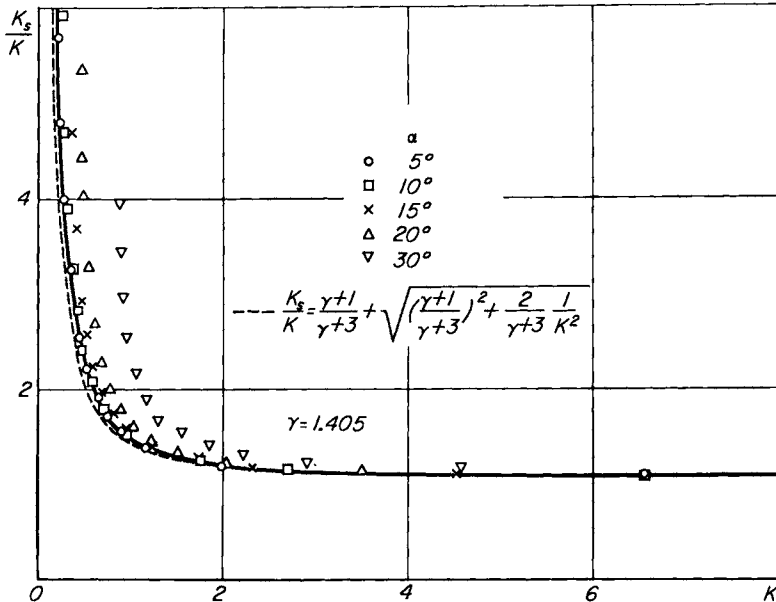


FIG. 2.12. Angle between bow shock wave and free stream direction for supersonic flow past a cone.

given, however. The calculations carried out in [19] by means of numerical integration were for the spherically symmetric case ($\nu = 3$), and hence they are not of interest for aerodynamic applications. Results of calculations for $\nu = 2$ are given in [20] and [21].

The following derivation of the requirement $2n/[\nu(n+1)] > -1$ for the existence of a solution was given in [21] and [22]. According to equation (2.8) the drag acting on the forward portion of the body is equal to

$$D = \int_0^R p(2\pi R)^{\nu-1} dR.$$

For the case considered,

$$p = \frac{2}{\gamma+1} \frac{\Phi(0)}{\Phi'(0)} \rho_1 C^2 \left(\frac{n+1}{C} R \right)^{2n/n+1},$$

so that

$$D = \frac{2\pi^{\nu-1}}{\gamma+1} \frac{\Phi(0)}{\Phi'(0)} \rho_1 C^2 \left(\frac{n+1}{C} \right)^{2n/n+1} \int_0^R R^{(2n/n+1)+\nu-1} dR. \quad (2.18)$$

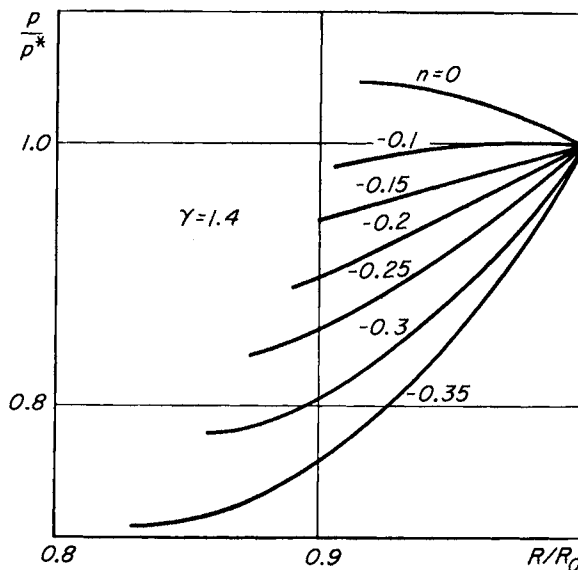


FIG. 2.13. Pressure distributions in the flow around axisymmetric power law bodies.

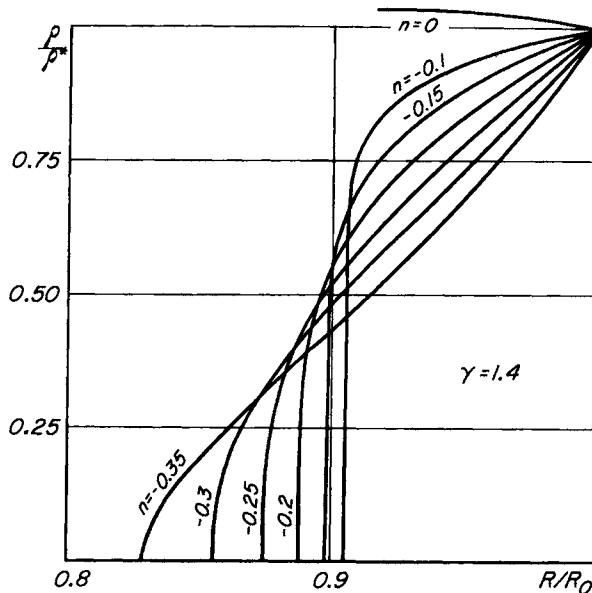


FIG. 2.14. Density distributions in the flow around axisymmetric power law bodies.

The integral on the right-hand side of this expression diverges for $2n/[\nu(n+1)] \leq -1$. In other words, in accordance with the equivalence principle the drag of the forward portion of a power law body has a finite value only for $n > -\nu/(\nu+2)$; that is, $n > -\frac{1}{3}$ for two-dimensional bodies, and $n > -\frac{1}{2}$ for bodies of revolution.

For the cylindrically symmetric case ($\nu = 2$) with $\gamma = 1.4$, the radial distributions of pressure, density, and velocity of the gas are shown for several values of n in Figs. 2.13 to 2.15. These curves were constructed from the tabular results given in [20]. Some numerical values from these tables are shown in Table 2.1.

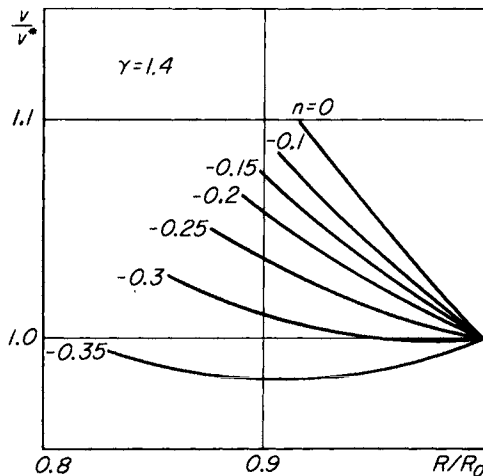


FIG. 2.15. Transverse velocity distributions in the flow around axisymmetric power law bodies.

The pressure increases somewhat from the shock wave to the piston for the case $n = 0$, i.e., for flow past a cone. For negative values of n , i.e., for flows past axisymmetric convex bodies, the pressure on the piston is higher than the pressure behind the shock wave down to values of n roughly equal to -0.075 . For smaller values of n the pressure decreases toward the piston, the more sharply for the smaller n .

Values of the ratio of the pressure on the piston to the pressure behind the shock wave are shown in Fig. 2.16 by the open circles. These results were obtained from the numerical solution of the problem given in [20]. The curve passing through these circles corresponds to an approximate solution of the problem to be given in Section 8 of the next chapter.

TABLE 2.1
SELF-SIMILAR POWER LAW SOLUTIONS
CYLINDRICALLY SYMMETRIC CASE ($\nu = 2$); $\gamma = 1.4$

$n = 0$				$n = -0.10$			
R/R_0	p/p^*	ρ/ρ^*	v/v^*	R/R_0	p/p^*	ρ/ρ^*	v/v^*
1.000	1.0000	1.0000	1.0000	1.000	1.000	1.0000	1.0000
0.995	1.0052	1.0040	1.0059	0.995	1.001	0.9960	1.0041
0.990	1.0105	1.0077	1.0116	0.990	1.001	0.9910	1.0083
0.985	1.0154	1.0112	1.0174	0.985	1.002	0.9860	1.0126
0.980	1.0202	1.0145	1.0233	0.980	1.002	0.9800	1.0168
0.975	1.0244	1.0175	1.0289	0.975	1.002	0.9740	1.0210
0.970	1.0284	1.0203	1.0346	0.970	1.001	0.9670	1.0254
0.965	1.0320	1.0228	1.0403	0.965	1.001	0.9600	1.0297
0.960	1.0352	1.0251	1.0460	0.960	1.000	0.9520	1.0340
0.955	1.0383	1.0273	1.0516	0.955	0.999	0.9435	1.0384
0.950	1.0407	1.0291	1.0573	0.950	0.998	0.9346	1.0428
0.945	1.0430	1.0307	1.0630	0.945	0.997	0.9238	1.0473
0.940	1.0451	1.0321	1.0688	0.940	0.996	0.9127	1.0518
0.935	1.0468	1.0332	1.0746	0.935	0.994	0.8995	1.0563
0.930	1.0481	1.0341	1.0803	0.930	0.992	0.8838	1.0610
0.925	1.0490	1.0347	1.0862	0.925	0.990	0.8657	1.0658
0.920	1.0496	1.0351	1.0921	0.920	0.988	0.8436	1.0707
0.915	1.0497	1.0352	1.0982	0.915	0.987	0.8140	1.0754
0.9149	1.0497	1.0352	1.0983	0.910	0.986	0.7690	1.0803
				0.9050	0.982	0	1.0855
$n = -0.15$				$n = -0.20$			
R/R_0	p/p^*	ρ/ρ^*	v/v^*	R/R_0	p/p^*	ρ/ρ^*	v/v^*
1.000	1.0000	1.0000	1.0000	1.000	1.0000	1.0000	1.0000
0.995	0.9960	0.9912	1.0024	0.995	0.9945	0.9855	1.0022
0.990	0.9940	0.9810	1.0056	0.990	0.9900	0.9700	1.0044
0.985	0.9905	0.9710	1.0089	0.985	0.9840	0.9550	1.0066
0.980	0.9890	0.9607	1.0122	0.980	0.9790	0.9400	1.0090
0.975	0.9861	0.9502	1.0156	0.975	0.9735	0.9230	1.0114
0.970	0.9840	0.9388	1.0190	0.970	0.9680	0.9076	1.0138
0.965	0.9813	0.9267	1.0226	0.965	0.9630	0.8910	1.0165
0.960	0.9780	0.9138	1.0262	0.960	0.9580	0.8740	1.0191
0.955	0.9752	0.9004	1.0297	0.955	0.9530	0.8560	1.0219
0.950	0.9725	0.8870	1.0334	0.950	0.9480	0.8380	1.0246
0.945	0.9695	0.8720	1.0371	0.945	0.9440	0.8190	1.0274
0.940	0.9660	0.8555	1.0408	0.940	0.9380	0.7988	1.0303
0.935	0.9630	0.8382	1.0447	0.935	0.9330	0.7776	1.0333
0.930	0.9600	0.8190	1.0486	0.930	0.9290	0.7550	1.0365
0.925	0.9567	0.7966	1.0528	0.925	0.9240	0.7330	1.0396
0.920	0.9534	0.7727	1.0567	0.920	0.9190	0.7050	1.0430
0.915	0.9500	0.7435	1.0609	0.915	0.9150	0.6770	1.0462
0.910	0.9470	0.7030	1.0650	0.910	0.9110	0.6440	1.0497
0.905	0.9450	0.6590	1.0694	0.905	0.8980	0.6009	1.0532
0.900	0.9430	0.5730	1.0739	0.900	0.8950	0.5550	1.0568
0.8971	0.9420	0	1.0760	0.895	0.8940	0.4930	1.0601
				0.890	0.8920	0.3700	1.0643
				0.888	0.8910	0	1.0654

TABLE 2.1 (cont.)

$n = -0.25$				$n = -0.30$			
R/R_0	p/p^*	ρ/ρ^*	v/v^*	R/R_0	p/p^*	ρ/ρ^*	v/v^*
1.000	1.0000	1.0000	1.0000	1.000	1.0000	1.0000	1.0000
0.995	0.9910	0.9792	1.0009	0.995	0.9804	0.9719	0.9984
0.990	0.9821	0.9585	1.0018	0.990	0.9680	0.9440	0.9979
0.985	0.9736	0.9377	1.0029	0.985	0.9547	0.9175	0.9976
0.980	0.9652	0.9171	1.0041	0.980	0.9425	0.8901	0.9975
0.975	0.9570	0.8960	1.0053	0.975	0.9320	0.8642	0.9974
0.970	0.9490	0.8750	1.0066	0.970	0.9205	0.8390	0.9975
0.965	0.9413	0.8541	1.0082	0.965	0.9098	0.8135	0.9976
0.960	0.9333	0.8328	1.0097	0.960	0.8990	0.7870	0.9979
0.955	0.9265	0.8112	1.0113	0.955	0.8906	0.7635	0.9983
0.950	0.9192	0.7891	1.0130	0.950	0.8809	0.7380	0.9987
0.945	0.9121	0.7668	1.0149	0.945	0.8721	0.7135	0.9994
0.940	0.9054	0.7442	1.0168	0.940	0.8632	0.6887	1.0001
0.935	0.8986	0.7206	1.0188	0.935	0.8551	0.6642	1.0009
0.930	0.8921	0.6963	1.0209	0.930	0.8472	0.6397	1.0017
0.925	0.8857	0.6712	1.0231	0.925	0.8392	0.6145	1.0028
0.920	0.8797	0.6456	1.0254	0.920	0.8334	0.5895	1.0040
0.915	0.8737	0.6183	1.0277	0.915	0.8257	0.5640	1.0052
0.910	0.8679	0.5893	1.0302	0.910	0.8178	0.5379	1.0065
0.905	0.8625	0.5583	1.0328	0.905	0.8130	0.5116	1.0080
0.900	0.8572	0.5245	1.0354	0.900	0.8057	0.4844	1.0095
0.895	0.8521	0.4860	1.0382	0.895	0.8000	0.4560	1.0111
0.890	0.8475	0.4424	1.0410	0.890	0.7952	0.4264	1.0128
0.885	0.8431	0.3874	1.0440	0.885	0.7908	0.3952	1.0146
0.880	0.8390	0.3101	1.0470	0.880	0.7870	0.3618	1.0167
0.875	0.8358	0	1.0500	0.875	0.7840	0.3260	1.0185
				0.870	0.7830	0.2844	1.0206
				0.865	0.7820	0.2352	1.0228
				0.860	0.7810	0.1690	1.0251
				0.858	0.7800	0	1.0266

 $n = -0.35$

R/R_0	p/p^*	ρ/ρ^*	v/v^*	R/R_0	p/p^*	ρ/ρ^*	v/v^*	R/R_0	p/p^*	ρ/ρ^*	v/v^*
1.000	1.0000	1.0000	1.0000	0.940	0.8277	0.6302	0.9831	0.880	0.7348	0.3326	0.9832
0.995	0.9815	0.9630	0.9979	0.935	0.8179	0.6047	0.9826	0.875	0.7299	0.3195	0.9839
0.990	0.9635	0.9287	0.9959	0.930	0.8078	0.5795	0.9822	0.870	0.7259	0.2955	0.9847
0.985	0.9463	0.8940	0.9940	0.925	0.7993	0.5549	0.9817	0.865	0.7219	0.2715	0.9854
0.980	0.9309	0.8611	0.9923	0.920	0.7903	0.5309	0.9815	0.860	0.7188	0.2439	0.9864
0.975	0.9158	0.8296	0.9907	0.915	0.7819	0.5065	0.9813	0.855	0.716	0.2197	0.9873
0.970	0.9011	0.7987	0.9892	0.910	0.7735	0.4828	0.9813	0.850	0.714	0.1925	0.9885
0.965	0.8870	0.7681	0.9880	0.905	0.7662	0.4592	0.9814	0.845	0.713	0.1635	0.9896
0.960	0.8744	0.7389	0.9868	0.900	0.7586	0.4355	0.9816	0.840	0.712	0.1316	0.9908
0.955	0.8616	0.7109	0.9858	0.895	0.7526	0.4127	0.9818	0.835	0.712	0.0926	0.9921
0.950	0.8496	0.6838	0.9847	0.890	0.7464	0.3893	0.9822	0.830	0.712	0.0392	0.9935
0.945	0.8392	0.6575	0.9839	0.885	0.7405	0.3662	0.9827	0.828	0.712	0	0.9937

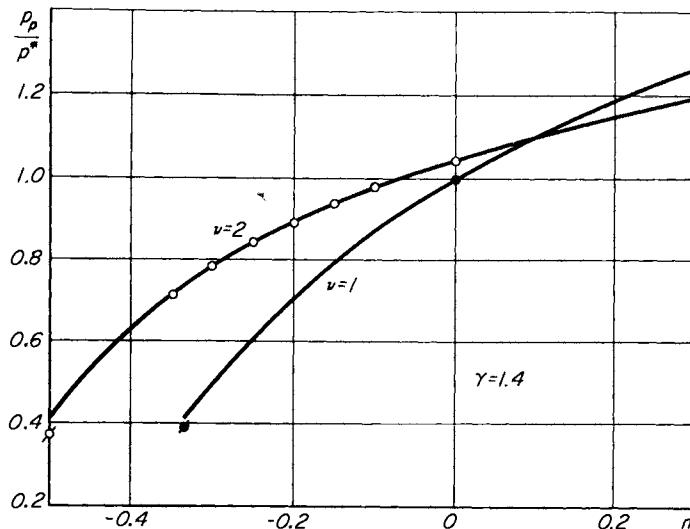


FIG. 2.16. Ratio of surface pressure to pressure behind the shock wave for power law bodies.

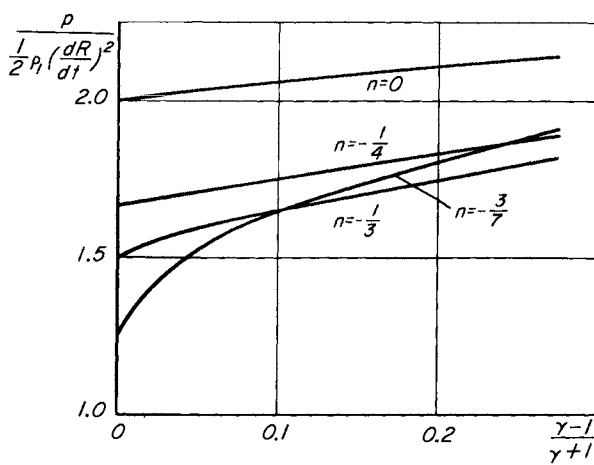


FIG. 2.17. Surface pressure on power law bodies as a function of the parameter $\epsilon = (\gamma - 1)/(\gamma + 1)$, which characterizes the specific heat ratio.

(Looking ahead somewhat, we note that the other curve on this figure corresponds to the motion of a plane piston.) Figure 2.17 illustrates the influence of the specific heat ratio γ on the value of the pressure on the piston [23]. For $n = 0$ or slightly less than zero the influence of γ on the pressure is negligible. This influence only becomes strong when n approaches $-\frac{1}{2}$. This observation will be used in Section 6 of Chapter III for the development of an approximate method for calculating gas flows with strong shock waves.

The density distribution between the shock wave and the piston (see Fig. 2.14) is characterized by the fact that the density remains finite everywhere for $n = 0$, while for $n < 0$ the density at the piston is zero, and for $n > 0$ the density on the piston is infinite. (This follows from the second of equations (2.15) and from the fact that the pressure on the piston remains finite for all n .) The existence of a region of low density

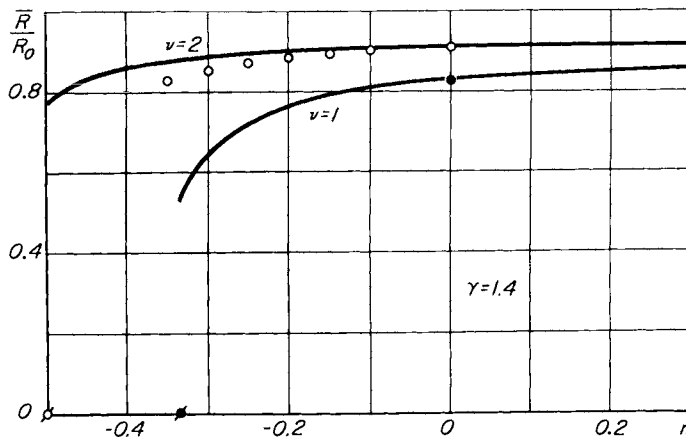


FIG. 2.18. Ratio of body radius to shock wave radius for flows around power law bodies.

near the piston for $n < 0$ results in an increase of the ratio of the shock wave radius to the piston radius with decreasing n . This decrease is slow at first, but becomes very rapid for $n \rightarrow -\frac{1}{2}$. Values of the ratio \bar{R}/R_0 for several values of n are shown in Fig. 2.18 by the open circles (the other curves and circles have the same meaning as in Fig. 2.16).

In anticipation of what will follow later (Chapter III, Section 6), we note that in spite of the increase in the distance between the shock wave

and the piston for a decrease in n , the bulk of the gas remains concentrated in a relatively thin layer near the shock wave. We also note that the presence of a region of low density near the surface of the body is of interest in that it can facilitate the cooling of the surface at hypersonic speeds.

Using equation (2.18), the following formula for the drag coefficient can be easily obtained:

$$C_D = \frac{2^{\nu-1}}{\gamma + 1} \frac{(n+1)^3}{2n + \nu(n+1)} \frac{\mathcal{P}(0)}{\mathcal{R}^2(0)} \tau^2, \quad (2.19)$$

where τ is the thickness ratio of the body defined as the ratio of the maximum diameter to the length. Here C_D is the drag coefficient based on the maximum cross-sectional area $\pi^{\nu-1} \bar{R}_{\max}^\nu$, and in the case of the airfoil ($\nu = 1$) on half the drag. The dependence of $\mathcal{P}(0)$ and $\mathcal{R}(0)$ on n and γ is determined by the numerical solution of the piston problem. Values of C_D/τ^2 for axisymmetric bodies are shown (open circles) as a function of n in Fig. 2.19. From this figure it follows that for a given

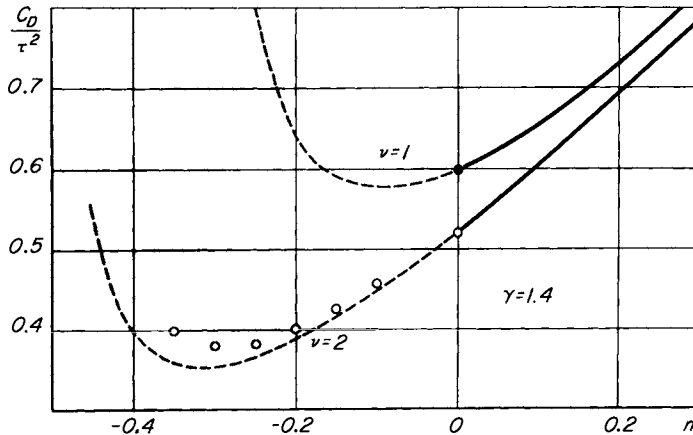


FIG. 2.19. Drag coefficient for power law bodies with given thickness ratio.

body length there exists a value of n for which the drag of the body is a minimum. This value is roughly equal to -0.29 . In a similar manner, Fig. 2.20 shows values of C_D as a function of n for a fixed volume V and a fixed maximum cross-sectional radius of the body. These results were calculated from the relation

$$C_D = \frac{2^{\nu+1} \pi^{2(\nu-1)}}{\gamma + 1} \frac{(n+1)^3}{[2n + \nu(n+1)][1 + \nu(n+1)]^2} \left(\frac{\bar{R}_{\max}^{\nu+1}}{V} \right)^2 \frac{\varphi(0)}{\vartheta^2(0)}. \quad (2.20)$$

Here the volume V is given by

$$V = \frac{\pi^{\nu-1} \bar{R}_{\max}^{\nu} x_{\max}}{[1 + \nu(n+1)]},$$

and in the case of the airfoil ($\nu = 1$) is equal to half the transverse area of the airfoil. Minimum drag is attained in the axisymmetric case for $n = 0$ (as far as can be deduced from the numerical results), when

$$C_D \left(\frac{V}{\bar{R}_{\max}^3} \right)^2 = 2.28.$$

For a body of minimum drag with a given length, $C_D = 0.38\tau^2$, whereas for a cone ($n = 0$) of the same length, $C_D = 0.52\tau^2$. Thus if a body has a conical forebody blunting of the nose may not increase the hypersonic

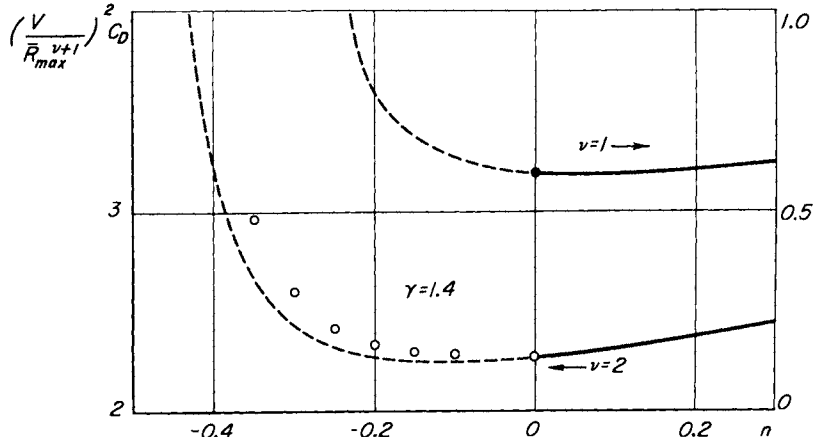


FIG. 2.20. Drag coefficient for power law bodies with given volume and given maximum cross section.

drag, but may even decrease it. (We have already mentioned this behavior in Section 2 of the Introduction. We recall that at hypersonic speeds a blunted nose is more advantageous than a sharp one for cooling.)

Exact solutions of one-dimensional unsteady flow problems can be obtained in other cases besides the self-similar, one-dimensional unsteady

motions already considered which are related to supersonic flows past power law bodies. We note, in particular, the self-similar motion produced in a gas by a violent explosion [16]. (This solution and its application to aerodynamic problems on the basis of the equivalence principle will be examined in Chapter V.) In addition there is the self-similar motion which corresponds to the case when the single dimensionless independent variable μ has the form

$$\mu = \frac{m}{\rho_1 R^* e^{t/\tau}},$$

that is, when the piston expands according to the exponential law

$$\tilde{R} = R^* e^{t/\tau}. \quad (2.21)$$

A self-similar solution also exists for planar symmetry when

$$\mu = \frac{m}{\rho_1 R^* \ln(t/\tau)}.$$

These motions have been studied in the books [16] and [24]. In [25] it was shown that these solutions can be obtained as limits of the previously considered self-similar motions for which

$$\mu = \frac{m}{\frac{\rho_1}{\nu} \left(\frac{C t^{n+1}}{n+1} \right)^{\nu}}.$$

In Table 2.2 are presented results [26] for calculating the flow resulting from the motion of a cylindrical piston described by (2.21). We note that this piston motion corresponds to the flow past a body whose contour extends to infinity in both directions and whose surface has a common point with the shock wave only at infinity; see Fig. 2.21. (In this figure the thickness of the layer between the body and the shock wave has been greatly enlarged for purposes of illustration.) The solution of this type for planar motions, as for solutions of other self-similar motions with shock waves propagating into a gas at rest, can be used to construct flows past airfoils with attached bow waves at the leading edge. Assigning to the quantity m in the function $R = R_0 \mathcal{R}(m/m^*)$ various constant values, we indeed obtain a family of curves which

TABLE 2.2
SELF-SIMILAR EXPONENTIAL SOLUTION,
CYLINDRICALLY SYMMETRIC CASE ($\nu = 2$); $\gamma = 1.4$

R/R_0	p/p^*	ρ/ρ^*	v/v^*	m/m^*
1.0000	1.0000	1.0000	1.0000	1.0000
0.9962	1.0492	1.0786	1.0197	0.9507
0.9924	1.0841	1.1433	1.0325	0.9010
0.9888	1.1166	1.2121	1.0442	0.8509
0.9853	1.1518	1.2917	1.0558	0.8002
0.9820	1.1852	1.3775	1.0665	0.7504
0.9791	1.2177	1.4701	1.0762	0.7004
0.9763	1.2489	1.5698	1.0849	0.6514
0.9735	1.2815	1.6898	1.0934	0.6001
0.9710	1.3129	1.8220	1.1011	0.5482
0.9687	1.3425	1.9674	1.1078	0.4980
0.9667	1.3700	2.1258	1.1136	0.4507
0.9647	1.3944	2.3280	1.1194	0.3992
0.9629	1.4283	2.5557	1.1243	0.3507
0.9612	1.4593	2.8675	1.1292	0.2970
0.9586	1.5232	3.6848	1.1365	0.2033
0.9563	1.5646	5.9430	1.1430	0.0956
0.9552	1.5856	∞	1.1462	0.0000

correspond to streamlines in the equivalent steady motion (one such line is shown in Fig. 2.21). Every such line can be taken as the contour of one side of an airfoil. In this way we can construct flows past various symmetrical and unsymmetrical airfoils. Using cylindrically symmetric solutions, we can similarly construct flows past axisymmetric bodies

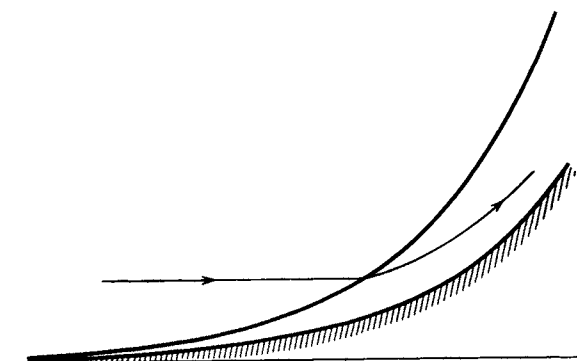


FIG. 2.21. Flow past a body of exponential shape.

whose external surfaces are formed by rotating the chosen streamlines about the axis of symmetry. We can, in this case, remove the cylindrical part of the body situated upstream of the shock wave and consider the body to have a circular hole in front through which the air passes. (This is a so-called annular body. Bodies of such shape are used as intakes in jet engines.)

For the purpose of constructing flows past airfoils or annular bodies of revolution, we can use the self-similar solutions which correspond to the propagation of a shock wave according to the power law (2.13) with an arbitrary value of n ($n \neq -1$), including also those values of n which do not satisfy the condition $n > -\nu/(\nu + 2)$. For values of n which do not satisfy this condition, the solution can be continued from $\mu = 1$ (the shock wave) to $\mu < 1$ but not to $\mu = 0$ (the piston). In fact the continuation can only be carried to some value $\mu = \mu_{\min} > 0$ for which a limit line appears in the flow.[†] For a fixed value of $m > 0$, in the equivalent steady flow we obtain a segment of a streamline which corresponds to a change of m^* (i.e., time) from m to m/μ_{\min} . This streamline segment can be taken to be the contour of an airfoil or body of revolution.

[†] This fact was also pointed out by G. L. Grodzovskii (oral communication) and by Grigoryan [22].

CHAPTER III

NEWTON'S LAW OF RESISTANCE; TANGENT-CONE AND TANGENT-WEDGE METHODS; THE BUSEMANN FORMULA AND THE BOUNDARY LAYER METHOD

1. Newton's law of resistance

The practical importance of the problem of determining the forces acting on bodies at hypersonic speeds has aroused considerable interest in the development of methods for calculating the surface pressures on bodies moving at these speeds. The well-developed linearized method is suitable only for the calculation of flows past slender bodies at low values of the similarity parameter K . This method has been described in great detail in a number of textbooks on aerodynamics and will not be discussed further.

In general, the system of equations describing hypersonic flows past bodies admits some simplification (Chapter I, Section 4 and Chapter II, Section 3), but the system nevertheless remains complicated and does not readily lend itself to solution. Only the boundary conditions at the bow shock wave (Chapter I, Section 4) become simpler for hypersonic flows past bodies (whose thicknesses are not necessarily small). However this fact does not make the solution of the problem any easier in comparison with the general case.

To calculate purely supersonic two-dimensional or axisymmetric flows one can employ different versions of the method of characteristics. Effective methods for calculating three-dimensional supersonic flows or two-dimensional and axisymmetric flows with detached shock waves are only now beginning to be developed (see, for example, [1-3]).

The equations for hypersonic flows past slender bodies with sharp noses can be reduced to the equations for unsteady one-dimensional gas motion (Chapter II, Section 3). For $K \sim 1$ or $K \gg 1$, an effective method for calculating such unsteady flows with planar or cylindrical

symmetry is the numerical method of characteristics. At the present time, other finite difference methods are being developed which seem to offer prospects for the future (see Chapter I, Section 2). These methods, as well as the method of characteristics, are rather time consuming, however, and require the use of high speed computing machines. This is not always convenient for the qualitative analysis of various flow properties or for a rapid estimate of the aerodynamic characteristics of a body.

As already mentioned in the preceding chapter, the study of self-similar unsteady gas flows is of great interest in ascertaining the features of flows past bodies at hypersonic speeds. However, the number of self-similar problems of unsteady flow with planar or cylindrical symmetry which can be applied to supersonic flows past bodies is not very large. On the whole, the problems considered in the present book (see Chapter II, Section 5 and Chapter V, Section 2) exhaust all such solutions.

In view of what has been said, it is of interest to find those physical features of hypersonic flows which allow us to further simplify the equations and at the same time ensure effective solutions for more or less wide classes of bodies. The boundary layer method presented in this chapter and the method to which Chapter IV is devoted, in which the reflected disturbances from the surface of the bow shock wave are neglected, are both based on the physical nature of hypersonic flows past bodies. Both these methods are of interest not only because with their aid one can calculate particular flows, but also because in the process of deriving them we obtain important qualitative information about the general properties of hypersonic flows.

For rapid calculations of the aerodynamic characteristics of bodies, it is also desirable to have simple formulas which may not even be strictly valid from physical or mathematical considerations, but which are good approximations to more exact solutions for the surface pressure distributions on bodies of a variety of classes. Newton's law of resistance gives such a simple formula for the pressure. For airfoils with sharp leading edges or for bodies of revolution with sharp noses, the pressure on the forward portion can also be found by the tangent-wedge or tangent-cone methods, respectively. These approximate methods for the determination of surface pressures in hypersonic flows will be given in this chapter.

The first attempt to determine the resistance of bodies to motion in

gases and liquids from the general laws of mechanics is due to Newton [4]. Newton assumed that the medium flowing around the body was composed of identical non-interacting particles equidistant from each other. When such particles collide with the surface of the body, their component of momentum normal to the surface is altered, with the result that a pressure force is exerted on the body. According to Newtonian theory the pressure on an element of the body surface depends only on the orientation of this element with respect to the incident particle flow, and does not depend on the shape of the rest of the body. It is then evident that the drag of the body is determined solely from the shape of its forward portion if only this part of the body undergoes collisions with the particles. From Newtonian theory it is not possible to find the pressure on those parts of the body surface which lie in the "aerodynamic shadow" (Fig. 3.1) and, according to the theory, that pressure is equal to zero.

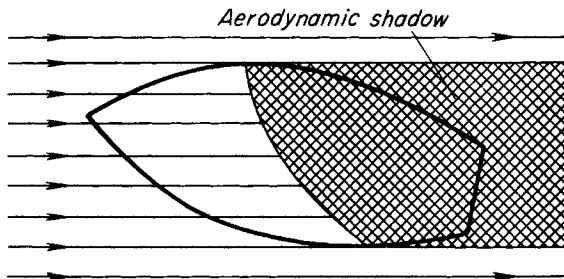


FIG. 3.1. Flow past a body according to the Newtonian model.

In order to determine the value of the pressure produced by the incidence of particles on a body according to Newtonian theory, let us consider an element of surface F which is inclined at an angle α to the direction of the incident flow. The mass of particles which collide with this surface element per unit time is equal to

$$\rho V F \sin \alpha,$$

where ρ is the density of the medium and V is the velocity of the particles. The force acting on the element F as a result of the collisions depends on the nature of the interaction between the particles and the body surface. For inelastic collisions the normal component of this force is equal to

$$\rho V^2 F \sin^2 \alpha.$$

This follows from the fact that the momentum per unit mass in the direction normal to the surface is changed by an amount $V \sin \alpha$. The pressure, defined as the ratio of the normal force to the area on which the force acts, is then equal to

$$p = \rho V^2 \sin^2 \alpha.$$

For inelastic collisions with a smooth surface, the component of momentum tangential to the surface is conserved, and the particles continue to move by inertia along the surface. So long as the motion of the particles is an inertial one, they will move with constant velocity along the geodesic lines of the surface.

The formula obtained by Newton served for more than two centuries as the basis for calculating the drag of bodies moving in air and for determining wind loadings on structural elements—this in spite of the fact that Newton himself expressed doubt as to the possibility of applying his idealized results to flows of real fluids. Indeed, experiments which were carried out on low speed flows in liquids soon after the publication of the “Principia Mathematica” did not corroborate the Newtonian formula [5].

But as was already mentioned in Chapter I in connection with a flat plate at an angle of attack, the hypersonic flow pattern closely resembles that conceived by Newton in his theory of inelastic collisions of particles with a body [5–7]. In this pattern the bow shock wave is close to the surface, so that the disturbance in the flow produced by the body is not propagated upstream. Hence the free stream gas particles almost reach the surface of the body without changing their velocity, and then after crossing the shock wave move in a thin layer between the shock wave and the body surface.

From equations (1.17) and (1.18) it follows that the shock on a flat plate approaches the plate surface when the Mach number is increased, and the pressure on the surface increases (with the free stream pressure held constant). In the limit $M \rightarrow \infty$, the pressure on the surface of the plate is given by the expression

$$p = \frac{2}{\gamma + 1} \rho_1 V^2 \sin^2 \beta.$$

The relation between the flow deflection angle α and the shock angle β takes the form

$$\cot \alpha = \tan \beta \left(\frac{\gamma + 1}{2 \sin^2 \beta} - 1 \right).$$

Thus, for $M \rightarrow \infty$ and $\gamma \rightarrow 1$ the shock wave approaches coincidence with the plate surface and the pressure on the surface agrees with the pressure calculated by the Newtonian formula.

We note that according to the Newtonian theory the surface pressures are the same on a flat plate at an angle of attack α and on a cone of half-angle α in an axisymmetric flow. According to the exact theory these pressures differ from each other for $M = \infty$ and $\gamma > 1$. Figure 3.2a shows the exact dependence on the angle α of the pressure coefficients on a wedge and on a cone for $M = \infty$ and $\gamma = 1.4$. (The values for the cone were obtained by numerical integration of the ordinary differential equations for conical flow, and are taken from the tables of [8].) The same figure also shows the approximate dependence corresponding to the Newtonian formula. Figure 3.2b shows the analogous comparison of the dependence of the shock wave inclination angle β on the angle α . It follows from Fig. 3.2a that the Newtonian formula is in rather good agreement with the exact value of the cone pressure for $M = \infty$, even if $\gamma = 1.4$. For the wedge the agreement with the exact solution for the same value of γ is less satisfactory.

Let us give some further examples of the comparison of the Newtonian formula with more exact calculations and with experimental data for the hypersonic flow of air past bodies. Figure 3.3 shows experimental data, taken from [9], for the surface pressure distribution on a circular cone at an angle of attack for $M = 6.9$. The solid curve shows the values for the pressure obtained by the Newtonian formula.

It has been observed [10]† that a substantial improvement in the agreement of Newtonian calculations with experimental data for symmetric two-dimensional and axisymmetric flows could be obtained if the Newtonian formula

$$C_p = 2 \sin^2 \alpha \quad (3.1)$$

† *Editor's note:* This observation was noted first in Lees, L., Hypersonic Flow, *Proc. 5th Internat. Aero. Conf., Los Angeles*, Inst. Aero. Sci., New York, 241–276 (1955).

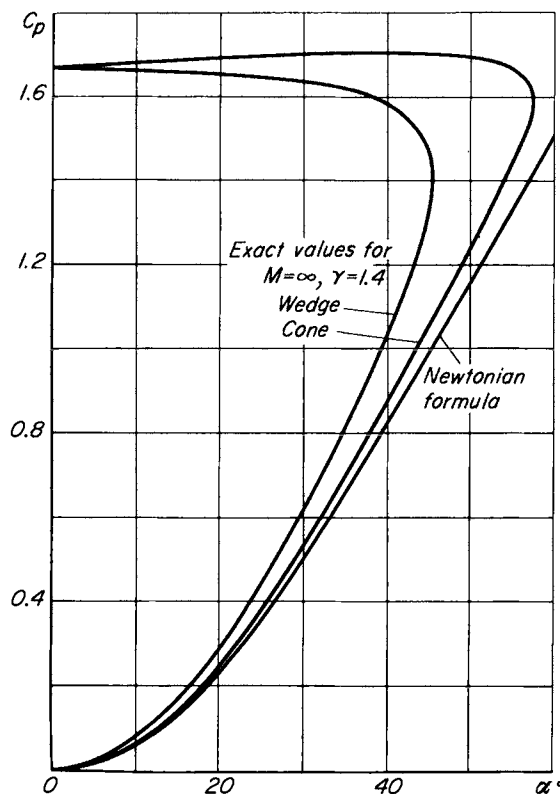


FIG. 3.2a. Surface pressure for a wedge and cone according to the exact theory for $M = \infty$ and $\gamma = 1.4$, and according to the Newtonian model.

were modified and represented in the following manner:

$$C_p = C_p^* \frac{\sin^2 \alpha}{\sin^2 \alpha_0}. \quad (3.2)$$

Here C_p^* is the value of the pressure coefficient at the leading edge or nose of the body, found from the theory of supersonic flow of an ideal gas, and α_0 is the angle between the tangent to the body contour at this point and the free stream direction. For bodies with blunted noses, $\sin \alpha_0 = 1$, and the dependence of C_p^* on M and γ is easily determined with the aid of the normal shock relations and the Bernoulli integral:

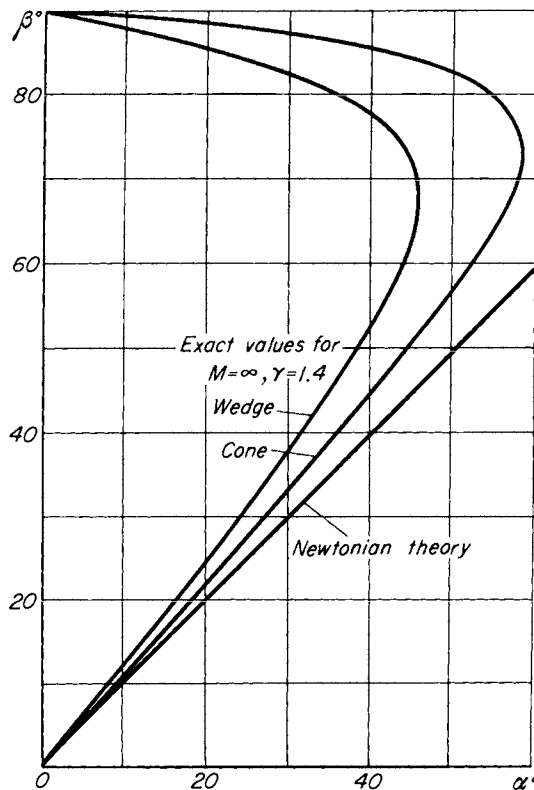


FIG. 3.2b. Angle between bow shock and free stream for a wedge and cone according to the exact theory for $M = \infty$ and $\gamma = 1.4$, and according to the Newtonian model.

$$C_p^* = \frac{2}{\gamma M^2} \left[\left(\frac{\gamma + 1}{2} M^2 \right)^{\gamma/(\gamma-1)} \left(\frac{\gamma + 1}{2\gamma M^2 - \gamma + 1} \right)^{1/(\gamma-1)} - 1 \right]$$

(the Rayleigh formula). Figure 3.4 shows the value of C_p^* as a function of Mach number for $\gamma = 1.4$ as calculated from this formula. For $M = \infty$

$$C_p^* = \frac{2}{\gamma} \left(\frac{\gamma + 1}{2} \right)^{\gamma/(\gamma-1)} \left(\frac{\gamma + 1}{2\gamma} \right)^{1/(\gamma-1)}.$$

For values of γ equal to 1, 9/7, 7/5, and 5/3, the value of C_p^* for $M = \infty$ is equal to 2.00, 1.88, 1.84, and 1.76, respectively.

For flows past sharp-nosed bodies of revolution and airfoils with

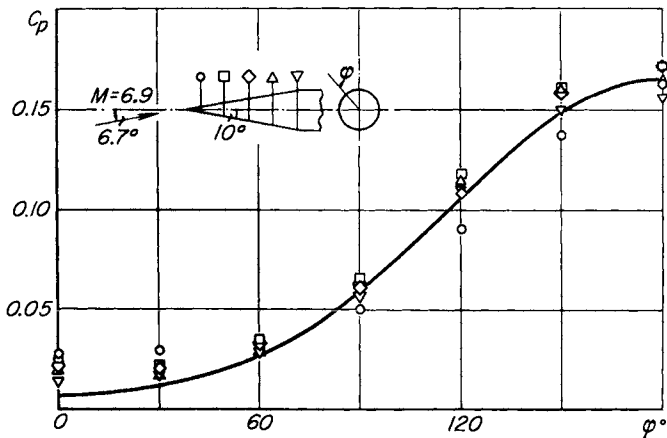


FIG. 3.3. Surface pressure distribution on a cone at angle of attack. Comparison of the Newtonian formula with experiment.

attached shock waves, the value of C_p^* should be found from the solutions for flow past a cone or a wedge. Unfortunately the exact value of C_p^* for a wedge is expressed in terms of M and α_0 only in implicit form, while

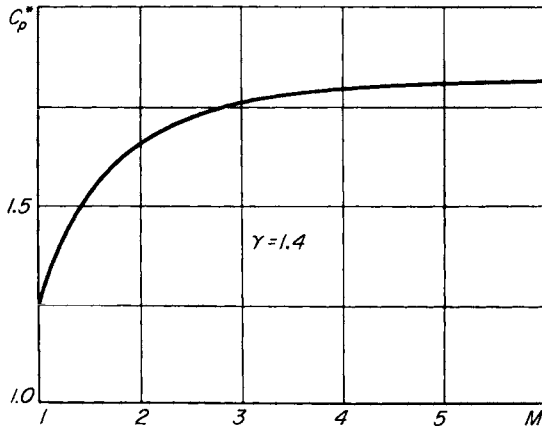


FIG. 3.4. Stagnation point pressure coefficient for supersonic flow past blunt-nosed bodies.

for a cone it can be found only by numerical means. For slender wedges and cones at hypersonic speeds, however, one can obtain approximate analytic expressions for C_p^* . For a wedge such an expression for C_p^* follows from equations (1.20) and (1.21):

$$C_p^* = \frac{4}{\gamma + 1} \frac{K_s^2 - 1}{K^2} \alpha_0^2,$$

$$K_s = \frac{\gamma + 1}{4} K + \sqrt{\left(\frac{\gamma + 1}{4} K\right)^2 + 1}.$$

Approximate expressions for C_p^* for a cone will be considered in Section 3 of this chapter.

The formula (3.2) in which C_p^* is determined in accordance with the above-mentioned considerations will be called the modified Newtonian formula.

In the figures below, experimental data is given for the surface pressure distributions on various blunt-nosed bodies. Figure 3.5 shows data

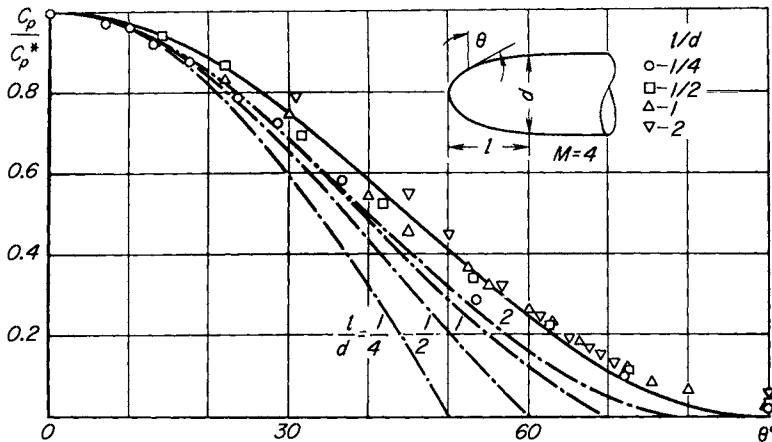


FIG. 3.5. Surface pressure distributions for axisymmetric flows past cylinders with ellipsoidal caps. Comparison of modified Newtonian (—) and Busemann (---) theories with experiment.

for circular cylinders with ellipsoidal caps which have fineness ratios of $\frac{1}{4}$, $\frac{1}{2}$, 1, and 2 in an axisymmetric flow at $M = 4.0$.† (Schlieren photographs of the flow patterns around these bodies are shown in Fig. 3.6.) Figure 3.7 shows the surface pressure distributions on a cone with a spherical cap at $M = 5.6$ to 5.8 [10]. Figure 3.8 gives the surface pressures on a circular cylinder transverse to the flow direction at $M = 3.0$,*

† These tests were carried out by V. I. Shul'gin at the request of the author.

* Experimental data due to G. M. Ryabinkov.

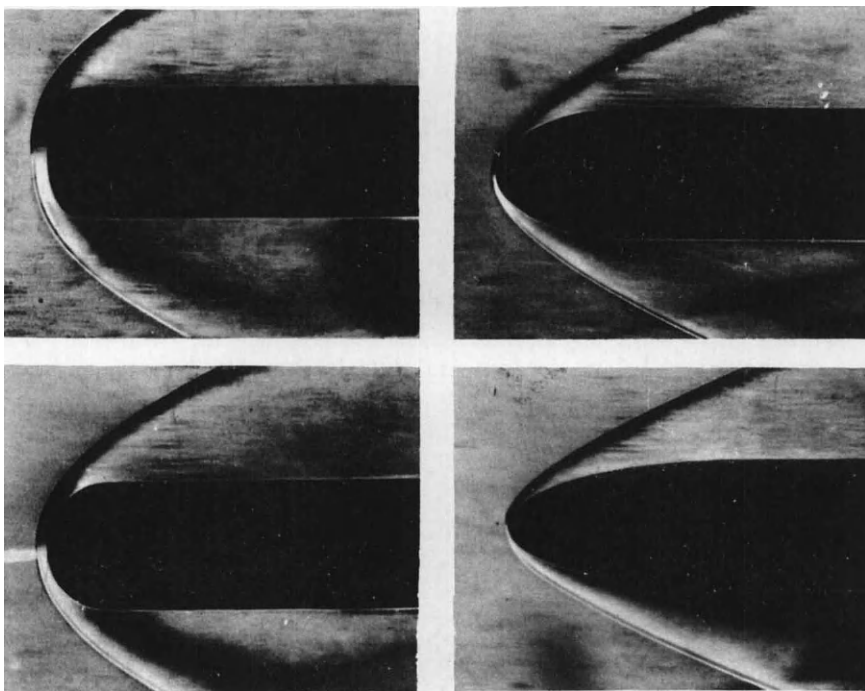


FIG. 3.6. Schlieren photographs of flow past cylinders with ellipsoidal caps at $M = 4$.

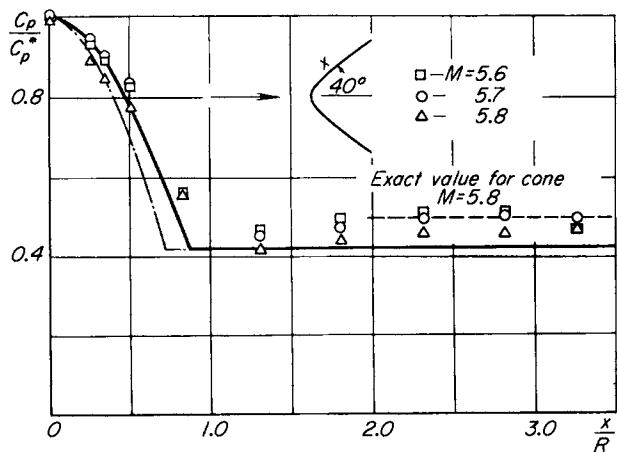


FIG. 3.7. Surface pressure distributions on a cone with a spherical cap. Comparison of modified Newtonian (—) and Busemann (---) theories with experiment.

4.0 [11], and 5.8 [10]. The solid curves in these figures represent the values of the pressure coefficients calculated from the modified Newtonian formula. The dashed lines plotted in Fig. 3.8 represent the pressures found from a numerical solution of the flow past a cylinder with

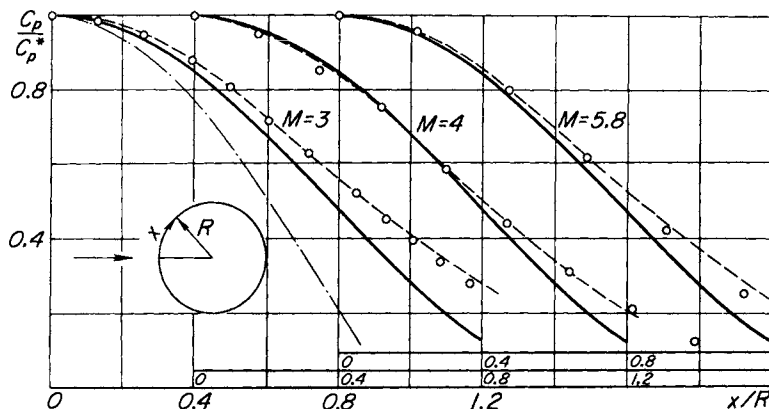


FIG. 3.8. Pressure distributions on the front side of a circular cylinder transverse to the flow direction. Comparison of modified Newtonian (—) and Busemann (---) theories, and exact numerical calculations (- - -) with experiment.

the aid of a high speed computing machine [2]. The results given in these figures show that the modified Newtonian formula agrees well with experiment for flows past bodies of revolution, although the agreement is somewhat poorer for flows past two-dimensional profiles.

2. Use of the Newtonian formula for determining aerodynamic characteristics of bodies and for finding bodies of minimum drag

On the basis of the results presented in the previous section we may conclude that the Newtonian formula can be used to determine the hypersonic aerodynamic characteristics of wedge or conelike bodies and of bodies similar to those depicted in Figs. 3.5 to 3.8, in those cases where a high degree of accuracy is not required.* We shall employ this formula for the comparative analysis of the aerodynamic characteristics of some

* Additional considerations concerning the accuracy of the Newtonian formula will be presented in Section 4 of this chapter.

simple bodies at hypersonic speeds, as well as for finding body shapes having the lowest drag at these speeds.

Let us consider a plane-convex airfoil whose cross section has the form of an isosceles triangle, and a biconvex airfoil of diamond cross section both of which have the same maximum thickness ratio τ (Fig. 3.9).

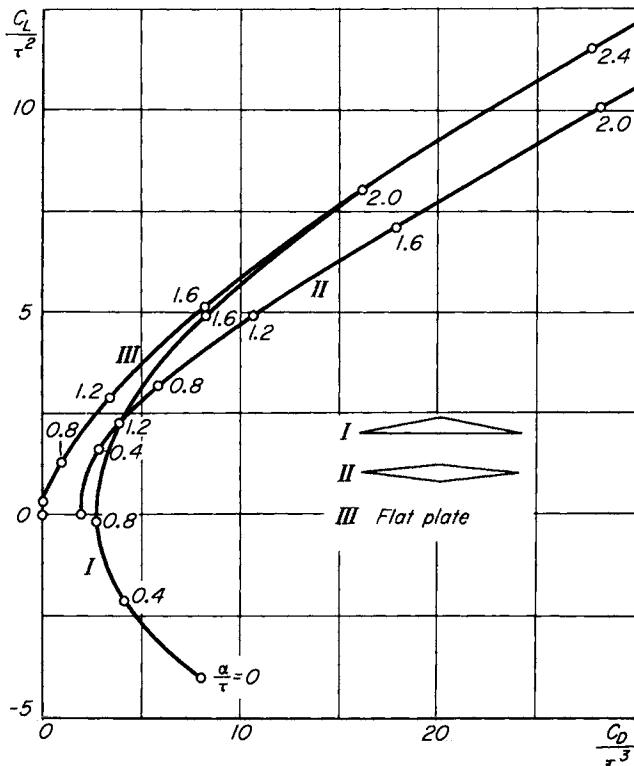


FIG. 3.9. Polar diagrams for airfoils at hypersonic speeds constructed by use of the Newtonian formula.

Limiting ourselves to small thickness ratios and small angles of attack α , we shall obtain from the Newtonian formula expressions for the drag and lift coefficients of these airfoils. For an airfoil of triangular section

$$\frac{C_D}{\tau^3} = 2 \left(\frac{\alpha}{\tau} \right)^3 + \left(2 - \frac{\alpha}{\tau} \right)^3,$$

$$\frac{C_L}{\tau^2} = 2 \left(\frac{\alpha}{\tau} \right)^2 - \left(2 - \frac{\alpha}{\tau} \right)^2.$$

The second terms in these expressions need be taken into account only for $\alpha/\tau < 2$. For large angles of attack the pressure on the upper surfaces of the airfoil becomes zero and the airfoil behaves like a flat plate. For a diamond shaped airfoil

$$\frac{C_D}{\tau^3} = \left(1 + \frac{\alpha}{\tau}\right)^3 + \left|1 - \frac{\alpha}{\tau}\right|^3,$$

$$\frac{C_L}{\tau^2} = \left(1 + \frac{\alpha}{\tau}\right)^2 - \left|1 - \frac{\alpha}{\tau}\right| \left(1 - \frac{\alpha}{\tau}\right).$$

In agreement with the results which follow from the similarity law for hypersonic flows past slender bodies, which was developed in Section 2 of Chapter II, the quantities C_D/τ^3 and C_L/τ^2 for both airfoils depend only on the ratio α/τ . Figure 3.9 shows the polar diagrams, calculated neglecting skin friction,* for these two airfoils and for a flat plate airfoil which has the highest lift-drag ratio at supersonic speeds (i.e., the ratio C_L/C_D). From an examination of Fig. 3.9 it can be seen that the triangular airfoil with a flat lower surface possesses a definite advantage in comparison with the diamond airfoil. For sufficiently large angles of attack the lift-drag ratio of the triangular airfoil is higher than for the diamond airfoil. We note that for moderate supersonic speeds the excess aerodynamic pressure on the forward-facing parts of the surface is proportional to the first power of the angle between the flow and the surface. Furthermore, the pressure decrease on those parts of the surface located in the aerodynamic shadow is of the same order of magnitude as the pressure increase on the forward-facing parts of the surface (Ackeret theory). Therefore, at moderate supersonic speeds the diamond airfoil possesses a higher lift-drag ratio than the triangular one.

The conclusion as to the advantage of the triangular over the diamond airfoil at hypersonic speeds is actually more general. For hypersonic speeds, when the pressure on the forward-facing parts of the surface is proportional to the square of the angle between the flow and the surface, and the pressure in the aerodynamic shadow is zero, then the decisive role in the development of the aerodynamic forces acting on the airfoil is played by the lower surface of the airfoil making a larger angle with the

* Polar diagrams for the triangular and diamond airfoils calculated by more exact relations will be presented in Fig. 4.5.

free stream. Hence the lift-drag ratio at such speeds of an airfoil with a flat lower surface is higher than that of a biconvex airfoil with the same thickness ratio.

A similar conclusion can also be drawn for bodies in three-dimensional flows. In Fig. 3.10 are given the polar diagrams (neglecting skin friction)

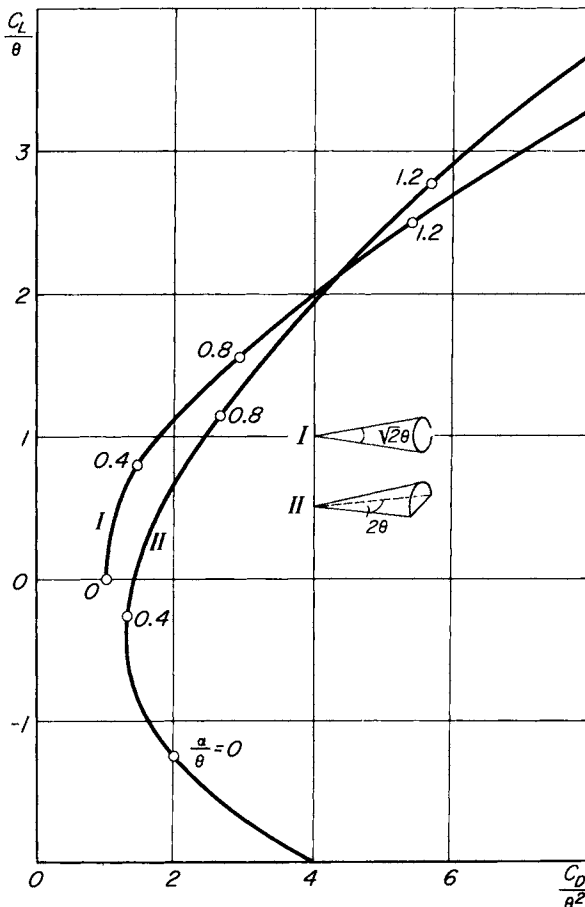


FIG. 3.10. Polar diagrams for a cone and half-cone at hypersonic speeds constructed by use of the Newtonian formula.

for two slender bodies having the same maximum cross-sectional area and the same length. The bodies are a circular cone of half-angle $\theta/\sqrt{2}$ and a cone of semicircular cross section with a half-angle θ . Once again

the lift-drag ratio of the half-cone is higher than that of the circular cone. This fact, first shown in [12], can have an important influence on the choice of the forebody shape of a vehicle which employs lift and which is intended for flight at hypersonic speeds.

Let us now apply the Newtonian formula to find bodies which have the lowest drag at hypersonic speeds. As already pointed out (Chapter II, Section 1), the drag associated with the appearance of shock waves can be most important at these speeds, and is essentially dependent on the shape of the body. For flows past bodies which are not very slender, it exceeds by far the drag due to viscous forces. Therefore it is natural to attempt to find by theoretical means those body shapes which have the lowest drag at a given velocity in an ideal gas, and which satisfy certain supplementary constraints (bodies which have given volumes and lengths, for example, or given transverse and axial dimensions, etc.).

A great many problems concerned with the determination of body shapes of minimum drag in supersonic flow have been solved within the framework of linearized theory. According to this theory the two-dimensional airfoil of minimum drag for a given maximum thickness ratio has a diamond cross section with the location of the maximum thickness at the center of the chord [13]. Within the framework of linearized theory, airfoils which have minimum drag for other supplementary constraints are also made up of straight line segments. We note, for example, that for $M = 2$ with a maximum thickness ratio equal to 0.1, the drag coefficient of the optimum airfoil is 0.0226, whereas the drag coefficient of the airfoil formed by two circular arcs is 0.0308.

The first minimum-drag problem for a body of revolution in supersonic flow was solved by von Kármán [14]. He determined the shape of the forebody of minimum drag for a given length. Its equation has the form

$$\frac{y}{y_1} = \sqrt{\frac{2}{\pi} \sin^{-1} \sqrt{x} - \frac{2}{\pi} \sqrt{x(1-x)(1-2x)}}.$$

(Here the length of the body is taken to be unity, the x -axis is in the direction of the free stream velocity, and the y -axis is perpendicular to it.) The drag coefficient of such a forebody is equal to $4y_1^2$, while the drag coefficient of an ogival shaped forebody is approximately 15 per cent greater than this value.

Besides von Kármán's solution, some other solutions are also known

for minimum-drag problems for bodies of revolution. For example, the problem of determining the shape of a body which has minimum drag for a given volume and given length has been solved [15], and the shape of an annular body which has minimum drag for a given length, entrance area of the annulus, and a given maximum cross-sectional area has also been determined [16]. In addition, within the limits of linearized theory a number of variational problems have been solved for three-dimensional supersonic flows. We note a recently published paper [17] devoted to this question.

Despite the availability of a considerable number of solutions of linearized problems concerned with minimum-drag bodies in supersonic flow, these solutions cannot be applied at hypersonic speeds for the reasons already given. But for such speeds the Newtonian formula can be used for the solution of variational problems concerned with finding minimum-drag bodies. The first such solution was given by Newton himself [4]. We shall reproduce here the result which he obtained. According to the formula

$$p = \rho_1 V^2 \sin^2 \alpha,$$

the drag force acting on the surface of an airfoil or body of revolution of length l is equal to

$$D = \rho_1 V^2 \int_0^l (2\pi y)^{\nu-1} \frac{y'^3}{1+y'^2} dx, \quad (3.3)$$

where $\nu = 1$ for two-dimensional flow and $\nu = 2$ for axisymmetric flow. This expression enables us to solve various problems concerned with the determination of the shape of minimum-drag bodies. As an example let us consider the simplest case, when the coordinates of the front and rear ends of the body are given—i.e., $y(0) = y_0$, $y(l) = y_1$ (in two-dimensional flow one can always take $y_0 = 0$). As is well known, the determination of the minimum of equation (3.3) for the drag force is reduced to the solution of the differential equation

$$\frac{\partial F}{\partial y} - \frac{d}{dx} \frac{\partial F}{\partial y'} = 0, \quad (3.4)$$

where

$$F = y^{\nu-1} \frac{y'^3}{1+y'^2}.$$

Since in the case being considered the function F does not contain x explicitly,

$$\frac{dF}{dx} = \frac{\partial F}{\partial y} y' + \frac{\partial F}{\partial y'} y'',$$

so that from equation (3.4) we obtain

$$0 = \frac{dF}{dx} - \left(y' \frac{d}{dx} \frac{\partial F}{\partial y'} + y'' \frac{\partial F}{\partial y'} \right) = \frac{dF}{dx} - \frac{d}{dx} \left(y' \frac{\partial F}{\partial y'} \right).$$

The integral of this equation is

$$F - y' \frac{\partial F}{\partial y'} = \text{const},$$

which upon substitution of the values of F and $\partial F/\partial y'$ takes the form

$$\frac{y^{\nu-1} y'^3}{(1 + y'^2)^2} = \text{const}. \quad (3.5)$$

Thus in a two-dimensional flow ($\nu = 1$) the extremals are straight lines so that the body of minimum drag in Newtonian theory is a wedge, as in linearized theory. (In the exact theory of supersonic flow of an ideal gas this result is not correct; see Chapter IV, Section 4.) In axisymmetric flow ($\nu = 2$) the equation for the extremals can be easily represented in parametric form by taking as the parameter the quantity $p = y'$, which is the tangent of the local inclination angle of the body to the free stream flow. According to the equality (3.5)

$$y = C \frac{(1 + p^2)^2}{p^3}.$$

By integrating the relation $dx = dy(p)/p$, we then obtain

$$x = C \left(\frac{3}{4p^4} + \frac{1}{p^2} + \ln p \right) + C_1.$$

In Fig. 3.11 the dependence of y upon x as given by the above relations is presented in graphical form.* The curve has a cusp point for $p = \sqrt{3}$.

* In a recently published paper [18] this dependence was obtained by a numerical integration of the equation for the extremals (3.3). For $p > \sqrt{3}$ the results do not correspond to the correct solution.

In the construction of the curve, the scale constants C and C_1 in the expressions for y and x were chosen so that the cusp point coincides with the point $x = 0, y = 1$. (For finding the minimum-drag configurations only the lower branch of the curve should be used. On this branch the

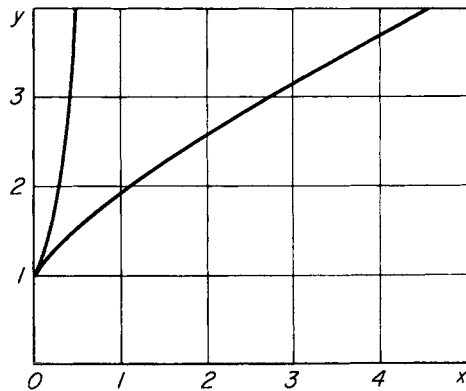


FIG. 3.11. Body of revolution having minimum drag, when the pressure is determined by the Newtonian formula.

Legendre condition $\partial^2 F / \partial y'^2 \geq 0$, which here implies $p \leq \sqrt{3}$, is fulfilled.) Let us denote by $Y_N(p)$ and $X_N(p)$ the dependence of y and x upon p corresponding to the constants which were chosen. Then if the length of the body is taken equal to unity, the shape of the body of minimum drag for given y_0 and y_1 is determined by the expressions

$$y = \frac{Y_N(p)}{X_N(p_1) - X_N(p_0)},$$

$$x = \frac{X_N(p) - X_N(p_0)}{X_N(p_1) - X_N(p_0)}.$$

Here p_0 and p_1 are obviously related to y_0 and y_1 by

$$y_0 = \frac{Y_N(p_0)}{X_N(p_1) - X_N(p_0)},$$

$$y_1 = \frac{Y_N(p_1)}{X_N(p_1) - X_N(p_0)}.$$

The Newtonian solution has been used to study the properties of minimum-drag bodies at hypersonic speeds in [19].*

* *Editor's note:* See also [30].

3. Tangent-cone and tangent-wedge methods

The satisfactory agreement at hypersonic speeds of the results of pressure calculations by the Newtonian formula (3.1) with experiment and with the results of more exact theoretical calculations is evidence of the fact that at such speeds the pressure on the forward facing surfaces of the body is determined principally by the local angle between the surface and the free stream flow. This feature of the flow suggests an idea for examining flows at hypersonic speeds past airfoils with sharp leading edges or bodies of revolution with sharp noses. The idea is to take the pressure at any point on the surface equal to the pressure on a wedge (for flow past airfoils) or on a cone (for flow past bodies of revolution) which is tangent to the point being considered, and which is subject to the same flow. This method was proposed by S. V. Vallander in 1949 and was termed the tangent-cone method (for the calculation of the pressure on bodies of revolution in axisymmetric flows) or the tangent-wedge method (for the calculation of the pressure on airfoils).*

For all their simplicity, the inconvenience of the tangent-cone and tangent-wedge method consists in the fact, pointed out earlier, that, in general, the dependence of the wedge pressure on the wedge angle can be represented only in implicit form, and the solution of the problem of flow past a cone can be obtained only by numerical means. For this reason it is not possible to exactly represent pressure distributions on bodies in simple analytic form. In order to avoid this difficulty, one can use various approximate analytic solutions for the wedge and cone flows. The simplest such solution is given by the Newtonian formula (3.1). Thus the method of calculating supersonic flows past sharp-nosed airfoils and bodies of revolution using this formula can be considered as one of the variants of the tangent-cone or tangent-wedge method. It is possible to find more exact analytic expressions for the pressure on a wedge or cone, however, which are more suitable for hypersonic speeds. For a wedge the pressure can be determined by equations (1.20) and (1.21). We shall now give one of the methods for obtaining expressions

* *Editor's note:* This method was presented by Vallander in his doctoral thesis at Leningrad University. The actual terminology he employed was "the method of tangent cones" and "the method of tangent wedges." For independent Western references on these methods the reader is referred to Hayes and Probstein [26].

for the pressure on a cone [20]. (These same expressions will be obtained by other means further on in the present chapter.)

The system of equations which describes the axisymmetric flow past a circular cone can be set up in the following manner: Let us denote by u the velocity component of the gas along a ray emanating from the apex of the cone at an angle ϑ to its axis, and by v the velocity component along the normal to the ray in the meridian plane (Fig. 3.12). If $s(\vartheta)$ is

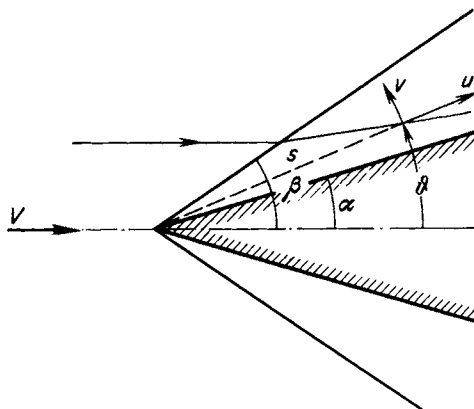


FIG. 3.12. Supersonic flow past a cone.

the distance along the ray from the apex of the cone to a streamline, then

$$s d\vartheta = ds \frac{v}{u}.$$

Taking into consideration the fact that the flow parameters are constant along each ray (see, for example, [21, 22]), it is a simple matter to write the conditions of conservation of mass and the condition of irrotationality of the flow (the condition of the absence of circulation around a closed contour) as

$$\frac{d}{d\vartheta} \rho v s^2 \sin \vartheta = 0$$

and

$$\frac{du}{d\vartheta} - v = 0. \quad (3.6)$$

We now use the Bernoulli integral

$$a^2 = C - \frac{\gamma - 1}{2} (u^2 + v^2)$$

and the condition of isentropic flow, which may be expressed as

$$a^2 = \gamma \frac{p}{\rho} = \gamma C_1 \rho^{\gamma-1}$$

(C and C_1 are constants). After eliminating s , the continuity equation is easily transformed to the following form:

$$\frac{dv}{d\vartheta} + u = \frac{a^2(u + v \cot \vartheta)}{v^2 - a^2}. \quad (3.7)$$

In order to solve equations (3.6) and (3.7) it is necessary to formulate the boundary conditions on the surface of the cone where $\vartheta = \alpha$, and at the bow shock wave where $\vartheta = \beta$. Since the angle β is found from the solution and is not known beforehand, it follows that the total number of boundary conditions necessary to solve the problem is three.

For $\vartheta = \alpha$ one must fulfill the flow condition

$$v = 0.$$

We shall take as the conditions to be fulfilled for $\vartheta = \beta$, the momentum equation along the tangent to the shock and the continuity equation

$$u_2 = V \cos \beta, \quad -v_2 = \frac{\rho_1}{\rho_2} V \sin \beta. \quad (3.8)$$

(Two other relations at the shock are necessary to determine the constants C and C_1 .) Let us assume that the surface of the bow shock is near the surface of the cone, so that the quantity $\vartheta - \alpha$ is small in the flow region of interest to us between the shock wave and the cone. Then we can approximately represent the unknown functions u and v in the form of the leading terms of their expansions in powers of the difference $\vartheta - \alpha$. Since $v = 0$ for $\vartheta = \alpha$, it follows from equations (3.6) and (3.7) that on the surface of the cone

$$u' = 0, \quad v' = u'' = -2u_e.$$

Therefore near the cone surface

$$\frac{u}{u_c} = 1 - (\vartheta - \alpha)^2, \quad \frac{v}{u_c} = -2(\vartheta - \alpha).$$

In order to determine the relation between β and α we substitute these expressions into equations (3.8) at the bow wave. Neglecting higher order quantities, we obtain after substitution

$$\beta - \alpha = \frac{1}{2} \frac{\rho_1}{\rho_2} \beta. \quad (3.9)$$

For a perfect gas with constant specific heats the density ratio ρ_1/ρ_2 is determined by the relation [see (1.10)]

$$\frac{\rho_1}{\rho_2} = \frac{\gamma - 1}{\gamma + 1} + \frac{2}{\gamma + 1} \frac{1}{M^2 \sin^2 \beta}.$$

We note that if $\rho_1/\rho_2 \rightarrow 0$, i.e., if for a perfect gas $\gamma \rightarrow 1$ and $M \rightarrow \infty$, then $\beta \rightarrow \alpha$ and the layer of disturbed gas between the cone surface and the bow shock wave becomes infinitely thin and the shock wave coincides with the cone surface. Thus, the assumption made above, that the difference $\beta - \alpha$ is small, is justified for large values of the Mach number and for γ not very different from one.

When not only the difference $\beta - \alpha$ is small but the quantity β is also small (hypersonic flow past a slender cone), then in accord with the hypersonic similarity law for slender bodies we obtain from equation (3.9)

$$K_s - K = \frac{1}{2} \frac{\gamma - 1}{\gamma + 1} \left(K_s + \frac{2}{\gamma - 1} \frac{1}{K_s} \right), \quad (3.10)$$

where $K = M\alpha$ and $K_s = M\beta$. From this relation we find

$$\frac{K_s}{K} = \frac{\gamma + 1}{\gamma + 3} + \sqrt{\left(\frac{\gamma + 1}{\gamma + 3} \right)^2 + \frac{2}{\gamma + 3} \frac{1}{K^2}}.$$

This equation is compared in Fig. 2.12 with the values of K_s/K obtained by means of numerical integration of the exact equations for conical flow [8]. Equation (3.10) corresponds to the dashed curve in Fig. 2.12. The solid line in this figure corresponds to the dependence found using the equivalence principle. This dependence is well approximated by the relation

$$\frac{K_s}{K} = \sqrt{\frac{\gamma + 1}{2} + \frac{1}{K^2}}. \quad (3.11)$$

This relation will be obtained in Chapter V, Section 4 from another approximate solution of the problem of hypersonic flow past a slender cone.

To use the tables of [8] for obtaining the exact values of K_s/K , it was assumed that $K = M \tan \alpha$ and $K_s = M \tan \beta$. An examination of Fig. 2.12 shows that the approximate formulas (3.10) and (3.11) are good approximations to the exact values of K_s/K over the range of angles α and free stream Mach numbers for which the hypersonic similarity law is valid, i.e., for which there exists a single relationship between K_s and K .

In order to determine the value of the pressure on the cone p_c we use the adiabatic condition and write the ratio p_c/p_1 in the following form:

$$\frac{p_c}{p_1} = \frac{p_c}{p_2} \frac{p_2}{p_1} = \left(\frac{a_c^2}{a_2^2} \right)^{\gamma/\gamma-1} \frac{p_2}{p_1}. \quad (3.12)$$

We find the second factor in this expression from the relation across the bow shock wave

$$\frac{p_2}{p_1} = \frac{2\gamma}{\gamma + 1} K_s^2 - \frac{\gamma - 1}{\gamma + 1}.$$

In order to find the first factor we employ the Bernoulli integral which gives the following relationship between the variables behind the shock wave and at the surface of the cone:

$$\frac{a_c^2}{a_2^2} = 1 + \frac{\gamma - 1}{2} \frac{u_2^2}{a_2^2} \left[1 - \left(\frac{u_c}{u_2} \right)^2 + \left(\frac{v_2}{a_2} \right)^2 \right].$$

On using the approximate expressions $u_2/u_c = 1 - (\beta - \alpha)^2$ and $v_2/u_c = -2(\beta - \alpha)$ it follows that

$$\frac{a_c^2}{a_2^2} \approx 1 + (\gamma - 1) \frac{a_1^2}{a_2^2} (K_s - K)^2,$$

so that

$$\frac{p_c}{p_2} \approx 1 + \gamma \frac{a_1^2}{a_2^2} (K_s - K)^2.$$

Substituting the expressions for p_c/p_2 and p_2/p_1 into equation (3.12), we find after some simple calculation

$$C_p M^2 = \frac{2}{\gamma} \left(\frac{p_c}{p_1} - 1 \right) = \frac{4}{\gamma + 1} (K_s^2 - 1) + 2(K_s - K)^2 \frac{\gamma + 1}{\gamma - 1 + \frac{2}{K_s^2}}. \quad (3.13)$$

Here K_s and K are related by (3.10). In Fig. 2.5 a comparison is given of the values of C_p/α^2 calculated by equation (3.13) (dashed curve) with the exact values [8].

It follows from equation (3.13) that for $M = \infty$

$$\frac{C_p}{\alpha^2} = 2 \frac{(\gamma + 1)(\gamma + 7)}{(\gamma + 3)^2}.$$

For values of γ equal to 1, 9/7, 7/5, and 5/3, the right-hand side of this expression is equal to 2.00, 2.06, 2.08, and 2.12, respectively. Equations (3.13) and (3.10) or (3.11) can serve as the basic analytic relations in the tangent-cone method.

In order to use this method for the calculation of pressure distributions on slender bodies of revolution, the angle α must be identified with the local value of the tangent of the inclination angle of the body to the free stream direction, so that

$$K = M \frac{dy}{dx} = M\tau \frac{d\bar{y}}{d\bar{x}} = K_0 \frac{d\bar{y}}{d\bar{x}}.$$

Here τ is the thickness ratio, and \bar{x} and \bar{y} are the body coordinates made dimensionless with respect to the body length and maximum diameter, respectively.

As an example of the application of the tangent-cone method let us consider the flow past a family of parabolic bodies [23]. For such bodies

$$K = K_0(1 - \bar{x}).$$

Since $K \rightarrow 0$ for $\bar{x} \rightarrow 1$, it is evident that the condition $K > 1$, which must be met in order that equations (3.13) and (3.10) apply, is not fulfilled near the rear of the body. The pressure distribution (for $\gamma = 1.4$) is given by the equation

$$\frac{2}{\gamma} \left(\frac{p}{p_1} - 1 \right) = 1.041 K_0^2 (1 - \bar{x})^2 - 0.454 + \sqrt{1.084 K_0^4 (1 - \bar{x})^4 + 1.656 K_0^2 (1 - \bar{x})^2}.$$

For values of K_0 equal to 1.0, 1.5, 2.0, and 2.29, a comparison is presented in Fig. 3.13 of the pressure distributions calculated by this equation

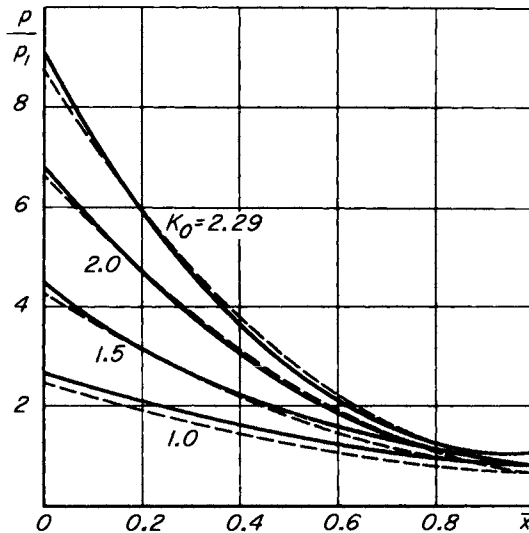


FIG. 3.13. Surface pressure distributions on ogives: --- tangent-cone; —— method of characteristics.

(dashed curves) with the distributions obtained by the method of characteristics (solid curves). There is satisfactory agreement between the exact and approximate values everywhere except in the vicinity of the base of the bodies.

Figure 3.14 shows a graph of the function $F(K_0)$ which enters into the drag law:

$$\begin{aligned} F(K_0) &= C_D M^2 \\ &= 0.347 K_0^2 - 0.454 - \frac{1}{K_0^4} [4.278 N^3 - (1.382 K_0^2 + 1.055)^2 N \\ &\quad + (0.608 K_0^2 + 0.464) \ln (2.400 N + 1.309 K_0^2 + 1)], \end{aligned}$$

where

$$N = \sqrt{0.297 K_0^4 + 0.454 K_0^2},$$

and where C_D is based on the cross-sectional area at the rear of the body. The points plotted in this figure represent the values obtained by the method of characteristics calculations. As can be seen from this figure,

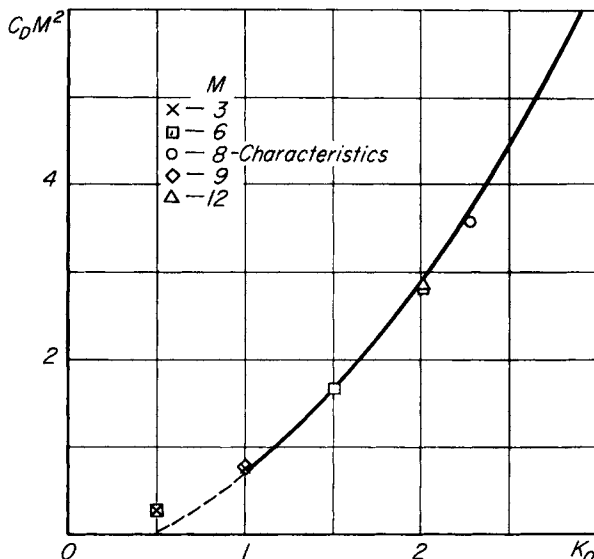


FIG. 3.14. Drag of ogives. Comparison between tangent-cone and method of characteristic calculations.

the tangent-cone method using equations (3.13) and (3.10) or (3.11) to calculate the pressure gives very satisfactory results for the determination of the drag coefficient for $K_0 > 1$, at least in the range $\tau < \frac{1}{3}$ and $M > 3$.

4. The Busemann formula

It was shown before that for a perfect gas with $\gamma = 1$ and $M = \infty$, the gas particles in wedge or axisymmetric cone flow move along straight lines in an infinitely thin layer adjacent to the surface in which the density of the gas is infinitely large. The pressure on the surface of the wedge and cone coincides with the pressure behind the shock wave and is determined by the Newtonian formula

$$p = \rho_1 V^2 \sin^2 \alpha.$$

In supersonic flows past bodies, the normal velocity component of the gas behind the shock wave is expressed in general by the relation [see (1.9)]

$$v_n = \left(1 - \frac{\rho_1}{\rho_2}\right) D,$$

where D is the normal component of the propagation velocity of the bow wave. If the density ratio across the shock becomes indefinitely large, i.e., if for a perfect gas we let $\gamma \rightarrow 1$ and $M \rightarrow \infty$ in equation (1.18), then the bow wave coincides with the body surface, since the boundary condition at the body surface $v_n = V_n$ (V_n is the normal velocity component of points on the body surface) is satisfied for this case.

On the other hand the pressure on the body surface is not generally equal to the pressure behind the shock wave, since the gas particles move along curvilinear trajectories, so that one must take account of the centrifugal forces which balance the pressure difference between points behind the shock wave and points on the body surface [24]. Despite the

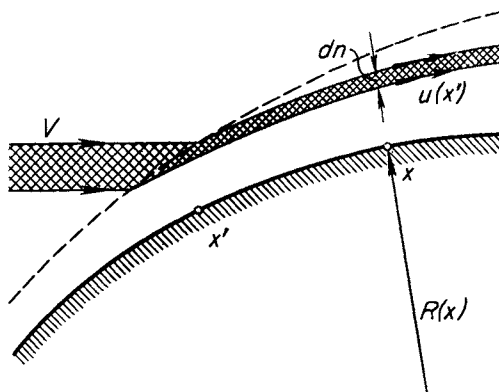


FIG. 3.15. Sketch for derivation of the Busemann formula.

infinitesimal thickness of the layer, this pressure difference has a finite value because of the infinite density of the gas in the layer. The value of the pressure difference depends on the distribution of gas velocity and density across the layer. Based on the postulate of inelastic collisions and the absence of frictional forces, we assume that the velocity of a particle

remains unchanged after collision with the surface and that the particles move along the geodesic lines of the surface. Under this assumption we shall determine the pressure difference in the layer for two-dimensional and axisymmetric flows.* Let us consider the motion of the particles along the surface of the body after collision; see Fig. 3.15. (The layer in which the moving particles are affected by the body, depicted between the dashed line and the body contour in this figure, must be thought of as infinitely thin.) At the point x , the pressure difference dp in the infinitesimal layer composed of particles which collided with the surface near the point x' and which have the velocity $u(x')$, is equal to

$$dp = \frac{\rho(x, x') u^2(x')}{R(x)} dn. \quad (3.14)$$

Here $R(x)$ is the radius of curvature of the body and dn is the thickness of the above-mentioned infinitesimal layer along the outward normal to the surface. From the condition of conservation of mass in the layer we obtain

$$\rho(x, x') u(x') l(x) dn = \rho_1 V dF(x'),$$

where $l(x)$ is equal to 1 and $2\pi r(x)$, respectively, for two-dimensional and axisymmetric flows; F is the cross-sectional area of the body in a plane normal to the direction of the free stream flow, and r is the radial coordinate for the body of revolution.

Using this expression together with

$$R = - \frac{dx}{d\alpha} = - \frac{1}{\sin \alpha} \frac{dr}{d\alpha},$$

we can transform the relation (3.14) into

$$dp = - \rho_1 V \sin \alpha \frac{d\alpha}{dF} u(x') dF(x').$$

Since the velocity component of a particle tangential to the body surface is unaltered by the collision, $u(x') = V \cos \alpha(x')$. Integrating the equa-

* The effect of centrifugal forces on flows past bodies of revolution is analyzed in [25] with various assumptions concerning the distribution of the flow parameters in the layer. The centrifugal force calculation for flows past bodies of arbitrary shape under the assumptions made in the present section was given in [26] and [27].

tion for dp and taking into account the fact that at the outer boundary of the layer $p = \rho_1 V^2 \sin^2 \alpha$, we find the pressure on the body surface to be

$$p = \rho_1 V^2 \left(\sin^2 \alpha + \sin \alpha \frac{d\alpha}{dF} \int_{F_0}^F \cos \alpha dF \right). \quad (3.15)$$

In contrast to the Newtonian formula, the pressure at a given point on the surface according to this expression is determined not only by the local orientation of the surface with respect to the free stream flow, but also by the shape of the surface upstream of this point.

The formula (3.15) was first given in [24], so that we shall call it the Busemann formula. For later use we rewrite the Busemann formula in the following modified form:

$$C_p = \frac{C_p^*}{\sin^2 \alpha_0} \left(\sin^2 \alpha + \sin \alpha \frac{d\alpha}{dF} \int_{F_0}^F \cos \alpha dF \right).$$

Here C_p^* and α_0 have the same values as in the modified Newtonian formula (3.2).

Equation (3.15) can only be used for $p > 0$, as with the Newtonian formula. At the point where the pressure becomes zero, the layer of condensed gas becomes detached from the body. Between the moving gas and the body surface a region of vacuum is formed so that the pressure on the surface everywhere in this region is equal to zero. The shape of this free layer of condensed gas is easily found by equating to zero the right-hand side of equation (3.15) for the pressure [28].* It follows that for the calculation of the drag of a body using the formula (3.15), the integral is taken only along that part of the surface where the pressure is greater than zero.

We find for slender sharp-nosed bodies, replacing the sine of the angle α by the value of the angle itself and the cosine of the angle by one in the formula (3.15),

$$p = \rho_1 V^2 \left(r'^2 + \frac{1}{\nu} rr'' \right), \quad (3.16)$$

* Editor's note: See also [26].

or in the modified form,

$$C_p = \frac{C_p^*}{\sin^2 \alpha_0} \left(r'^2 + \frac{1}{\nu} rr'' \right)$$

where $r = r(x)$ is the equation of the body. According to the expression (3.16), the pressure on an element of the body surface depends only on the local geometrical characteristics of the element, in contrast to the formula (3.15).

We shall present results using the formula (3.15) for finding the pressure distributions on bodies in air ($\gamma = 1.4$). This formula takes into account not only the pressure which arises from collisions of the particles with the body but also the effect of the centrifugal forces in the layer. In Figs. 3.5, 3.7, and 3.8 comparisons are given of the Newtonian pressure coefficients on various body surfaces with more exact theoretical

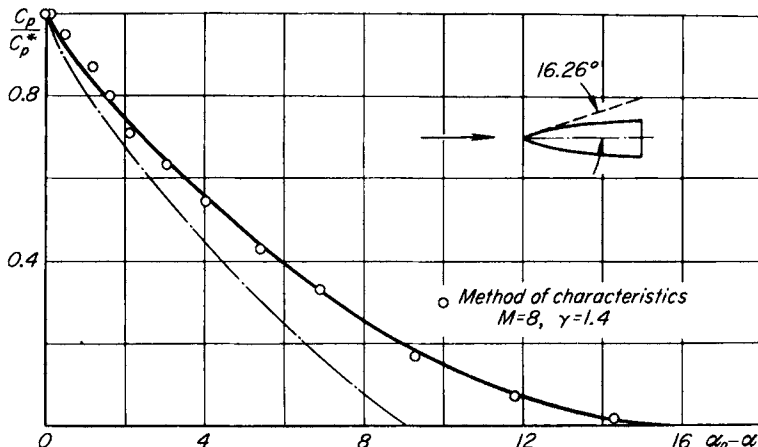


FIG. 3.16. Surface pressure distribution on an ogive. Comparison between modified Newtonian and Busemann formulas and method of characteristics calculations.

values and with the results of experiments. The dashed-dotted lines in these figures show the values of C_p/C_p^* computed according to the modified Busemann formula. Still another comparison with more exact calculations is shown in Fig. 3.16. There the pressure distribution found by the method of characteristics [25] at $M = 8$ and $\gamma = 1.4$ on a circular-arc ogive of revolution with a half-angle of 16.26° at the nose is compared

with the modified Newtonian formula (solid line) and with the modified Busemann formula (dashed-dotted line).

Examination of Figs. 3.5, 3.7, 3.8, and 3.16 shows that the use of the Busemann formula for finding pressure distributions in flows with $\gamma = 1.4$ gives poorer results than the Newtonian formula, which in the cases examined gives quite satisfactory results. The high degree of accuracy of the Newtonian formula for the calculation of hypersonic flows past some bodies with $\gamma = 1.4$ is explained by the compensating action of two factors. The pressure directly behind the shock wave is higher than the pressure given by the Newtonian formula, because for $\gamma = 1.4$ the angle β between the shock wave and the free stream direction is larger than the angle α between the body surface and the free stream, which enters into the Newtonian formula. The pressure near the shock wave for flow past a *convex* body is *decreased* toward the body surface by taking into account the centrifugal forces, and this effect to a large extent compensates the increased value of the pressure behind the shock wave. For flow past *concave* contours both factors act in the same direction (the pressure *increases* from the shock wave to the body as a result of the centrifugal forces) and the Newtonian formula gives less accurate results.

To corroborate these conclusions we turn to the cases considered in Section 5 of Chapter II: flows past bodies described by power law and exponential functions. If we pass to the equivalent one-dimensional unsteady flows, then according to the Newtonian formula

$$\frac{p}{\frac{1}{2}\rho_1(d\bar{R}/dt)^2} = 2.$$

From Fig. 2.17, which was based on exact calculations (using the equivalence principle), it follows that with $\gamma = 1.4$ (i.e., for $(\gamma - 1)/(\gamma + 1) = 1/6$) the quantity $p/[\frac{1}{2}\rho_1(d\bar{R}/dt)^2]$ lies between 1.7 and the cone value of 2.1 for a convex body of revolution. Thus it does not differ very greatly from the value given by the Newtonian formula. On the other hand, for a body of revolution which has a concave contour in the form of an exponential function,

$$\frac{p}{\frac{1}{2}\rho_1(d\bar{R}/dt)^2} = 2.90$$

according to the exact calculations given in Table 2.2 of Section 5, Chapter II. This is almost one and a half times the value given by the Newtonian formula. The direct application of the Newtonian formula to the body depicted in Fig. 3.17 also does not give satisfactory results for the determination of the pressure downstream of the corner.

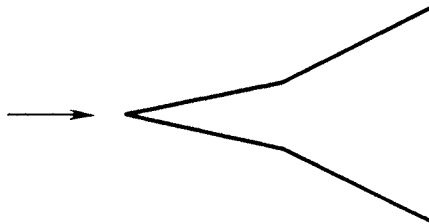


FIG. 3.17. Body with a corner.

When the compression of the gas across the shock wave is increased, which occurs for a perfect gas when $M \rightarrow \infty$ and $\gamma \rightarrow 1$, the difference between the shock angle and the inclination angle of the surface is decreased. Then the factor which compensates for the decrease of pressure across the layer due to the presence of centrifugal forces in the flow around convex bodies tends to vanish. Therefore, for hypersonic speeds and γ close to 1 the Newtonian formula must overestimate the pressure in flows past convex surfaces, and underestimate the pressure in flows past concave surfaces. With an increased condensation of the gas in the layer and with the corresponding decrease in the thickness of the layer, the Busemann formula becomes more exact; and when the thickness of the layer tends to zero, the Busemann formula gives the exact value of the pressure.

We shall confirm this conclusion with two examples. As the first example let us consider power law bodies. According to the Busemann formula,

$$\frac{p}{\frac{1}{2} \rho_1 \left(\frac{dR}{dt} \right)^2} = 2 \left[1 + \frac{n}{\nu(n+1)} \right].$$

These values of the pressure agree with the exact values which were shown in Fig. 2.17, for $M = \infty$ and $\gamma = 1$. The dependence of the pressure upon γ is not very strong for values of n which are not close to $-\nu/(\nu+2)$, so that the Busemann formula can also be used for values

of γ which are appreciably greater than 1. For $n > 0$ this dependence is still weaker. Thus in the case considered previously of the flow past a body of revolution described by an exponential function,

$$\frac{p}{\frac{1}{2} \rho_1 \left(\frac{dR}{dt} \right)^2} = 3$$

according to the Busemann formula, while the exact value for $\gamma = 1.4$ is equal to 2.90. (For a two-dimensional profile, $p/[\frac{1}{2}\rho_1(d\bar{R}/dt)^2] = 4$ according to the Busemann formula.)

The second example concerns the flow past an airfoil with sharp leading and trailing edges. Figure 3.18 shows the pressure coefficient on a circular arc airfoil with a thickness ratio of 0.1, computed for $M = \infty$ and $\gamma = 1.40$ and 1.05 according to formulas (3.1) (solid curves) and (3.15) (dashed-dotted curves). The circles in this figure are the values of the pressure coefficient obtained by the method of characteristics [29]. (The meaning of the dashed lines in Fig. 3.18 will be explained

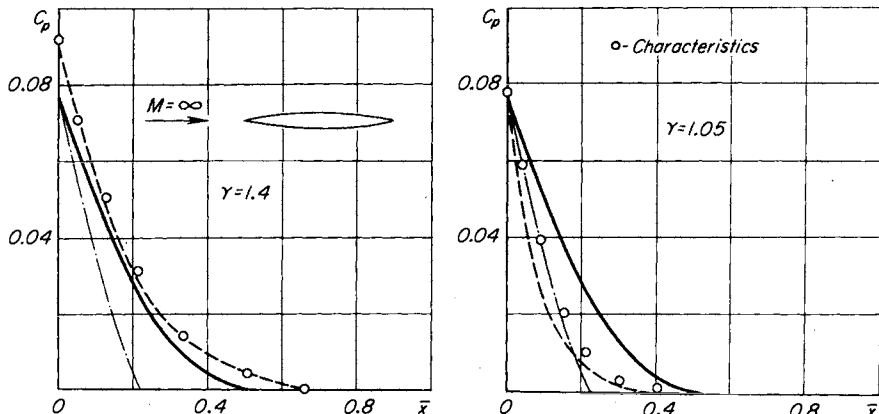


FIG. 3.18. Pressure distribution along an airfoil for $\gamma = 1.4$ and $\gamma = 1.05$ according to the Newtonian (—) and Busemann (---) formulas.

in Chapter IV.) For $\gamma = 1.4$, taking into account the centrifugal forces [formula (3.15)] leads to a considerable decrease in the pressure in comparison with the exact values, while the Newtonian formula gives satisfactory results [particularly in the modified form (3.2)]. For $\gamma = 1.05$,

on the other hand, the pressures obtained from the Newtonian formula are much greater than the exact values. In this case equation (3.15) gives results which are nearly correct.

5. The determination of body shapes of minimum drag using the Busemann formula

It was shown in the previous section that when the gas is strongly compressed across the bow shock wave, the surface pressure depends only on the shape of the body, and is determined for two-dimensional or axisymmetric flows by the Busemann formula

$$p = \rho_1 V^2 \left(\sin^2 \alpha + \sin \alpha \frac{d\alpha}{dF} \int_{F_0}^F \cos \alpha dF \right), \quad (3.17)$$

which can be rewritten in the equivalent form

$$p = \rho_1 V^2 \frac{d}{dF} \left(F - \cos \alpha \int_{F_0}^F \cos \alpha dF \right).$$

Integrating the resulting expression for the pressure coefficient along the body surface, the drag coefficient for an airfoil or body of revolution is found to be

$$C_D = 2 \left(1 - \frac{\cos \alpha_1}{F_1 - F_0} \int_{F_0}^{F_1} \cos \alpha dF \right). \quad (3.18)$$

We may conclude from this formula that for an annular body of revolution the drag is related to the annular area $F_1 - F_0$.

According to equation (3.18) the body drag depends not only on the integral, whose value is determined by the shape of the body—i.e., the function $\alpha(F)$ —but it depends moreover on the value of α for $F = F_1$. This latter condition is related to the fact that the shock layer can be deflected near the base of the body, in which case $\alpha_1 \neq \lim_{F \rightarrow F_1} \alpha$.*

* The angle α_1 can be made greater than the value $\lim_{F \rightarrow F_1} \alpha$ by fitting a deflecting shield at the base of the body. According to Hayes [26], to decrease the deflection one can mount a “turning cowl” (termed by Hayes a “thrust cowl”), which does not introduce additional drag, near the base of the body at a small distance from the surface.

Equation (3.18) for the drag coefficient enables one to solve a variety of variational problems for bodies with minimum external drag.[†] As with our previous use of the Newtonian formula, let us again consider the usual problem of determining the shape of a body having minimum drag for specified values of y_0 and y_1 (the length of the body is taken equal to unity). Taking into consideration the fact that α_1 need not be equal to $\lim_{F \rightarrow F_1} \alpha$, we shall separately maximize the integral and the factor multiplying it [26]. The factor in front of the integral necessarily takes on its extremal value for $\alpha_1 = 0$. In order to find the maximum of the integral we shall transform equation (3.18) from the variable of integration F to the variable x —the distance from the nose of the body measured in the direction of the free stream flow [31]. After carrying out the transformation we obtain

$$C_D = 2 \left[1 - \frac{\nu \cos \alpha_1}{y_1^\nu - y_0^\nu} \int_0^1 \frac{y^{\nu-1} y' dx}{(1 + y'^2)^{1/2}} \right]. \quad (3.19)$$

In this relation the expression under the integral does not contain the variable x explicitly. Hence the corresponding equation for the extremals $y(x)$ must be integrable by quadrature, as was the case when the Newtonian formula was used to determine the pressure. By simple calculation we find the first integral of the equation for the extremals in the following form:

$$\frac{y^{\nu-1} y'^3}{(1 + y'^2)^{3/2}} = \text{const.}$$

For two-dimensional flow ($\nu = 1$) the extremals are straight lines. For axisymmetric bodies ($\nu = 2$) the relation between y and x can be easily expressed in parametric form by again taking p as the parameter, where p is the tangent of the local inclination angle of the body to the axis of symmetry ($p = y'$). We then obtain

[†] The problem of bodies of revolution with minimum external drag at hypersonic speeds was also considered in [30]. This paper was, however, unavailable to the author. *Editor's note:* The analysis in this paper omits the centrifugal correction to the pressure on the body.

$$y = \frac{Y(p)}{X(p_1) - X(p_0)},$$

$$x = \frac{X(p) - X(p_0)}{X(p_1) - X(p_0)}, \quad (3.20)$$

where

$$Y(p) = \frac{(1 + p^2)^{3/2}}{p^3},$$

$$X(p) = \frac{3\sqrt{1 + p^2}}{4p^2} \left(\frac{1}{p^2} + \frac{1}{2} \right) + \frac{3}{16} \ln \frac{\sqrt{1 + p^2} - 1}{\sqrt{1 + p^2} + 1}.$$

The relation between the specified quantities y_0 and y_1 and the constants p_0 and p_1 which appear in the formulas (3.20) can be found from the obvious relations

$$y_0 = \frac{Y(p_0)}{X(p_1) - X(p_0)}, \quad y_1 = \frac{Y(p_1)}{X(p_1) - X(p_0)}. \quad (3.21)$$

The values of the functions $Y(p)$ and $X(p)$ for several values of p are given in Table 3.1.

TABLE 3.1
VALUES OF THE FUNCTIONS $Y(p)$ AND $X(p)$

p	X	Y	p	X	Y
0	∞	∞	0.50	14.6	11.2
0.10	7570	1010	1.0	1.26	2.82
0.15	1650	343	2.0	0.135	1.40
0.20	486	133	5.0	0.009	1.06
0.30	99.3	42.0	∞	0	1.00

A graph of the relation between Y and X is shown in Fig. 3.19 for large values of p . This curve, appropriately scaled, represents a body of revolution having minimum drag at hypersonic speeds. According to equation (3.17) the surface pressure distribution on an axisymmetric body having minimum drag is expressed by the following relation:

$$C_p = 2 \sin^2 \alpha \left[1 - \frac{1}{6} \left(1 - \frac{1}{4} \sin^2 \alpha - \frac{3}{8} \sin^4 \alpha + \frac{3}{8} \frac{\sin^6 \alpha}{\cos \alpha} \ln \tan \frac{\alpha}{2} \right) \right].$$

This relation is plotted in Fig. 3.20.

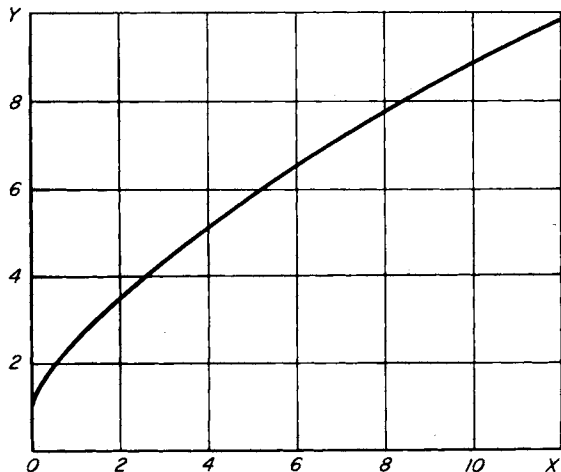


FIG. 3.19. Body of revolution having minimum drag, when the pressure is determined by the Busemann formula.

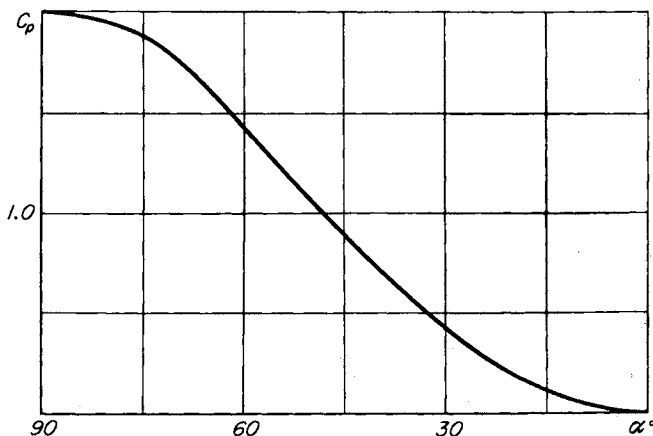


FIG. 3.20. Dependence of the pressure coefficient on the local inclination angle of the surface with respect to the free stream direction for a minimum-drag body.

For all minimum-drag bodies the dependence of the pressure coefficient on the local inclination angle of the surface with respect to the free stream direction is the same, provided the surface pressure is everywhere greater than zero. It is important to note that according to equations (3.20) and (3.21), $\lim_{F \rightarrow F_1} \alpha \neq 0$; therefore, the body shape which was

found will in fact be a body of minimum drag only if a "turning cowl" is mounted at the base of the body (see footnote on p. 128). In general, according to equations (3.19) and (3.20) the drag coefficient for axisymmetric bodies of optimum shape has the form

$$C_D = 2 \left\{ 1 - \frac{6p_1^6}{(1+p_1^2)^3 \left(1 - \frac{y_0^2}{y_1^2} \right)} \left[(1+p_1^2)^{1/2} \left(\frac{1}{16p_1^2} + \frac{7}{24p_1^4} + \frac{1}{6p_1^6} \right) + \frac{1}{32} \ln \frac{\sqrt{1+p_1^2} - 1}{\sqrt{1+p_1^2} + 1} \right]_{p_0}^{p_1} \right\}. \quad (3.22)$$

This expression together with equations (3.21) implicitly determines the dependence of C_D on the specified quantities y_0 and y_1 for a minimum-drag body.*

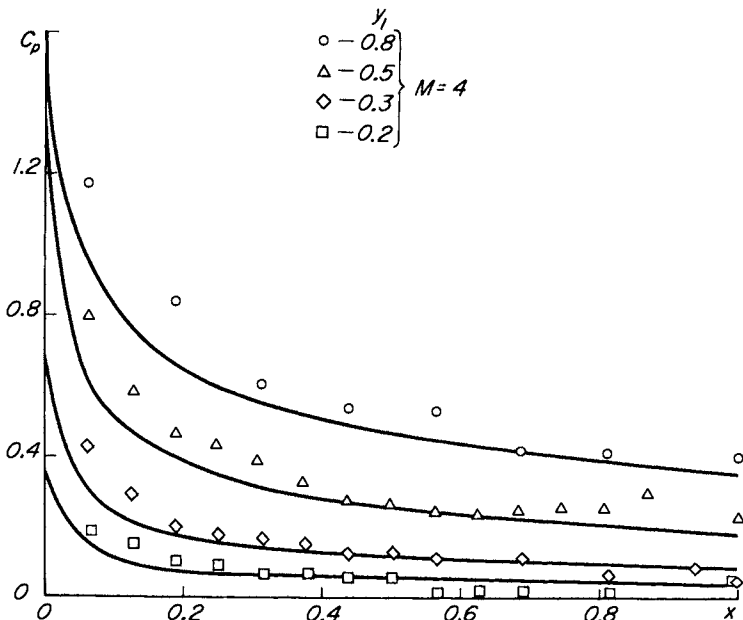


FIG. 3.21. Surface pressure distributions on minimum-drag bodies.

* If $(1+p_1^2)^3$ is replaced by $(1+p_1^2)^{7/2}$, equation (3.22) is also valid for a flow which is not deflected at the base of the body.

According to the first of equations (3.21), the initial radius y_0 of bodies having minimum drag for a specified length is different from zero. For a specified thickness ratio $2y_1$, the quantity y_0 can vary from y_1 to some minimum value which corresponds to $p_0 = \infty$. For this value of p_0 we have $Y(p_0) = 1$, $X(p_0) = 0$, so that

$$y_1 = \frac{Y(p_1)}{X(p_1)}, \quad \frac{y_0}{y_1} = \frac{p_1^3}{(1 + p_1^2)^{3/2}} = \sin^3 \alpha_1. \quad (3.23)$$

The solid curves shown in Fig. 3.21 were calculated for $p_0 = \infty$ and for several values of the thickness ratio, using the previously given formula for the pressure distribution on an optimum body. Characteristic of these curves is the sharp drop in pressure along the body from the stagnation point. This feature is significant in connection with reducing the cooling requirements on the forward portion of a body at limiting hypersonic speeds. Also plotted in Fig. 3.21 are experimental values of the pressure coefficient for $M = 4^*$; they agree satisfactorily with the theoretical curves. Profiles of bodies of optimum shape and schlieren photographs of the flows past them (without cowls to deflect the flow) are shown in Fig. 3.22.

For $p_0 = \infty$, equation (3.22) for the drag coefficient takes the form

$$C_D =$$

$$2 \left[1 - \sqrt{1 + p_1^2} \left(1 - \frac{\frac{5}{4} p_1^2 + \frac{21}{8} p_1^4 - \frac{3}{16} \frac{p_1^6}{\sqrt{1 + p_1^2}} \ln \frac{\sqrt{1 + p_1^2} - 1}{\sqrt{1 + p_1^2} + 1}}{1 + 3p_1^2 + 3p_1^4} \right) \right]. \quad (3.24)$$

Values of the drag coefficient for bodies of optimum shape are given in Table 3.2 for various thickness ratios (along with the corresponding values of y_0/y_1) as calculated from equations (3.23) and (3.24).

For small thickness ratios the quantity y_0/y_1 is very small (even for bodies with thickness ratios of 0.5, this quantity is less than 0.01), so that for practical purposes it can be taken equal to zero. Bodies of optimum shape give significantly less drag than cones of the same length.

* Experimental data obtained by A. L. Gonor.

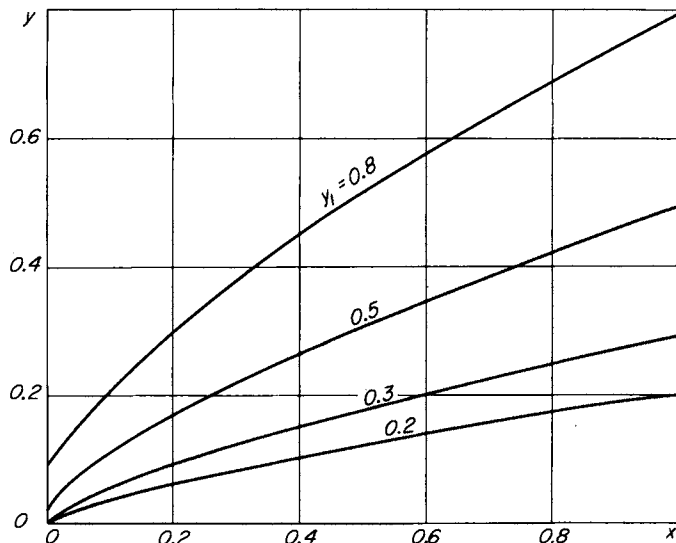
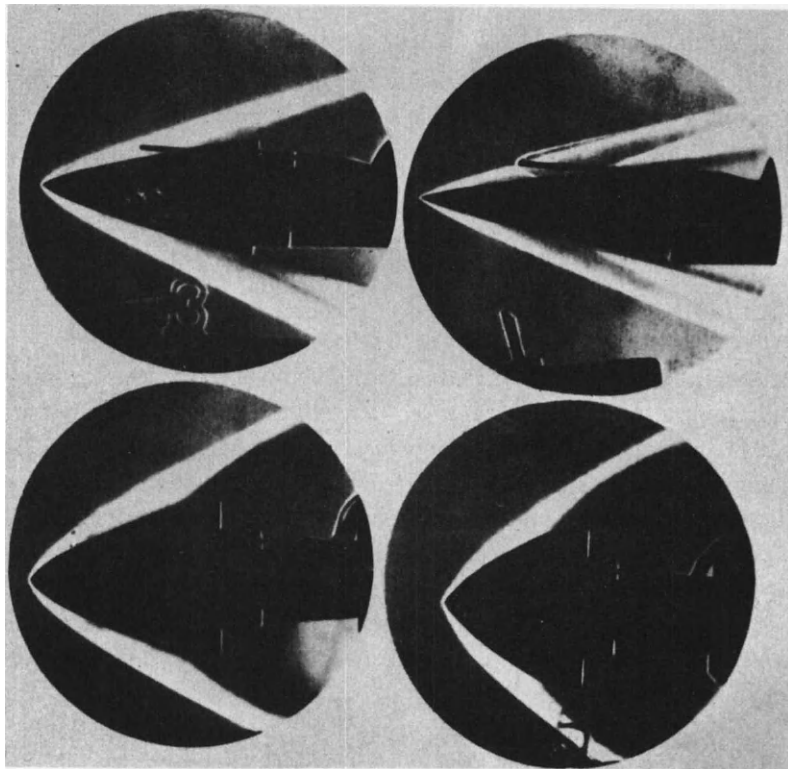


FIG. 3.22. Minimum-drag body shapes, and schlieren photographs of the flows past them (without turning cowls).

TABLE 3.2
DRAG COEFFICIENTS OF MINIMUM-DRAG BODIES WITH VARIOUS
THICKNESS RATIOS FOR $p_0 = \infty$

p_1	y_1	C_D	$\frac{y_0}{y_1}$	p_1	y_1	C_D	$\frac{y_0}{y_1}$
0	0	0	0.000	0.30	0.423	0.136	0.024
0.05	0.067	0.004	0.000	0.50	0.767	0.317	0.089
0.10	0.135	0.015	0.000	1.0	2.24	0.738	0.355
0.15	0.208	0.034	0.003	2.0	10.4	1.35	0.714
0.20	0.274	0.059	0.008	5.0	118	1.64	0.944

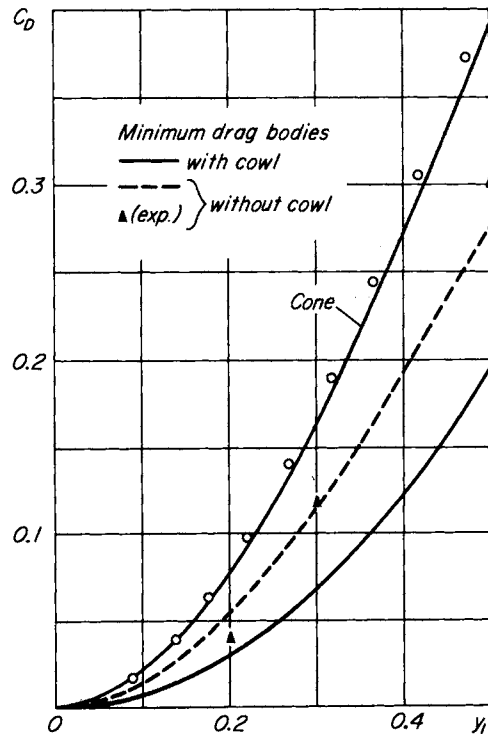


FIG. 3.23. Drag coefficients of minimum-drag bodies with different thickness ratios.

According to equation (3.18) the drag coefficient of a cone is given by the relation

$$C_D = \frac{2y_1^2}{1 + y_1^2}.$$

The drag of the optimum body shape is less than half the drag of the cone with the same thickness ratio.

The upper curve in Fig. 3.23 was calculated according to the approximate expression given above for the drag coefficient of a cone, while the circles are the exact values for $M = \infty$ and $\gamma = 1.4$ [8]. The two lower curves give the theoretical values of C_D for bodies of optimum shape with (solid line) and without (dotted line) deflection of the shock layer at the base of the body. The triangles on this figure are the values of C_D obtained from the experimental data on optimum shape bodies (without turning cowls) which was given in Fig. 3.21.

If we wish to exclude the possibility of using a turning cowl, we must maximize the integral in equation (3.18) together with the factor in front of it, in which case it is natural to require as an additional condition that the pressure on the body be nonnegative everywhere. Hayes found (although not strictly rigorously) bodies of minimum drag for this statement of the problem [26].

6. Boundary layer method

We shall now consider in more detail the flow properties when the density ratio across the bow shock wave is very large. The equation of conservation of mass across the bow shock wave, and the components of the momentum equation along the normal \mathbf{n} to the wave and along the tangent to it in the plane which contains the free stream vector velocity \mathbf{V} and the normal \mathbf{n} , can in general be written in the following form:

$$\begin{aligned} p_2 - p_1 &= \left(1 - \frac{\rho_1}{\rho_2}\right) \rho_1 V^2 \sin^2 \beta, \\ \cot \beta &= \left\{ \frac{1 - (\rho_1/\rho_2)}{2} \pm \sqrt{\left[\frac{1 - (\rho_1/\rho_2)}{2} \right]^2 - \frac{\rho_1}{\rho_2} \tan^2 \alpha} \right\} \cot \alpha, \\ V_2 \cos(\beta - \alpha) &= V_1 \cos \beta. \end{aligned} \quad (3.25)$$

Here α is the flow deflection angle and β is the angle between the bow wave and the free stream direction in the plane defined above.

In the limiting case of very strong compression of the gas across the shock wave—i.e., when $\rho_1/\rho_2 \ll 1$ —the conditions (3.25) take the form

$$p_2 - p_1 = \rho_1 V^2 \sin^2 \alpha, \quad \beta = \alpha, \quad V_2 = V_1 \cos \alpha.$$

These relations are independent of the thermodynamic properties of the gas and of the energetic processes which take place when the gas crosses the bow wave. From these conditions it follows that for strong compressions, the gas motion behind the bow shock wave takes place in a highly condensed thin layer along the body surface, and the change in pressure across the bow wave coincides with the change in pressure given by the Newtonian formula. The parameter which defines the extent to which the flow approximates this limit state is the characteristic value of the ratio of the density of the gas in the free stream flow to that in the layer behind the bow wave. We note that the maximum value of the flow deflection angle across the shock wave (which corresponds to the maximum value of $\tan \alpha$ for which the square root in expression (3.25) is real) is defined by the relation

$$\tan \alpha = \frac{1}{2} \left(1 - \frac{\rho_1}{\rho_2} \right) \sqrt{\frac{\rho_2}{\rho_1}}.$$

It follows from the above relation that when the density ratio ρ_2/ρ_1 across the shock wave becomes indefinitely large, the limit angle tends to ninety degrees.

For the flow of a perfect gas with constant specific heats, the density ratio across the bow wave is expressed from equation (1.17) by

$$\frac{\rho_1}{\rho_2} = \frac{\gamma - 1}{\gamma + 1} + \frac{2}{\gamma + 1} \frac{1}{M^2 \sin^2 \beta}.$$

For such a gas the minimum value of the quantity ρ_1/ρ_2 is reached for $M = \infty$ and is equal to $(\gamma - 1)/(\gamma + 1)$, i.e., $(\rho_1/\rho_2)_{\min} = 1/6$ for $\gamma = 1.4$. Thus the maximum value of the limiting flow deflection angle across a shock wave for a perfect gas with constant specific heats is reached in the limit $M = \infty$, when according to the preceding relation $\tan \alpha_{\max} = (\gamma^2 - 1)^{-1/2}$, that is, $\alpha_{\max} = 45^\circ 35'$ for $\gamma = 1.4$. For $\gamma \rightarrow 1$

the angle $\alpha_{\max} \rightarrow \pi/2$. As pointed out in the Introduction, when bodies are moving in a gas at very high speeds, and excitation of the vibrational degrees of freedom of the molecules and dissociation and ionization of the air components become important, then the temperature behind the bow shock wave is actually much lower than the temperature calculated under the assumption of constant specific heats. Since the pressure behind a strong shock wave depends only weakly on the thermodynamic properties of the gas, it follows that the actual compression of the gas is much larger than that given by the formula

$$\left(\frac{\rho_2}{\rho_1}\right)_{\max} = \frac{\gamma + 1}{\gamma - 1}$$

with $\gamma = 1.4$. So too will the limiting flow deflection angles across the shock be larger than defined by the relation $\tan \alpha_{\max} = (\gamma^2 - 1)^{-1/2}$ with $\gamma = 1.4$.

The preceding considerations suggest the idea of considering the flow behind a strong shock wave as a boundary layer-type flow near the shock, and to use for the calculation of such a flow, and for the calculation of general hypersonic flows, an expansion of the solution in a power series in the parameter ϵ , where ϵ is equal to the ratio of the density of the gas ahead of the shock wave to the characteristic value of the density of the gas behind it. This method was proposed by the author in [32–34] and was applied to the solution of various one-dimensional unsteady gas flow problems in [35–37] and to hypersonic gas flows in [38–41]. Somewhat later, a similar method was proposed independently in [28, 42, 43] and applied to the calculation of the flow near the stagnation point of blunt bodies in a hypersonic stream.

We shall limit our considerations to two-dimensional and axisymmetric flows. (The application of the method to the calculation of nonaxisymmetric conical flows has been carried out in [40] and [41]). The flows will be examined in the usual curvilinear system of coordinates applied in boundary layer theory. In a coordinate system of this type (depicted in Fig. 3.24) the position of a point M is defined by its distance $y = NM$ along a normal from the body surface and by the arc length $x = ON$ along the body measured from some point O . For steady flow, the equations describing the motion in the region between the shock wave and body surface take the following form in this coordinate system:

$$\begin{aligned}
 \rho \left(\frac{u}{1 + \frac{y}{R}} \frac{\partial u}{\partial x} + v \frac{\partial u}{\partial y} + \frac{uv}{R + y} \right) &= - \frac{1}{1 + \frac{y}{R}} \frac{\partial p}{\partial x}, \\
 \rho \left(\frac{u}{1 + \frac{y}{R}} \frac{\partial v}{\partial x} + v \frac{\partial v}{\partial y} - \frac{u^2}{R + y} \right) &= - \frac{\partial p}{\partial y}, \\
 \frac{\partial}{\partial x} (\rho u r^{r-1}) + \frac{\partial}{\partial y} \left[\rho v r^{r-1} \left(1 + \frac{y}{R} \right) \right] &= 0, \\
 \frac{u}{1 + \frac{y}{R}} \frac{\partial S}{\partial x} + v \frac{\partial S}{\partial y} &= 0.
 \end{aligned} \tag{3.26}$$

In these equations u and v are the velocity components in the x and y directions respectively; p , ρ , and S are as previously the pressure, density, and entropy per unit mass; R is the radius of curvature of the body sur-

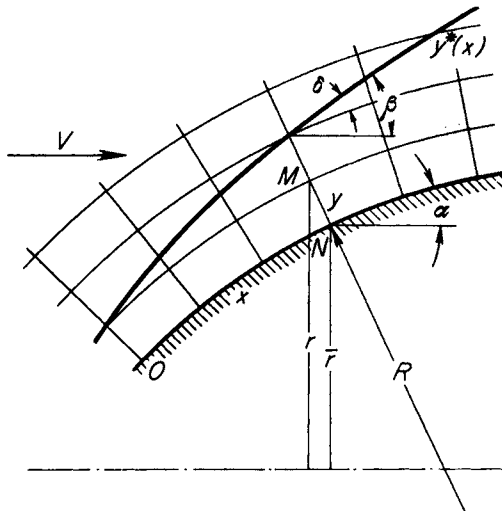


FIG. 3.24. Coordinate system and notation in boundary layer method.

face, and $v = 1$ or 2 for two-dimensional or axisymmetric flows respectively. For axisymmetric flows r is the distance of a point from the axis of symmetry. In this case, $r = \bar{r} + y \cos \alpha$, where \bar{r} is the distance from the axis of symmetry to the body surface, and α is the angle between the tangent to the surface and the axis of symmetry.

It is convenient to transform the system of equations (3.26) to new independent variables ψ and x , where ψ is the stream function.* Introducing the stream function ψ by means of the equality

$$d\psi = \rho u r^{r-1} dy - \rho v r^{r-1} \left(1 + \frac{y}{R}\right) dx,$$

we replace the continuity equation by the equations

$$\frac{\partial y}{\partial \psi} = \frac{1}{\rho u r^{r-1}}, \quad \frac{\partial y}{\partial x} = \left(1 + \frac{y}{R}\right) \frac{v}{u}. \quad (3.27)$$

Since†

$$\frac{\partial}{\partial x} \Big|_{\psi} = \frac{\partial}{\partial x} \Big|_y + \frac{\partial}{\partial y} \frac{\partial y}{\partial x},$$

then

$$\frac{u}{1 + (y/R)} \frac{\partial}{\partial x} \Big|_y + v \frac{\partial}{\partial y} = \frac{u}{1 + (y/R)} \frac{\partial}{\partial x} \Big|_{\psi}.$$

Using these transformation formulas we can reduce the remaining equations in (3.26) to the form

$$\begin{aligned} \rho u \frac{\partial u}{\partial x} + \rho v \frac{\partial v}{\partial x} + \frac{\partial p}{\partial x} &= 0, \\ \frac{1}{1 + \frac{y}{R}} \frac{\partial v}{\partial x} - \frac{u}{R + y} &= -r^{r-1} \frac{\partial p}{\partial \psi}, \\ \frac{\partial}{\partial x} \frac{p}{\rho^r} &= 0. \end{aligned} \quad (3.28)$$

(The first equation of this system is obtained from the first two equations of (3.26), the second from the second of (3.26), and the third from the fourth of (3.26).)

In the chosen system of coordinates, the velocity components normal

* Such a transformation was used by Kibel' [22] in the case of two-dimensional flows of an ideal gas with $R = \infty$. In boundary layer theory a similar transformation is due to von Mises [44].

† The symbol $\partial/\partial x|_{\psi}$ denotes differentiation with y held constant.

and tangential to the bow shock wave, and ahead of and behind the shock, may be written in the form

$$\begin{aligned} v_{1n} &= -V \sin \beta, & v_{2n} &= -u \sin (\beta - \alpha) + v \cos (\beta - \alpha), \\ v_{1t} &= V \cos \beta, & v_{2t} &= u \cos (\beta - \alpha) + v \sin (\beta - \alpha). \end{aligned}$$

Since

$$\tan (\beta - \alpha) = \frac{y^{*'}}{1 + (y^*/R)},$$

where $y = y^*(x)$ is the equation of the shock wave, the conditions at the bow shock wave can be expressed in the following form:

$$\begin{aligned} p_2 &= \frac{2}{\gamma + 1} \rho_1 V^2 \sin^2 \beta - \frac{\gamma - 1}{\gamma + 1} p_1, \\ \frac{\rho_1}{\rho_2} &= \frac{\frac{uy^{*'}}{1 + (y^*/R)} - v}{V \left(\sin \alpha + \cos \alpha \frac{y^{*'}}{1 + (y^*/R)} \right)} = \frac{\gamma - 1}{\gamma + 1} + \frac{2}{\gamma + 1} \frac{1}{M^2 \sin^2 \beta}, \\ u + \frac{vy^{*'}}{1 + (y^*/R)} &= V \left(\cos \alpha - \sin \alpha \frac{y^{*'}}{1 + (y^*/R)} \right). \end{aligned} \tag{3.29}$$

The first of these relations shows that for bodies of finite thickness (for which $\sin^2 \beta$ is not a small quantity), the pressure p_2 behind the shock has the same order of magnitude as the free stream dynamic pressure. From the last two relations we may conclude; first that the ratio of the free stream density ρ_1 to the density behind the shock ρ_2 must equal the ratio of the scales which measure y and x ; and secondly, as has already been pointed out, that for a perfect gas with constant specific heats this ratio of scales is a small quantity if the sum

$$\frac{\gamma - 1}{\gamma + 1} + \frac{2}{\gamma + 1} \frac{1}{M^2 \sin^2 \beta}$$

is small, i.e., if $M^2 \sin^2 \beta \gg 1$ (limiting hypersonic flows) and if the value of the specific heat ratio is close to one.

We now take into account the estimates which were obtained for the quantities appearing in equations (3.27) and (3.28), and consider the

orders of magnitude of these quantities to be the same in the entire flow region. On this basis we seek a solution of the equations in the form of a series in powers of the small parameter ϵ , which characterizes the ratio of the density of the gas ahead of the shock to that behind it, in the following form:

$$\begin{aligned} y &= \epsilon y_0 + \dots, \\ u &= u_0 + \epsilon u_1 + \dots, \\ v &= \epsilon v_0 + \dots, \\ p &= p_0 + \epsilon p_1 + \dots, \\ \rho &= \frac{\rho_0}{\epsilon} + \rho_1 + \dots. \end{aligned} \quad (3.30)$$

For a perfect gas with constant specific heats, we may take for the small parameter ϵ the quantity $(\gamma - 1)/(\gamma + 1)$.

Substituting these series into equations (3.27) and (3.28), we obtain the following relations for determining the first terms of the series:

$$\begin{aligned} \frac{\partial y_0}{\partial \psi} &= \frac{1}{\rho_0 u_0 r^{\nu-1}}, & v_0 &= u_0 \frac{\partial y_0}{\partial x}, \\ \frac{\partial u_0}{\partial x} &= 0, & \frac{u_0}{R} &= r^{\nu-1} \frac{\partial p_0}{\partial \psi}, \\ \frac{\partial}{\partial x} \frac{p_0^{1/\gamma}}{\rho_0} &= 0. \end{aligned} \quad (3.31)$$

The functions u_1 , p_1 , and ρ_1 satisfy the equations

$$\begin{aligned} \rho_0 u_0 \frac{\partial u_1}{\partial x} + \frac{\partial p_0}{\partial x} &= 0, \\ \frac{\partial v_0}{\partial x} - \frac{u_1}{R} &= - \frac{u_0}{R} \left[\frac{y_0}{R} + (\nu - 1) \frac{y_0}{\bar{r}} \cos \alpha \right] - \bar{r}^{\nu-1} \frac{\partial p_1}{\partial \psi}, \\ \frac{\partial}{\partial x} \left(\frac{p_1}{\rho_0} - \gamma \frac{\rho_1}{\rho_0} \right) &= 0. \end{aligned} \quad (3.32)$$

Both these systems of equations are integrable by quadrature. (It is easy to satisfy oneself that the systems of equations which determine

the terms in the series (3.30) for higher powers of ϵ are also integrable by quadrature.)

From the system (3.31) we obtain

$$\begin{aligned} u_0 &= u_0(\psi), \quad p_0^{1/\gamma} = \vartheta_0(\psi)\rho_0, \\ p_0 &= \frac{1}{R\tilde{r}^{\nu-1}} \int_{\psi_0^*}^{\psi} u_0 d\psi + p^*(x), \\ y_0 &= \frac{1}{\tilde{r}^{\nu-1}} \int_0^{\psi} \frac{d\psi}{\rho_0 u_0} + \bar{y}(x), \\ v_0 &= u_0 \frac{\partial y_0}{\partial x}. \end{aligned} \quad (3.33)$$

Here $u_0(\psi)$, $\vartheta_0(\psi)$, $p^*(x)$, and $\bar{y}(x)$ are arbitrary functions. The lower limit of integration ψ_0^* in the equation for p_0 will be defined below.

From the second system (3.32) we obtain

$$\begin{aligned} u_0 u_1 + \frac{\gamma}{\gamma - 1} \vartheta_0(\psi) p_0^{(\gamma-1)/\gamma} &= i_1(\psi), \\ \frac{p_1}{p_0} - \gamma \frac{p_1}{\rho_0} &= \vartheta_1(\psi), \\ p_1 &= \frac{1}{\tilde{r}^{\nu-1}} \int_{\psi_0^*}^{\psi} \left\{ \frac{u_1}{R} - \frac{\partial v_0}{\partial x} - \frac{u_0}{R} \left[\frac{y_0}{R} + (\nu - 1) \frac{y_0}{\tilde{r}} \cos \alpha \right] \right\} d\psi + p_1^*(x), \end{aligned} \quad (3.34)$$

where $i_1(\psi)$, $\vartheta_1(\psi)$, and $p_1^*(x)$ are arbitrary functions.

The relations obtained in (3.33) and (3.34) determine an approximate solution of the equations of motion of an ideal gas. For supersonic flow past a body, the arbitrary functions which enter into these equations must be found from the conditions (3.29) at the shock wave and from the condition at the given body surface. Taking $\psi = 0$ at the surface of the body, this latter condition has the form

$$y = 0 \quad \text{for} \quad \psi = 0,$$

from which it follows that $\bar{y}(x) = 0$.

The conditions (3.29) at the shock wave must be satisfied for $\psi = \psi^*(x)$, where

$$\begin{aligned}\psi^*(x) &= \frac{\rho^0 V}{\nu} (r^{*\nu} - r_0^\nu) \\ &= \frac{\rho^0 V}{\nu} (\bar{r}^\nu - r_0^\nu) + \epsilon \rho^0 V \bar{r}^{\nu-1} y_0^* \cos \alpha + O(\epsilon^2) \\ &= \psi_0^* + \epsilon \psi_1^* + O(\epsilon^2).\end{aligned}$$

Here, and in what follows, the free stream flow parameters are denoted by a superscript 0 in order to avoid confusion with the subscript 1 terms in the series (3.30). Transforming the relations (3.29) by use of this formula, we obtain the conditions which must be satisfied by the functions appearing in the expansions (3.30). For $\psi = \psi_0^*$ they are

$$\begin{aligned}u_0 &= V \cos \alpha, \quad u_1 = -u_{0\psi} \psi_1^* - V y_0^* \sin \alpha, \\ p_0 &= \rho^0 V^2 \sin^2 \alpha, \\ p_1 &= -p_{0\psi} \psi_1^* + \rho^0 V^2 (2y_0^{*\prime} \sin \alpha \cos \alpha - \sin^2 \alpha) - p^0, \quad (3.35) \\ \rho_0 &= \frac{\rho^0}{1 + \frac{2}{\gamma - 1} \frac{1}{M^2 \sin^2 \alpha}}, \\ \rho_1 &= -\rho_{0\psi} \psi_1^* + \frac{\rho_0^2}{\rho^0} \frac{4 \cos \alpha}{(\gamma - 1) M^2 \sin^3 \alpha} y_0^{*\prime}.\end{aligned}$$

Here y_0^* is the value of $y_0(x, \psi)$ for $\psi = \psi_0^*$, and $u_{0\psi}, p_{0\psi}, \rho_{0\psi}$ are the derivatives of the functions u_0, p_0, ρ_0 with respect to ψ . The condition

$$v_0 = u_0 y_0^{*\prime} - V \sin \alpha \frac{\rho^0}{\rho_0},$$

which follows from conservation of mass at the shock, is satisfied identically by ψ_0^* as chosen. Thus, at the shock wave

$$\begin{aligned}v_0 &= u_0 \frac{\partial}{\partial x} \left(\frac{1}{\bar{r}^{\nu-1}} \int_0^{\psi_0^*} \frac{d\psi}{\rho_0 u_0} + \frac{1}{\bar{r}^{\nu-1}} \int_{\psi_0^*}^{\psi} \frac{d\psi}{\rho_0 u_0} \right) \\ &= u_0 y_0^{*\prime} - \frac{1}{\bar{r}^{\nu-1}} \frac{1}{\rho_0} \frac{dy_0^*}{dx} = u_0 y_0^{*\prime} - V \sin \alpha \frac{\rho^0}{\rho_0}.\end{aligned}$$

The six conditions (3.35) enable one to determine the six remaining undetermined functions in equations (3.33) and (3.34). We thus obtain the quantities y_0 , u_0 , v_0 , p_0 , ρ_0 in the form

$$\begin{aligned} y_0 &= \frac{1}{\tilde{r}^{\nu-1}} \int_0^\psi \frac{d\psi}{\rho_0 u_0}, \quad u_0 = V \cos \alpha(x^*), \quad v_0 = u_0 \frac{\partial y_0}{\partial x}, \\ p_0 &= \rho^0 V^2 \sin^2 \alpha(x) - \frac{1}{R \tilde{r}^{\nu-1}} \int_{\psi^*} u_0 d\psi \\ &= \rho^0 V^2 \left[\sin^2 \alpha(x) + \sin \alpha(x) \frac{d\alpha}{dF} \int_{x^*}^x \cos \alpha(x^*) dF \right], \\ \rho_0 &= \frac{\rho^0}{1 + \frac{2}{\gamma-1} \frac{1}{M^2 \sin^2 \alpha(x^*)}} \left[\frac{p_0}{\rho^0 V^2 \sin^2 \alpha(x^*)} \right]^{1/\gamma}. \end{aligned} \quad (3.36)$$

We see that the first terms in the expansions (3.30) of the velocity u and the pressure p agree with the corresponding values obtained from the Busemann formula. However, the first terms of the series (3.30) enable one to calculate the entire flow field—i.e., the shock wave shape and the velocity and density distributions (and hence also the temperature distribution) in the layer between the shock wave and the body. The next terms in the expansions, specified by equations (3.34) and (3.35), enable one to more accurately determine the density, pressure, and velocity distributions.

Equations (3.36) show that to first approximation the pressure distribution along the body does not depend on the free stream Mach number. The flow as a whole, however, and in particular the position of the bow shock wave, changes with Mach number, approaching the previously determined limit for $M \rightarrow \infty$.

We note the following important criterion for the application of the theory. As shown by the appropriate formula in (3.36), for the motion of the gas particles along a curved path the pressure at some point of the disturbed region is in first approximation equal to the sum of two terms: the pressure behind the bow wave at that value of x , plus the pressure which balances the centrifugal forces acting on the gas particles between

the given point and the point on the bow wave. For bodies with convex contours these terms have different signs, and the first term decreases along a streamline in the downstream direction while the integral in the second term increases (since ψ_0^* increases and at the same time $u_0(\psi)$ also increases along the outer edge of the layer). Therefore if the decrease in the curvature of the body in the downstream direction is not sufficiently rapid, the drop in pressure between the bow shock wave and a given streamline caused by centrifugal forces will at some point exceed the increase in pressure across the shock wave. As a result the first approximation to the pressure will become zero, and thereafter will be negative. It is apparent that this condition will first be reached at the body surface. Along with p_0 , the density ρ_0 also becomes zero. The point where this occurs is a singular point in the present theory. The basic assumptions of the theory break down somewhat before this point; these basic assumptions being that the density of the gas in the layer behind the shock wave is much larger than the density of the gas in the free stream, and consequently that the thickness of the layer between the body surface and the bow wave is small. Thus the calculation of the flow by the present method can only be carried out up to somewhere in the neighborhood of this singular point.

7. Use of the equivalence principle in the boundary layer method

In Chapter II an analogy was established between hypersonic flows past slender bodies and unsteady one-dimensional gas flows produced by the motion of a piston in a gas. According to this analogy, axisymmetric flows past bodies of revolution correspond to unsteady flows with cylindrical symmetry, and flows past airfoils correspond to unsteady flows with planar symmetry. The basic means for calculating such flows with shock waves present is the numerical method of characteristics with various modifications. Exact solutions of unsteady one-dimensional flows with shock waves have been obtained in only a few cases, mainly for self-similar motions. We shall present here an approximate method for calculating self-similar and nonself-similar unsteady one-dimensional gas flows with very strong and moderately strong shock waves, based on the idea described previously of considering the flow behind a strong shock wave as a kind of boundary layer near the surface of the wave. We shall also apply the method to the calculation of hypersonic flows

past slender bodies (see [34] and [36]). This same method was later suggested in [39].

As in Section 4 of Chapter II, we shall take as the basic unknown functions the distance R of the particles from the axis (or plane) of symmetry, the density ρ , and the pressure p . We shall let the independent variables be the time t and the Lagrangian coordinate m defined by the relation $dm = \rho^0 r^{\nu-1} dr$ (r is the value of R at the initial instant of time, ρ^0 is the initial density, and $\nu = 1$ or 2 for the planar or cylindrical case respectively; for spherically symmetric problems one would take $\nu = 3$). With these assumptions the equations of continuity, motion, and energy for adiabatic flows of a perfect gas can be written in the following manner (see equations (2.10) in Section 4, Chapter II):

$$\begin{aligned}\frac{\partial R}{\partial m} &= \frac{1}{\rho R^{\nu-1}}, \\ \frac{\partial^2 R}{\partial t^2} &= -R^{\nu-1} \frac{\partial p}{\partial m}, \\ \frac{\partial}{\partial t} \frac{p}{\rho^\gamma} &= 0.\end{aligned}\tag{3.37}$$

Let us once again assume that the density of the gas behind the shock wave (in the layer between the shock wave and the piston surface) is much larger than that ahead of the shock wave. In accordance with this assumption we will seek solutions of the system (3.37) in the form of expansions in powers of the small parameter ϵ , which characterizes the density ratio of the gas across the shock, as follows:

$$\begin{aligned}R &= R_0 + \epsilon R_1 + \dots, \\ p &= p_0 + \epsilon p_1 + \dots, \\ \rho &= \frac{\rho_0}{\epsilon} + \rho_1 + \dots.\end{aligned}\tag{3.38}$$

We obtain the system of equations

$$\frac{\partial R_0}{\partial m} = 0, \quad \frac{\partial^2 R_0}{\partial t^2} = -R_0^{\nu-1} \frac{\partial p_0}{\partial m}, \quad \frac{\partial}{\partial t} \frac{p_0}{\rho_0^\gamma} = 0,$$

for the functions R_0 , p_0 , and ϑ_0 . Integrating we find

$$\begin{aligned} R_0 &= R_0(t), \\ p_0 &= P(t) - \frac{\ddot{R}_0}{R_0^{\nu-1}} m, \\ \vartheta_0 &= \frac{p_0^{1/\gamma}}{\vartheta_0(m)}, \end{aligned} \quad (3.39)$$

where $R_0(t)$, $P(t)$, $\vartheta_0(m)$ are arbitrary functions.

The functions R_1 , p_1 , and ρ_1 satisfy the equations

$$\begin{aligned} \frac{\partial R_1}{\partial m} &= \frac{1}{\rho_0 R_0^{\nu-1}}, \\ R_0^{\nu-1} \frac{\partial p_1}{\partial m} &= (\nu - 1) \frac{\ddot{R}_0}{R_0} R_1 - \frac{\partial^2 R_1}{\partial t^2}, \\ \frac{\partial}{\partial t} \left(\frac{p_1}{p_0} - \gamma \frac{\rho_1}{\rho_0} \right) &= 0, \end{aligned}$$

and are determined by the following relations:

$$\begin{aligned} R_1 &= \frac{1}{R_0^{\nu-1}} \int_{m^*}^m \frac{\vartheta_0(m)}{p_0^{1/\gamma}} dm + R_1^*(t), \\ p_1 &= (\nu - 1) \frac{\ddot{R}_0}{R_0^{\nu}} \int_{m^*}^m R_1 dm - \frac{1}{R_0^{\nu-1}} \int_{m^*}^m \frac{\partial^2 R_1}{\partial t^2} dm + p_1^*(t), \\ \frac{p_1}{p_0} - \gamma \frac{\rho_1}{\rho_0} &= \vartheta_1(m). \end{aligned} \quad (3.40)$$

Here $R_1^*(t)$, $p_1^*(t)$, and $\vartheta_1(m)$ are arbitrary functions, and m^* is the lower limit of integration which can be chosen in a number of ways corresponding to the simplest manner of writing the equations.

Equations (3.39) and (3.40) give in explicit form expressions for the first two terms in the expansions (3.38) of the unknown quantities in powers of ϵ . The arbitrary functions which enter in these expressions must be determined from the conditions at the shock wave and at the piston surface.

The condition of conservation of mass, the momentum theorem, and the law of conservation of energy have the following forms at the shock wave for the case being considered (see equations (2.11) in Section 4, Chapter II):

$$\begin{aligned} m^* &= \frac{\rho^0 R_0^{*\nu}}{\nu}, \\ p^* &= \frac{2}{\gamma + 1} \rho^0 D^2 - \frac{\gamma - 1}{\gamma + 1} p^0, \\ \rho^* &= \frac{\frac{\gamma + 1}{\gamma - 1} \rho^0}{1 + \frac{2}{\gamma - 1} \frac{a^{0*}}{D^2}}. \end{aligned} \quad (3.41)$$

We shall consider that the function $R_0(t)$ in equations (3.39) represents the motion of the shock wave. Then from equations (3.41) we can obtain the conditions at the shock wave for the first terms in the expansions of the unknown functions. With $m^* = \rho^0 R_0^{*\nu}/\nu$, they are

$$\begin{aligned} R_0 &= R_0(t), & R_1 &= 0, \\ p_0 &= \rho^0 \dot{R}_0^2, & p_1 &= -p^0 - \rho^0 \dot{R}_0^2, \\ \rho_0 &= \frac{\rho^0}{1 + [2/(\gamma - 1)](a^{0*}/\dot{R}_0^2)}, & \rho_1 &= 0. \end{aligned}$$

(All succeeding terms in the series (3.38) must vanish at the shock wave.) The conditions written above permit the determination of the arbitrary functions in equations (3.39) and (3.40). In the final expressions for the unknown quantities it is convenient to replace the Lagrangian variable m by the variable τ , which is related to m by the equation $m = \rho^0 R_0^{*\nu}(\tau)/\nu$. It is evident that $\tau(m)$ is the instant of time at which the shock wave crosses the particle with Lagrangian coordinate m , so that $m^* = \rho^0 R_0^{*\nu}(\tau)/\nu$. After substituting the values of the arbitrary functions in the expressions for the quantities p_0 and ρ_0 , they take the form

$$\begin{aligned} p_0 &= \rho^0 \dot{R}_0^2 + \rho^0 \frac{R_0 \ddot{R}_0}{\nu} - \frac{\ddot{R}_0}{R_0^{\nu-1}} m, \\ \rho_0 &= \frac{\rho^0}{1 + \frac{2}{\gamma - 1} \frac{a^{0*}}{\dot{R}_0^2(\tau)}} \frac{p_0^{1/\gamma}}{[\rho^0 \dot{R}_0^2(\tau)]^{1/\gamma}}. \end{aligned} \quad (3.42)$$

The functions R_1 , p_1 , and ρ_1 are determined by the relations

$$\begin{aligned} R_1 &= -\frac{1}{R_0^{\nu-1}} \int_{\tau}^t \frac{\left[1 + \frac{2}{\gamma-1} \frac{a^{0^2}}{\dot{R}_0^2(\tau)}\right] R_0^{\nu-1}(\tau) \dot{R}_0^{(2/\nu)+1}(\tau) d\tau}{\left[\dot{R}_0^2 + \frac{R_0 \ddot{R}_0}{\nu} \left(1 - \frac{R_0^\nu(\tau)}{R_0^\nu}\right)\right]^{1/\nu}}, \\ p_1 &= (\nu-1) \frac{\ddot{R}_0}{R_0^\nu} \int_{m^*}^m R_1 dm - \frac{1}{R_0^{\nu-1}} \int_{m^*}^m \frac{\partial^2 R_1}{\partial t^2} dm - p^0 - \rho^0 \dot{R}_0^2, \\ \rho_1 &= \frac{\rho_0}{\gamma} \left[\frac{p_1}{p_0} + 1 + \frac{a^{0^2}}{\gamma \dot{R}_0^2(\tau)} \right]. \end{aligned} \quad (3.43)$$

To complete the solution of the problem it is necessary to express the function $R_0(t)$ in terms of the specified piston motion $\bar{R}(t)$, using the conditions at the piston surface. The following equality must then be satisfied for $\tau = 0$:

$$R = R_0 + \epsilon R_1 + O(\epsilon^2) = \bar{R}(t).$$

From the above relation,

$$\begin{aligned} R_0 - \frac{\gamma-1}{\gamma+1} \frac{1}{R_0^{\nu-1}} \int_0^t \frac{\left[1 + \frac{2}{\gamma-1} \frac{a^{0^2}}{\dot{R}_0^2(\tau)}\right] R_0^{\nu-1}(\tau) \dot{R}_0^{(2/\nu)+1}(\tau) d\tau}{\left[\dot{R}_0^2 + \frac{R_0 \ddot{R}_0}{\nu} \left(1 - \frac{R_0^\nu(\tau)}{R_0^\nu}\right)\right]^{1/\nu}} \\ = \bar{R}(t) + O(\epsilon^2). \end{aligned} \quad (3.44)$$

If in this integral equation we replace the function R_0 by the function \bar{R} in the term which contains the integral, leading to a change in the right-hand side of $O(\epsilon^2)$, we obtain a relation which expresses the function R_0 explicitly in terms of the given function \bar{R} . That is,

$$R_0 = \bar{R} + \frac{\gamma-1}{\gamma+1} \frac{1}{\bar{R}^{\nu-1}} \int_0^t \frac{\left[1 + \frac{2}{\gamma-1} \frac{a^{0^2}}{\dot{\bar{R}}^2(\tau)}\right] \bar{R}^{\nu-1}(\tau) \dot{\bar{R}}^{(2/\nu)+1}(\tau) d\tau}{\left[\dot{\bar{R}}^2 + \frac{\bar{R} \ddot{\bar{R}}}{\nu} \left(1 - \frac{\bar{R}^\nu(\tau)}{\bar{R}^\nu}\right)\right]^{1/\nu}}. \quad (3.45)$$

When the motion of the piston is known, i.e., when the body shape is given in a hypersonic flow, equations (3.42) and (3.43) together with

the relations (3.44) or (3.45) determine the approximate expressions for all the flow parameters.

8. Boundary layer method: examples

Let us consider some examples of the application of the boundary layer method to the calculation of hypersonic flows past bodies.

1. Flow Past a Slender Wedge or a Slender Cone

Let us make use of the equivalence principle by taking

$$\bar{R} = Ut,$$

$$R_0 = Dt$$

in the equivalent unsteady flow problem for these bodies. (According to the equivalence principle, $x = Vt$, so that $U = V \tan \alpha$, $D = V \tan \beta$, where to the approximation considered $\tan \alpha \approx \alpha$, $\tan \beta \approx \beta$). Substituting the expression $R_0 = Dt$ into equations (3.42) and (3.43), we obtain after some simple calculations

$$\begin{aligned} p_0 &= \rho^0 D^2, \quad \rho_0 = \frac{\rho^0}{1 + \frac{2}{\gamma - 1} \frac{a^{02}}{D^2}}, \\ R_1 &= - \left(1 + \frac{2}{\gamma - 1} \frac{a^{02}}{D^2} \right) \left[1 - \left(\frac{\tau}{t} \right)^{\nu} \right] \frac{Dt}{\nu}, \\ p_1 &= \frac{\nu - 1}{2\nu} \rho^0 D^2 \left(1 + \frac{2}{\gamma - 1} \frac{a^{02}}{D^2} \right) \left[1 - \left(\frac{\tau}{t} \right)^{2\nu} \right] - p^0 - \rho^0 D^2, \\ \rho_1 &= \frac{\nu - 1}{2\nu} \left[1 - \left(\frac{\tau}{t} \right)^{2\nu} \right] \frac{\rho^0}{\gamma}. \end{aligned} \quad (3.46)$$

Here the quantity τ is related to the Lagrangian coordinate r by $r = D\tau$. According to equation (3.44), the dependence of D on U has the following form:

$$D \left[1 - \frac{1}{\nu} \frac{\gamma - 1}{\gamma + 1} \left(1 + \frac{2}{\gamma - 1} \frac{a^{02}}{D^2} \right) \right] = U. \quad (3.47)$$

To the approximation considered, equations (3.46) and (3.47) give the complete solution of the equivalent problem of the unsteady gas flow

resulting from the motion of a piston at constant speed. One can easily satisfy oneself that this approximate solution agrees with the exact solution for planar symmetry ($\nu = 1$). For spherical symmetry ($\nu = 3$), comparison of the results of the approximate relations (3.46) and (3.47) with the results of exact calculations [45] also shows their high degree of accuracy for values of U/a^0 greater than 1.5 to 2.0. Such a comparison has been carried out in [36].

In order to pass from the equivalent problem of unsteady motion of a gas displaced by a piston to the problem of hypersonic flow past a wedge or cone, let us put $U/a^0 = (V/a^0) \tan \alpha = K$ and $D/a^0 = (V/a^0) \tan \beta = K_s$, as we did previously in Chapter II. Then according to equation (3.47) the relation between K_s and K has the form

$$K_s - K = \frac{1}{\nu} \frac{\gamma - 1}{\gamma + 1} \left(K_s + \frac{2}{\gamma - 1} \frac{1}{K_s} \right). \quad (3.48)$$

In accordance with equations (3.46) we obtain for the pressure coefficient on the surface of a wedge or cone

$$C_p M^2 = 2 \left[\frac{2}{\gamma + 1} (K_s^2 - 1) + \frac{\gamma - 1}{\gamma + 1} \frac{\nu - 1}{2\nu} \left(K_s^2 + \frac{2}{\gamma - 1} \right) \right]. \quad (3.49)$$

Equations (3.48) and (3.49) with $\nu = 2$ are the same as equations (3.10) and (3.13), which were obtained previously as the basic relations in the tangent-cone method. The results of comparison of these equations with exact calculations for flow past a cone are given in Figs. 2.12 and 2.5.

2. Limiting Hypersonic Flows Past Power Law Bodies

We have in the equivalent problems of one-dimensional unsteady motion

$$\bar{R} = C \frac{t^{n+1}}{n + 1},$$

$$R_0 = C_1 \frac{t^{n+1}}{n + 1}.$$

Here the ratio a^0/D must be considered negligibly small, in which case the motion is a self-similar one. The exact solution of this problem was considered in Section 5 of Chapter II. Approximate solutions are given

by equations (3.42) and (3.43) which, after substitution of the expression for R_0 , take the following form:

$$\begin{aligned} p_0 &= p_0^* \left[1 + \frac{n}{\nu(n+1)} \left(1 - \frac{m}{m^*} \right) \right], \quad \rho_0 = \rho^0 \left(\frac{p_0}{\rho^0 C_1^2 \tau^{2n}} \right)^{1/\gamma}, \\ R_1 &= -\frac{1}{\nu} R_0 I \left(\gamma, \frac{2n}{\nu(n+1)}, \frac{m}{m^*} \right), \\ p_1 &= p_0^* \left\{ I' \left(\frac{m}{m^*} \right) \left(\frac{m}{m^*} \right)^2 - \frac{1}{\nu} \left(\frac{n}{n+1} + \frac{\gamma+1}{\nu} \right) I \left(\frac{m}{m^*} \right) \frac{m}{m^*} \right. \\ &\quad \left. - \frac{1}{\nu} \left(\frac{2n}{\nu(n+1)} + 1 + \nu \right) \int_{m/m^*}^1 I d\frac{m}{m^*} \right\}, \\ \rho_1 &= \frac{\rho_0}{\gamma} \left(\frac{p_1}{p_0} + 1 \right). \end{aligned} \quad (3.50)$$

Here

$$\frac{2}{\gamma+1} p_0^* = \frac{2}{\gamma+1} \rho^0 C_1^2 t^{2n} = p^*$$

is the pressure behind the shock wave front, and

$$\begin{aligned} m^* &= \frac{\rho^0 R_0'}{\nu}, \quad m = \frac{\rho^0 R_0'(\tau)}{\nu} \\ I \left(\gamma, \frac{2n}{\nu(n+1)}, \frac{m}{m^*} \right) &= \int_{m/m^*}^1 \left[\frac{x^{2n/\nu(n+1)}}{1 + \frac{n}{\nu(n+1)}(1-x)} \right]^{1/\gamma} dx. \end{aligned}$$

The relation between the constants C_1 and C required for the complete solution of the problem is determined by equation (3.44), and has the form

$$\frac{\bar{R}}{R_0} = \frac{C}{C_1} = 1 - \frac{\gamma-1}{\gamma+1} \frac{1}{\nu} I \left(\gamma, \frac{2n}{\nu(n+1)}, 0 \right). \quad (3.51)$$

This expression gives the ratio of the piston radius to the shock wave radius. The thickness of the gas layer between the piston and the shock wave $R_0 - \bar{R}$ is given by

$$\frac{\gamma-1}{\gamma+1} \frac{1}{\nu} I \left(\gamma, \frac{2n}{\nu(n+1)}, 0 \right) R_0 \equiv \frac{1}{\nu} \frac{\gamma}{\gamma+1} \frac{\gamma-1}{\gamma+\kappa} F \left(\frac{1}{\gamma}, 1; 2 + \frac{\kappa}{\gamma}, -\frac{\kappa}{2} \right) R_0,$$

where F is the hypergeometric function, and where for abbreviation the notation $\kappa = 2n/\nu(n+1)$ has been introduced. From this identity it follows that for $\kappa \rightarrow -1$, i.e., for $n \rightarrow -\nu(\nu+2)$, the thickness of the gas layer is not small even for $\gamma \rightarrow 1$, being of the order of R_0 . Thus for $n \rightarrow -\nu/(\nu+2)$ the basic assumption of the theory that the extent of the layer is small breaks down. The accuracy of the derived expression for R (as well as for the gas velocity $\partial R/\partial t$) decreases for small values of m if n approaches $-\nu/(\nu+2)$.

In accordance with equations (3.50) the pressure at the piston surface has the following value:

$$p_p = p_0^* \left\{ 1 + \frac{n}{\nu(n+1)} - \frac{\gamma-1}{\gamma+1} \frac{1}{\nu} \right. \\ \times \left[\frac{2n}{\nu(n+1)} + 1 + \nu \right] \int_0^1 I d \frac{m}{m^*} \left. \right\} = p^* \varphi(0). \quad (3.52)$$

We note that this expression will continue to remain accurate for $n \rightarrow -\nu/(\nu+2)$, since the rapid increase in the thickness of the gas layer between the shock wave and the piston for $n \rightarrow -\nu/(\nu+2)$ is governed by the appearance near the piston of a region in which the gas has a very low density, and consequently in which the pressure of the gas cannot be significantly altered.

The curves in Figs. 2.16 and 2.18 give the values of p_p/p^* and \bar{R}/R_0 for $\nu = 1$ and 2 as computed by the approximate formulas, with terms of order $(\gamma-1)/(\gamma+1)$ taken into account. As already pointed out in Chapter II, the open circles on these figures correspond to values obtained from the solution of the exact equations by means of numerical integration [46]. The dark circles correspond to the exact solution of the problem of plane piston motion at constant speed. The crossed open and dark circles correspond to the exact solutions of the violent explosion problem with a cylindrical and a planar charge, respectively, and will be described in Chapter V.

Let us also apply our approximate solution to determine the drag coefficient of power law bodies. To do this we introduce the approximate values of $\mathfrak{A}(0) = \bar{R}/R_0$ and $\mathfrak{P}(0) = p_p/p^*$ from equations (3.51) and (3.52) into the previously obtained expressions (2.19) and (2.20). Results of calculations for $\nu = 2$ and $\gamma = 1.4$ are shown in Figs. 2.19 and 2.20.

With the exception of values of n close to $-\frac{1}{2}$, the agreement of the approximate solution with the exact values is very satisfactory even for $n < 0$ (which corresponds to the dashed parts of the curves). If in the approximate solution we take into account only the leading terms, i.e., if we neglect terms of order $(\gamma - 1)/(\gamma + 1)$ and higher, then the expressions for C_D become quite simple [39]. In this case, according to equations (3.51) and (3.52), we must set

$$\frac{\bar{R}}{R_0} = 1, \quad \frac{p_p}{p^*} = \frac{\gamma + 1}{2} \left[1 + \frac{n}{\nu(n + 1)} \right],$$

so that equations (2.19) and (2.20) take the following forms:

$$C_D = \frac{(n + 1)^2}{2} \cdot \frac{n(\nu + 1) + \nu}{n(\nu + 2) + \nu} \tau^2$$

and

$$C_D = \frac{2^\nu \pi^{2(\nu-1)}}{\nu} \frac{(n + 1)^2}{n(\nu + 2) + \nu} \frac{n(\nu + 1) + \nu}{(vn + 1 + \nu)^2} \cdot \left(\frac{\bar{R}_{\max}^{\nu+1}}{V} \right)^2.$$

From the first of the above relations we can readily show that the drag coefficient C_D for a given thickness ratio has a minimum for $n = -0.136$ with $\nu = 1$, and a minimum for $n = -\frac{1}{3}$ with $\nu = 2$. The corresponding values of C_D are $0.460\tau^2$ and $\frac{1}{3}\tau^2$ (for a wedge or a cone, $C_D = \frac{1}{2}\tau^2$ to the approximation considered).

For a fixed volume and fixed maximum cross-sectional radius, the body of minimum drag with $\nu = 1$ is a wedge ($n = 0$), while with $\nu = 2$, C_D has a minimum for $n = -0.130$. The corresponding values of C_D are $\frac{1}{2}(\bar{R}_{\max}^2/V)^2$ and $2.16(\bar{R}_{\max}^3/V)^2$ (for a cone, $C_D = 2.19(\bar{R}_{\max}^3/V)^2$).

3. Flow Past an Annular Conical Body [38]

As a simple example of the solution of a nonself-similar problem by the boundary layer method, let us consider the supersonic flow past a body of revolution in the form of a truncated cone with an annulus (Fig. 3.25). To analyze the flow we shall apply the formulas obtained in Section 6, but without assuming that the inclination angle at the nose of the body is necessarily small. For this body

$$R(x) = \infty, \quad \bar{r} = r_0 + x \sin \alpha,$$

where r_0 is the radius of the annulus entrance.

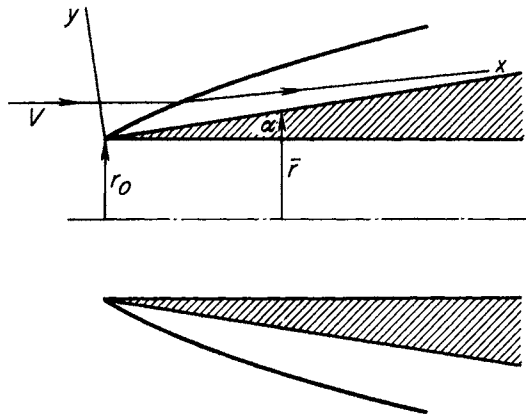


FIG. 3.25. Flow past a truncated cone with an annulus.

From the conditions (3.35) at the shock wave and from the conditions at the wall, the values of the arbitrary functions in the expressions (3.33) are found to be

$$u_0(\psi) = V \cos \alpha, \quad p^*(x) = \rho^0 V^2 \sin^2 \alpha,$$

$$\vartheta_0(\psi) = \frac{1}{\rho^0} \left(1 + \frac{2}{\gamma - 1} \frac{1}{M^2 \sin^2 \alpha} \right) (\rho^0 V^2 \sin^2 \alpha)^{1/\gamma}, \quad \tilde{y}(x) = 0.$$

All these functions are thus reduced to constants. Substituting into equations (3.33) and taking into account the fact that $\nu = 2$, we obtain

$$y_0 = \frac{\psi}{\rho_0 u_0 \bar{r}}, \quad u_0 = V \cos \alpha, \quad v_0 = -\frac{\psi \sin \alpha}{\rho_0 \bar{r}^2},$$

$$p_0 = \rho^0 V^2 \sin^2 \alpha, \quad \rho_0 = \frac{\rho^0}{1 + \frac{2}{\gamma - 1} \frac{1}{M^2 \sin^2 \alpha}}. \quad (3.53)$$

The function y_0^* which determines the shock wave shape can be found by replacing the stream function ψ in the expression for y_0 by its value at the shock wave ψ_0^* :

$$y_0^* = \frac{\psi_0^*}{\rho_0 u_0 \bar{r}} = \frac{\rho^0 V}{\rho_0 u_0} \cdot \frac{\bar{r}^2 - r_0^2}{2\bar{r}}. \quad (3.54)$$

Using equations (3.53) and the boundary conditions (3.35), we find from equations (3.34), after some simple calculations, the functions u_1 , p_1 , and ρ_1 :

$$\begin{aligned} u_1 &= - \frac{\rho^0 V \sin^2 \alpha}{\rho_0 \cos \alpha} \frac{\psi + \rho^0 V r_0^2}{2\psi + \rho^0 V r_0^2}, \\ p_1 &= \rho^0 V^2 \sin^2 \alpha \frac{\rho^0}{\rho_0} \left[1 + \frac{1}{4} \left(1 + \frac{r_0^2}{\bar{r}^2} \right)^2 - \left(\frac{\psi}{\rho^0 V \bar{r}^2} \right)^2 \right] - (\rho^0 V^2 \sin^2 \alpha + p^0), \\ \rho_1 &= \rho_0 \left\{ \frac{\rho^0}{\gamma \rho_0} \left[\frac{1}{4} \left(1 + \frac{r_0^2}{\bar{r}^2} \right)^2 - \left(\frac{\psi}{\rho^0 V \bar{r}^2} \right)^2 \right] \right. \\ &\quad \left. + \left(\frac{4}{(\gamma - 1) M^2 \sin^2 \alpha} - \frac{\rho^0}{\gamma \rho_0} \right) \frac{\rho^0 V r_0^2}{2\psi + \rho^0 V r_0^2} + \frac{4}{(\gamma - 1) M^2 \sin^2 \alpha} \right\}. \end{aligned} \quad (3.55)$$

Equations (3.53) and (3.55) give the expressions for all the unknown quantities in the flow region behind the shock wave. In particular the pressure distribution along the wall is determined by the expression

$$\begin{aligned} p - p^0 &= \rho^0 V^2 \sin^2 \alpha \left\{ 1 + \frac{\gamma - 1}{\gamma + 1} \frac{1}{4} \right. \\ &\quad \times \left(1 + \frac{2}{(\gamma - 1) M^2 \sin^2 \alpha} \right) \left(1 + \frac{1}{\left(1 + \frac{x}{r_0} \sin \alpha \right)^2} \right)^2 \left. \right\}. \end{aligned}$$

Integrating the excess pressure along the body surface, we obtain for the drag coefficient of an annular conical body

$$C_D = \frac{D}{\pi(\bar{r}^2 - r_0^2)\rho^0 \frac{V^2}{2}} = 2 \left[1 + \frac{\gamma - 1}{\gamma + 1} \frac{1}{4} \frac{\rho^0}{\rho_0} \left(1 + f - \frac{2f \ln f}{1 - f} \right) \right] \sin^2 \alpha. \quad (3.56)$$

Here $f = r_0^2/\bar{r}^2$ is the ratio of the area of the annulus entrance to the area of the rear section of the cone. For $f \rightarrow 1$ the right-hand side of this expression becomes the drag coefficient of a wedge:

$$C_D^{\text{wedge}} = 2 \left[1 - \frac{\gamma - 1}{\gamma + 1} \frac{\rho^0}{\rho_0} \right] \sin^2 \alpha.$$

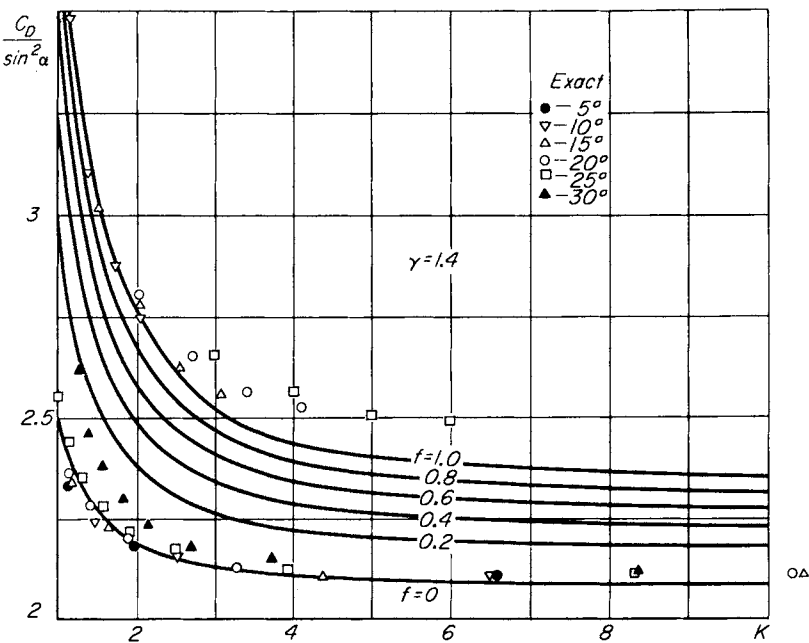


FIG. 3.26. Drag coefficients for annular conical bodies. Comparison of exact values for $f = 0$ and 1 with equation (3.56).

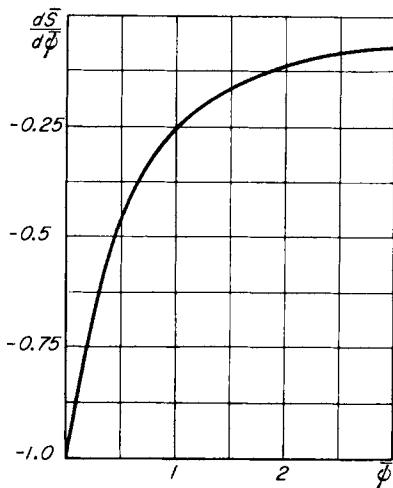


FIG. 3.27. Distribution of vorticity in the flow between body surface and shock wave for an annular conical body.

For $f \rightarrow 0$, it becomes the drag coefficient of a cone:

$$C_D^{\text{cone}} = 2 \left[1 - \frac{\gamma - 1}{\gamma + 1} \frac{1}{4} \frac{\rho^0}{\rho_0} \right] \sin^2 \alpha.$$

Curves of $C_D/\sin^2 \alpha$ as a function of the parameter $K = M \sin \alpha$, calculated from equation (3.56) for several values of f with $\gamma = 1.4$, are presented in Fig. 3.26. On the same figure are shown some exact values of $C_D/\sin^2 \alpha$ for $f = 0$ and $f = 1.0$.

According to equation (3.54), the shock curvature resulting from the flow past an annular conical body decreases rapidly with an increase in the x -coordinate. It follows that the vorticity in the flow rapidly decreases from the body surface to the shock wave. At a sufficient distance downstream of the nose, the vorticity is concentrated in an extremely thin layer near the surface of the body. The derivative $dS/d\psi$ (S is the entropy per unit mass) whose magnitude characterizes the vorticity is given by

$$\frac{dS}{d\bar{\psi}} = - \frac{\gamma - 1}{\gamma + 1} c_v \frac{1 - (2/M^2 \sin^2 \alpha)}{(1 + \bar{\psi})^2}, \quad \bar{\psi} = \frac{\psi}{\rho^0 (V r_0^2 / 2)}.$$

A graph of this relation is shown in Fig. 3.27, where we have denoted

$$S = \bar{S} \frac{\gamma - 1}{\gamma + 1} c_v \left(1 - \frac{2}{M^2 \sin^2 \alpha} \right).$$

CHAPTER IV

METHODS USING SHOCK AND SIMPLE WAVE RELATIONS

1. General remarks on the methods of calculating supersonic flows past airfoils

In this chapter we shall consider supersonic flows past airfoils with sharp leading edges. The local inclination angle of the surface of the airfoil with respect to the free stream direction and the free stream Mach number are assumed to be such that the bow wave is attached and the flow velocity is completely supersonic in those portions of the disturbed region which affect the flow near the airfoil.

Under these assumptions the calculation of the flow can be carried out by the method of characteristics. The method of characteristics, however, as pointed out in Chapter III, is rather time consuming and in general does not yield relations for the dependence of the aerodynamic characteristics of the airfoil upon its geometrical parameters, the angle of attack, or the free stream parameters (the Mach number M and the specific heat ratio γ). Therefore it is natural to seek approximate methods for calculating flows past airfoils which do not have this shortcoming. The simplest of such methods is the small disturbance theory based on the linearization of the flow equations. In this method, the local value of the pressure coefficient on an airfoil is given by the relation [1]

$$C_p = \frac{2}{\sqrt{M^2 - 1}} \theta, \quad (4.1)$$

where θ is the angle between an element of the surface and the free stream direction. Equation (4.1) enables us to determine the aerodynamic characteristics of any airfoil without difficulty. In particular we find for a flat plate at an angle of attack α ,

$$C_L = \frac{C_D}{\alpha} = \frac{4\alpha}{\sqrt{M^2 - 1}}.$$

This expression was used in Chapter I to plot the dashed lines in Fig. 1.7.

Let us briefly consider other frequently used methods for calculating the surface pressures on airfoils in supersonic flows,* without dwelling in detail on the small disturbance theory based on the linearization of the flow equations. Under the assumptions which were set forth at the beginning of this section, the flow on either side of the airfoil does not influence the flow on the opposite side. Therefore we can limit our considerations to only the upper surface of the airfoil, for example. When the region occupied by the flow expands behind the leading edge of the airfoil (Fig. 4.1,a), an expansion is generated at the surface of the

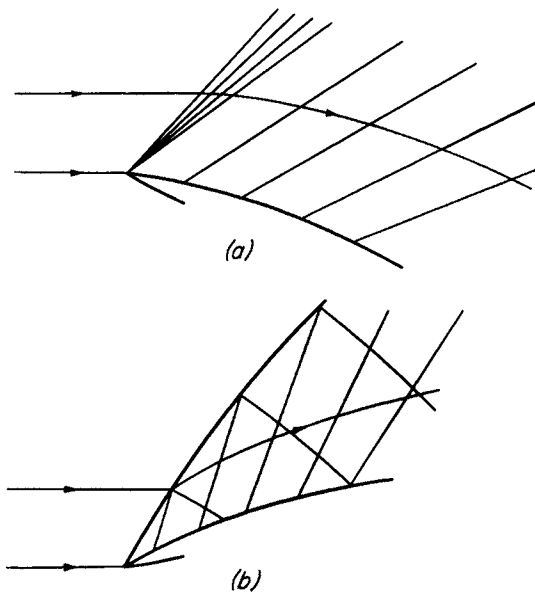


FIG. 4.1. Supersonic flow past an airfoil.

airfoil. Such a flow is a simple wave flow composed of a system of plane sound waves along each of which the flow parameters remain constant. The previous reasoning (see Chapter I, Section 3) for a simple wave produced by flow past a flat plate can also be applied without change to the present, more general case of flow past a curved surface. Thus

* More detailed treatments of these methods have been given, for example, in [1] and [2].

the flow parameters in a simple wave are determined as before by equations (1.13) and (1.14), and by the relations which follow from the adiabatic condition, the Bernoulli integral, and the equation of state. In particular one can calculate the surface pressure on an airfoil with these relations.

If behind the leading edge of the airfoil the region occupied by the incident flow becomes narrower (Fig. 4.1,b), a shock wave is formed in the flow. For a curved airfoil the flow behind the shock ceases to be isentropic and is no longer a simple wave. If the shock is weak, however, the entropy changes across it can be neglected (see, for example, [1]) and as before one can use the simple wave relations for calculating the pressure on the airfoil. It is easy to estimate the error connected with using the simple wave relations for calculating the pressure distribution along an airfoil. To do this one can compare the value of the pressure coefficient at the leading edge of the airfoil computed according to the exact oblique shock relations and according to the simple wave relations. Such a comparison has been made for $\gamma = 1.4$ in Fig. 4.2. The solid lines

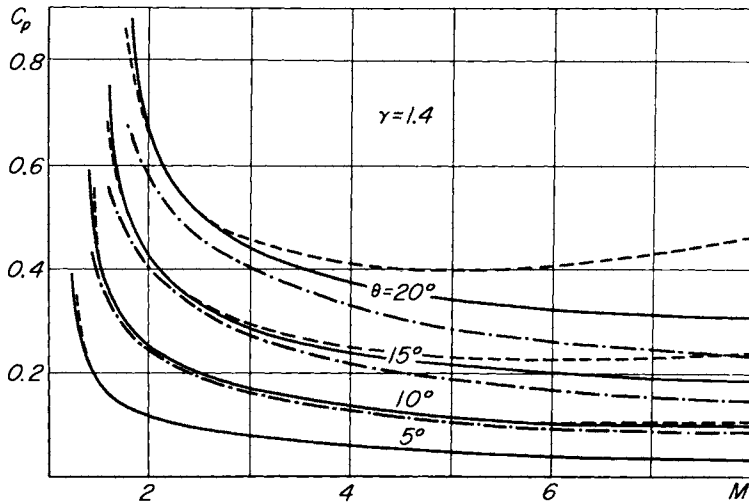


FIG. 4.2. Pressure coefficient at the leading edge of an airfoil: — oblique shock relations; - - simple wave relations; — · — equation (4.2).

give the exact values of the pressure and the dashed lines are the values calculated from the simple wave relations. (The curves obtained from the oblique shock relations are terminated at the left end of the figure at

the lowest value of the Mach number for which it is possible to deflect a flow across a shock wave for the given angle θ . The curves obtained from the simple wave relations are terminated at the point where the flow velocity behind the wave has dropped to the velocity of sound—further deflection through a simple wave is not possible.)

The close agreement of the curves for small θ and not very large values of the Mach number suggests the idea of using an expansion of C_p in terms of θ for a shock and simple wave, and comparing the expansions. From the simple wave relations and from the oblique shock relations we obtain respectively [1]:

$$C_p = a_1\theta + a_2\theta^2 + a_3\theta^3 + \dots$$

and

$$C_p = a_1\theta + a_2\theta^2 + (a_3 + a_{1d})\theta^3 + \dots,$$

where

$$a_1 = \frac{2}{\sqrt{M^2 - 1}}, \quad a_2 = \frac{2 - 2M^2 + \frac{1}{2}(\gamma + 1)M^4}{(M^2 - 1)^2},$$

$$a_3 = \frac{\frac{4}{3} - 2M^2 + \frac{5}{3}(\gamma + 1)M^4 - \frac{1}{6}(5 + 7\gamma - 2\gamma^2)M^6 + \frac{1}{6}(\gamma + 1)M^8}{(M^2 - 1)^{7/2}},$$

$$a_{1d} = \frac{\frac{1}{6}(\gamma + 1)M^4[\frac{1}{8}(3\gamma - 5)M^4 + \frac{1}{2}(3 - \gamma)M^2 - 1]}{(M^2 - 1)^{7/2}}.$$

The coefficients a_1 , a_2 , and a_3 are positive for all $M > 1$ and all $\gamma > 1$, but the coefficient a_{1d} changes sign with changing Mach number. For $\gamma = 1.4$ the quantity a_{1d} is negative outside the interval $1.245 < M < 2.540$ and positive inside. In absolute value the quantity a_{1d} is much less than a_3 .

For large values of the Mach number the coefficients a_1 , a_2 , a_3 , and a_{1d} have the following asymptotic forms:

$$a_1 = \frac{2}{M}, \quad a_2 = \frac{\gamma + 1}{2}, \quad a_3 = \frac{\gamma + 1}{6}M, \quad a_{1d} = \frac{(\gamma + 1)(3\gamma - 5)}{48}M.$$

These expressions are found to be in accord with the hypersonic similarity law. They can be obtained directly from the approximate equations for C_p through a simple wave (1.16) and through a shock wave (1.21) which are valid for large Mach numbers and small flow deflection angles.

The error resulting from the use of the simple wave relations for calculating the pressure at the leading edge of an airfoil can be taken as a

measure of the calculation error at all points of the surface, since the shock has its maximum strength near the leading edge. Thus simple wave theory gives an error in the pressure (and for the other flow parameters as well) of the order of θ^3 . Therefore in calculating the pressure behind a shock wave on an airfoil with the aid of simple wave relations, it is quite reasonable to neglect terms of order θ^3 and in this way retain the expression for C_p in the form

$$C_p = a_1\theta + a_2\theta^2. \quad (4.2)$$

This method for determining the pressure on an airfoil is due to Busemann (second-order theory).

In Fig. 4.2 the dashed-dotted lines are the values of C_p calculated from equation (4.2). In Fig. 4.3 a comparison is given for $\gamma = 1.4$ of the values

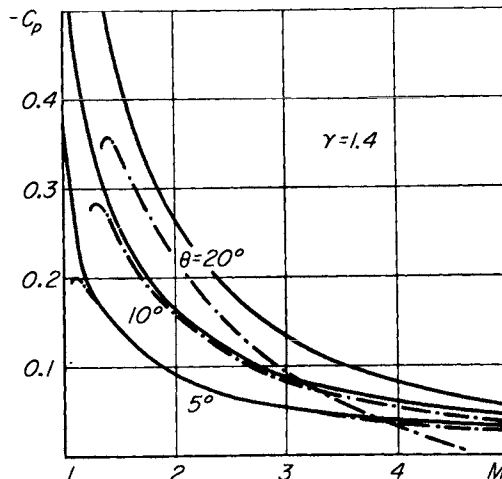


FIG. 4.3. Pressure coefficient through an expansion wave: — exact simple wave relation; - - - equation (4.2).

of C_p computed from this equation with the exact simple wave values for an expansion flow. For large values of the Mach number the agreement of the approximate values of C_p with the exact values becomes poorer, even for small θ . The explanation is that the radius of convergence of the series for C_p is proportional to M^{-1} for large M . The expressions (1.16) and (1.21) show that the corresponding series for flow past a flat plate converges only for $M\theta < 2/(\gamma - 1)$ and $M\theta < 4/(\gamma + 1)$, respec-

tively. Thus the linear theory, the Busemann second-order theory, and other more exact theories which take into account terms of order θ^3 and θ^4 (the theory of Donov, see [1]) can be used for the calculation of the pressure distribution along airfoils only when the quantity $M\theta$ is sufficiently small.

2. Exact method using shock and simple wave relations

For supersonic flows of an ideal gas past some airfoils, the pressure distribution along the surface can be calculated exactly using the shock wave relations and the simple wave solution (this possibility was first pointed out in [3]). Let a section OA of the contour of an airfoil near the leading edge be a straight line (Fig. 4.4). For supersonic flow with an

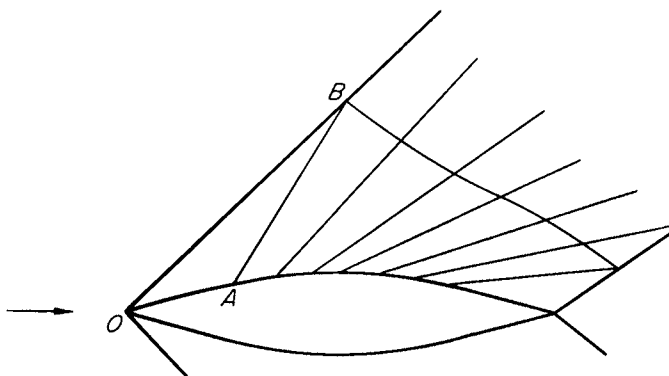


FIG. 4.4. Flow past an airfoil with a straight segment at the leading edge.

attached shock wave past such an airfoil, the flow in the region between the surface of the airfoil, the shock wave, and a characteristic segment AB is uniform. In this region the values of all the flow parameters can be found as functions of the free stream Mach number M_1 and the flow deflection angle at the leading edge of the airfoil $\bar{\theta}$ with the aid of the shock wave relations. A simple wave joins the uniform flow along the straight characteristic AB , so that at points on the airfoil surface downstream of the point A which do not fall under the region of influence of the point B , the pressure is determined by the simple wave solution. If the airfoil lies entirely outside the region of influence of the point B , the pressure everywhere on the surface can be found from the shock and simple wave relations:

The pressure coefficient at points on the surface of such an airfoil can be represented in the following form:

$$C_p = C_{p2} + \frac{\rho_2 V_2^2}{\rho_1 V_1^2} \tilde{C}_p(M_2, \theta - \bar{\theta}).$$

The pressure coefficient on the straight portion of the airfoil C_{p2} and also the quantities $\rho_2 V_2^2 / \rho_1 V_1^2$ and M_2 are determined from the shock wave conditions (1.17) and (1.18) by the free stream Mach number M_1 and the angle $\bar{\theta}$. The dependence of the pressure coefficient \tilde{C}_p through the simple wave upon the Mach number M_2 ahead of the simple wave and upon the flow deflection angle $\theta - \bar{\theta}$ through the wave is found by means of equation (1.14) and the relation

$$\frac{p}{p_2} = \left(\frac{1 + \frac{\gamma - 1}{2} M_2^2}{1 + \frac{\gamma - 1}{2} M^2} \right)^{\gamma/(\gamma-1)}$$

According to the equations of Section 3, Chapter I, the following approximate equalities are valid for hypersonic speeds and small values of the angle $\bar{\theta}$:

$$\begin{aligned} C_{p2} &= \frac{4}{\gamma + 1} \frac{K_s^2 - 1}{M_1^2}, \\ \frac{\rho_2}{\rho_1} &= \frac{1}{\frac{\gamma - 1}{\gamma + 1} + \frac{2}{\gamma + 1} \frac{1}{K_s^2}}, \quad \frac{V_2}{V_1} = 1, \\ M_2 &= \frac{M_1}{\sqrt{\left(\frac{2\gamma}{\gamma + 1} K_s^2 - \frac{\gamma - 1}{\gamma + 1} \right) \left(\frac{\gamma - 1}{\gamma + 1} + \frac{2}{\gamma + 1} \frac{1}{K_s^2} \right)}}, \\ \tilde{C}_p &= \frac{2}{\gamma M_2^2} \left\{ \left[1 - \frac{\gamma - 1}{2} M_2 (\bar{\theta} - \theta) \right]^{2\gamma/\gamma-1} - 1 \right\}. \end{aligned} \quad (4.3)$$

Here the quantity $K_s = M_1 \beta$ (β is the inclination angle of the shock wave with respect to the free stream direction) is related to the quantity $K = M_1 \bar{\theta}$ by the equation

$$K_s = \frac{\gamma + 1}{4} K + \sqrt{\left(\frac{\gamma + 1}{4} K \right)^2 + 1}.$$

By substituting these approximate expressions for the corresponding quantities in the equation for C_p , we can transform this equation to the form [4]

$$C_p = \frac{2}{\gamma M_1^2} \left\{ g(K) \left[1 - f(K) \left(1 - \frac{\theta}{\bar{\theta}} \right) \right]^{2\gamma/\gamma-1} - 1 \right\}. \quad (4.4)$$

Here

$$g = \frac{2\gamma}{\gamma + 1} K_s^2 - \frac{\gamma - 1}{\gamma + 1},$$

$$f = \frac{\frac{\gamma - 1}{2} K}{\sqrt{\left(\frac{2\gamma}{\gamma + 1} K_s^2 - \frac{\gamma - 1}{\gamma + 1} \right) \left(\frac{\gamma - 1}{\gamma + 1} + \frac{2}{\gamma + 1} \frac{1}{K_s^2} \right)}}.$$

Equation (4.4) enables us to easily determine the aerodynamic characteristics of slender airfoils at hypersonic speeds which satisfy the conditions for the application of the method set forth at the beginning of this section. To facilitate the calculations, values of the functions g and f for $\gamma = 1.4$ are given in Table 4.1 as a function of the parameter $K = M_1 \bar{\theta}$.

If the angle of attack of the airfoil is sufficiently large, a shock is not formed on the upper surface of the airfoil, and the pressure distribution on this surface can be found from the simple wave relation (1.16). (Equation (1.16) can be obtained from equation (4.4) by setting $K_s = 1$ and $\bar{\theta} = 0$.) In this case the pressure on the upper surface of the airfoil is less than the pressure in the undisturbed flow, a fact which is favorable to the development of lift. As the flight velocity increases, the pressure on the upper surface of the airfoil decreases, and for $M_1 \theta < 2/(\gamma - 1)$ the pressure is zero. This corroborates the conclusion drawn in Section 2 of Chapter III from the Newtonian formula—namely that at hypersonic speeds the value of the lift on an airfoil is determined principally by the pressure distribution on the lower surface at those angles of attack for which an expansion flow is produced on the upper surface of the airfoil. At such speeds, therefore, the maximum lift is attained by an airfoil with a flat lower surface, and any convexity of the lower surface of the airfoil results in a decrease of lift. If the angle of attack or flight Mach number are so large that the pressure on the upper surface

TABLE 4.1
VALUES OF $g(K)$ AND $f(K)$ FOR $\gamma = 1.4$

K	$g(K)$	$f(K)$	K	$g(K)$	$f(K)$
0	1.000	0	5.0	44.14	0.3466
0.05	1.072	0.009901	5.2	47.56	0.3487
0.10	1.148	0.01961	5.4	51.13	0.3506
0.15	1.230	0.02912	5.6	54.82	0.3523
0.20	1.316	0.03845	5.8	58.66	0.3539
0.25	1.406	0.04760	6.0	62.62	0.3553
0.30	1.502	0.05656	6.2	66.73	0.3566
0.35	1.604	0.06537	6.4	70.96	0.3578
0.40	1.710	0.07393	6.6	75.33	0.3589
0.45	1.823	0.08235	6.8	79.83	0.3600
0.50	1.941	0.09058	7.0	84.47	0.3610
0.55	2.065	0.09863	7.2	89.24	0.3618
0.60	2.195	0.1071	7.4	94.14	0.3626
0.65	2.332	0.1142	7.6	99.19	0.3633
0.70	2.474	0.1217	7.8	104.4	0.3640
0.75	2.624	0.1290	8.0	109.7	0.3647
0.80	2.780	0.1362	8.5	123.5	0.3661
0.85	2.943	0.1431	9.0	138.2	0.3673
0.90	3.112	0.1499	9.5	153.8	0.3684
0.95	3.289	0.1565	10.0	170.2	0.3693
1.00	3.473	0.1630	10.5	187.4	0.3701
1.1	3.862	0.1753	11.0	205.4	0.3707
1.2	4.280	0.1869	11.5	224.3	0.3714
1.3	4.728	0.1978	12.0	244.1	0.3719
1.4	5.206	0.2064	12.5	264.7	0.3723
1.5	5.715	0.2178	13.0	286.1	0.3727
1.6	6.256	0.2269	13.5	308.3	0.3731
1.7	6.827	0.2354	14.0	331.4	0.3735
1.8	7.431	0.2433	14.5	355.4	0.3738
1.9	8.066	0.2507	15.0	380.2	0.3740
2.0	8.734	0.2577	16.0	432.3	0.3745
2.1	9.411	0.2646	17.0	487.7	0.3749
2.2	10.17	0.2702	18.0	546.5	0.3752
2.3	10.93	0.2759	19.0	608.6	0.3755
2.4	11.73	0.2812	20.0	674.2	0.3757
2.5	12.56	0.2862	22.0	815.3	0.3761
2.6	13.42	0.2908	24.0	969.8	0.3764
2.7	14.32	0.2951	26.0	1,138	0.3766
2.8	15.25	0.2992	28.0	1,319	0.3768
2.9	16.21	0.3030	30.0	1,514	0.3770
3.0	17.21	0.3066	35.0	2,060	0.3772
3.2	19.30	0.3130	40.0	2,690	0.3774

TABLE 4.1 (cont.)

K	$g(K)$	$f(K)$	K	$g(K)$	$f(K)$
3.4	21.52	0.3187	45.0	3,404	0.3775
3.6	23.88	0.3287	50.0	4,202	0.3776
3.8	26.37	0.3280	60.0	6,050	0.3777
4.0	29.00	0.3322	70.0	8,233	0.3778
4.2	31.76	0.3358	80.0	10,750	0.3778
4.4	34.65	0.3389	90.0	13,610	0.3779
4.6	37.68	0.3418	100.0	16,800	0.3779
4.8	40.84	0.3443	∞	∞	0.3780

of the airfoil is everywhere zero, then such a flat-bottomed airfoil will behave aerodynamically like an infinitely thin flat plate.

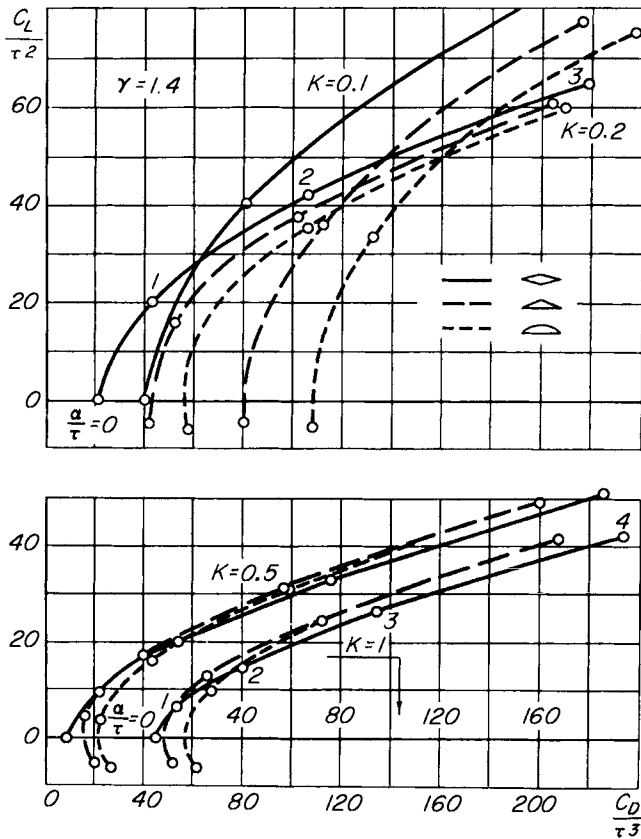


FIG. 4.5. Polar diagrams for slender airfoils at hypersonic speeds.

As an example, polar diagrams (i.e., the dependence of C_L on C_D) are shown in Fig. 4.5, calculated from equation (4.4) for airfoils of triangular and diamond section* [5] for values of $K = M_1\tau$ from 0.1 to 1.0 (τ is the thickness ratio of the airfoil). (The curves for large values of K are practically the same as the curves for $K = 1$.) For $K \geq 0.5$ the lift-drag ratio C_L/C_D is greater for a triangular airfoil than for a diamond airfoil, excluding a small region corresponding to low values of lift. This advantage of the triangular airfoil becomes greater with an increase of the parameter K . We recall that this fact was indicated previously (Section 2, Chapter III) with regard to limiting hypersonic flows past airfoils, for which the pressure was calculated by the Newtonian formula.

3. Interaction of disturbances with a shock wave

If the surface of the airfoil is curved at the leading edge, vorticity will be present in the flow. The flow calculation can then no longer be carried out by the method of the previous section, since the entire airfoil is located in the region of influence of the disturbances reflected from the bow shock wave. The vorticity and disturbances reflected from the shock wave can be neglected for weak bow shocks and the flow near the airfoil surface can, as before, be considered a simple wave with the entropy corresponding to the entropy of the undisturbed stream. In this case the waves give rise to a curved shock but the shock does not produce a feedback effect on the simple wave flow.

If the bow shock is sufficiently strong, it is no longer possible to neglect the vorticity in the flow and it becomes necessary to take into account the interaction of the flow near the airfoil with the bow shock. The question of the interaction with a shock wave of disturbances which are incident on it from a region of supersonic flow behind the shock was first examined in [6]. This type of interaction, as well as the interaction of disturbances in the free stream flow with a shock wave, was investigated independently by the author in 1950. Part of this work was later repeated in other papers [4, 7, 8]. Some of the results obtained by the author are reproduced in this and the following section.

Let us consider a two-dimensional or axisymmetric flow with a shock

* The method of determining the polar diagram shown in this figure for the circular-arc airfoil will be given in Section 5 of the present chapter.

wave present. We place the origin of the coordinates at some point O on the shock wave and choose the axis Ox in such a way that its direction differs by only a small amount from the streamline direction behind the shock. We let the direction of the incident undisturbed flow be Ox' . The axes Ox and Ox' together with their normals Oy and Oy' form two systems of coordinates in the plane of flow (Fig. 4.6). We shall denote by

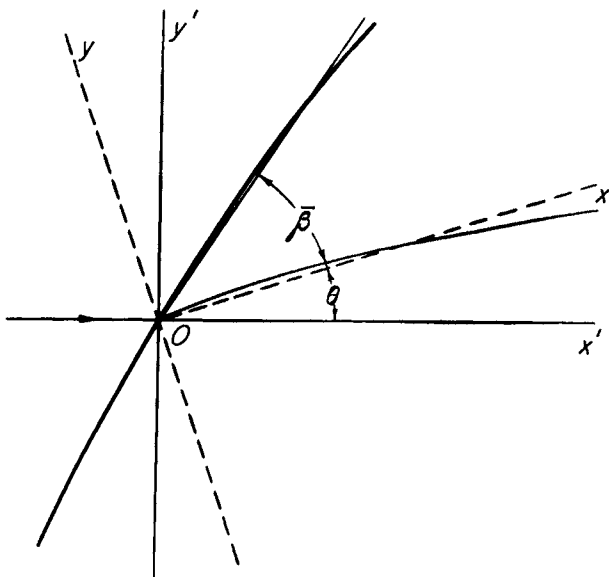


FIG. 4.6. Coordinate systems for studying the flow near a shock wave.

θ the angle between the axes Ox and Ox' , by u and v the projections of the velocity on the axes Ox and Oy , respectively, and by U and V the projections of the velocity on the axes Ox' and Oy' , respectively. The subscripts 1 and 2 denote quantities in the flow regions ahead of and behind the shock, respectively.

To determine the flow behind the shock we shall use the previously derived system of equations (3.26). For the case being considered, on putting $R = \infty$ and $r = r_0 + x \sin \theta + y \cos \theta$ (where r_0 is the distance of the origin from the axis of symmetry) the system reduces to the following form:

$$\rho u \frac{\partial u}{\partial x} + \rho v \frac{\partial u}{\partial y} = - \frac{\partial p}{\partial x},$$

$$\begin{aligned} \rho u \frac{\partial v}{\partial x} + \rho v \frac{\partial v}{\partial y} &= - \frac{\partial p}{\partial y}, \\ \frac{\partial \rho u}{\partial x} + \frac{\partial \rho v}{\partial y} + (\nu - 1) \frac{\rho u \sin \theta + \rho v \cos \theta}{r_0 + x \sin \theta + y \cos \theta} &= 0, \\ u \frac{\partial}{\partial x} \frac{p}{\rho^\gamma} + v \frac{\partial}{\partial y} \frac{p}{\rho^\gamma} &= 0. \end{aligned} \quad (4.5)$$

It follows from the choice of direction of the axis Ox that the equation of a streamline behind the shock can be written in the form

$$y = \epsilon' Y(x).$$

Here ϵ' is a small quantity which characterizes the deviation of the streamline from the chosen direction Ox . The function $Y(x)$ together with its derivative are of the order of unity in the flow region being considered (the characteristic dimension of which we shall take equal to unity).

With small disturbances present in the free stream flow, the flow parameters can be represented in the form

$$\begin{aligned} p_1 &= \bar{p}_1 + \epsilon'' p'_1, & U &= \bar{U} + \epsilon'' U', \\ \rho_1 &= \bar{\rho}_1 + \epsilon'' \rho'_1, & V &= \epsilon'' V'. \end{aligned} \quad (4.6)$$

Here \bar{p}_1 , $\bar{\rho}_1$, and \bar{U} are constants corresponding to the undisturbed free stream, and ϵ'' is a small quantity which characterizes the deviation of the free stream from a uniform rectilinear flow. The functions p_1 , ρ_1 , U , and V which describe the flow upstream of the shock wave will be considered as given.

It is evident that for the case of axial symmetry, the flow region near the point O will approximate a two-dimensional flow to the extent that the dimension of this flow region is small in comparison with its distance r_0 from the axis of symmetry. Therefore one can introduce another small parameter $\epsilon''' = (\nu - 1)/r_0$ which characterizes the deviation of an axi-symmetric flow from a two-dimensional flow.

In order to determine the disturbed flow behind the shock wave we must relate the flow parameters on both sides of the shock by the following conditions [see equations (1.5)]:

$$\begin{aligned}\rho_2(u_2 \sin \beta - v_2 \cos \beta) &= \rho_1(u_1 \sin \beta - v_1 \cos \beta), \\ \rho_2(u_2 \sin \beta - v_2 \cos \beta)^2 + p_2 &= \rho_1(u_1 \sin \beta - v_1 \cos \beta)^2 + p_1, \quad (4.7) \\ u_2 \cos \beta + v_2 \sin \beta &= u_1 \cos \beta + v_1 \sin \beta, \\ \frac{u_2^2 + v_2^2}{2} + \frac{\gamma}{\gamma-1} \frac{p_2}{\rho_2} &= \frac{u_1^2 + v_1^2}{2} + \frac{\gamma}{\gamma-1} \frac{p_1}{\rho_1}.\end{aligned}$$

Let us now represent the quantities characterizing the flow behind the shock wave as the sums of leading terms which are linear with respect to the small parameters ϵ' , ϵ'' , and ϵ''' plus terms of higher order, i.e.,

$$\begin{aligned}u_2 &= \bar{u}_2(1 + \epsilon' u' + \epsilon'' u'' + \epsilon''' u''' + \dots), \\ v_2 &= \bar{v}_2(\epsilon' v' + \epsilon'' v'' + \epsilon''' v''' + \dots), \\ p_2 &= \bar{p}_2(1 + \epsilon' p' + \epsilon'' p'' + \epsilon''' p''' + \dots), \quad (4.8) \\ \rho_2 &= \bar{\rho}_2(1 + \epsilon' \rho' + \epsilon'' \rho'' + \epsilon''' \rho''' + \dots).\end{aligned}$$

Here \bar{u}_2 , \bar{p}_2 , and $\bar{\rho}_2$ are constants which correspond to the state of the gas behind an oblique shock with a flow deflection angle θ .

In what follows we shall limit ourselves to finding only the terms of first degree in the small parameters. For brevity we introduce the notation

$$\epsilon\varphi(x, y) \equiv \epsilon' \varphi'(x, y) + \epsilon'' \varphi''(x, y) + \epsilon''' \varphi'''(x, y),$$

and then substitute the expressions (4.8) into equations (4.5). On dropping terms higher than first order in ϵ , we obtain the following system of linear equations (variational equations) for the determination of ϵu , ϵv , ϵp , and $\epsilon\rho$:

$$\begin{aligned}\frac{\partial \epsilon u}{\partial x} + \frac{1}{\gamma M_2^2} \frac{\partial \epsilon p}{\partial x} &= 0, \\ \frac{\partial \epsilon v}{\partial x} + \frac{1}{\gamma M_2^2} \frac{\partial \epsilon p}{\partial y} &= 0, \\ \frac{\partial \epsilon p}{\partial x} - \gamma \frac{\partial \epsilon \rho}{\partial x} &= 0, \\ \frac{\partial \epsilon u}{\partial x} + \frac{\partial \epsilon \rho}{\partial x} + \frac{\partial \epsilon v}{\partial y} + \epsilon''' \sin \theta &= 0,\end{aligned} \quad (4.9)$$

where we have denoted $M_2^2 = \bar{u}_2^2 / (\gamma p_2 / \rho_2)$.

Let us now linearize the boundary conditions (4.7) at the shock wave. We shall represent the shock inclination angle in the form

$$\beta = \bar{\beta} + \epsilon\beta',$$

where $\bar{\beta}$ is the inclination angle with respect to the axis Ox of the shock wave in the undisturbed flow which corresponds to the flow deflection angle θ . We then introduce this expression together with the expressions (4.8) into the conditions (4.7).

Taking into account the relations between the flow parameters in the basic flow, we obtain after linearization the following conditions at the shock wave:

$$\begin{aligned} \epsilon u - \epsilon v \cot \bar{\beta} + \epsilon p + \left(1 - \frac{\bar{\rho}_1}{\bar{\rho}_2}\right) \epsilon \beta' \cot \bar{\beta} &= \epsilon'' L_1, \\ 2\epsilon u - 2\epsilon v \cot \bar{\beta} + \epsilon p + \frac{1}{\gamma M_2^2 \sin^2 \bar{\beta}} \epsilon p &= \epsilon'' L_2, \\ \epsilon u + \epsilon v \tan \bar{\beta} + \left(\frac{\bar{\rho}_2}{\bar{\rho}_1} - 1\right) \epsilon \beta' \tan \bar{\beta} &= \epsilon'' L_3, \\ \epsilon u + \frac{1}{(\gamma - 1)M_2^2} (\epsilon p - \epsilon p) &= \epsilon'' L_4. \end{aligned} \quad (4.10)$$

Here we have introduced for brevity the notation

$$\begin{aligned} L_1 &= U' - V' \cot (\theta + \bar{\beta}) + \rho'_1, \\ L_2 &= \frac{1}{\bar{\rho}_2 \bar{u}_2^2 \sin^2 \bar{\beta}} \{ \bar{\rho}_1 \bar{U}^2 \sin^2 (\bar{\beta} + \theta) [2U' - 2 \cot (\bar{\beta} + \theta) V' + \rho'_1] + \bar{\rho}_1 p'_1 \}, \\ L_3 &= U' + V' \tan (\bar{\beta} + \theta), \\ L_4 &= \frac{\bar{U}^2}{\bar{u}_2^2} \left[U' + \frac{1}{(\gamma - 1)M_1^2} (p'_1 - \rho'_1) \right]. \end{aligned}$$

It is apparent that to the present approximation it is sufficient that the conditions (4.10) be satisfied not at the points

$$y = x \tan \bar{\beta} + \frac{1}{\cos^2 \bar{\beta}} \int_0^x \epsilon \beta' dx \quad (4.11)$$

on the shock itself, but at points on the straight line $y = x \tan \bar{\beta}$ at the corresponding abscissas ($\cos^2 \bar{\beta}$ can be considered sufficiently large).

For supersonic velocities behind the shock, the system of equations (4.9) is easily integrated in general form. The existence of the integrals

$$\epsilon u + \frac{1}{\gamma M_2^2} \epsilon p = \epsilon F_1(y),$$

$$\epsilon p - \gamma \epsilon u = -\gamma \epsilon F_2(y),$$

follows immediately from the first and third equations. (In linear approximation these integrals are equivalent to the Bernoulli integral and the adiabatic condition.) The perturbations in the total enthalpy and entropy of the gas which propagate with the gas particles along streamlines can be expressed through the functions $F_1(y)$ and $F_2(y)$. Using the above integrals and the remaining two equations of the system (4.9), we obtain

$$(M_2^2 - 1) \frac{\partial^2 \epsilon p}{\partial x^2} - \frac{\partial^2 \epsilon p}{\partial y^2} = 0.$$

For $M_2 > 1$ the general solution of this equation for ϵp along with the expressions for the other unknown functions can be written in the form

$$\begin{aligned} \epsilon p &= \gamma M_2^2 [\epsilon F_3(x - \sqrt{M_2^2 - 1}y) - \epsilon F_4(x + \sqrt{M_2^2 - 1}y)], \\ \epsilon u &= \epsilon F_1(y) - \epsilon F_3(x - \sqrt{M_2^2 - 1}y) + \epsilon F_4(x + \sqrt{M_2^2 - 1}y), \\ \epsilon v &= \sqrt{M_2^2 - 1} [\epsilon F_3(x - \sqrt{M_2^2 - 1}y) \\ &\quad + \epsilon F_4(x + \sqrt{M_2^2 - 1}y)] - \epsilon''' y \sin \theta, \\ \epsilon \rho &= \epsilon F_2(y) + M_2^2 [\epsilon F_3(x - \sqrt{M_2^2 - 1}y) - \epsilon F_4(x + \sqrt{M_2^2 - 1}y)]. \end{aligned} \tag{4.12}$$

The functions $F_3(x - \sqrt{M_2^2 - 1}y)$ and $F_4(x + \sqrt{M_2^2 - 1}y)$ describe the disturbances which propagate along the two families of characteristics in the directions toward and away from the shock wave, respectively.

The general solution which was obtained for the system of equations (4.9) contains the four arbitrary functions F_1 , F_2 , F_3 , F_4 . The boundary conditions (4.10) relate the values of these functions on the shock wave to the quantity β' which characterizes the shock shape. Putting the expressions (4.12) into the shock conditions (4.10) and denoting $\sqrt{M_2^2 - 1}$ by $\cot \alpha$, we obtain for $y = x \tan \bar{\beta}$

$$\begin{aligned}
& \epsilon F_1 + \epsilon F_2 + \cot \alpha (\cot \alpha - \cot \bar{\beta}) \epsilon F_3 - \cot \alpha (\cot \alpha + \cot \bar{\beta}) \epsilon F_4 \\
& \quad + \left(1 - \frac{\bar{\rho}_1}{\bar{\rho}_2} \right) \epsilon \beta' \cot \bar{\beta} = \epsilon'' L_1 - \epsilon''' x \sin \theta, \\
& 2\epsilon F_1 + \epsilon F_2 + (\cot \alpha - \cot \bar{\beta})^2 \epsilon F_3 - (\cot \alpha + \cot \bar{\beta})^2 \epsilon F_4 \\
& \quad = \epsilon'' L_2 - 2\epsilon''' x \sin \theta, \\
& \epsilon F_1 + \tan \bar{\beta} (\cot \alpha - \cot \bar{\beta}) \epsilon F_3 + \tan \bar{\beta} (\cot \alpha + \cot \bar{\beta}) \epsilon F_4 \quad (4.13) \\
& \quad + \left(\frac{\bar{\rho}_2}{\bar{\rho}_1} - 1 \right) \epsilon \beta' \tan \bar{\beta} = \epsilon'' L_3 + \epsilon''' x \tan^2 \beta \sin \theta, \\
& \epsilon F_1 - \frac{1}{(\gamma - 1) M_2^2} \epsilon F_2 = \epsilon'' L_4.
\end{aligned}$$

From these relations we can readily express the functions F_1 , F_2 , F_4 , and β' at the shock in terms of the function F_3 . In particular it is not difficult to obtain the following relation between the functions F_4 and F_3 :

$$\epsilon F_4 \left[\left(1 + \frac{\tan \bar{\beta}}{\tan \alpha} \right) x \right] + \lambda \epsilon F_3 \left[\left(1 - \frac{\tan \bar{\beta}}{\tan \alpha} \right) x \right] = \epsilon'' \bar{L}(x) + \epsilon''' \bar{C}x. \quad (4.14)$$

Here

$$\begin{aligned}
\lambda &= \frac{a - b}{a + b}, \quad \bar{C} = \frac{a}{a + b} \tan \alpha \tan \bar{\beta} \sin \theta, \\
\bar{L}(x) &= - \frac{2 \tan^2 \bar{\beta}}{a + b} \left\{ \left(1 + \frac{\gamma - 1}{2} M_2^2 \right) \frac{\bar{\rho}_2}{\bar{\rho}_1} \sin^2 \bar{\beta} L_1 \right. \\
&\quad + \frac{1}{2} \left[\cot^2 \bar{\beta} - (1 - (\gamma - 1) M_2^2) \frac{\bar{\rho}_2}{\bar{\rho}_1} \right] \sin^2 \bar{\beta} L_2 - \left(1 + \frac{\gamma - 1}{2} M_2^2 \right) \cos^2 \bar{\beta} L_3 \\
&\quad \left. + \frac{\gamma - 1}{2} M_2^2 \left(\frac{\bar{\rho}_2}{\bar{\rho}_1} \sin^2 \bar{\beta} + \cos^2 \bar{\beta} \right) L_4 \right\}.
\end{aligned}$$

The quantities a and b are expressed by the relations

$$\begin{aligned}
a &= 2 \frac{\tan \bar{\beta}}{\tan \alpha} \left[1 - \frac{\gamma - 1}{2} M_2^2 \sin^2 \bar{\beta} \left(\frac{\bar{\rho}_2}{\bar{\rho}_1} - 1 \right) \right], \\
b &= 1 + \frac{\bar{\rho}_2}{\bar{\rho}_1} \frac{\tan^2 \bar{\beta}}{\tan^2 \alpha} - \gamma M_2^2 \sin^2 \bar{\beta} \left(\frac{\bar{\rho}_2}{\bar{\rho}_1} - 1 \right).
\end{aligned} \quad (4.15)$$

Let us first consider the case when the free stream is undisturbed and the flow is plane parallel, i.e., $\epsilon'' = \epsilon''' = 0$. Then from equation (4.14) and the expression for ϵp in (4.12) it follows that if we take as a measure of the flow disturbance the corresponding change in pressure, the quantity λ will represent the reflection coefficient of a disturbance from the shock wave. This reflection coefficient is the ratio of the amplitude of the disturbance reflected from the shock wave (along the characteristic $x + \sqrt{M_2^2 - 1}y = \text{const.}$) to the amplitude of the disturbance incident on the shock wave (along the characteristic $x - \sqrt{M_2^2 - 1}y = \text{const.}$).

From the previously used expression for the density ratio across the shock wave

$$\frac{\bar{\rho}_1}{\bar{\rho}_2} = \frac{\gamma - 1}{\gamma + 1} + \frac{2}{(\gamma + 1)M_1^2 \sin^2(\bar{\beta} + \theta)},$$

and from the symmetry of the relations at the shock with respect to the subscripts 1 and 2, it follows that

$$\frac{\bar{\rho}_2}{\bar{\rho}_1} = \frac{\gamma - 1}{\gamma + 1} + \frac{2}{(\gamma + 1)M_2^2 \sin^2 \bar{\beta}}.$$

These expressions enable us to obtain the inequalities

$$1 < \frac{\bar{\rho}_2}{\bar{\rho}_1} < \frac{\gamma + 1}{\gamma - 1},$$

$$\frac{\gamma - 1}{2\gamma} < M_2^2 \sin^2 \bar{\beta} < 1, \quad \frac{\gamma + 1}{2\gamma} < M_2^2 \sin^2 \bar{\beta} \frac{\bar{\rho}_2}{\bar{\rho}_1} < 1.$$

Replacing every term on the right-hand sides of equations (4.15) by its minimum value, we obtain

$$\frac{a \tan \alpha}{2 \tan \bar{\beta}} > 1 - \frac{\gamma - 1}{2} + \frac{\gamma - 1}{2} \frac{\gamma - 1}{2\gamma} > 0,$$

$$\begin{aligned} b &= 1 + \frac{\bar{\rho}_2 \tan^2 \bar{\beta}}{\bar{\rho}_1 \tan^2 \alpha} + \gamma M_2^2 \sin^2 \bar{\beta} - \gamma \left(\frac{2}{\gamma + 1} + \frac{\gamma - 1}{\gamma + 1} M_2^2 \sin^2 \bar{\beta} \right) \\ &= \frac{\bar{\rho}_2 \tan^2 \bar{\beta}}{\bar{\rho}_1 \tan^2 \alpha} + \frac{2\gamma}{\gamma + 1} M_2^2 \sin^2 \bar{\beta} - \frac{\gamma - 1}{\gamma + 1} > \frac{\bar{\rho}_2 \tan^2 \bar{\beta}}{\bar{\rho}_1 \tan^2 \alpha} > 0. \end{aligned}$$

Since the quantity λ can be written in either of the forms

$$\lambda = \frac{a - b}{a + b} = 1 - \frac{2b}{a + b} = -1 + \frac{2a}{a + b},$$

it is clear that $|\lambda| < 1$. The quantity λ calculated for different values of the Mach number M_1 and for $\gamma = 1.4$ is shown in Fig. 4.7 as a function of the flow deflection angle θ .

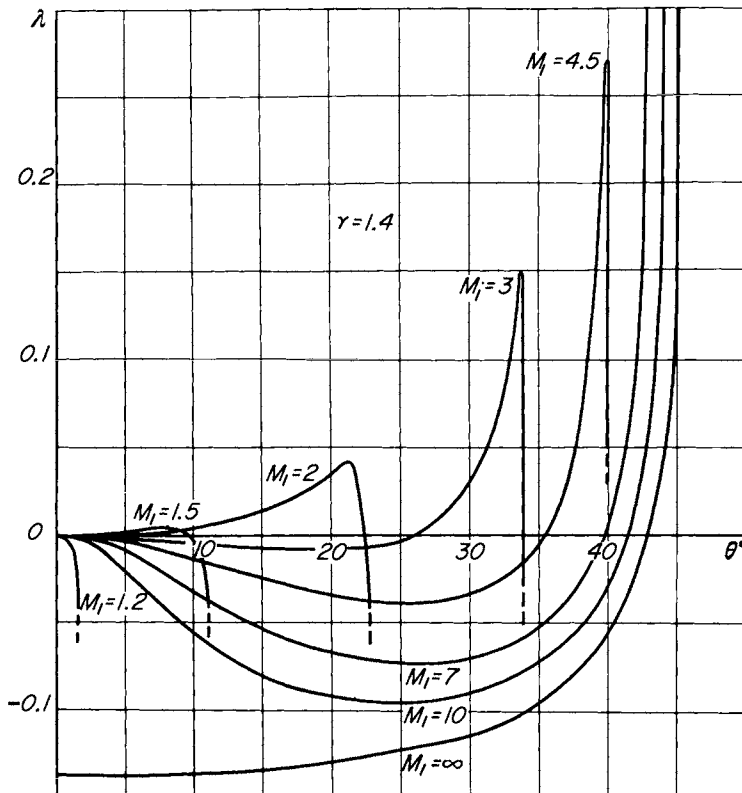


FIG. 4.7. Reflection coefficient of a disturbance from a shock wave surface.

Making use of the expressions (4.15) for small values of the angle θ and for Mach numbers which are not too large (i.e., for $M_1\theta \ll 1$), we can, by simple but tedious calculation, obtain the relation

$$\lambda = h(M_1)\theta^2 + O(\theta^3),$$

where

$$h(M_1) = \frac{\frac{1}{8}(\gamma + 1)M_1^4[\frac{1}{8}(3\gamma - 5)M_1^4 + \frac{1}{2}(3 - \gamma)M_1^2 - 1]}{(M_1^2 - 1)^3}.$$

For small values of θ the quantity λ is of the order of θ^2 . As is known, this permits one to neglect the interaction between the shock wave and the flow behind it when calculating the small terms of first and second order in the flow deflection angle. We note that for $\gamma < 5/3$ the function $h(M_1)$ vanishes for two values of the Mach number M_1 , and for $\gamma \geq 5/3$ it vanishes for one value. For $\gamma = 1.4$ the values of M_1 for which $h(M_1)$ vanishes are 1.245 and 2.540.

These considerations on the reflection of disturbances from a shock wave surface clarify the significance of the quantity a_{1d} (see Section 1 of this chapter), which distinguishes the pressure coefficient behind a shock from the pressure coefficient through a simple wave. Indeed for small values of θ the leading term in the expression for the pressure coefficient, which relates to the effect of the reflected disturbances from the shock, is equal to $\lambda a_1 \theta$ or $h a_1 \theta^2$. It follows from the appropriate relations that the product $h a_1$ is simply proportional to the coefficient a_{1d} .

The curves of Fig. 4.7 have a number of interesting features. First of all, from an examination of them it follows that the quantity $|\lambda|$ is small, particularly for small values of the Mach number M_1 . Only for large values of the Mach number M_1 , and also for those values of the flow deflection angle θ for which the Mach number M_2 is close to 1, does λ become appreciable. In the former case $\lambda = \lambda(\theta)$ has a very sharp maximum for a fixed M_1 . Furthermore, from an examination of the curves it follows that the quantity λ can be positive as well as negative, i.e., in some cases the reflection takes place without the disturbance changing sign, while in other cases the sign of the disturbance is changed due to the reflection.* For $\gamma = 1.4$ and for $M_1 < 1.245$, $\lambda = 0$ only for $\theta = 0$; in the range of Mach numbers M_1 from 1.245 to 2.540, λ vanishes for one value of θ (besides $\theta = 0$); and for $M_1 > 2.540$ it vanishes for two values of θ .

It is important to note that the reflection coefficient λ is rather sensitive to changes in γ . In order to estimate the effect of γ on the coefficient λ , we shall limit the calculations of λ to the case $M_1 = \infty$, since for a

* As a result of an error, the author of [6] arrived at the incorrect conclusion that for $M_1 \rightarrow \infty$ the reflection coefficient λ tends to -1 . In [8] it is incorrectly stated that $0 < \lambda < 1$, so that some of the conclusions of this reference are incorrect; in particular, the conclusion concerning the conservation of sign of the reflected disturbance [see *Referat. Zhur. (Abstract Journal)*, *Mekhanika* **3**, no. 2457 (1954)].

given γ the reflection coefficient takes on its maximum absolute value for $M_1 = \infty$. In Fig. 4.8, λ is shown as a function of θ for $M_1 = \infty$ and several values of γ . The reflection coefficient λ is seen to increase in absolute value for decreasing γ , excluding a small region near the values

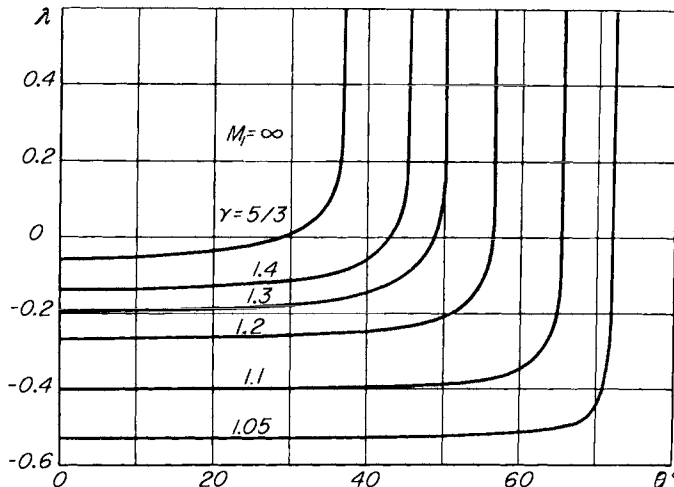


FIG. 4.8. Dependence of the reflection coefficient on the specific heat ratio for $M_1 = \infty$.

of θ which correspond to subsonic speeds behind the shock. This increase for a decrease of γ from 1.4 to, say, 1.3 is not very large. With a further decrease of γ , however, the absolute value of the coefficient λ begins to increase sharply, and for $\gamma = 1$ the coefficient becomes equal to -1 , i.e., the disturbances when reflected change their sign but retain their magnitude.

4. Flows past wedgelike bodies and slender airfoils at large angles of attack

Let us consider the supersonic flow past a body whose shape is close to a wedge, under the condition that the velocity behind the attached shock wave remains supersonic. To describe the flow between the body surface and the bow shock, we can make use of the solution obtained in the previous section by considering the streamline

$$y = \epsilon' Y(x)$$

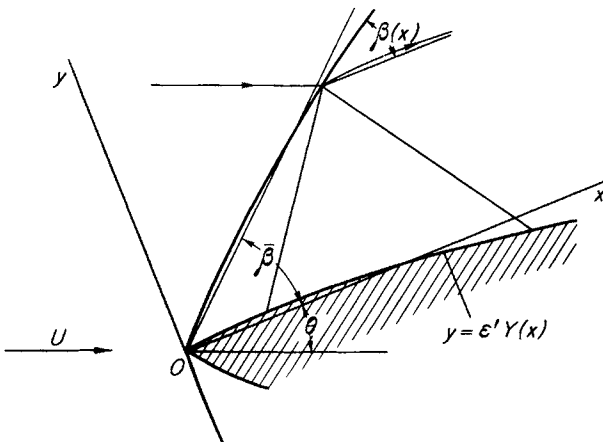


FIG. 4.9. Flow past a wedgelike airfoil.

which passes through the point 0 (Fig. 4.9), to represent the contour of one side of the body.* On this line the streamline condition

$$\frac{v_2}{u_2} = \epsilon' Y'(x)$$

must be fulfilled. In accordance with equations (4.8), let us substitute into this condition $v_2 = \bar{u}_2 \epsilon v + \dots$ and $u_2 = \bar{u}_2(1 + \epsilon u + \dots)$. Then using equations (4.12) for ϵu and ϵv and dropping terms of order ϵ^2 , we find

$$\epsilon F_3(x) + \epsilon F_4(x) = \epsilon' \frac{Y'(x)}{\sqrt{M_2^2 - 1}}. \quad (4.16)$$

Using this relation we can eliminate the function F_4 from equation (4.14) and in this way obtain one equation to determine the function F_3 . This relation is

$$\begin{aligned} \epsilon F_3 \left[\left(1 + \frac{\tan \bar{\beta}}{\tan \alpha} \right) x \right] - \lambda \epsilon F_3 \left[\left(1 - \frac{\tan \bar{\beta}}{\tan \alpha} \right) x \right] \\ = \epsilon' \tan \alpha Y' \left[\left(1 + \frac{\tan \bar{\beta}}{\tan \alpha} \right) x \right] - \epsilon'' \bar{L}(x) - \epsilon''' \bar{C}x. \quad (4.17) \end{aligned}$$

* A slender airfoil at large angle of attack is one such body. In this case the flow on the other side of the airfoil is a simple expansion wave.

We now introduce the new variable

$$\xi = \left(1 + \frac{\tan \bar{\beta}}{\tan \alpha}\right) x$$

and denote by k the quantity

$$k = \frac{1 - (\tan \bar{\beta}/\tan \alpha)}{1 + (\tan \bar{\beta}/\tan \alpha)}. \quad (4.18)$$

Equation (4.17) then takes the form

$$\epsilon F_3(\xi) - \lambda \epsilon F_3(k\xi) = \epsilon' \tan \alpha Y'(\xi) - \epsilon'' L(\xi) - \epsilon''' C \xi, \quad (4.19)$$

where

$$L(\xi) = \bar{L} \left[\frac{\xi}{1 + (\tan \bar{\beta}/\tan \alpha)} \right],$$

$$C = \frac{a}{a+b} \frac{\tan \alpha \tan \bar{\beta} \sin \theta}{1 + (\tan \bar{\beta}/\tan \alpha)}.$$

Thus the problem of supersonic flow past a wedgelike body is reduced to the solution of the functional equation (4.19), which can be separated into three equations of the form

$$F_3(\xi) - \lambda F_3(k\xi) = f(\xi). \quad (4.20)$$

Let us now solve this equation. Since α is the inclination angle with respect to the axis Ox of a characteristic downstream of the shock, then $\alpha > \bar{\beta}$, so that from equation (4.18), $k > 0$. It is also obvious that $k < 1$. The function $f(\xi)$ will be considered defined and piecewise continuous on the segment $[0, X]$, where X can be indefinitely large. We shall show that for the stated conditions equation (4.20) has a unique solution which is finite on the segment $[0, X]$, and we shall construct this solution.

It is not difficult to verify that the series

$$F_3(\xi) = \sum_{n=0}^{\infty} \lambda^n f(k^n \xi) \quad (4.21)$$

formally satisfies equation (4.20) for every ξ . If the function $f(\xi)$ is piecewise continuous on the segment $[0, X]$ and $\xi = 0$ is not a point of

discontinuity, then only a finite number of the leading terms of this series are discontinuous. The remaining terms in the series will be continuous and since

$$|\lambda^n f(k^n \xi)| \leq |\lambda|^n N,$$

where

$$N = \max_{0 \leq \xi \leq X} |f(\xi)|,$$

their sum exists and this sum is also a continuous function on the segment $[0, X]$. Hence the series (4.21) is actually a solution of equation (4.20). But since the function $F_3(\xi)$ must also be twice piecewise differentiable, it is still necessary to prove the convergence of the series obtained by double differentiation of the series (4.21) with respect to ξ . This series is convergent. The proof of this is similar to the proof just given.

In order to prove that the solution (4.21) of equation (4.20) is a solution which is unique and finite on the segment $[0, X]$, it is sufficient to show that the corresponding homogeneous equation

$$F(\xi) - \lambda F(k\xi) = 0$$

does not have finite solutions other than the solution $F(\xi) \equiv 0$. It is evident that

$$F(\xi) = \lambda F(k\xi) = \dots = \lambda^n F(k^n \xi).$$

Let the function F remain finite while the argument tends to zero. Since $|\lambda| < 1$, by choosing n sufficiently large we can for every ξ make the right-hand side of the equality

$$F(\xi) = \lambda^n F(k^n \xi)$$

as small in absolute value as we like. Thus it follows that the left-hand side, which does not depend on n , is identically zero, i.e.,

$$F(\xi) \equiv 0.$$

Therefore equation (4.20) has a unique solution. As a matter of fact if we assume that there are two solutions, their difference must satisfy the homogeneous equation, and from what was just shown this difference

must equal zero. Thus we have proved that the function F_3 defined by the series (4.21) is a unique and finite solution of equation (4.20).

If $f(\xi)$ is represented in the form of a power series (or a polynomial), i.e.,

$$f(\xi) = \sum_{n=0}^{\infty} a_n \xi^n,$$

then the solution (4.21) takes the form

$$F_3(\xi) = \sum_{n=0}^{\infty} \frac{a_n}{1 - \lambda k^n} \xi^n.$$

Returning to equation (4.19), we obtain

$$\begin{aligned} \epsilon F_3(\xi) &= \epsilon' \tan \alpha \sum_{n=0}^{\infty} \lambda^n Y'(k^n \xi) - \epsilon'' \sum_{n=0}^{\infty} \lambda^n L(k^n \xi) \\ &\quad - \epsilon''' \frac{a \tan^2 \alpha \tan \bar{\beta} \sin \theta}{2(b \tan \alpha + a \tan \bar{\beta})} \xi. \end{aligned} \quad (4.22)$$

Having found the function F_3 , the determination of the functions F_1 , F_2 , F_4 , and β' , and hence the description of the entire flow downstream of the shock wave and the shock wave shape, presents no difficulty.

Let us determine the relation for the pressure distribution along the surface downstream of the shock wave. To do this we transform the expression for the pressure in (4.12), using the relation (4.16) between the functions F_3 and F_4 , and then introduce the solution (4.22). We obtain as the result

$$\begin{aligned} \epsilon p(x, 0) &= \epsilon' \frac{\gamma M_2^2}{\sqrt{M_2^2 - 1}} \left[Y'(x) + 2 \sum_{n=1}^{\infty} \lambda^n Y'(k^n x) \right] \\ &\quad - \epsilon'' 2\gamma M_2^2 \sum_{n=0}^{\infty} \lambda^n L(k^n x) - \epsilon''' \frac{\gamma M_2^2 a \tan \bar{\beta} \sin \theta}{\sqrt{M_2^2 - 1}(b + a \sqrt{M_2^2 - 1} \tan \bar{\beta})} x. \end{aligned} \quad (4.23)$$

As before, let the free stream be undisturbed and let the flow be a plane parallel one. Then $\epsilon'' = \epsilon''' = 0$, and equation (4.23) for the pressure distribution can be written:

$$p'(x, 0) = \frac{\gamma M_2^2}{\sqrt{M_2^2 - 1}} \left[Y'(x) + 2 \sum_{n=1}^{\infty} \lambda^n Y'(k^n x) \right]. \quad (4.24)$$

(A. A. Dorodnitsyn in 1949 obtained this relation by a slightly different method.) In particular, if the function $Y'(x)$ is given in the form of a power series (or a polynomial), that is,

$$Y'(x) = \sum_{n=0} \alpha_n x^n$$

then

$$p'(x, 0) = \frac{\gamma M_2^2}{\sqrt{M_2^2 - 1}} \sum_{n=0} \frac{1 + \lambda k^n}{1 - \lambda k^n} \alpha_n x^n.$$

The relations obtained are generalizations of the well known relations of linearized theory for determining the pressure on a slightly curved wall in a supersonic flow. They become the linearized relations for $\theta = 0$ (since then $M_2 = M_1$ and $\lambda = 0$). From an examination of equation (4.24) it is obvious that with a shock wave present, the pressure acting

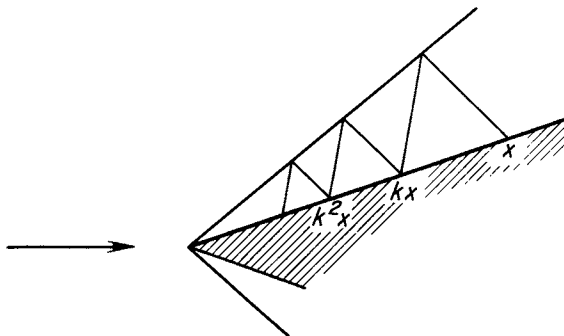


FIG. 4.10. Reflection of a disturbance from the shock wave and from the body surface.

on the surface at a point with abscissa x depends not only upon the inclination angle of the surface itself, but also upon the inclination angle of the surface at the points with abscissas kx , k^2x , etc. One can show that the n th term of the series in equation (4.24) corresponds to a disturbance which has struck the point having the abscissa x after n multiple reflections from the shock wave surface (Fig. 4.10).

The wave drag coefficient for one side of a wedgelike body can be written in the form

$$\begin{aligned} C_D &= \frac{1}{qh} \int_0^l p_2 \sin(\theta + \theta') dx = \frac{\bar{p}_2 l}{qh} \int_0^1 (1 + \epsilon' p')[\sin \theta + \cos \theta \epsilon' Y'(x)] dx \\ &= \frac{\bar{p}_2}{q} + \epsilon' \frac{\bar{p}_2 l}{qh} \int_0^1 [p' \sin \theta + \cos \theta Y'(x)] dx \\ &= C_D^{\text{edge}} + \delta C_D, \end{aligned}$$

where x is made dimensionless with respect to the length l as indicated. Here $q = \bar{p}_1 \bar{U}^2 / 2$, $h = l \sin \theta$, C_D^{edge} is the wave drag coefficient for a straight wall, and δC_D is the increment in wave drag coefficient when the straight wall is replaced by a slightly curved wall (first variation in C_D). Taking into account the fact that $Y(0) = Y(1) = 0$, and using equation (4.24) for $p'(x, 0)$, we find

$$\delta C_D = \frac{\bar{p}_2}{q} \frac{2\gamma M_2^2}{\sqrt{M_2^2 - 1}} \sum_{n=1}^{\infty} \lambda^n \epsilon' Y(k^n).$$

From the fact that the first variation in the drag coefficient for $\lambda \neq 0$ is different from zero and can be made negative, it follows that in contrast to the linearized theory result [9], a wedge is not the shape for which the wave drag is a minimum for a given ratio of thickness to length of the body. It is an easy matter to give a physical explanation of this fact. For simplicity let us limit ourselves to the case when only the first term in the series for δC_D is different from zero. To be specific, we shall consider that for a given M_1 and θ , the coefficient λ is positive. Then in order that δC_D be negative it is necessary that $Y(k) < 0$. The decrease in wave drag is explained here by the fact that an expansion produced by the local negative values of $Y'(x)$ to the left of the point $x = k$ (Fig. 4.11) reflects from the shock wave without changing sign (since $\lambda > 0$), resulting in a decrease of pressure on the portion of the body surface toward the right. On the other hand, a compression produced by the fact that the local values of $Y'(x)$ to the right of the point $x = k$ are positive, does not strike the body surface after reflection from the shock. By itself (without taking into account reflections from the shock wave),

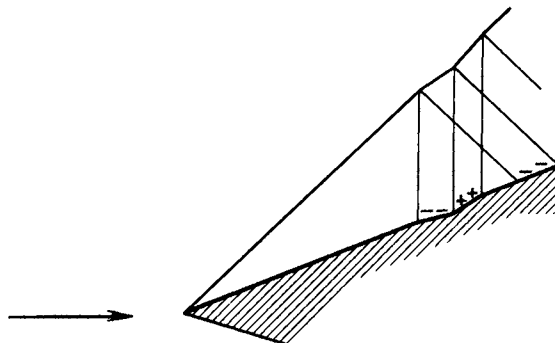


FIG. 4.11. Sketch for explanation of influence of reflected disturbances on the drag coefficient of a wedgelike body.

the change of the wall contour has an effect on the value of the wave drag only in the next approximation.

Let us now use equation (4.24) to calculate the surface pressure on slender wedgelike airfoils in a hypersonic flow. We represent the angle between the tangent to the body contour and the free stream direction in the form

$$\theta = \bar{\theta}[1 - \vartheta(x)], \quad \vartheta(0) = 0, \quad |\vartheta(x)| \ll 1.$$

Employing equations (4.3), which are correct for small $\bar{\theta}$ and $M_1 \gg 1$, we reduce equation (4.24) after some simple transformations to the following form:

$$C_p M_1^2 = \frac{4}{\gamma + 1} (K_s^2 - 1) - 2K \sqrt{\frac{\frac{2\gamma}{\gamma + 1} K_s^2 - \frac{\gamma - 1}{\gamma + 1}}{\frac{\gamma - 1}{\gamma + 1} + \frac{2}{\gamma + 1} \frac{1}{K_s^2}}} \times \left[\vartheta(x) + 2 \sum_{n=1}^{\infty} \lambda^n \vartheta(k^n x) \right], \quad (4.25)$$

where $K = M_1 \bar{\theta}$. The dependence of the reflection coefficient λ and the quantity k on the hypersonic similarity parameter K are determined by the relations

$$\lambda = \frac{a - b}{a + b},$$

$$a = 2 \frac{M_2}{M_1} (K_s - K) \left[1 - \frac{\gamma - 1}{\gamma + 1} \frac{M_2^2}{M_1^2} (K_s - K)^2 \frac{1 - \frac{1}{K_s^2}}{\frac{\gamma - 1}{\gamma + 1} + \frac{2}{\gamma + 1} \frac{1}{K_s^2}} \right],$$

$$b = 1 + \frac{M_2^2}{M_1^2} (K_s - K)^2 \frac{\frac{2\gamma}{\gamma + 1} \frac{1}{K_s^2} - \frac{\gamma - 1}{\gamma + 1}}{\frac{\gamma - 1}{\gamma + 1} + \frac{2}{\gamma + 1} \frac{1}{K_s^2}},$$

$$k = \frac{1 - \frac{M_2}{M_1} (K_s - K)}{1 + \frac{M_2}{M_1} (K_s - K)}.$$

The dependence of λ and k upon K for $\gamma = 1.4$ is shown in Fig. 4.12. For limiting hypersonic flows past slender bodies, λ and k tend to the constants

$$\lambda \rightarrow \frac{1 - \sqrt{\frac{\gamma}{2(\gamma - 1)}}}{1 + \sqrt{\frac{\gamma}{2(\gamma - 1)}}}, \quad k \rightarrow \frac{1 - \sqrt{\frac{\gamma - 1}{2\gamma}}}{1 + \sqrt{\frac{\gamma - 1}{2\gamma}}}.$$

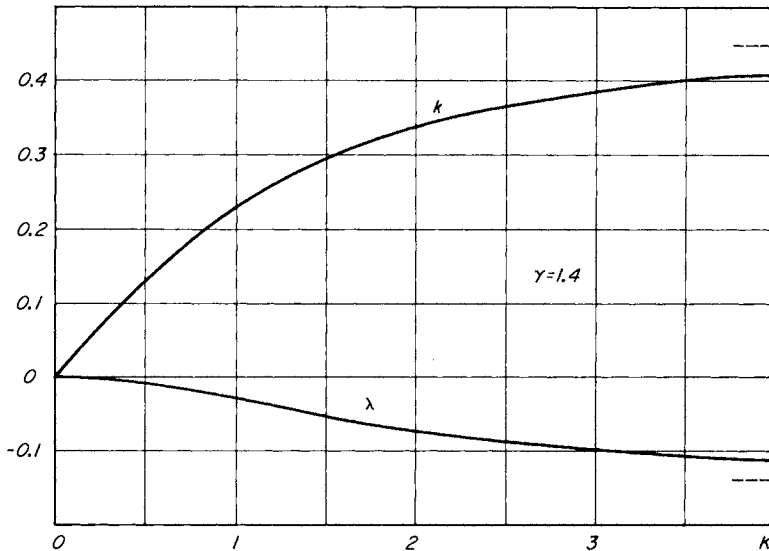


FIG. 4.12. Dependence of the quantities λ and k upon the hypersonic similarity parameter K .

If we neglect the reflection of disturbances from the shock wave (i.e., consider $\lambda = 0$), equation (4.25) agrees with equation (4.4) which was derived in Section 2 of the present chapter, if in the latter equation we limit ourselves to those terms linear in $1 - (\theta/\bar{\theta})$. This fact can be easily proved and is of course to be expected.

In [10] equation (4.25) was obtained, without employing the general expression (4.23), for the case when the function $\vartheta(x)$ is a power series in x . This was done by considering unsteady flows with planar symmetry and applying the equivalence principle. This equation was obtained by the same technique in [11] for the general form of the function $\vartheta(x)$.

Let us now consider the flow near the nose of the annular body of revolution depicted in Fig. 3.25. We assume that the free stream is undisturbed and the body is generated from a straight line, that is, $\epsilon' = \epsilon'' = 0$. Equations (4.12) and (4.22) show that the quantities p''' , ρ''' , u''' , and v''' in this case are linear functions of x and y , i.e., we retain the linear terms in the expansions of the functions p_2 , ρ_2 , u_2 , and v_2 in power series in x and y . In particular, from equation (4.23)

$$p'''(x, 0) = - \frac{\gamma M_2^2 a \tan \bar{\beta} \sin \theta}{\sqrt{M_2^2 - 1}(b + a \tan \bar{\beta} \sqrt{M_2^2 - 1})} x. \quad (4.26)$$

This expression determines the pressure gradient at the leading edge. Computed values of $\partial(p_2/\bar{p}_2)/\partial(x/r_0)$ for $\gamma = 1.4$ and several values of the Mach number M_1 are shown in Fig. 4.13.

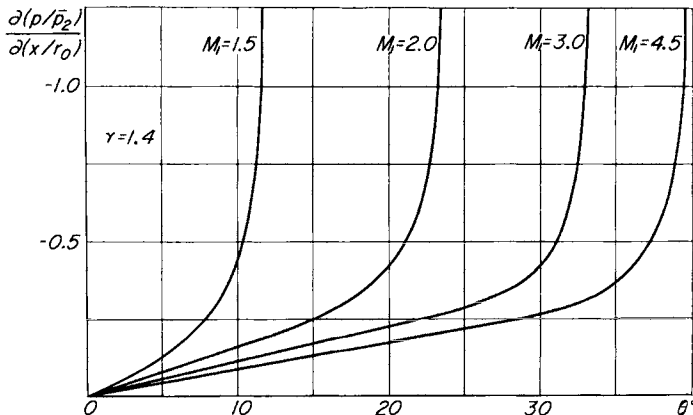


FIG. 4.13. Pressure gradient at the leading edge of an annular body of revolution.

It is also easy to obtain the shock wave equation near the leading edge of this body. This equation has the form

$$y = x \tan \bar{\beta} + \epsilon''' B x^2,$$

where B is found from the conditions (4.13) and equation (4.11). The problem of determining the flow near the leading edge of the axisymmetric body considered was studied within the present approximations in [12].

For hypersonic speeds and small flow deflection angles equation (4.26) can be written in the following form

$$\begin{aligned} \frac{C_p}{\theta^2} &= \frac{C_{p2}}{\theta^2} - \frac{2a \frac{M_1}{M_2} (K_s - K)}{K^2 \left[b + a \frac{M_2}{M_1} (K_s - K) \right] \left(\frac{\gamma - 1}{\gamma + 1} + \frac{2}{\gamma + 1} \frac{1}{K_s^2} \right) r_0} \frac{\theta x}{r_0} \\ &= \frac{C_{p2}}{\theta^2} - N(K) \frac{\theta x}{r_0}. \end{aligned}$$

A plot of the function N for $\gamma = 1.4$ is shown in Fig. 4.14.

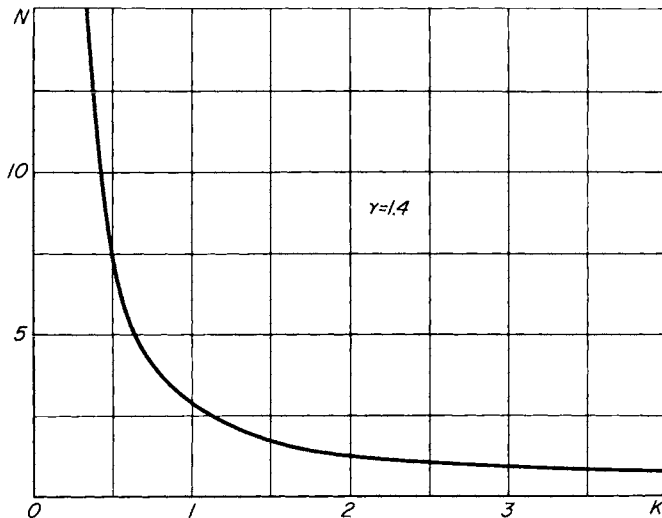


FIG. 4.14. Dependence of the quantity N , characterizing the pressure distribution near the nose of an annular body of revolution, upon the hypersonic similarity parameter K .

5. Approximate method using shock and simple wave relations (shock-expansion method)

The method given in Section 2 of the present chapter allows an exact calculation of the pressure on an airfoil only when the surface lies wholly outside the region of influence of the curved part of the bow shock wave. If the surface is located within the region of influence of this part of the bow shock, it is necessary to take into account the surface pressure changes produced by the disturbances reflected from the bow shock (and from the strong vorticity layers if they are present) which originate at the upstream parts of the airfoil. We note, however, that the strength of the disturbances reflected from the shock is small in general, even for hypersonic speeds, as was shown in Section 3. Therefore we can neglect the influence of the reflected disturbances for an approximate determination of the pressure distribution along an airfoil, i.e., consider the pressure (and hence also the flow deflection angle) as constant along the outgoing characteristics from the airfoil. In general, the velocity and density (and consequently the temperature, speed of sound, and Mach number) are variable along characteristics of this family (owing to the presence of disturbances propagated along the streamlines). Thus the characteristics are not straight, as in a simple wave, when we take the nonlinear effects into account. However, the variations of pressure and flow deflection angle along streamlines are still governed by the same relations as in a simple wave, but with different values of the entropy on different streamlines.

For approximate calculations of surface pressures on airfoils with curved contours we can therefore use shock and simple wave relations (shock-expansion method), as in Section 2. The conditions for the validity of this method of calculation were investigated in detail in [4] and [13]. In the present section we shall follow the first of these references.

As an example, Fig. 4.15 shows the distributions of the pressure coefficient along the surface of a symmetric airfoil with a parabolic contour and a thickness ratio equal to 0.1 for $M_1 = 5, 15$, and ∞ with $\gamma = 1.4$. The solid curves are the values calculated by the method of characteristics. The dashed-dotted curves were obtained from equation (4.4), which was derived using the shock and simple wave relations and the additional assumptions that the airfoil is slender and that $M_1 \gg 1$. Using the shock

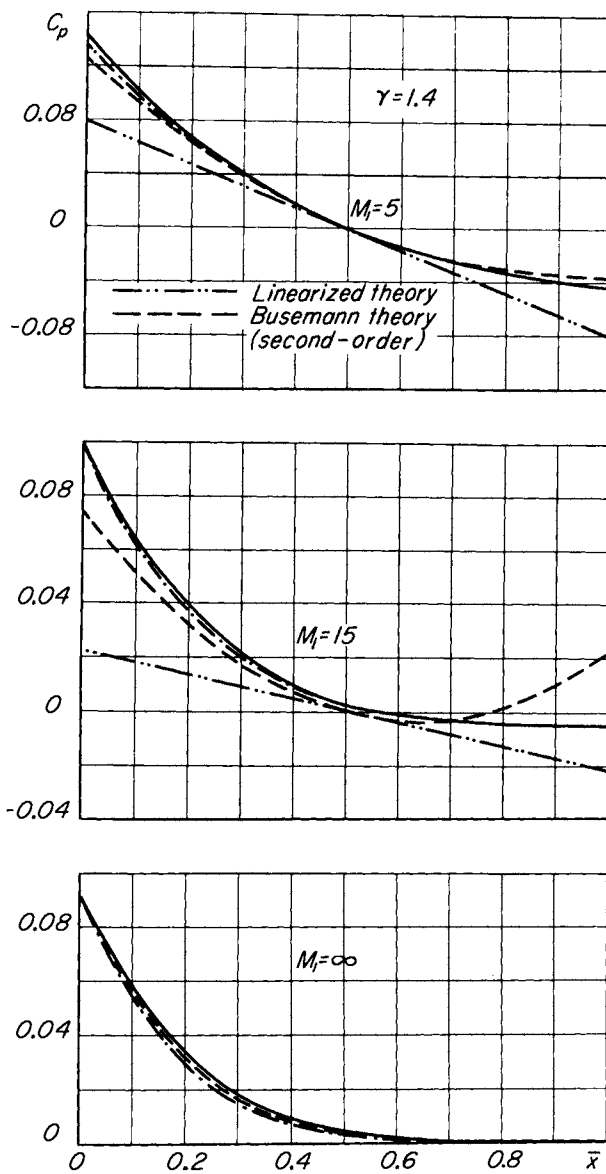


FIG. 4.15. Surface pressure on a symmetric airfoil with a thickness ratio equal to 0.1: — method of characteristics; - - - shock-expansion method; - - · - equation (4.4); - · - - linearized theory; - - - Busemann theory (second-order).

and simple wave relations without these assumptions (shock-expansion method) gives the pressure coefficient shown by the dashed lines in Fig. 4.15 for the case $M_1 = \infty$. The shock-expansion method values of C_p differ very little from the exact ones for the lower values of C_p . With a decrease in the Mach number this difference becomes even less significant, and for $M_1 \leq 5$, it practically disappears.

This result is easily explained by the behavior of the reflection coefficient λ (Fig. 4.7). In the range of Mach numbers and flow deflection angles at the shock which are being considered, the coefficient λ is negative, and its absolute value increases with an increase of Mach number. Consequently, the expansion waves emanating from the convex surface of the airfoil are reflected from the shock as compression waves, and these reflections are stronger for larger Mach numbers. These reflected waves are not taken into account in the shock-expansion method and this fact is the source of the discrepancy between the approximate and exact values of the pressure coefficient on the airfoil.[†]

We note that even with the use of equation (4.4)* the discrepancy between the approximate and exact values of C_p is not large. In order to compare the results with those of other approximate theories, we have also plotted in Fig. 4.15 the values of C_p corresponding to the linearized theory [equation (4.1)] and to the second-order Busemann theory [equation (4.2)], both of which were referred to in Section 1 of the present chapter. It can be seen that even for $M_1 = 5$ equation (4.4) is more accurate than the second-order theory given by equation (4.2).

[†]Editor's note: The neglect of the reflected waves from the shock is not the entire source of the discrepancy between the approximate and exact values of the surface pressure. There is also a tendency of the waves which reflect from the shear (vorticity) layers in the flow as expansions and from the shock wave as compressions to cancel. [See Waldman, G. D., and Probstein, R. F., An analytic extension of the shock-expansion method, *J. Aerospace Sci.* **28**, 119–132 (1961).]

* Equation (4.4) can be made still more accurate if we take into account the presence of the reflected disturbances, and in accordance with the treatment in Section 4 of the present chapter replace the quantity $1 - (\theta/\bar{\theta}) = \vartheta(x)$ by the sum

$$\vartheta(x) + 2 \sum_{n=1}^{\infty} \lambda^n \vartheta(k^n x).$$

In view of the smallness of λ it is sufficient to retain only the term corresponding to $n = 1$.

Detailed calculations show [4] that for $\gamma = 1.4$ the exact shock-expansion method can be applied to determine the pressure on a curved airfoil with sufficient accuracy for all supersonic speeds and for flow deflection angles through the shock wave up to 1° less than the angle for which the velocity behind the shock becomes sonic (i.e., in the range of Mach numbers M_1 and angles θ for which the reflection coefficient λ remains small compared to unity).

With $\gamma = 1.4$ equation (4.4) can be used with an error of less than 10 percent for $M_1 > 3$ and $\theta < 25^\circ$. As an example, in Fig. 4.5 are shown polar diagrams for a circular arc airfoil for a range of values of K from 0.1 to 1.0 obtained by using equation (4.4).

From what was said in Section 3 of this chapter concerning the increase in the absolute value of the reflection coefficient λ with decreasing γ , it can be seen that the method of the present section will become less accurate for γ close to unity. To illustrate this point, the shock-expansion values of the pressure coefficient on a circular-arc airfoil have been plotted in Fig. 3.18 (dashed lines) for $M_1 = \infty$ and two values of the specific heat ratio: $\gamma = 1.4$ and $\gamma = 1.05$. For $\gamma = 1.4$ the values of C_p calculated by the shock-expansion method are very close to those obtained by the method of characteristics, while for $\gamma = 1.05$ the approximate and exact values of C_p are markedly different.

Thus the small parameter method of the preceding chapter and the method of the present section complement each other. The first of these methods gives satisfactory results for γ close to unity, while the second one can be applied for values of γ not too close to unity.

The shock-expansion method essentially simplifies the entire calculation of the flow pattern. In particular it makes the method of characteristics significantly less time-consuming [4]. There have been attempts to obtain expressions for the flow parameters between the shock wave and airfoil surface by analytic means, within the approximations of this method [14, 15].

6. Generalization to flows past bodies of revolution

A simple method for the calculation of hypersonic flows past bodies of revolution with or without angle of attack was proposed in [16]. According to this method the flow in every meridian plane is calculated in the same manner as in Section 5, with the difference that the initial

flow parameters at the nose of the body in every such plane are taken either from the theoretical solution of the problem of flow past a cone or from corresponding experimental data. Hence the pressure on a body of revolution is determined in this method by the conical shock and Prandtl-Meyer relations.

Graphs of the pressure distribution calculated by this method are presented in Fig. 4.16 for an ogive with a fineness ratio equal to 3 for several values of the Mach number M_1 with $\gamma = 1.4$ (solid lines). The dashed lines on this figure give the values of the pressure calculated by the method of characteristics, and the circles are experimental data. (For $M_1 = 6.30$ the solid and dashed curves coincide. The experimental points are not shown for this Mach number since the experiments were carried out at low values of the Reynolds number for which viscosity was shown to have a significant effect on the flow.) In the examples given, the values of the similarity parameter K varied from 0.91 to 2.10. The approximate values of the pressure are in good agreement with the exact values for K greater than 1, and this agreement improves with increasing K .

Let us turn now to an example of the application of this method to flows past bodies of revolution at angles of attack. Figure 4.17 presents the results of pressure measurements on ogives with fineness ratios of 3 and 5 for $M_1 = 5.05$ and for two angles of attack (5° and 15°). The pressure was measured on three sections: top, bottom, and side. The flow parameters near the nose of the body for use in the calculation were determined experimentally by measurements of the flow past a cone with the same apex angle as the angle at the nose of the body and with the same angle of attack. The agreement obtained between the experimental data and the calculated results is quite satisfactory. A comparison is given in Fig. 4.18 of the shape of the bow wave in the plane of symmetry of the flow, as calculated by the generalized method and as obtained experimentally. These results are for the same two bodies as before, with $M_1 = 5.05$ and an angle of attack of 10° . Also shown in this figure, for comparison, is the shape of the bow wave for flow past a cone with a corresponding apex angle (dashed curves). The shape of the shock wave calculated by the generalized method agrees well with the experimental shape. From these results we may conclude that the shock-expansion method using the conical shock and simple wave relations can be applied

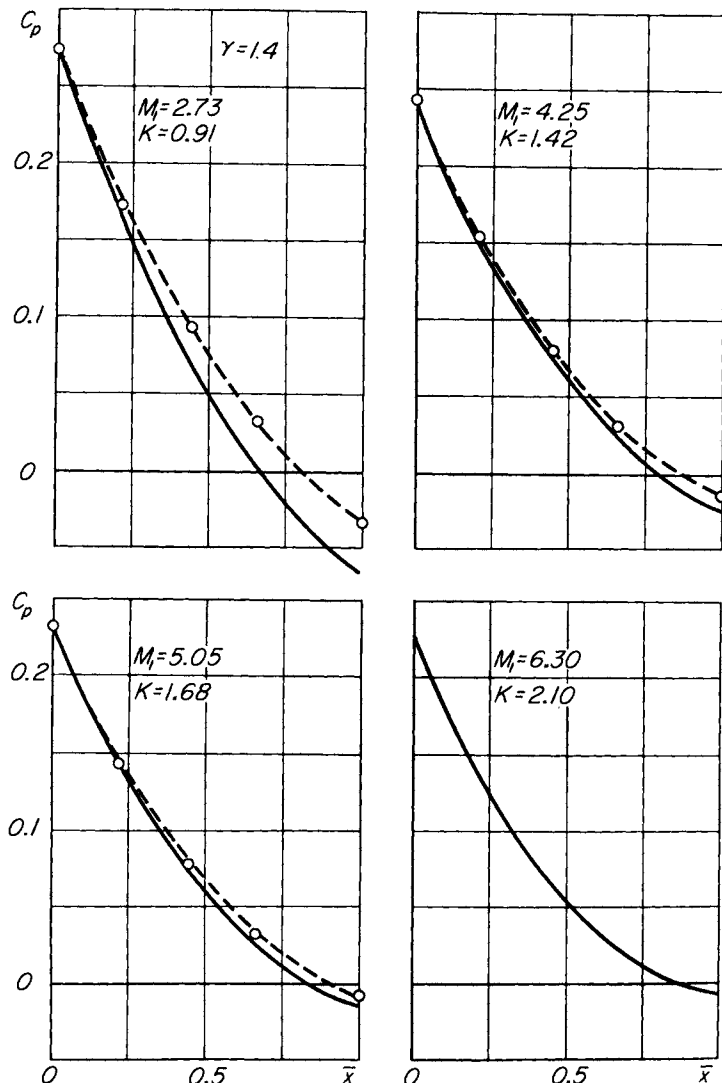


FIG. 4.16. Pressure distributions on an ogive of fineness ratio 3: — shock-expansion method using conical shock and expansion wave relations; --- method of characteristics; O-experiment.

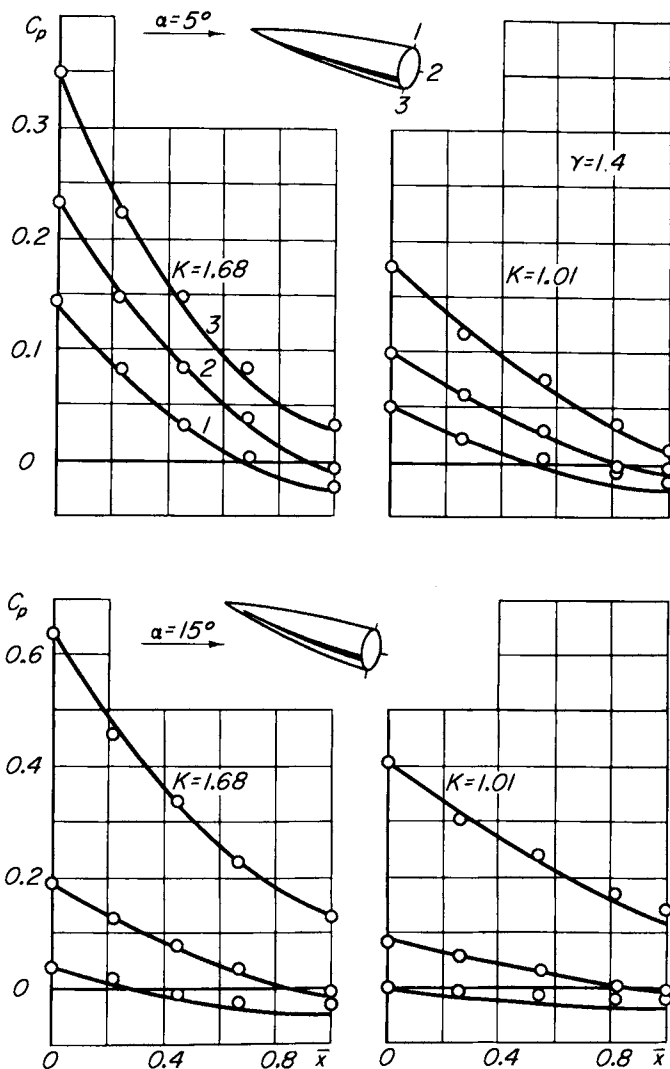


FIG. 4.17. Pressures at $M_1 = 5.05$ on ogives of fineness ratios 3 and 5 at angle of attack; — calculation; \circ —experiment.

to the calculation of flows past bodies of revolution for $M_1 > 5$ and $K > 1$.

We note that this method can also be used to calculate pressures on bodies of revolution at moderate supersonic speeds. The values of the

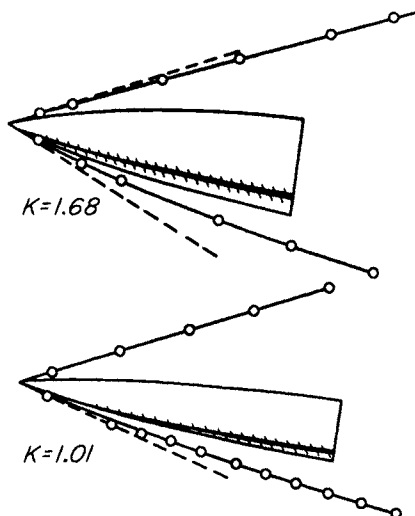


FIG. 4.18. Shape of bow wave for flows past ogives of fineness ratios 3 and 5 at 10° angle of attack and $M_1 = 5.05$: —— calculation; ○—experiment; - - - shape of bow shock wave for a cone.

pressure coefficient which are obtained, however, must be multiplied by a coefficient which depends on the Mach number and the fineness ratio of the body [17].

CHAPTER V

EFFECT OF SLIGHT LEADING EDGE BLUNTING ON HYPERSONIC FLOWS PAST BODIES

1. Introductory remarks and formulation of the problem

In the present chapter the theory of hypersonic flow past slender, sharp-nosed bodies given in Chapter II is generalized to the case where the leading edge or nose of the body is slightly blunted. Such a generalized theory is of great value, since in the practical design of vehicles it is not possible to attain wings with ideally sharp leading edges or bodies with ideally sharp noses. Even for small models which are very carefully constructed the thickness of the tip is of the order of several microns. Moreover, after a short period of time in a supersonic wind tunnel the sharp tip of the model will have deteriorated with the result that its effective thickness becomes of the order of twenty microns. In the case of large scale objects one can hardly speak of tip thicknesses less than one or several tenths of a millimeter.

Not only are ideally sharp leading edges or noses difficult to produce, but their fragility makes them impractical. In addition, a sharp nose on a body traveling at hypersonic flight speeds would make it impossible to transfer from the gas to the body the large amount of heat which is generated in the flow near the nose. In practice, therefore, in place of ideally sharp bodies one always deals with bodies which are slightly blunted. By this we mean bodies for which the dimension characterizing the blunting is small in comparison with the axial dimension. It is this type of configuration which we shall consider in the present chapter.

For supersonic flow on a blunt-nosed body a detached shock wave is formed, behind which there is a subsonic region. This materially complicates the theoretical study of the flow, particularly if the small dimension characterizing the blunting necessitates a consideration of viscous effects in the nose region of the body.*

* Available experimental data [1, 2] indicates a considerable dependence on Reynolds number of the flow pattern near the blunted leading edge of a flat plate, for Reynolds numbers based on the characteristic dimension of the blunting of the order of several thousand or less.

An attempt has been made to develop a semiempirical method to account for the effect of blunting the leading edge of a slender airfoil on a flow at a moderate supersonic speed [3]. The basic idea of this method is explained with the aid of Fig. 5.1. The flow in the region

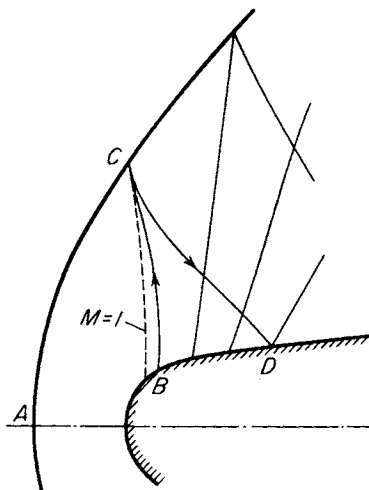


FIG. 5.1. Flow near the blunt leading edge of an airfoil at supersonic speed.

between the shock wave segment AC and the limiting characteristic BC , which originates at the surface of the body and which has a common point with the sonic line, is the same for different airfoils with the same leading edge shape. If the interaction of the disturbances which propagate along the characteristics in the direction of the body with the disturbances which come from the body is neglected, then the pressure on the surface to the right of the point B can be determined. This pressure is obtained by superposing the pressure computed for the given airfoil from the second-order Busemann formula [equation (4.2)] with the pressure associated with the propagation of the disturbances toward the body. These inward propagating disturbances do not depend on the shape of the airfoil, at least on the portion of the surface BD where they are strongest. Thus, to calculate the pressure distribution along different airfoils which have the same leading edge shape it is sufficient to have data on the flow past one of these airfoils—for example, a flat plate. Experimental data on flow past flat plates with elliptically shaped leading edges, with ratios of the major to minor axis ranging from 0 (flat

face leading edge) to 8, has been obtained in [4] for Mach numbers from 1.4 to 1.8. Analysis of results obtained by the above mentioned method shows that the effect of a slight blunting of the leading edge on the flow past an airfoil at a moderate supersonic speed introduces only a small correction to the theoretical result for flow past an airfoil with a sharp leading edge. The drag of the blunted airfoil can be obtained simply by adding the drag due to blunting (determined experimentally, for example) to the drag of the remaining part of the airfoil. The drag of the remaining part of the airfoil is computed from the results for an ideally sharp body, disregarding the effect on the drag of the disturbances arising in the subsonic region, since their strength is small.

The narrow extent of the flow region near the blunt nose of a body in comparison with the characteristic dimension of the body itself does not, however, always justify neglecting its effect on the flow in the scale of the entire body. In fact, as we established previously (see Chapter III), at hypersonic speeds the drag of an element of body surface is approximately proportional to the square of the sine of the inclination angle of the element to the flow direction. Therefore if we denote the characteristic dimension of the bluntness by d , the drag due to bluntness for an airfoil ($\nu = 1$) or body of revolution ($\nu = 2$) will be of the order of

$$C_D \frac{1}{2} \rho_1 V^2 d^\nu,$$

where C_D is of the order of unity. The drag of the remaining part of a slender body having a length L and a characteristic surface inclination angle α will be

$$\alpha^2 \cdot \frac{1}{2} \rho_1 V^2 (L\alpha)^\nu.$$

It follows that the force acting on the blunt nose and the force on the remaining part of the body are of the same magnitude if

$$\frac{C_D^{1/\nu} d}{L} \sim \alpha^{(2+\nu)/\nu}.$$

These theoretical considerations illustrate the fact that at hypersonic speeds a slight blunting of the leading edge of a flat plate can significantly alter the flow pattern and the pressure distribution in a region whose

dimensions are hundreds or thousands of times greater than the dimension of the bluntness itself. Experimental data also illustrates this fact [2].

If the dimension of the blunt portion of the body is very small in comparison with its axial dimension, we may expect to obtain a good approximation to the description of the flow phenomena if we neglect the alteration in body shape due to the blunting, but replace the effect of the bluntness on the flow by concentrated forces acting on the flow at the blunt nose. This formulation of the problem of hypersonic flows past slender, blunt-nosed bodies was given in [5, 6] and further developed in [7, 8].

Following the formulation given in [5], we shall consider a body whose forward surfaces have a small inclination to the direction of motion, with the exception of a small blunt forward portion, moving in a gas with a velocity V . The dimension of the blunt portion will be assumed sufficiently small that it can be neglected when considering the flow in a region of the order of the axial dimension of the body. However, we shall replace the effect of the bluntness on the flow, which can manifest itself in a large region despite its small size, by concentrated forces acting on the gas at the blunt nose. It is necessary to consider the magnitude of the concentrated forces as known, either from experiment or from theoretical considerations of the flow in the neighborhood of the nose of the body. At hypersonic speeds these forces can be determined approximately, for example, from the Newtonian formula.

We shall restrict our considerations to symmetric flows past airfoils or bodies of revolution. In the first case we shall treat the flow in the upper half plane (in a layer between two adjacent parallel planes), and in the second case the flow above the axis of symmetry in a meridian plane (in an angular region between adjacent planes which pass through the axis of the body). Let us replace the effect of the bluntness on the gas in these layers by the resultants of the forces due to the bluntness which act in the direction of flight and normal to it. We shall denote these resultant forces by D and L , respectively, defined per unit depth for two-dimensional flows and per 2π radians of azimuthal angle for axisymmetric flows. In order to calculate the total forces which replace the effect of the bluntness on the flow it is necessary to take into account the pressure forces, and in some cases (when viscosity has an appreciable influence on the flow near the nose) the viscous forces. (For very small

dimensions of the bluntness the viscous effects can be of the same order as, or even appreciably greater than, the pressure effects.) For flow past a blunted airfoil with a detached shock wave it is also necessary to include in the magnitudes of D and L the pressure forces (and viscous forces) which act on the gas in the upper half plane between the detached shock wave and the leading edge of the body.

The force D , acting in the direction of motion of the body, does work on the gas which increases its energy. As a result of the bluntness effect, the energy of the gas in a layer of unit depth perpendicular to the flight direction is increased by an amount $E = D \cdot 1$. Although the resultant force L does not do work, it imparts an impulse to the gas as does the force D . In this layer of unit depth, the impulse imparted to the gas by the blunting in the direction normal to the flight path is equal to $I = L/V$.

We shall now make use of the equivalence of a hypersonic flow past a slender body to a plane unsteady gas motion, developed in Chapter II (equivalence principle). In accordance with our previous remarks, the equivalent problem of unsteady motion for a blunt-nosed slender body may be stated as follows. At some instant of time an amount of energy E is released in a gas which is initially at rest (an explosion takes place) on a plane (or straight line), imparting to the gas an impulse I along the normal to the plane (or straight line); the energy E and impulse I are per unit area or per unit length of charge, respectively, for two-dimensional or axisymmetric flow. At this instant of time a plane (or cylindrical) piston begins to move from the point of the explosion with a velocity U . It is then required to determine the resulting gas motion. In order to relate the stated problem of unsteady motion to the problem of steady flow past a body with a velocity V in the direction of the x -axis, we set $E = D$, $I = L/V$, $U = V \tan \alpha$, and introduce the time t by means of the relation $x = Vt$. Here α is the local inclination angle with respect to the x direction of the surface of the airfoil or body of revolution.

When the effect of the initial pressure of the gas on the motion can be neglected, and $I = 0$ and $U = 0$ (a violent explosion), Sedov ([9, 10]; see also [11]) has found an analytic solution with spherical, planar, and cylindrical symmetry. For the violent spherical explosion a numerical solution was also given by Taylor [12]. These results were subsequently rederived in a number of other papers [13–15]. The motion which arises

from such a violent explosion is a self-similar one and corresponds to a limiting hypersonic flow past a blunted flat plate (for two-dimensional flow) or a right circular cylinder with its flat face normal to the stream direction (for axisymmetric flow).*

For more general conditions an exact solution for the problem of an explosion subsequently followed by the motion of a piston can be obtained in each specific case only by complicated numerical methods similar to those used in the solution for a point spherical explosion [16–18]. Such problems can also be solved by expanding the solution in powers of $(\gamma - 1)/(\gamma + 1)$, as described in Section 7 of Chapter III. In this method equations (3.42) and (3.43) provide expressions for the values of the flow parameters in the disturbed region behind the shock wave in terms of the shock wave motion $R_0(t)$. In order to determine the function $R_0(t)$ for the gas motion which results from an explosion followed by the motion of a piston, we apply the conservation of energy law [19]. According to this law the total energy (kinetic plus internal) of the moving gas at each instant of time must equal the sum of the energy E released by the explosion, the initial energy of the gas, and the work done due to the motion of the piston, i.e.,

$$\int_{v-v_0} \left[\frac{1}{2} \left(\frac{\partial R}{\partial t} \right)^2 + \frac{1}{\gamma - 1} \frac{p}{\rho} \right] \rho \, dv = E + \int_v \frac{1}{\gamma - 1} p^0 \, dv + \int_0^t p_p \, dv_0(t). \quad (5.1)$$

Here $v - v_0$ is the volume occupied by the moving gas, v_0 is the volume displaced by the piston, and p_p is the pressure on the piston. Using the first two terms in the expansions (3.38) we obtain from the energy equation (5.1)

* *Editor's note:* The correspondence of unsteady solutions with steady hypersonic flow solutions requires that the equivalence principle be applicable. For slender blunt bodies, however, the equivalence principle fails locally in the vicinity of the blunt nose itself, but more important, it fails also in a layer of high entropy near the surface of the body. The effect of this high entropy layer or "hot core" of gas associated with the strong nose shock can impose restrictions on the direct application of unsteady solutions to steady hypersonic flows past blunt-nosed bodies. Discussions and analyses of this feature of the problem may be found, for example, in [28–31].

$$\begin{aligned}
& \left[\frac{\dot{R}_0^2}{2} - \frac{a^{0^2}}{\gamma(\gamma-1)} \right] m^* + \int_0^{m^*} \left\{ \frac{\gamma-1}{\gamma+1} \dot{R}_0 \frac{\partial R_1}{\partial t} + \frac{1}{\gamma+1} \frac{p_0}{\rho_0} \right. \\
& \quad \times \left. \left[1 + \frac{\gamma-1}{\gamma+1} \left(\frac{p_1}{p_0} - \frac{\rho_1}{\rho_0} \right) \right] \right\} dm \\
& = \bar{E} + \int_0^{\bar{R}} \left(p_{0p} + \frac{\gamma-1}{\gamma+1} p_{1p} \right) \bar{R}^{r-1} d\bar{R} + O(\epsilon^2).
\end{aligned}$$

Here $\bar{E} = E/[2(\nu-1)\pi + \delta_\nu]$, where $\delta_1 = 1$, and $\delta_2 = \delta_3 = 0$. Let us now transform from integration with respect to m to integration with respect to τ , and use the fact that

$$\frac{p_1}{p_0} - \frac{\rho_1}{\rho_0} = \frac{p_1}{p_0} - \gamma \frac{\rho_1}{\rho_0} + O(\epsilon) = - \left[1 + \frac{a^{0^2}}{\gamma \dot{R}_0^2(\tau)} \right] + O(\epsilon)$$

(see Section 7, Chapter III). We then obtain an integro-differential equation for determining the function $R_0(t)$, although because of its rather lengthy form we shall not write it down here. With the function $\bar{R}(t)$ given, this equation can be solved, for example, by a successive approximation method in which the simplest scheme is to represent the function $R_0(t)$ in the form of a power series in $\epsilon = (\gamma-1)/(\gamma+1)$.

2. Flows past a flat plate with a flat leading edge, and a right circular cylinder with its end normal to the free stream

Let us consider (Fig. 5.2) the hypersonic flow past a flat plate of thickness d with a blunt leading edge. (One could also consider an infinitely thin plate, but with finite viscous forces acting on a small portion near the leading edge.) For the equivalent problem of one-dimensional unsteady motion with planar symmetry it is necessary to assume $E \neq 0$ and $U = 0$ in this case—i.e., we must consider the motion which results from the explosion of a charge distributed over a plane in a gas at rest. The parameters which serve to define this motion are the initial gas pressure p_1 , the initial density ρ_1 , the energy of the explosion E (per unit area of charge), the specific heat ratio γ , the distance r from the plane of the explosion, and the time t . Since we can construct only three independent dimensionless combinations from these parameters (for

example, γ , $p_1 r/E$, and $p_1^{3/2} t/\rho_1^{1/2} E$), then from a basic theorem of the theory of similarity and dimensional analysis [11] all independent variables will, after reduction to dimensionless form, be functions only of these three parameters. After replacing t and E according to the relations

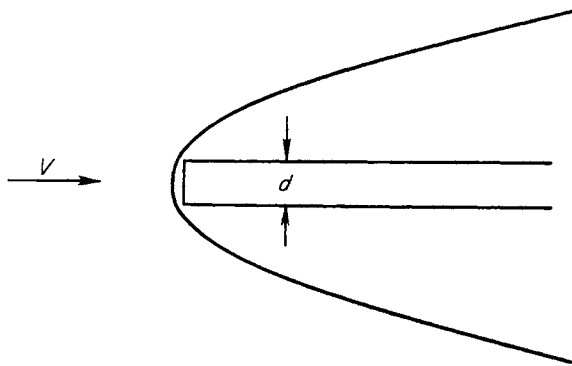


FIG. 5.2. Flow past a flat plate of finite thickness.

$t = x/V$ and $2E = 2D = C_D \frac{1}{2} \rho_1 V^2 d$ (C_D is the drag coefficient of the blunt leading edge), we find that for hypersonic flow past a flat plate with a blunt leading edge, the dimensionless dependent variables depend only on the variables γ , $(x/d)(C_D M^3)^{-1}$, and $(r/d)(C_D M^2)^{-1}$. Thus the correct functional relationship for the pressure distribution along the plate surface $r = 0$ takes the form

$$\frac{\Delta p}{p_1} = P \left(\gamma, \frac{1}{C_D M^3} \frac{x}{d} \right). \quad (5.2)$$

In particular, it follows from this relation that the extent of the region of high pressure near the leading edge of the plate is spread downstream very strongly by an increase in the Mach number (the downstream spread is proportional to M^3).

The shape of the bow shock wave for flow past a blunted flat plate is expressed by the functional dependence

$$\frac{1}{C_D M^2} \frac{r^*}{d} = R \left(\gamma, \frac{1}{C_D M^3} \frac{x}{d} \right). \quad (5.3)$$

The functions P and R can be determined by means of a numerical solution to the explosion problem, though this would entail the use of a

high speed computer. As mentioned previously, up to the present time such computations have been carried out only for the spherically symmetric case (point explosion) with $\gamma = 1.4$. For very strong shock waves, the counterpressure p_1 is negligibly small in comparison with the pressure behind the shock and can have no effect on the flow. Hence in this case the parameter p_1 together with the Mach number are not essential, so that the functional relations (5.2) and (5.3) should have the form

$$\frac{\Delta p}{\frac{1}{2} \rho_1 V^2} = \kappa(\gamma) C_D^{2/3} \left(\frac{x}{d} \right)^{-2/3} \quad (5.4)$$

and

$$\frac{r^*}{d} = \kappa_1(\gamma) C_D^{1/3} \left(\frac{x}{d} \right)^{2/3}. \quad (5.5)$$

The functions $\kappa(\gamma)$ and $\kappa_1(\gamma)$ cannot be determined from similarity and dimensional analysis considerations alone; their values can be obtained from the exact solution for the explosion of a plane charge, in

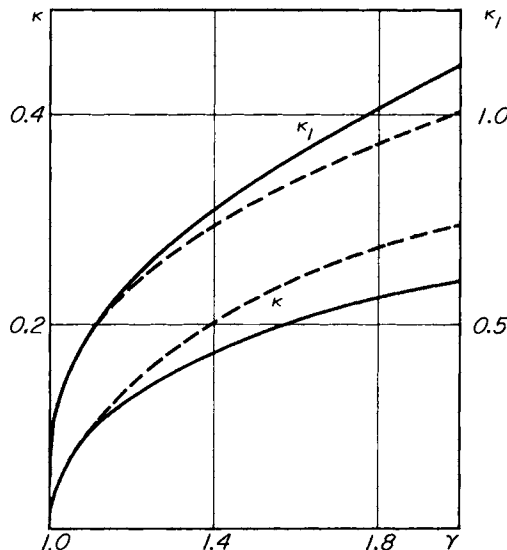


FIG. 5.3. The functions $\kappa(\gamma)$ and $\kappa_1(\gamma)$.

which the counterpressure is neglected [11]. These values are shown in Fig. 5.3 by the solid curves. In Table 5.1 are given the values of

p/p^* , ρ/ρ^* , and v/v^* obtained from this solution as functions of r/r^* and m/m^* . These functions specify the distribution of pressure, density, and transverse velocity between the shock wave and plate surface.

TABLE 5.1
EXACT SIMILAR SOLUTION FOR VIOLENT EXPLOSION,
Two-DIMENSIONAL CASE ($\nu = 1$); $\gamma = 1.4$

$\frac{r}{r^*}$	$\frac{p}{p^*}$	$\frac{\rho}{\rho^*}$	$\frac{v}{v^*}$	$\frac{m}{m^*}$
1	1	1	1	1
0.9797	0.9162	0.8625	0.9699	0.8873
0.9420	0.7915	0.6659	0.9156	0.7151
0.9013	0.6923	0.5160	0.8599	0.5722
0.8565	0.6120	0.3982	0.8017	0.4501
0.8050	0.5457	0.3019	0.7390	0.3427
0.7419	0.4904	0.2200	0.6678	0.2448
0.7029	0.4661	0.1823	0.6263	0.1980
0.6553	0.4437	0.1453	0.5780	0.1514
0.5925	0.4229	0.1074	0.5172	0.1040
0.5396	0.4116	0.0826	0.4682	0.0741
0.4912	0.4038	0.0641	0.4244	0.0529
0.4589	0.4001	0.0536	0.3957	0.0415
0.4161	0.3964	0.0415	0.3580	0.0293
0.3480	0.3929	0.0263	0.2988	0.0156
0.2810	0.3911	0.0153	0.2410	0.0074
0.2320	0.3905	0.0095	0.1989	0.0038
0.1680	0.3901	0.0042	0.1441	0.0012
0.1040	0.3900	0.0013	0.0891	0.0002
0.0000	0.3900	0.0000	0.0000	0.0000

The right hand sides of equations (5.4) and (5.5) are the leading terms in an expansion of $\Delta p/\frac{1}{2}\rho_1 V^2$ and r^*/d for small values of the variable $x(C_D M^3 d)^{-1}$. The next terms in these expansions are to be found in [20, 21].† An approximate solution of the explosion problem for plane (and also line and point) charges was obtained in [19] by expanding the solution in a power series in $(\gamma - 1)/(\gamma + 1)$, in conjunction with the use of equation (5.1) to determine the function $R_0(t)$.

Let us compare the results of the present theory, as given by equations (5.2) and (5.3), with the more exact calculations for flow past a flat

† A method of evaluating these terms was developed by N. S. Mel'nikov (see [11]) who investigated the spherically symmetric case.

plate with a blunt leading edge [22], and with available experimental data. In Fig. 5.4a are shown the values, computed by the method of characteristics, of the pressure on a flat plate with a leading edge in the form of a wedge whose angle is such that the velocity behind the attached shock wave is sonic. These calculations were carried out for $\gamma = 1.4$ and Mach numbers of 5.00, 6.86, and 9.50. On this same figure is shown the pressure at $M = 14.0$ on a flat plate with a semicircular leading edge, as calculated by use of an approximate method in conjunction with the method of characteristics [23]. In correspondence with equation (5.2) the abscissa and ordinate are respectively $(x/d)(C_D M^3)^{-1}$ and $\Delta p/p_1$. (For the sonic-wedge leading edge C_D was determined from the oblique shock relations, and for the semicircular leading edge C_D was taken equal to $\frac{2}{3}C_p^*$, corresponding to the modified Newtonian formula.) Excluding the small region near the corner of the sonic-wedge flat plate, we see that in these coordinates all of the pressure distributions correlate and follow a single curve. In Fig. 5.4b the shape of the shock wave corresponding to the case of the flat plate with a sonic-wedge leading edge is shown. Here, as well, starting at a small distance from the leading edge all of the curves correlate and follow a single curve very closely.

The results which have been presented indicate the possibility of using the equivalence principle for studying hypersonic flows past slender, slightly blunted bodies. The straight line in Fig. 5.4a corresponds to the value of $\Delta p/p_1$ calculated from equation (5.4). This curve agrees satisfactorily with the main part of the curves, calculated by the method of characteristics, up to values of $(x/d)(C_D M^3)^{-1}$ of approximately 0.01.

Figure 5.5 illustrates the results of two series of tests on hypersonic flows past blunted flat plates. The first series of tests was carried out in a helium wind tunnel at a Mach number of the order of 12 [2]. The model was a 10° wedge, one side of which was placed parallel to the flow; the leading edge blunting was made by cutting a flat face normal to this side of the wedge. The second series of tests was carried out with a similar model, but with a wedge angle of 20° , in a wind tunnel operating on air at a Mach number of about 7 [24].

In the first series of experiments if the Reynolds number based on free stream conditions and the width of the bluntness is greater than five to six thousand the values of $\Delta p/p_1$ as a function of $(x/d)(C_D M^3)^{-1}$, for

different bluntness widths and different free stream Mach numbers, follow a single curve very closely when C_D is taken equal to C_p^* . They also agree with the theoretical dependence given by equation (5.4) with $\gamma = 5/3$. For Reynolds numbers below these values the effect of

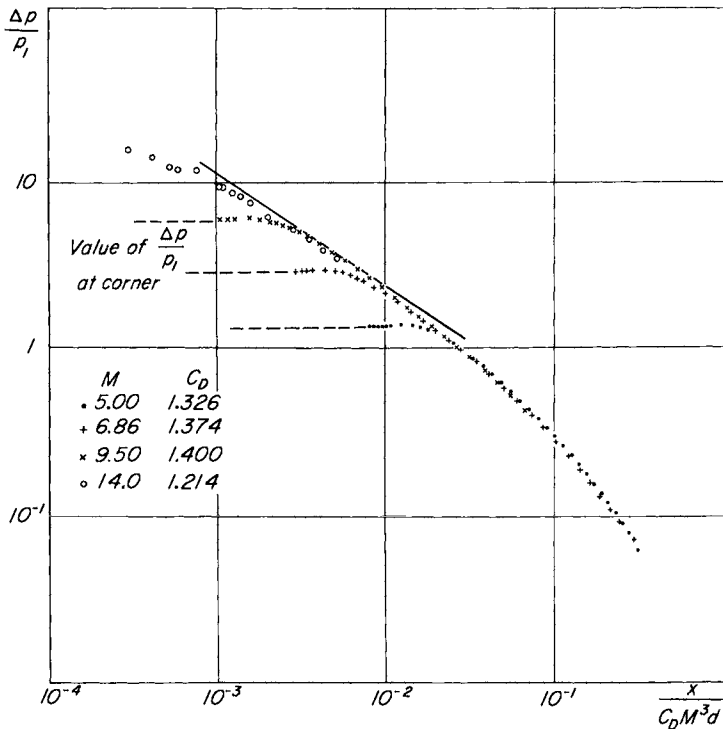


FIG. 5.4a. Pressure distribution on flat plates with sonic-wedge and semi-circular leading edges.

viscosity on the flow near the leading edge becomes important and the value of C_D needed to correlate the experiments rises sharply. In the second series of experiments the Reynolds numbers did not exceed 2000 and the effect of this was evidenced over the entire range which was investigated. For the largest Reynolds number the experimental values of the pressure agree well with equation (5.4) with $\gamma = 7/5$, if C_D is taken equal to C_p^* . For the lower Reynolds numbers, as in the first series of tests, C_D increases sharply.

Thus the experimental data also confirm the conclusions of the theory.

Moreover, the data show that the effect of viscosity can be neglected in determining the drag coefficient of the blunt leading edge C_D , if the Reynolds number exceeds 2000 to 6000 (a more precise estimate of this number is not possible from the available data). We also note that

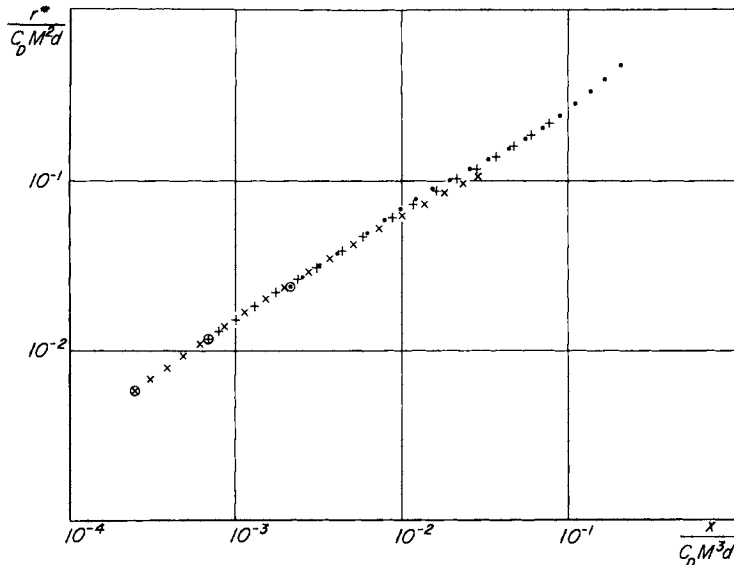


FIG. 5.4b. Shock wave shape for flow past a flat plate with a sonic-wedge leading edge.

according to the theory (Fig. 5.3), the effect of the bluntness is decreased with a decrease in the specific heat ratio γ . This decrease in the bluntness effect for a change of γ from $5/3$ to $7/5$ is not very large. The test results (see Fig. 5.5) confirm this conclusion.

Let us turn now to a consideration of the hypersonic flow past a right circular cylinder of diameter d with its flat end normal to the stream (see Fig. 5.6). Repeating the same reasoning as that used for a flat plate, we find that in this case the flow is determined by the dimensionless parameters γ , $(x/d)(\sqrt{C_D M^2})^{-1}$, and $(r/d)(\sqrt{C_D M})^{-1}$. In particular the pressure distribution on the surface of the cylinder and the shock wave shape are expressed by the functional relations

$$\frac{\Delta p}{p_1} = P \left(\gamma, \frac{1}{\sqrt{C_D M^2}} \frac{x}{d} \right)$$

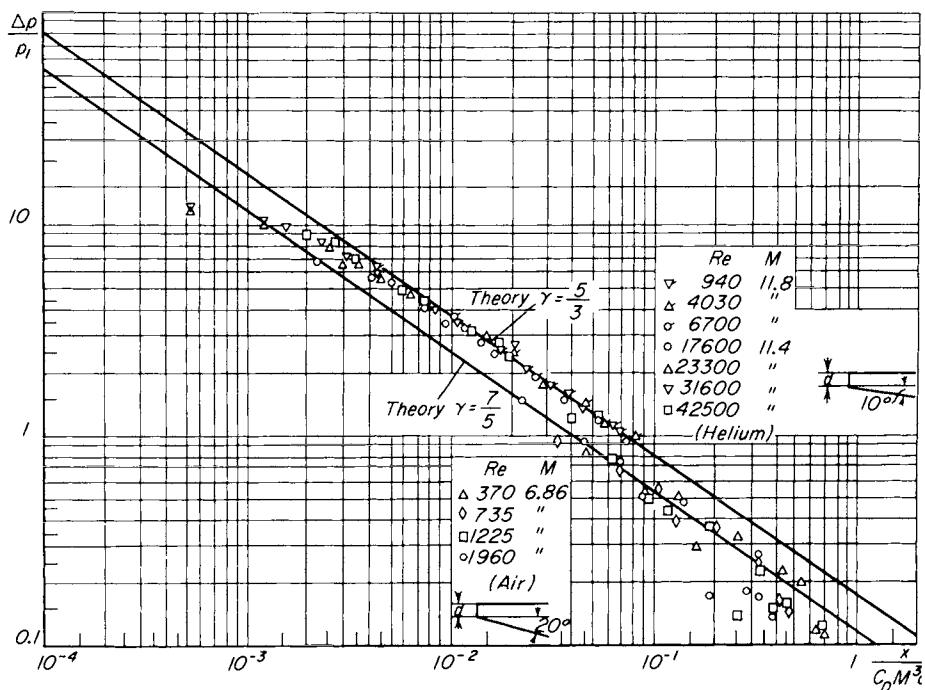


FIG. 5.5. Experimental data on the pressure distribution on a blunted flat plate at hypersonic speeds.

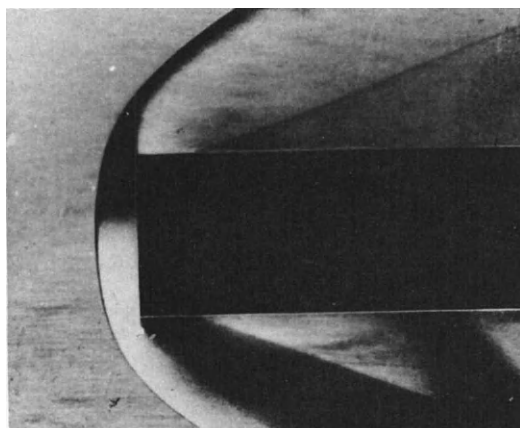


FIG. 5.6. Schlieren photograph of supersonic flow past a cylinder.

and

$$\frac{1}{\sqrt{C_D} M} \frac{r^*}{d} = R \left(\gamma, \frac{1}{\sqrt{C_D} M^2} \frac{x}{d} \right).$$

For limiting hypersonic speeds these expressions take the form

$$\frac{\Delta p}{\frac{1}{2} \rho_1 V^2} = \bar{\kappa}(\gamma) \sqrt{C_D} \frac{d}{x} \quad (5.6)$$

and

$$\frac{r^*}{d} = \bar{\kappa}_1(\gamma) C_D^{1/4} \left(\frac{x}{d} \right)^{1/2}. \quad (5.7)$$

Graphs of the functions $\bar{\kappa}(\gamma)$ and $\bar{\kappa}_1(\gamma)$, plotted from the exact solution for a violent explosion with a line charge [11], are shown by the solid lines in Fig. 5.7. In Table 5.2 are given the values obtained from this

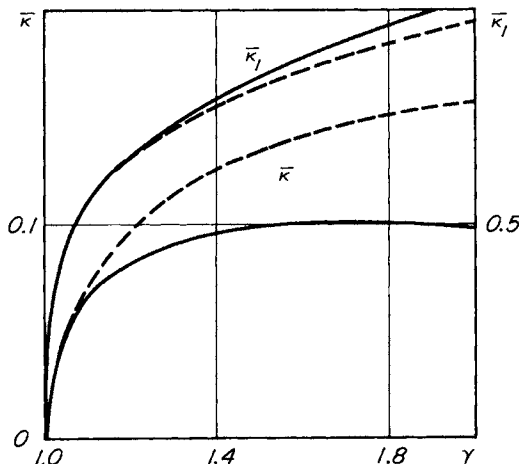


FIG. 5.7. The functions $\bar{\kappa}(\gamma)$ and $\bar{\kappa}_1(\gamma)$.

exact solution of p/p^* , ρ/ρ^* , and v/v^* as functions of r/r^* and m/m^* . These results specify the distribution of pressure, density, and transverse velocity between the shock wave and the cylinder surface.

Equation (5.6) indicates the presence of a region of high pressure near the blunt end of the cylinder. For limiting hypersonic speeds the extent of the high pressure region grows in proportion to M^2 (with the absence of any Reynolds number effect on C_D); with decreasing γ the extent of this region decreases.

Unfortunately experimental data on the pressure distribution and shape of the shock for hypersonic flow past a cylinder with a small diameter to length ratio are unavailable. In Figs. 5.8a and b are shown

TABLE 5.2
EXACT SIMILAR SOLUTION FOR VIOLENT EXPLOSION,
AXISYMMETRIC CASE ($\nu = 2$); $\gamma = 1.4$

$\frac{r}{r^*}$	$\frac{p}{p^*}$	$\frac{\rho}{\rho^*}$	$\frac{v}{v^*}$	$\frac{m}{m^*}$
1	1	1	1	1
0.9998	0.9985	0.9973	0.9996	0.9908
0.9802	0.8659	0.7653	0.9645	0.7941
0.9644	0.7832	0.6285	0.9374	0.6665
0.9476	0.7124	0.5164	0.9097	0.5565
0.9295	0.6514	0.4234	0.8812	0.4819
0.9096	0.5983	0.3451	0.8514	0.3770
0.8725	0.5266	0.2427	0.7998	0.2616
0.8442	0.4884	0.1892	0.7638	0.1989
0.8094	0.4545	0.1414	0.7226	0.1366
0.7629	0.4242	0.0975	0.6720	0.0903
0.7242	0.4074	0.0718	0.6327	0.0614
0.6894	0.3969	0.0545	0.5989	0.0428
0.6390	0.3867	0.0362	0.5521	0.0248
0.5745	0.3794	0.0208	0.4943	0.0117
0.5180	0.3760	0.0123	0.4448	0.0056
0.4748	0.3746	0.0079	0.4073	0.0030
0.4222	0.3737	0.0044	0.3621	0.0014
0.3654	0.3733	0.0021	0.3133	0.0005
0.3000	0.3730	0.0008	0.2571	0.0001
0.2500	0.3729	0.0003	0.2143	0.0000
0.2000	0.3729	0.0001	0.1714	0.0000
0.1500	0.3729	0.0000	0.1286	0.0000
0.1000	0.3729	0.0000	0.0857	0.0000
0.0000	0.3729	0.0000	0.0000	0.0000

experimental data [6] on the shape of the bow wave and on the pressure on a short cylinder at $M = 7.7$. The solid lines on these figures correspond to equations (5.6) and (5.7), and the dashed line to a relation which takes into account the counterpressure [21].

In concluding this section we note that the solution for the explosion of a plane or line charge also describes the flow past an arbitrary airfoil or body of revolution in a region whose dimensions are large

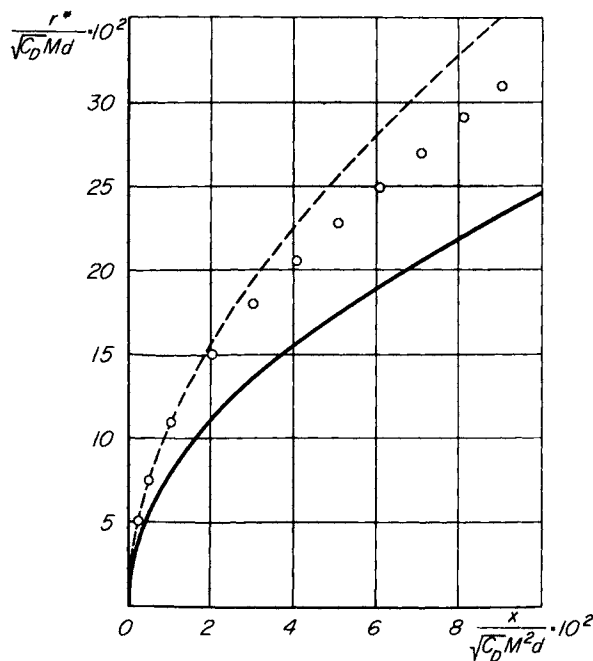


FIG. 5.8a. Bow wave shape for flow past a cylinder: ○-experiment, $M = 7.7$; —— equation (5.7); - - - formula from [21].

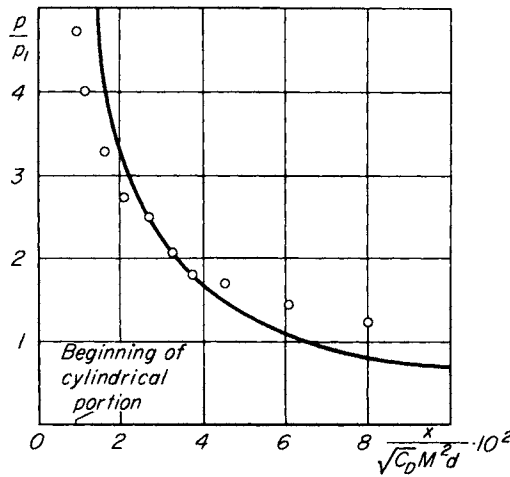


FIG. 5.8b. Surface pressure on a cylinder: ○-experiment, $M = 7.7$; —— equation (5.6).

in comparison with the transverse dimension of the body. In this case, in order to describe the flow in the region where the shock wave is not strong, it is of course necessary to use the solution which takes into account the counterpressure.

3. Flow past a slender wedge with a blunt leading edge

As the simplest example of hypersonic flow past an airfoil with a slightly blunted leading edge let us consider the flow past a slightly blunted wedge. For this case, in the equivalent problem of unsteady gas motion with planar symmetry we have $E \neq 0$ and $U = V \tan \alpha = \text{const}$ (α is the half-angle of the wedge). This motion is not self-similar even when the initial gas pressure can be neglected in comparison with the pressure behind the shock wave. An approximate solution to this problem can be obtained by expanding the solution in a power series in $(\gamma - 1)/(\gamma + 1)$. A brief description of the application of the method to problems of the type being considered can be found at the end of Section 1 of the present chapter. However, bearing in mind that in general this method is rather laborious, we shall in what follows derive a simplification of the method which will permit us to obtain a solution by elementary means and at the same time retain a satisfactory degree of accuracy.

We recall that the central idea in the method of expanding the solution in a power series in $(\gamma - 1)/(\gamma + 1)$ is that when the gas is strongly compressed across the shock wave, most of the gas in the disturbed region is concentrated in a thin layer close to the shock wave. The principal change in pressure also occurs in this layer, while in the rest of the region (which actually need not be present) the change in pressure is very small as a result of the low density. In order to obtain a solution in elementary form we shall assume that the thickness of the layer near the shock wave, which is taken to contain the entire mass of gas, is negligibly small and that the pressure change in the disturbed region outside of this layer can be neglected.

Applying the energy equation (5.1) to the gas inside the disturbed region, we obtain

$$\frac{1}{2} \rho_1 v \left(\frac{\partial R}{\partial t} \right)^2 + \frac{p}{\gamma - 1} (v - v_0) = E + \frac{p_1 v}{\gamma - 1} + \int_0^t p dv_0(t). \quad (5.8)$$

Here $v - v_0$ is the volume of gas in the disturbed region and v_0 is the volume displaced by the piston. In the case of planar symmetry v is the distance from the plane of the explosion to the shock wave and v_0 is the distance to the piston. In order to determine from this equation the shock wave motion $R_0(t)$, and together with it all the flow characteristics (from equations (3.42) and (3.43) of Chapter III), we can use the leading terms in the expansions of the functions R and p in powers of $(\gamma - 1)/(\gamma + 1)$, i.e.,

$$\frac{\partial R}{\partial t} = \dot{R}_0, \quad p = \rho_1 \dot{R}_0^2 + \rho_1 \frac{R_0 \ddot{R}_0}{v}.$$

To make the entire theory more elementary in character, however, we shall use the impulse equation as the second relation for determining the functions $R_0(t)$ and $p(t)$. This equation has the following form:

$$\rho_1 v \frac{\partial R}{\partial t} = I + \int_0^t (p - p_1) S dt, \quad (5.9)$$

where S is the surface area of the shock wave; in the case of planar symmetry $S = 1$.

In equations (5.8) and (5.9) the quantity $\partial R / \partial t$ is the gas velocity, which is the same for all particles. Let us now assume that the velocity of the gas particles throughout the layer is the same as at points behind the shock wave; i.e., we will take†

$$\frac{\partial R}{\partial t} = \frac{2}{\gamma + 1} \left(\dot{R}_0 - \frac{a_1^2}{\dot{R}_0} \right). \quad (5.10)$$

For a given piston motion $v_0(t)$, equations (5.8) to (5.10) permit the functions $R_0(t)$ and $p(t)$ to be determined.

For flow past a wedge, $v_0 = Ut$, $v = R_0$, and $S = 1$. To simplify the problem we shall limit our considerations to the case where the effect of the counterpressure on the motion can be neglected. (To consider the counterpressure does not, however, introduce any basic difficulties.)

† One can, with somewhat less exactitude, take $\partial R / \partial t = \dot{R}_0$; we note that this relation agrees with equation (5.10) in the case of infinite condensation of the gas across the shock wave, i.e., for $\gamma \rightarrow 1$ and $p_1 \rightarrow 0$.

Dropping the pressure p_1 from equations (5.8) and (5.9) and the term a_1^2/R_0 in equation (5.10), we obtain one equation to determine the shock wave motion:

$$\begin{aligned} \rho_1 R \cdot \frac{1}{2} \left(\frac{2}{\gamma + 1} \dot{R} \right)^2 + \frac{1}{\gamma - 1} (R - Ut) \frac{d}{dt} \left(\rho_1 R \frac{2}{\gamma + 1} \right) \dot{R} \\ = E - IU + \rho_1 U R \frac{2}{\gamma + 1} \dot{R}. \end{aligned}$$

Here the subscript 0 has been dropped from R .

We shall for the moment not consider the case $U = 0$, which was examined more exactly in Section 2. Let us introduce as a length scale $L = (E - IU)/\rho_1 U^2$, as a time scale L/U , and as a measure of the pressure the scale $\rho_1 U^2$. The equation written above then assumes the form

$$\frac{1}{\gamma - 1} (R - t) \frac{d}{dt} (R \dot{R}) = \frac{\gamma + 1}{2} + R \dot{R} - \frac{1}{\gamma + 1} R \dot{R}^2. \quad (5.11)$$

This equation has a unique solution $R^*(t)$, which satisfies the condition $R(0) = 0$ and which exists for all $t \geq 0$. For small values of t

$$R^* = \left[\frac{9}{4} \frac{(\gamma + 1)^2(\gamma - 1)}{3\gamma - 1} \right]^{1/3} t^{2/3}.$$

For large t the solution tends to the asymptotic limit

$$R = \frac{\gamma + 1}{2} t + \gamma - 1, \quad (5.12)$$

which is an exact solution of equation (5.11).

Since $R^* \dot{R}^* = O(t^{1/3})$ for $t \rightarrow 0$, the solution $R^*(t)$ corresponds to the case $I = 0$. For small values of the wedge half-angle α the quantity $IU = L \tan \alpha$ is small in comparison with the quantity $E = D$ (L is of the order of D or smaller). This then allows us to use the solution R^* in order to estimate the effect on a hypersonic flow of slightly blunting the leading edge of a slender wedge.

Transforming to the variables which characterize the steady flow problem, we find that the shape of the shock is determined by the relation

$$\frac{r^*}{d} = \frac{C_D}{4 \tan^2 \alpha} R^* \left(\frac{4 \tan^3 \alpha}{C_D} \frac{x}{d}, \gamma \right). \quad (5.13)$$

For the pressure distribution along the wedge we obtain the following expression:

$$\frac{p}{\rho_1 V^2 \tan^2 \alpha} = \dot{W} \left(\frac{4 \tan^3 \alpha}{C_D} \frac{x}{d}, \gamma \right), \quad (5.14)$$

where by $\dot{W}(t, \gamma)$ we have denoted the function $2R^*R^*/(\gamma + 1)$. Graphs of the relations (5.13) and (5.14) are shown in Figs. 5.9 and 5.10. In Fig. 5.9 the shock location for flow past a wedge with a sharp leading edge is also shown.

It follows from equations (5.13) and (5.12) that the shock wave angle for flow past the blunted wedge approaches the shock angle in the downstream direction for flow past the sharp leading edge wedge, although the shock itself is displaced farther from the wedge surface than for the

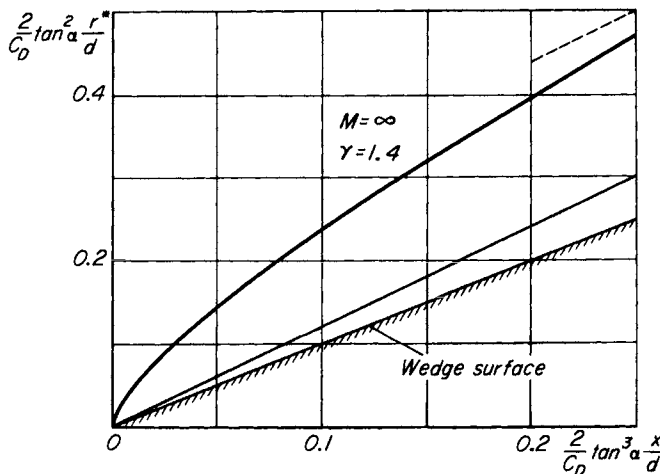


FIG. 5.9. Bow wave shape for flow past a slightly blunted wedge.

sharp leading edge case. This added displacement is caused by a layer of gas near the surface of the wedge which passed through the strong part of the shock wave near the leading edge and which therefore has a high temperature and low density. From equations (5.13) and (5.12) this displacement is given by

$$\frac{\gamma - 1}{4} \frac{C_D}{\tan^2 \alpha} d;$$

i.e., it can be appreciable for slender wedges.

A detailed comparison with experiment of the results of the calculations was not made because of the lack of experimental data at the time of writing. We have, however, shown in Fig. 5.11a a schlieren photograph of the flow over a blunted 10° wedge at a Mach number of 13.8

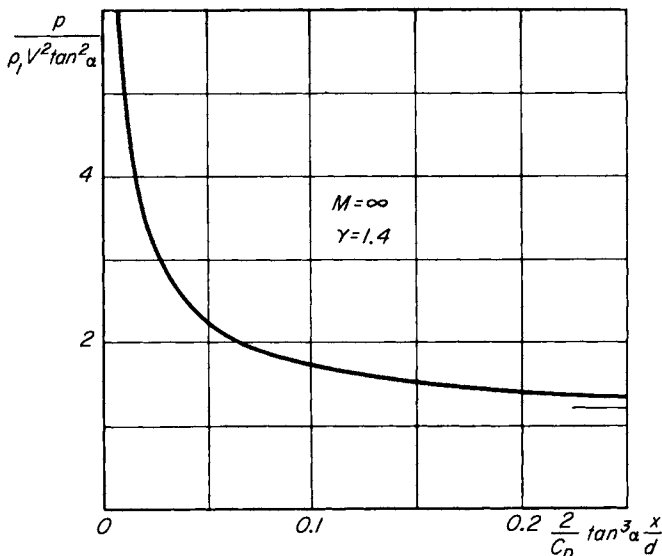


FIG. 5.10. Surface pressure distribution on a slightly blunted wedge.

in air [25].† Figure 5.11b is presented in order to give a qualitative comparison of the flow picture with that obtained from equation (5.13) with $\gamma = 7/5$. In the upper half-plane the free stream flow is in the direction of the wedge surface, which corresponds to the case $\alpha = 0$ in this equation. Using the asymptotic expression of the function R^* for small t , we find that for $\alpha = 0$

$$\frac{p}{\frac{1}{2} \rho_1 V^2} = \left[\frac{\sqrt{2}}{3} \frac{(\gamma + 1)^{1/2}(\gamma - 1)}{3\gamma - 1} \right]^{2/3} C_D^{2/3} \left(\frac{d}{x} \right)^{2/3},$$

$$\frac{r^*}{d} = \left[\frac{9}{16} \frac{(\gamma + 1)^2(\gamma - 1)}{3\gamma - 1} \right]^{1/3} C_D^{1/3} \left(\frac{x}{d} \right)^{2/3}.$$

† *Editor's note:* The width of the bluntness is 0.0142 in, and the Reynolds number based on this width and free stream conditions is 3150. In [25] the schlieren photograph shown is for helium, although the measured shock shape corresponding to Fig. 5.11a is given in Fig. 22 of this reference.

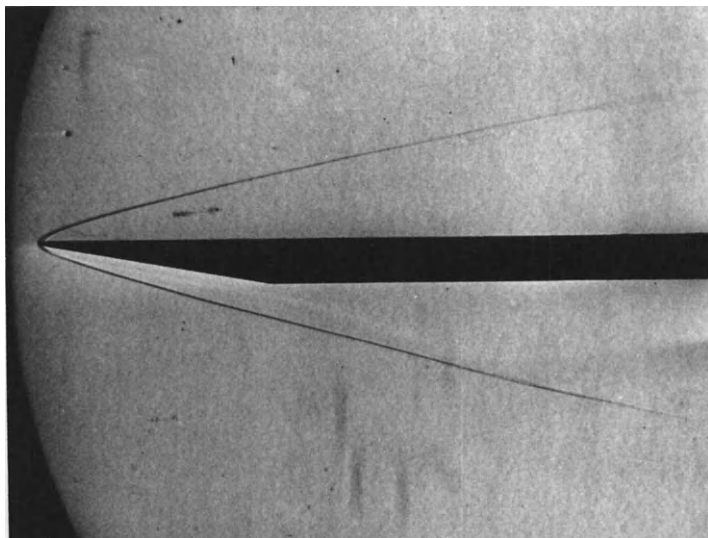


FIG. 5.11a. Schlieren photograph of flow past a slightly blunted 10° wedge in air at $M = 13.8$. (Armament Research and Development Establishment, courtesy of Her Majesty's Stationery Office. British Crown Copyright reserved.)

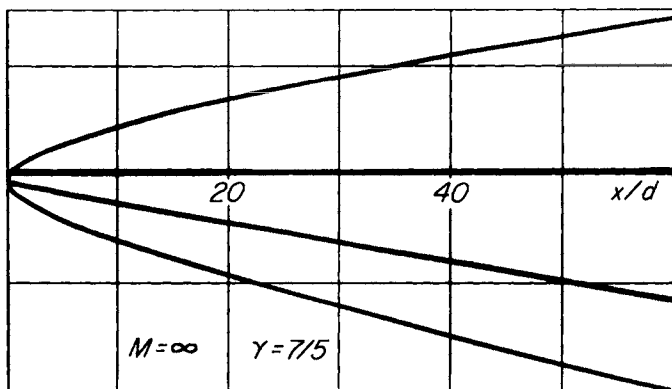


FIG. 5.11b. Picture of flow past a slightly blunted wedge at $M = \infty$ with $\gamma = 7/5$.

In order to judge the accuracy of these expressions we have plotted by means of the dashed lines in Fig. 5.3 the bracketed quantities raised to their respective powers which appear on the right hand sides of these expressions. These factors correspond to the functions $\kappa(\gamma)$ and $\kappa_1(\gamma)$ in equations (5.4) and (5.5), which were obtained from the exact solution for flow past a blunted flat plate with $M = \infty$.

The total drag D_1 of a blunted wedge of length l is given by

$$D_1 = 2D + 2 \int_0^l p \tan \alpha dx = 2D \left[1 + W \left(\frac{4 \tan^3 \alpha}{C_D} \frac{l}{d}, \gamma \right) \right].$$

(We remind the reader that D is half the drag of the blunting.) The drag coefficient of this wedge is expressed by the formula

$$C_D^{\text{wedge}} = \frac{2}{t} [1 + W(t, \gamma)] \tan^2 \alpha,$$

where

$$t = \frac{4}{C_D} \tan^3 \alpha \frac{l}{d}.$$

A graph of this relation for small values of t and $\gamma = 1.4$ is shown by the solid curve in Fig. 5.12. For large values of t the appropriate approximate dependence is given by

$$C_D^{\text{wedge}} = \left(\gamma + 1 + \frac{2\gamma}{t} \right) \tan^2 \alpha.$$

On this same figure we have plotted by means of the dashed line the value of C_D^{wedge} corresponding to the sum of the drag of the blunt leading edge and the drag of the sharp leading edge wedge:

$$C_D^{\text{wedge}} = \left(\gamma + 1 + \frac{2}{t} \right) \tan^2 \alpha.$$

As the results show, for slender wedges a slight blunting of the leading edge leads to a considerable increase in the drag coefficient C_D^{wedge} . Thus even for an l/d of 500, the drag of a blunt wedge of 6° half-angle is twice that of the wedge with a sharp leading edge. Therefore in computing

the drag it is important to take into account the effect of the blunting on the pressure distribution along the remaining part of the wedge surface. Hence in order to avoid significantly increasing the drag of wings

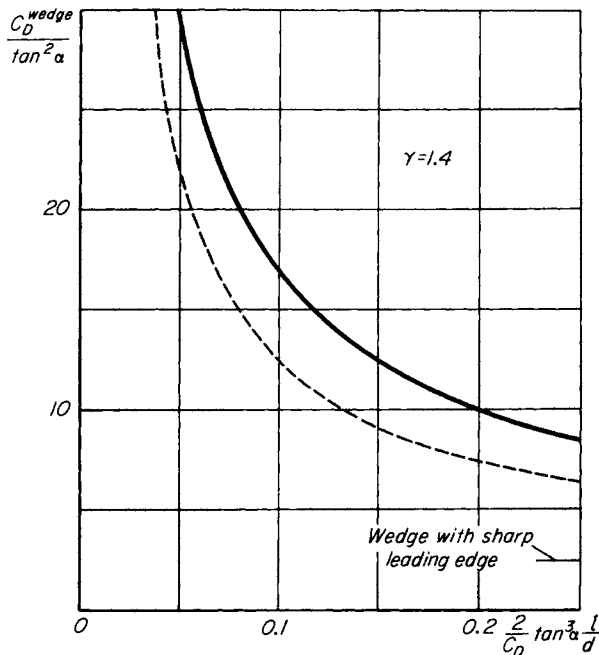


FIG. 5.12. Drag coefficient on a slightly blunted wedge: — including bluntness effect on wedge pressure distribution; - - - sum of bluntness drag and drag of sharp wedge.

and stabilizing surfaces at hypersonic speeds, it is necessary to have very carefully sharpened leading edges. As was pointed out in Section 1 of the present chapter, however, from a practical point of view this requirement is hardly feasible.

We should also point out that the center of pressure of an airfoil with a blunt leading edge is moved forward in comparison with the center of pressure of the same airfoil with a sharp leading edge. The extent of this displacement can be appreciable. For example, at limiting hypersonic speeds for a flat plate airfoil with a blunt leading edge, the center of pressure as given by equation (5.4) is located at the $\frac{1}{4}$ chord point

measured from the leading edge, and not at the center of the chord as would be the case for the infinitely thin flat plate.

In concluding the present section we note that the approximate solution which was developed gives for the case of the sharp leading edge wedge

$$\beta = \frac{\gamma + 1}{2} \alpha, \quad \frac{p}{\rho_1 V^2} = \frac{\gamma + 1}{2} \alpha^2$$

(β is the shock wave angle with respect to the free stream direction). These results agree with those obtained from the exact theory for $M = \infty$.

4. Flow past a slender blunted cone

We shall consider in this section an approximate formulation of the problem of flow past a slightly blunted slender cone, analogous to that considered for the wedge in the preceding section. In this case it is necessary to set $v = \pi R^2$, $v_0 = \pi U^2 t^2$, and $S = 2\pi R$ in the energy and impulse equations (5.8) and (5.9).

For the particle velocity in the disturbed region we shall apply equation (5.10), i.e., we shall take into consideration the initial pressure of the gas. Assuming that $U \neq 0$, we introduce as a length scale $L = (E/\pi\rho_1 U^2)^{1/2}$, as a time scale L/U ; and we shall denote by $\rho_1 U^2 \Delta p$ the pressure difference $p - p_1$. Then equations (5.8) and (5.9) take the following form:

$$\begin{aligned} \frac{1}{2} R^2 \left(\frac{2}{\gamma + 1} \right)^2 \left(\dot{R} - \frac{1}{K^2 \dot{R}} \right)^2 + \frac{R^2 - t^2}{\gamma - 1} \left(\Delta p + \frac{1}{\gamma K^2} \right) \\ = 1 + \frac{R^2}{\gamma - 1} \frac{1}{\gamma K^2} + 2 \int_0^t \left(\Delta p + \frac{1}{\gamma K^2} \right) t \, dt, \quad (5.15) \\ R^2 \frac{2}{\gamma + 1} \left(\dot{R} - \frac{1}{K^2 \dot{R}} \right) = \frac{IU}{E} + 2 \int_0^t \Delta p R \, dt. \end{aligned}$$

Here $K = U/(\gamma p_1 / \rho_1)^{1/2} = M \tan \alpha$ is the hypersonic similarity parameter.

For small values of t , the initial energy of the gas in the disturbed region and the work done by the piston are small in comparison with

the energy released by the explosion. Then the solution of the system of equations (5.15) reduces to an approximate solution of the problem of a violent explosion with cylindrical symmetry (as in Section 3, we take the quantity IU/E to be negligibly small), and is given by

$$\begin{aligned}\Delta p &= \sqrt{\frac{\gamma - 1}{4(3\gamma - 1)}} t^{-1}, \\ R &= \left[\frac{4(\gamma + 1)^2(\gamma - 1)}{3\gamma - 1} \right]^{1/4} t^{1/2}.\end{aligned}\tag{5.16}$$

From these relations it is easy to obtain the expressions corresponding to the functions $\bar{\kappa}(\gamma)$ and $\bar{\kappa}_1(\gamma)$ of equations (5.6) and (5.7). These values are shown by the dashed lines in Fig. 5.7.

The solution of equations (5.15), which for small t has the asymptotic form (5.16), can be obtained by a numerical integration. From these equations it can be shown that for large values of t the functions \dot{R} and Δp tend to constants (corresponding to the flow past a sharp-nosed cone):

$$\begin{aligned}\dot{R} &\rightarrow \sqrt{\frac{\gamma + 1}{2} + \frac{1}{K^2}}, \\ \Delta p &\rightarrow 1.\end{aligned}$$

In Fig. 2.12 is shown (solid line) a graph of the relation

$$\frac{K_s}{K} = \frac{\tan \beta}{\tan \alpha} = \sqrt{\frac{\gamma + 1}{2} + \frac{1}{K^2}},$$

which is obtained using the first of the above equations (β is the shock wave angle with respect to the free stream direction).

Calculations carried out for $K = \infty$ (i.e., for negligible counter-pressure) have shown the following interesting features concerning the behavior of the solution. The pressure coefficient on the cone is infinite at the nose and rapidly decreases in the downstream direction, taking on significantly lower values on some parts of the cone than the values for a sharp cone with the same apex angle (see curve in Fig. 5.13). Correspondingly, the angle β between the shock wave and flow direction has a minimum (see curve in Fig. 5.14). This qualitative behavior of the flow is maintained for values of the hypersonic similarity parameter

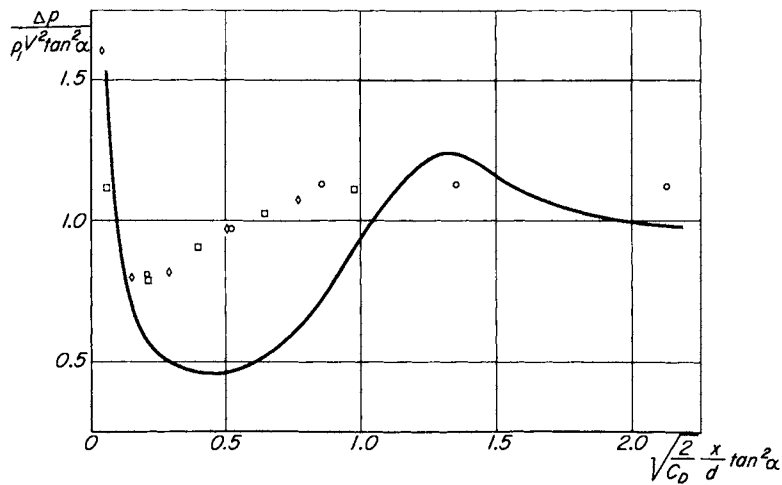


FIG. 5.13. Surface pressure on a slightly blunted cone; theory $K = \infty$, experiment $K = 1.2$ ($M = 6.85$).

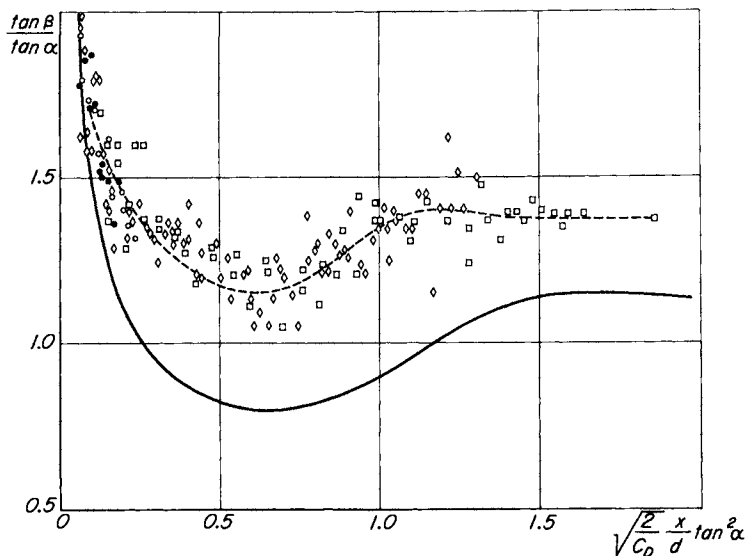


FIG. 5.14. Angle of bow wave with respect to free stream flow for a slightly blunted cone; theory $K = \infty$, experiment $K = 1.2$ ($M = 6.85$).

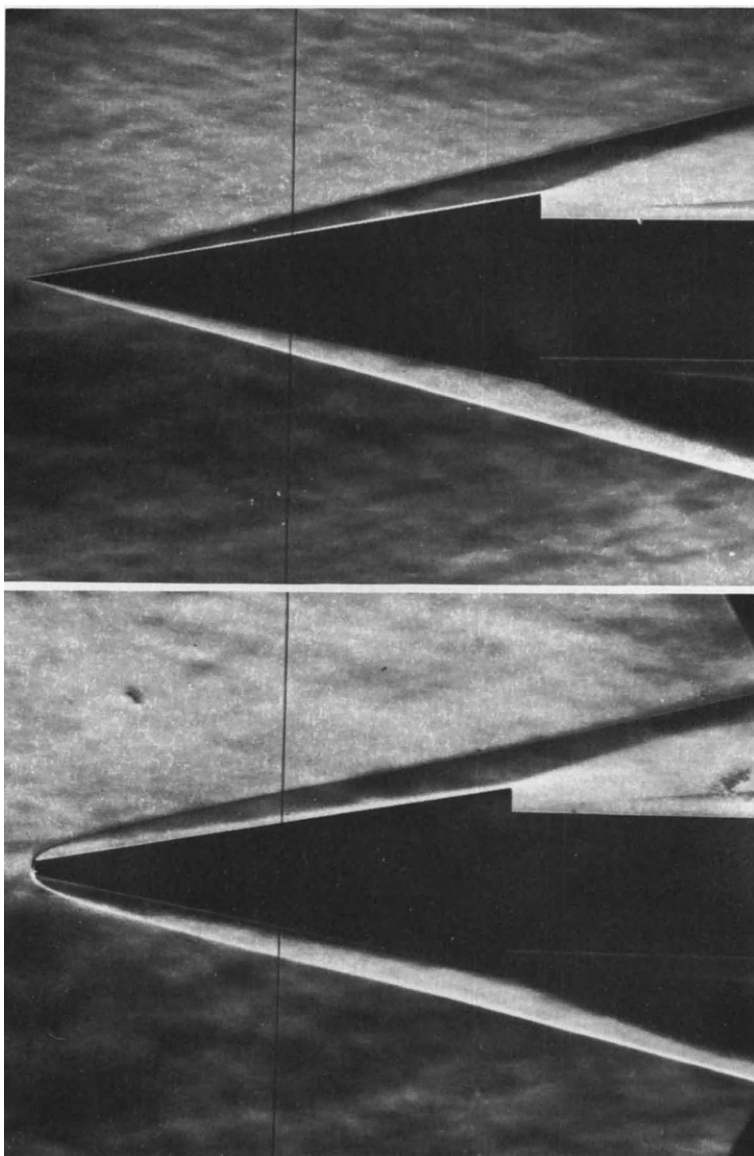


FIG. 5.15. Schlieren photographs of flow past a sharp and slightly blunted 10° half-angle cone in air at $M = 6.85$.

of the order of one. This is shown by the experimental data reported in [26] for the flow of air past a slightly blunted cone of 10° half-angle at a Mach number of 6.85 (i.e., for $K = 1.2$). The results of these experiments are plotted in Figs. 5.13 and 5.14, and in Fig. 5.15 are shown schlieren photographs taken from [26] of the flow past a sharp and blunted cone.

Since the pressure on an appreciable part of the surface of a blunted cone is lower than on the surface of the corresponding sharp-nosed cone, the total drag of the blunted cone can be less than the drag of the sharp-nosed cone. The drag coefficient of the blunted cone is given (for $K = \infty$) by the relation

$$C_D^{\text{cone}} = \frac{2}{l^2} \left(1 + 2 \int_0^t \Delta p \, t \, dt \right) \tan^2 \alpha,$$

where

$$t = 2 \sqrt{\frac{2}{C_D}} \frac{l}{d} \tan^2 \alpha.$$

A graph of this relation with $\gamma = 1.4$ is shown in Fig. 5.16. For

$$\frac{l}{d} \approx \frac{0.96}{\tan^2 \alpha} \sqrt{\frac{C_D}{2}}$$

the drag coefficient of the blunted cone has a minimum, at which point the relative decrease in drag, in comparison with that of the correspond-

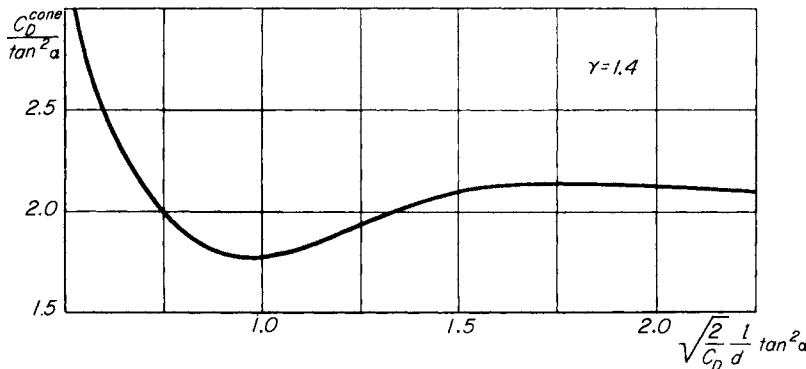


FIG. 5.16. Drag coefficient for a slightly blunted cone.

ing sharp-nosed cone, approaches 10%. Thus, in contrast to flows past airfoils, for limiting hypersonic flows past bodies of revolution a slight blunting of the nose, which is very desirable in connection with the need to cool the body, does not necessarily mean an increase in the drag.

5. Similarity law for flows past slightly blunted slender bodies

The formulation of the problem of flows past slightly blunted bodies, as presented in Section 1 of the present chapter, permits us to extend to such bodies the hypersonic similarity law developed in Section 2 of Chapter II for flows past slender, sharp-nosed bodies.[†] We shall limit our considerations to symmetric flows past bodies of revolution and airfoils; in addition, the shape of the blunting will be assumed symmetrical.

As was discussed previously, hypersonic flows past slightly blunted slender bodies correspond to the plane unsteady motions which result if, in a gas initially at rest with a density ρ_1 and pressure p_1 , there is an explosion of a line (for axisymmetric flow) or plane (for two-dimensional flow) charge releasing an energy density E which is accompanied by the subsequent motion of a piston (cylindrical or planar). In this motion the gas velocity v , its pressure p , and density ρ are determined by the following system of parameters:

$$\rho_1, \quad p_1, \quad \gamma; \quad E; \quad \alpha_1, \dots, \alpha_k; \quad r, \quad t.$$

Here $\alpha_1, \dots, \alpha_k$ are kinematic constants which enter into the relation for the piston motion.

In general, among the parameters $\alpha_1, \dots, \alpha_k$ there are two possessing independent dimensions. Without limiting the generality of the analysis, we shall assume that these two parameters have the dimensions of length and time, and we shall denote them respectively by r_0 and t_0 . If both the parameters E and p_1 must be considered (i.e., if for flow past a blunt body the counterpressure has an appreciable effect on the flow), then they can be replaced by the parameters

$$r_* = \left(\frac{E}{p_1}\right)^{1/\nu} \quad \text{and} \quad t_* = E^{1/\nu} \rho_1^{1/2} p_1^{-(\nu+2)/2\nu} \quad \left(\text{or} \quad a_1 = \left(\frac{\gamma p_1}{\rho_1}\right)^{1/2}\right),$$

[†]Editor's note: The extension of the hypersonic similarity law to slightly blunted slender bodies has been carried out independently by Cheng [27].

which have the dimensions of length and time (or velocity). Thus the system of independent parameters can be expressed in the form

$$\rho_1, \quad r_*, \quad t_* \quad (\text{or } a_1), \quad \gamma, \quad r_0, \quad t_0, \quad \alpha_3, \dots, \alpha_k, \quad r, \quad t.$$

In the relations

$$v = \frac{r_0}{t_0} v', \quad p = \rho_1 \frac{r_0^2}{t_0^2} p', \quad \rho = \rho_1 \rho' \quad (5.17)$$

the dimensionless functions v' , p' , and ρ' can only depend on the dimensionless combinations

$$\frac{r}{r_0}, \quad \frac{t}{t_0}, \quad \gamma, \quad \frac{r_0}{a_1 t_0}, \quad \frac{r_*}{r_0}, \quad (5.18)$$

and on the dimensionless constants α'_i , which enter into the relation describing the piston motion.

As was shown in Section 1 of the present chapter, in order to pass from the unsteady motions being considered to the equivalent steady flows past bodies, we must make the following change of variables in the relations (5.17) and (5.18):

$$r_0 \rightarrow \tau L, \quad t_0 \rightarrow \frac{L}{V}, \quad t \rightarrow \frac{x}{V}, \quad E \rightarrow D = C_D \frac{\rho_1 V^2}{2} d'.$$

Here L is the length of the body and τ is a parameter characterizing the thickness ratio of the body; the rest of the quantities have the same meaning as in the previous sections. Carrying out these substitutions the relations (5.17) take the form

$$v = \tau V v', \quad p = \rho_1 V^2 \tau^2 p', \quad \rho = \rho_1 \rho', \quad (5.19)$$

and we find that the dimensionless functions v' , p' , and ρ' depend only on the quantities

$$\frac{r}{\tau}, \quad x, \quad \gamma, \quad M\tau, \quad C_D^{1/\nu} M^{1+(2/\nu)} d \quad (\text{and upon } \alpha'_i) \quad (5.20)$$

(all lengths are made dimensionless with respect to the body length L). The functional equation expressing the body shape takes the form

$$\Phi \left(\frac{r}{\tau}, \quad x, \quad \alpha'_i \right) = 0. \quad (5.21)$$

From these expressions we may generalize the similarity law given in Section 2 of Chapter II to the case of slightly blunted bodies as follows: For hypersonic flows past slightly blunted affinely related bodies, which have different values of the parameter τ in the equation expressing their shape (5.21), the dimensionless quantities v' , p' , and ρ' in equations (5.19) will have the same values at corresponding points (i.e., at the same r/τ and x) if the parameters $K = M\tau$ and $K^* = C_D^{1/2}M^{1+(2/\nu)}d$ are the same. The parameter K is the well-known similarity criterion for hypersonic flows past sharp-nosed bodies; the parameter K^* is the additional similarity criterion when the body is slightly blunted.

In place of the parameter K^* one can introduce the parameter K^{**}

$$K^{**} = \frac{K^*}{K^{1+(2/\nu)}} = \frac{C_D^{1/2}d}{\tau^{1+(2/\nu)}},$$

which does not contain the Mach number. For limiting hypersonic flows where the counterpressure of the gas can be neglected, the Mach number will in general not enter into the system of independent parameters (5.20), so that in place of the similarity criteria K and K^* there remains only the criterion K^{**} . As shown in Section 1 of this chapter, for limiting hypersonic speeds the quantity K^{**} characterizes the ratio of the force due to blunting to the force from the remaining part of the body.

From a treatment similar to that in Section 2 of Chapter II, we find that the drag coefficient C_D of the blunted body can be expressed in the form

$$C_D = \tau^2 F(\gamma, K, K^*)$$

(where the drag coefficient is based on an appropriate cross-sectional area of the body), and for limiting hypersonic speeds in the form

$$C_D = \tau^2 F_\infty(\gamma, K^{**}).$$

The function F_∞ was determined approximately for the blunted wedge and cone in Sections 3 and 4 of the present chapter, and is shown graphically in Figs. 5.12 and 5.16. An appreciable effect of the blunting on the drag of these bodies is indicated for $K^{**} > 1$.

For flows past a wedge or circular cone the relation for the piston motion is determined by the one constant $U = V\tau$ which has the dimension of a velocity. In this case the system of dimensionless independent parameters may be written in the following form:

$$\frac{r}{(C_D M^2)^{1/\nu} d}, \quad \frac{x}{(C_D M^2)^{1/\nu} M d}, \quad \gamma, \quad M\tau,$$

or

$$K^{*-1}x, \quad \frac{r/\tau}{x}, \quad \gamma, \quad K.$$

We find for the pressure distribution along the surface of the wedge or cone and for the coordinate of the bow shock wave r^* the functional relations

$$\frac{\Delta p}{\rho_1 V^2 \tau^2} = P_\nu(K^{*-1}x, \gamma, K),$$

$$K^{*-1} \frac{r^*}{\tau} = R_\nu(K^{*-1}x, \gamma, K),$$

which for limiting hypersonic speeds take the form

$$\frac{\Delta p}{\rho_1 V^2 \tau^2} = P_{\nu\infty}(K^{**-1}x, \gamma),$$

$$K^{**-1} \frac{r^*}{\tau} = R_{\nu\infty}(K^{**-1}x, \gamma).$$

The functions $P_{\nu\infty}$ and $R_{\nu\infty}$ were determined approximately in Sections 3 and 4 of the present chapter, and graphs of them are given in Figs. 5.9, 5.10, 5.13, and 5.14.[†]

If $U = 0$, i.e., if we consider the flow past a blunted flat plate or a right circular cylinder with its end normal to the stream, then the dimensionless functions

$$\frac{v}{a_1}, \quad \frac{p}{p_1}, \quad \frac{\rho}{\rho_1}$$

depend only on the quantities

$$\frac{x}{(C_D M^2)^{1/\nu} M d}, \quad \frac{r}{(C_D M^2)^{1/\nu} d}, \quad \gamma.$$

This case was considered in detail in Section 2 of the present chapter.

[†] In Fig. 5.14 is given a curve of the derivative of $R_{2\infty}$, and not of the value of the function itself.

CITED REFERENCES

Editor's note:

Every effort has been made to supply a source of an English translation for the originally cited Russian reference if available. In some cases an English translation has also been given for cited references published in other languages. Russian titles have been translated into English, but where a translation is indicated the English title given is that of the translated version.

Prior to 1947 the Proceedings of the Soviet Academy of Sciences (*Doklady Akademii Nauk SSSR*) appeared both in Russian and in a foreign edition (*Comptes Rendus de l'Academie des Sciences de l'URSS*) in which the articles were published in English, French, or German. Where a cited reference may be found in the foreign edition reference to it has been made.

Since 1958 the Soviet journal *Applied Mathematics and Mechanics* (*Prikladnaya Matematika i Mekhanika*) has been translated into English. In those cases where a referenced article has appeared in the translated journal the page numbers of both the original and translated edition have been given. Translations of articles appearing in *Prikladnaya Matematika i Mekhanika* prior to 1958 can be purchased from the Pergamon Institute, 1404 New York Avenue, N.W., Washington 5, D. C. and are listed by number as "*Pergamon Transl.*". The translations listed as "*M.D. Friedman Transl.*" are available from Morris D. Friedman, Inc., P. O. Box 35, West Newton 65, Mass. Those translations listed as "*Sci. Transl. Cent.*" were prepared by the Scientific Translations Center of the Library of Congress and can be obtained at present from the SLA Translation Center, The John Crerar Library, 86 East Randolph St., Chicago 1, Ill. The sources of all other translations are self-explanatory. In those cases where two or more translations of the same article were available reference has been made to the one most accessible through libraries or to the one which can be purchased at the lowest price.

The transliteration of Russian names in the cited references, as well as in the text, has followed the system used by *Applied Mechanics*

Reviews and Science Abstracts, but with no distinction between e, ö, and ə or between и and Ѻ, and with y used for ѿ.

The abbreviations used for journals and reports are, as far as possible, those used by *Mathematical Reviews*. A list of these abbreviations may be found in any recent index number of this journal.

Introduction

1. Ackeret, J.
Air forces on airfoils moving faster than sound, *Flugtech. und Motorluftshifffart* **16**, 72–74 (1925). Transl. as *NACA Tech. Mem.* no. 317 (1925). Original reprinted in *Foundations of High Speed Aerodynamics* (G. F. Carrier, ed.) pp. 103–112. Dover, New York, 1951.
2. Ackeret, J.
Gasdynamik, *Handbuch der Physik*, Vol. VII, Ch. 5, pp. 289–342. Springer Verlag, Berlin, 1927. Transl. as *R. T. P. Transl.* no. 2119, Gt. Brit. Ministry of Aircraft Production.
3. Ackeret, J.
Über Luftkräfte bei grossen Geschwindigkeiten, insbesondere bei ebenen Strömungen, *Helv. Phys. Acta* **1**, 301–322 (1928).
4. von Kármán, T., and Moore, N. B.
Resistance of slender bodies moving with supersonic velocities with special reference to projectiles, *Trans. A.S.M.E.* **54**, 303–310 (1932). Reprinted in *Foundations of High Speed Aerodynamics* (G. F. Carrier, ed.) pp. 142–149. Dover, New York, 1951.
5. von Kármán, T.
The problem of resistance in compressible fluids, *Reale Accad. d'Italia, Fondazione Alessandro Volta, Proc. 5th Volta Cong.*, Rome, 222–277 (1935).
6. Busemann, A.
Aerodynamischer Auftrieb bei Überschallgeschwindigkeit, *Reale Accad. d'Italia, Fondazione Alessandro Volta, Proc. 5th Volta Cong.*, Rome, 328–360 (1935). Also *Luftfahrtforschung* **12**, 210–220 (1935). Reprinted in *Foundations of High Speed Aerodynamics* (G. F. Carrier, ed.), pp. 131–141. Dover, New York, 1951.
7. Epstein, P. S.
On the air resistance of projectiles, *Proc. Nat. Acad. Sci. U.S.A.* **17**, 532–547 (1931).
8. Rankine, W. J. M.
On the thermodynamic theory of waves of finite longitudinal disturbance, *Phil. Trans. Roy. Soc. London* **160**, 277–286 (1870). Reprinted in *Foundations of High Speed Aerodynamics* (G. F. Carrier, ed.), pp. 1–10. Dover, New York, 1951.

9. Hugoniot, H.
Sur la propagation du mouvement dans les corps et spécialement dans les gaz parfaits, *J. de l'École Polytech.* **58**, 1–125 (1889).
10. Prandtl, L.
Neue Untersuchungen über die strömende Bewegung der Gase und Dämpfe, *Phys. Z.* **8**, 23–32 (1907).
11. Meyer, T.
Über zweidimensionale Bewegungsvorgänge in einem Gas, das mit Überschallgeschwindigkeit strömt, *Doctorate dissertation*, Göttingen (1908). Also *Forschungsheft des Vereins deutscher Ingenieure, Berlin* **62**, 31–67 (1908). Reprinted in *Foundations of High Speed Aerodynamics* (G. F. Carrier, ed.), pp. 50–89. Dover, New York, 1951.
12. Taylor, G. I., and MacColl, J. W.
The air pressure on a cone moving at high speeds, *Proc. Roy. Soc. London, Ser. A* **139**, 278–311 (1933).
13. Prandtl, L., and Busemann, A.
Näherungsverfahren zur zeichnerischen Ermittlung von ebenen Strömungen mit Überschallgeschwindigkeit, *Stodola Festschrift*, Zürich and Leipzig, 499–509 (1929). Reprinted in *Foundations of High Speed Aerodynamics* (G. F. Carrier, ed.), pp. 120–130. Dover, New York, 1951.
14. Busemann, A.
Gasdynamik, *Handbuch der Experimentalphysik, Hydro-und-Aerodynamik*, Vol. IV, Part I, pp. 341–460. Akademische Verlagsgesellschaft, Leipzig, 1931. Transl. as *R. T. P. Transl.* nos. 2207–2212, Gt. Brit. Ministry of Aircraft Production.
15. Frankl', F. I.
Vortex motion and plane-parallel supersonic flow past bodies, *Collection, Reaktivnoe Dvizhenie (Jet Motion)*, Moscow, 1934.
16. Frankl', F. I.
Supersonic flow with axial symmetry, *Izv. Artil. Akad.* **1**, no. 6, Lenin-grad (1934).
17. Guderley, G.
Die Charakteristikenmethode für ebene und achsensymmetrische Überschallströmungen, *Jbuch. Deutschen Luftfahrtforschung*, I522–I535 (1940).
18. Busemann, A., and Walchner, O.
Profileigenschaften bei Überschallgeschwindigkeit, *Forschung auf dem Gebiet des Ingenieurwesens* **4A**, 87–92 (1933).
19. Donov, A. E.
A flat wing with sharp edges in a supersonic stream, *Izv. Akad. Nauk SSSR, Ser. Matem.* **3**, 603–626 (1939). Transl. as *NACA Tech. Mem.* no. 1394 (1956).
20. Crocco, L.
Transmission of heat from a flat plate to a fluid flowing at high velocity.

- Aerotecnica* **12**, 181–197 (1932). Transl. as *NACA Tech. Mem.* no. 690 (1932).
21. Frankl', F. I.
Laminar boundary layer in a compressible fluid, *TsAGI Rep.* no. 176 (1934).
22. Busemann, A.
Gasströmung mit laminarer Grenzschicht entlang einer Platte, *Z. Angew. Math. Mech.* **15**, 23–25 (1935).
23. von Kármán, T., and Tsien, H. S.
Boundary layer in compressible fluids, *J. Aero. Sci.* **5**, 227–232 (1938).
24. Kibel', I. A.
Boundary layer in compressible liquid with allowance for radiation, *C. R. (Dokl.) Acad. Sci. URSS* **25**, 275–279 (1939).
25. Crocco, L.
Una caratteristica trasformazione delle equazioni dello strato limite nei gaz, *Atti di Guidonia* no. 7 (1939).
26. Frankl', F. I., and Voishel', V. V.
Turbulent friction in the boundary layer of a flat plate in a two-dimensional compressible flow at high speeds, *TsAGI Rep.* no. 321 (1937). Transl. as *NACA Tech. Mem.* no. 1053 (1943).
27. Ferri, A.
Experimental results with airfoils tested in the high-speed tunnel at Guidonia, *Atti di Guidonia* no. 17 (1939). Transl. as *NACA Tech. Mem.* no. 946 (1940).
28. Ackeret, J.
Windkanäle für hohe Geschwindigkeiten, *Reale Accad. d'Italia, Fondazione Alessandro Volta, Proc. 5th Volta Cong., Rome*, 487–537 (1935).
29. Zemskii, O. M.
Supersonic wind tunnels, *VVA Rep.* no. 60, Moscow (1940).
30. Schlichting, H.
Airfoil theory at supersonic speed, *Luftfahrtforschung* **13**, 320–335 (1936).
Also *Jbuch. Deutschen Luftfahrtforschung*, II181–II197 (1937). Transl. as *NACA Tech. Mem.* no. 897 (1939).
31. Busemann, A.
Infinitesimal conical supersonic flow, *Jbuch. Deutschen Akad. Luftfahrtforschung, 1942/1943*, 455–470, Berlin, 1943. Transl. as *NACA Tech. Mem.* no. 1100 (1947). Original reprinted in *Foundations of High Speed Aerodynamics* (G. F. Carrier, ed.), pp. 103–112. Dover, New York, 1951.
32. Gurevich, M. I.
Lift force of an arrow-shaped wing, *Prikl. Mat. Mekh.* **10**, 513–520 (1946). Transl. as *NACA Tech. Mem.* no. 1245 (1949).
33. Karpovich, E. A., and Frankl', F. I.
The drag of a delta wing in supersonic flow, *Prikl. Mat. Mekh.* **11**, 495–496 (1947). *Sci. Transl. Cent.* no. RT-416.

34. Krasil'shchikova, E. A.
Disturbed motion of air caused by vibrations of a wing moving at supersonic speed, *Prikl. Mat. Mekh.* **11**, 147–164 (1947). *Sci. Transl. Cent.* no. RT-2946.
35. Galin, L. A.
Remarks on the wing of finite aspect ratio in supersonic flow, *Prikl. Mat. Mekh.* **11**, 383–386 (1947). *Sci. Transl. Cent.* no. RT-2947.
36. Puckett, A. E.
Supersonic wave drag of thin airfoils, *J. Aero. Sci.* **13**, 475–484 (1946).
37. von Kármán, T.
Supersonic aerodynamics—principles and applications, *J. Aero. Sci.* **14**, 373–402 (1947).
38. Fal'kovich, S. V.
On the theory of a wing of finite aspect ratio in supersonic flow, *Prikl. Mat. Mekh.* **11**, 391–394 (1947). *Sci. Transl. Cent.* no. RT-418.
39. Krasil'shchikova, E. A.
Effect of tips of wings moving at supersonic speed, *Dokl. Akad. Nauk SSSR* **58**, 543–546 (1947). *Sci. Transl. Cent.* no. RT-925. Tip effect on an oscillating wing at supersonic speeds, *Dokl. Akad. Nauk SSSR* **58**, 761–762 (1947).
40. Ward, G. N.
Supersonic flow past thin wings. I. General theory, *Quart. J. Mech. Appl. Math.* **2**, 136–152 (1949). II. Flow reversal theorem, *Quart. J. Mech. Appl. Math.* **2**, 374–384 (1949).
41. Stewart, H. J.
The lift of a delta wing at supersonic speeds, *Quart. Appl. Math.* **4**, 246–254 (1946).
42. Brown, C. E.
Theoretical lift and drag of thin triangular wings at supersonic speeds, *NACA Rep.* no. 839 (1946).
43. Jones, R. T.
Properties of low-aspect-ratio pointed wings at speeds below and above the speed of sound, *NACA Rep.* no. 835 (1946).
44. Ferrari, C.
Interference between wing and body at supersonic speeds—theory and numerical application, *J. Aero. Sci.* **15**, 317–336 (1948).
45. Hantzsch, W., and Wendt, H.
Zum Kompressibilitätseinfluss bei der laminaren Grenzschicht der ebenen Platte, *Ibuch. Deutschen Luftfahrtforschung*, I517–I521 (1940).
46. Emmons, H. W., and Brainerd, J. G.
Temperature effects in a laminar compressible-fluid boundary layer along a flat plate, *J. Appl. Mech.* **8**, A105–A110 (1941). Reprinted in *Foundations of High Speed Aerodynamics* (G. F. Carrier, ed.), pp. 173–178. Dover, New York, 1951.

47. Dorodnitsyn, A. A.
The boundary layer in a compressible gas, *Prikl. Mat. Mekh.* **6**, 449–486 (1942). *Pergamon Transl.* no. 445.
48. Dorodnitsyn, A. A., and Loitsyanskii, L. G.
On the theory of the transition from the laminar to the turbulent boundary layer, *Prikl. Mat. Mekh.* **9**, 269–285 (1945). *Pergamon Transl.* no. 443.
49. Howarth, L.
Concerning the effect of compressibility on laminar boundary layers and their separation, *Proc. Roy. Soc. London, Ser. A* **194**, 16–42 (1948).
50. Crocco, L.
The laminar-boundary layer in gases, *Monografie Scientifica di Aeronautica* No. 3, Rome, 1946. Transl. as *Rep. no. AL-684*, Aerophys. Lab., North American Aviation Inc., Los Angeles, Calif., 1948.
51. Kalikhman, L. E.
Heat transmission in the boundary layer, *Prikl. Mat. Mekh.* **10**, 449–474 (1946). Transl. as *NACA Tech. Mem.* no. 1229 (1949).
52. Newton, I.
Mathematical principles of natural philosophy (Philosophiae naturalis principia mathematica), transl. by A. Motte (1729), revised by A. Cajori, Book II, Sect. VII. Univ. of California Press, Berkeley, 1934. Reprinted 1946.
53. Busemann, A.
Flüssigkeits-und-Gasbewegung, *Handwörterbuch der Naturwissenschaften*, Vol. IV, 2nd edition, pp. 244–279. Gustav Fischer, Jena, 1933.
54. Tsien, H. S.
Similarity laws of hypersonic flows, *J. Math. Phys.* **25**, 247–251 (1946).
55. Fal'kovich, S. V.
Two-dimensional motion of a gas at large supersonic velocities, *Prikl. Mat. Mekh.* **11**, 459–464 (1947). *Sci. Transl. Cent.* no. RT-403.
56. Hayes, W. D.
On hypersonic similitude, *Quart. Appl. Math.* **5**, 105–106 (1947).
57. Bam-Zelikovich, G. M., Bunimovich, A. I., and Mikhailova, M. P.
The motion of slender bodies at hypersonic speeds, *Collection of Papers* no. 4, *Teoretich. Gidromekhanika (Theoretical Hydromechanics)*. Oborongiz, Moscow, 1949. See also, *Izv. Akad. Nauk SSSR, Otd. Tekhn. Nauk, Mekh. i Mashinostr.*, 1960, no. 1, 33–40.
58. Eggers, A. J., Jr.
Performance of long-range hypervelocity vehicles, *Jet Propulsion* **27**, 1147–1151 (1957).
59. Sänger, E., and Bredt, I.
A rocket drive for long range bombers; *Zentrale für Wissenschaftliches Berichtswesen über Luftfahrtforschung, Untersuchungen und Mitteilungen*

- no. 3538, Ainring, 1944. Transl. as *Rept. no. CGD32*, Bureau of Aeronautics, Navy Dept., Washington, 1946. See also,
 Sänger, E.
 Die Wege der Rückstoss-Flugtechnik, *Interavia* **3**, 617-622 (1948).
60. Kantrowitz, A.
 A survey of physical phenomena occurring in flight at extreme speeds, in *Proceedings of the Conference on High-Speed Aeronautics* (A. Ferri, N. J. Hoff, and P. A. Libby, eds.), pp. 335-339. Polytechnic Inst. of Brooklyn, Brooklyn, N. Y., 1955.
61. Logan, J. G.
 The calculation of the thermodynamic properties of air at high temperatures, *AFOSR Tech. Note* no. 56-344, Cornell Aero. Lab., Buffalo, N. Y., 1956.
62. Zel'dovich, Ya. B.
 Theory of Shock Waves and Introduction to Gasdynamics. Izdat. Akad. Nauk SSSR, Moscow and Leningrad, 1946.
63. Gunn, J. C.
 Relaxation time effects in gas dynamics, *Repts. and Mem.* no. 2338, Gt. Brit. Aero. Res. Counc., 1956.
64. Bethe, H. A., and Teller, E.
 Deviations from thermal equilibrium in shock waves, *Rep. no. X-117*, Ballistic Res. Lab., Aberdeen Proving Ground, Md., 1945.
65. Feldman, S.
 Some shock tube experiments on the chemical kinetics of air at high temperatures, *J. Fluid Mech.* **3**, 225-242 (1957).
66. Kulikovskii, A. G.
 On the flow of a conducting fluid around a magnetized body, *Dokl. Akad. Nauk SSSR* **117**, 199-202 (1957). M. D. Friedman Transl. no. K-172.
67. Kurzweg, H. H., and Wilson, R. E.
 Experimental hyperballistics, *Aero. Eng. Rev.* **15**, no. 12, 32-36 (1956).
68. Logan, J. G.
 Nitric oxide formation in hypersonic flow, *J. Aero. Sci.* **23**, 1123-1125 (1956).

Chapter I

1. Kochin, N. E., Kibel', I. A., and Roze, N. V.
 Theoretical Hydromechanics, Part 2, Gostekhizdat, Moscow and Leningrad, 3rd edition, 1948. Transl. in German as *Theoretische Hydromechanik*, Akademie Verlag, Berlin, 1954.
2. Zel'dovich, Ya. B.
 Theory of Shock Waves and Introduction to Gasdynamics. Izdat. Akad. Nauk SSSR, Moscow and Leningrad, 1946.

3. Courant, R., and Friedrichs, K. O.
Supersonic Flow and Shock Waves. Interscience, New York, 1957.
4. Friedrichs, K. O.
 Mathematical aspects of flow problems of hyperbolic type, in *General Theory of High Speed Aerodynamics* (W. R. Sears, ed.), Sect. B, pp. 31–60 (Vol. VI of *High Speed Aerodynamics and Jet Propulsion*). Princeton Univ. Press, Princeton, 1954.
5. von Neumann, J. (chairman)
 Discussion on the existence and uniqueness or multiplicity of solutions of the aerodynamical equations, in *Problems of Cosmical Aerodynamics*, Chapt. 10, pp. 75–84 (*Proc. of Symp. held by Int. Union Theor. and Appl. Mech. and Int. Astronomical Union*, Paris, 1949). Central Air Documents Office, Dayton, Ohio, 1951.
6. von Neumann, J., and Richtmyer, R. D.
 A method for the numerical calculation of hydrodynamic shocks, *J. Appl. Phys.* **21**, 232–237 (1950).
7. Lax, P. D.
 Weak solutions of nonlinear hyperbolic equations and their numerical computation, *Comm. Pure Appl. Math.* **7**, 159–193 (1954).
8. Godunov, S. K.
 Finite difference method for calculating shock waves, *Uspekhi. Mat. Nauk* **12**, no. 1 (73), 176–177 (1957).
9. Sobolev, S. L.
 General theory of the diffraction of waves on Riemann surfaces, *Trudy Matemat. Inst. Akad. Nauk SSSR* **9**, 39–105 (1935).
10. Hopf, E.
 The partial differential equation $u_t + uu_x = \mu u_{xx}$, *Comm. Pure Appl. Math.* **3**, 201–230 (1950).
11. Tikhonov, A. N., and Samarskii, A. A.
 On discontinuous solutions of a quasi-linear equation of first order, *Dokl. Akad. Nauk SSSR* **99**, 27–30 (1954).
12. Oleinik, O. A.
 Discontinuous solutions of nonlinear differential equations, *Uspekhi. Mat. Nauk* **12**, no. 3 (75), 3–73 (1957).
13. Linnell, R. D.
 Two-dimensional airfoils in hypersonic flows, *J. Aero. Sci.* **16**, 22–30 (1949).
14. Oswatitsch, K.
 Ähnlichkeitsgesetze für Hyperschallströmung, *Z. Angew. Math. Phys.* **2**, 249–264 (1951).
15. Charters, A. C., and Thomas, R. N.
 The aerodynamic performance of small spheres from subsonic to high supersonic velocities, *J. Aero. Sci.* **12**, 468–476 (1945).

16. Hodges, A. J.
The drag coefficient of very high velocity spheres, *J. Aero. Sci.* **24**, 755–758 (1957).
17. Stevens, V. I.
Hypersonic research facilities at the Ames aeronautical laboratory, *J. Appl. Phys.* **21**, 1150–1155 (1950).

Chapter II

1. Frankl', F. I., and Karpovich, E. A.
Gas Dynamics of Thin Bodies. Gostekhizdat, Moscow and Leningrad, 1948.
English translation (by M. D. Friedman), Interscience, New York, 1953.
2. Krasil'shchikova, E. A.
Finite Span Wings in Compressible Flow. Gostekhizdat, Moscow and Leningrad, 1952. Transl. as *NACA Tech. Mem.* no. 1383 (1956).
3. Heaslet, M. A., and Lomax, H.
Supersonic and transonic small perturbation theory, in *General Theory of High Speed Aerodynamics* (W. R. Sears, ed.), Sect. D, pp. 122–344 (Vol. VI of *High Speed Aerodynamics and Jet Propulsion*). Princeton Univ. Press, Princeton, 1954.
4. Tsien, H. S.
Similarity laws of hypersonic flows, *J. Math. Phys.* **25**, 247–251 (1946).
5. Fal'kovich, S. V.
Two-dimensional motion of a gas at large supersonic velocities, *Prikl. Mat. Mekh.* **11**, 459–464 (1947). *Sci. Transl. Cent.* no. RT-403.
6. Hayes, W. D.
On hypersonic similitude, *Quart. Appl. Math.* **5**, 105–106 (1947).
7. Bam-Zelikovich, G. M., Bunimovich, A. I., and Mikhailova, M. P.
The motion of slender bodies at hypersonic speeds, *Collection of Papers no. 4, Teoretich. Gidromekhanika (Theoretical Hydromechanics)*. Oborongiz, Moscow, 1949. See also, *Izv. Akad. Nauk SSSR, Otd. Tekhn. Nauk, Mekh. i Mashinostr.*, 1960, no. 1, 33–40.
8. Goldsworthy, F. A.
Two-dimensional rotational flow at high Mach number past thin aerofoils, *Quart. J. Mech. Appl. Math.* **5**, 54–63 (1952).
9. Van Dyke, M. D.
A study of hypersonic small-disturbance theory, *NACA Rep.* no. 1194 (1954).
10. Telenin, G. F.
Similarity Laws for Hypersonic Speeds. Oborongiz, Moscow, 1956.
11. Il'yushin, A. A.
The law of plane sections in hypersonic aerodynamics, *Prikl. Mat. Mekh.* **20**, 733–755 (1956). *Pergamon Transl.* (number and title omitted from list).

12. Neice, S. E., and Ehret, D. M.
Similarity laws for slender bodies of revolution in hypersonic flows, *J. Aero. Sci.* **18**, 527–530, 568 (1951).
13. Kopal, Z.
Tables of supersonic flow around cones, *Tech. Rep.* no. 1, Dept. of Elect. Eng., Mass. Inst. Tech., Cambridge, Mass., 1947.
14. Van Dyke, M. D.
The combined supersonic-hypersonic similarity rule, *J. Aero. Sci.* **18**, 499–500 (1951).
15. Shapiro, A. H.
The Dynamics and Thermodynamics of Compressible Fluid Flow, Vol. 2. Ronald Press, New York, 1953.
16. Sedov, L. I.
Similarity and Dimensional Methods in Mechanics. Gostekhizdat, Moscow, 4th edition, 1957. English translation (M. Holt, ed.), Academic Press, New York and London, 1959.
17. Sedov, L. I.
On some unsteady motions of a compressible fluid, *Prikl. Mat. Mekh.* **9**, 293–311 (1945). *Pergamon Transl.* no. 1221.
18. Taylor, G. I.
The air wave surrounding an expanding sphere, *Proc. Roy. Soc. London, Ser. A* **168**, 273–292 (1946).
19. Krasheninnikova, N. L.
On the unsteady motion of a gas displaced by a piston, *Izv. Akad. Nauk SSSR, Otd. Tekh. Nauk*, 1955, no. 8, 22–36.
20. Velesko, L. G., Grodzovskii, G. L., and Krasheninnikova, N. L.
Tables of flow parameters for power law bodies of revolution at hypersonic speeds, *TsAGI Rep.* (1956).
21. Lees, L., and Kubota, T.
Inviscid hypersonic flow over blunt-nosed slender bodies, *J. Aero. Sci.* **24**, 195–202 (1957).
22. Grigoryan, S. S.
Cauchy's problem and the problem of a piston for one-dimensional non-steady motions of gas (automodel motion), *Prikl. Mat. Mekh.* **22**, 179–187 (1958). Transl. in *J. Appl. Math. Mech.* **22**, 244–255 (1958).
23. Lees, L.
Recent developments in hypersonic flow, *Jet Propulsion* **27**, 1162–1178 (1957).
24. Stanyukovich, K. P.
Unsteady Motion of Continuous Media. Gostekhizdat, Moscow, 1955. English translation (M. Holt, ed.), Pergamon Press, New York and London, 1960.
25. Barenblatt, G. I.
On limiting self similar motions in the theory of unsteady filtration of a gas in a porous medium and the theory of the boundary layer, *Prikl. Mat. Mekh.* **18**, 409–414 (1954). *Pergamon Transl.* no. 99.

26. Gusev, V. N.

On unsteady self-similar motion of a gas displaced by a piston according to an exponential law, *TsAGI Rep., BNI* (1957).

Chapter III

1. Rusanov, V. V.
The method of characteristics for three-dimensional problems, *Collection of Papers no. 11, Teoretich. Gidromekhanika (Theoretical Hydromechanics)*. Oborongiz, Moscow, 3rd edition, 1953.
2. Belotserkovskii, O. M.
Flow past a circular cylinder with a detached shock, *Dokl. Akad. Nauk SSSR* **113**, 509–512 (1957). *M. D. Friedman Transl.* no. B-131.
3. Van Dyke, M. D.
The supersonic blunt-body problem—review and extension, *J. Aero/Space Sci.* **25**, 485–496 (1958).
4. Newton, I.
Mathematical principles of natural philosophy (Philosophiae naturalis principia mathematica), transl. by A. Motte (1729), revised by A. Cajori, Book II, Sect. VII. Univ. of California Press, Berkeley, 1934. Reprinted 1946.
5. von Kármán, T.
Isaac Newton and aerodynamics, *J. Aero. Sci.* **9**, 521–522, 548 (1942).
6. Epstein, P. S.
On the air resistance of projectiles, *Proc. Nat. Acad. Sci. U.S.A.* **17**, 532–547 (1931).
7. Zahm, A. F.
Superaerodynamics, *J. Franklin Inst.* **217**, 153–166 (1934).
8. Kopal, Z.
Tables of supersonic flow around cones, *Tech. Rep.* no. 1, Dept. of Elect. Eng., Mass. Inst. Tech., Cambridge, Mass., 1947.
9. McLellan, C. H.
Exploratory wind-tunnel investigation of wings and bodies at $M = 6.9$, *J. Aero. Sci.* **18**, 641–648 (1951).
10. Oliver, R. E.
An experimental investigation of flow about simple blunt bodies at a nominal Mach number of 5.8, *J. Aero. Sci.* **23**, 177–179 (1956).
11. Kim, C. S.
Experimental studies of supersonic flow past a circular cylinder, *J. Phys. Soc. Japan* **11**, 439–445 (1956).
12. Sänger, E.
Gleitkörper für sehr hohe Fluggeschwindigkeiten, *German Patent 411/42*, Berlin, 1939. See also Die Wege der Rückstoss-Flugtechnik, *Interavia* **3**, 557–565 (1948).

13. Ferri, A.
Elements of Aerodynamics of Supersonic Flows, pp. 133–135. Macmillan, New York, 1949.
14. von Kármán, T.
 The problem of resistance in compressible fluids, *Reale Accad. d'Italia, Fondazione Alessandro Volta, Proc. 5th Volta Cong.*, Rome, 222–277 (1935).
15. Heaslet, M. A., and Lomax, H.
 Supersonic and transonic small perturbation theory, in *General Theory of High Speed Aerodynamics* (W. R. Sears, ed.), Sect. D, pp. 122–344 (Vol. VI of *High Speed Aerodynamics and Jet Propulsion*). Princeton Univ. Press, Princeton, 1954.
16. Nikol'skii, A. A.
 On annular bodies of revolution with minimum external wave drag in supersonic flow, (originally *TsAGI Rep.*, 1950) in *Sbornik Teoreticheskikh Rabot Po Aerodinamike, TsAGI (Collection of Theoretical Works in Aerodynamics, TsAGI)*, pp. 56–63. Oborongiz, Moscow, 1957.
17. Kogan, M. N.
 On bodies of minimum drag in supersonic flow, *Prikl. Mat. Mekh.* **21**, 207–212 (1957). *Pergamon Transl.* no. 595a.
18. Carter, W. J.
 Optimum nose shapes for missiles in the superaerodynamic region, *J. Aero. Sci.* **24**, 527–532 (1957).
19. Grodzovskii, G. L.
 Certain peculiarities of the flow around bodies at high supersonic velocities, *Izv. Akad. Nauk SSSR, Otd. Tekhn. Nauk*, 1957, no. 6, 86–92. *M. D. Friedman Transl.* no. G-140.
20. Lees, L.
 Note on the hypersonic similarity law for an unyawed cone, *J. Aero. Sci.* **18**, 700–702 (1951).
21. Ferri, A.
Elements of Aerodynamics of Supersonic Flows, pp. 236 and ff. Macmillan, New York, 1949.
22. Kochin, N. E., Kibel', I. A., and Roze, N. V.
Theoretical Hydromechanics, Part 2. Gostekhizdat, Moscow and Leningrad, 3rd edition, 1948. Transl. in German as *Theoretische Hydromechanik*, Akademie Verlag, Berlin, 1954.
23. Probstein, R. F., and Bray, K. N. C.
 Hypersonic similarity and the tangent-cone approximation for unyawed bodies of revolution, *J. Aero. Sci.* **22**, 66–68 (1955).
24. Busemann, A.
 Flüssigkeits-und-Gasbewegung, *Handwörterbuch der Naturwissenschaften*, Vol. IV, 2nd edition, pp. 244–279. Gustav Fischer, Jena, 1933.
25. Grimminger, G., Williams, E. P., and Young, G. B. W.

- Lift on inclined bodies of revolution in hypersonic flow, *J. Aero. Sci.* **17**, 675–690 (1950).
26. Hayes, W. D.
 Newtonian flow theory in hypersonic aerodynamics, in *Advances in Aeronautical Sciences*, Vol. I, pp. 113–119. Pergamon Press, New York and London, 1959. See also,
 Hayes, W. D., and Probstein, R. F.
Hypersonic Flow Theory, pp. 70–138. Academic Press, New York, 1959.
27. Maikapar, G. I.
 Calculation (Effect) of the centrifugal forces on surface pressure for a body of arbitrary shape, *Prikl. Mat. Mekh.* **23**, 64–69 (1959). Transl. in *J. Appl. Math. Mech.* **23**, 83–91 (1959).
28. Lighthill, M. J.
 Dynamics of a dissociating gas. Part I. Equilibrium flow, *J. Fluid Mech.* **2**, 1–32 (1957).
29. Eggers, A. J., Jr., Syvertson, C. A., and Kraus, S.
 A study of inviscid flow about airfoils at high supersonic speeds, *NACA Rep.* no. 1123 (1953).
30. Eggers, A. J., Jr., Resnikoff, M. M., and Dennis, D. H.
 Bodies of revolution having minimum drag at high supersonic airspeeds, *NACA Rep.* no. 1306 (1957).
31. Gonor, A. L., and Chernyi, G. G.
 On minimum drag bodies at hypersonic speeds, *Izv. Akad. Nauk SSSR, Otd. Tekh. Nauk*, 1957, no. 7, 89–93. *M. D. Friedman Transl.* no. G-141.
32. Chernyi, G. G.
 Gas flow around a body at hypersonic speeds, *Dokl. Akad. Nauk SSSR* **107**, 221–224 (1956). *M. D. Friedman Transl.* no. C-106.
33. Chernyi, G. G.
 Adiabatic motion of a perfect gas with very strong shock waves, in *Trudy III Vsesoyuznovo Matem. S'ezda (Proc. of Third All-Union Mathematical Congress)*, Vol. 1. Izdat. Akad. Nauk SSSR, Moscow, 1956. See also [36] ff.
34. Chernyi, G. G.
 One-dimensional unsteady motion of a perfect gas with a strong shock wave, *Dokl. Akad. Nauk SSSR* **107**, 657–660 (1956). *M. D. Friedman Transl.* no. C-107.
35. Chernyi, G. G.
 The problem of a point explosion, *Dokl. Akad. Nauk SSSR* **112**, 213–216 (1957). Transl. as *Rep.* no. MOA TIL/T.4871, Ministry of Aviation (Gt. Brit.), 1959.
36. Chernyi, G. G.
 Adiabatic motion of a perfect gas with very strong shock waves; *Izv. Akad. Nauk SSSR, Otd. Tekhn. Nauk*, 1957, no. 3, 66–81.
37. Andriankin, E. I.
 Strong explosion in a medium with a density gradient, *Izv. Akad. Nauk SSSR, Otd. Tekhn. Nauk*, 1958, no. 2, 123–125.

38. Chernyi, G. G.
Hypersonic flow around a body by an ideal gas, *Izv. Akad. Nauk SSSR, Otd. Tekhn. Nauk*, 1957, no. 6, 77–85. *M. D. Friedman Transl.* no. C-111.
39. Cole, J. D.
Newtonian flow theory for slender bodies, *J. Aero. Sci.* **24**, 448–455 (1957).
40. Gonor, A. L.
Hypersonic flow around a cone at an angle of attack, *Izv. Akad. Nauk SSSR, Otd. Tekhn. Nauk*, 1958, no. 7, 102–105. *M. D. Friedman Transl.* no. G-154.
41. Gonor, A. L.
Hypersonic flow around conical bodies, *Izv. Akad. Nauk SSSR, Otd. Tekhn. Nauk, Mekh. i Mashinostr.*, 1959, no. 1, 34–40. *M. D. Friedman Transl.* no. G-163.
42. Chester, W.
Supersonic flow past a bluff body with a detached shock. I. Two-dimensional body, *J. Fluid Mech.* **1**, 353–365 (1956). II. Axisymmetrical body, *J. Fluid Mech.* **1**, 490–496 (1956).
43. Freeman, N. C.
On the theory of hypersonic flow past plane and axially symmetric bluff bodies, *J. Fluid Mech.* **1**, 366–386 (1956).
44. von Mises, R.
Bemerkungen zur Hydrodynamik, *Z. Angew. Math. Mech.* **7**, 425–431 (1927).
45. Taylor, G. I.
The air wave surrounding an expanding sphere, *Proc. Roy. Soc. London, Ser. A* **186**, 273–292 (1946).
46. Velesko, L. G., Grodzovskii, G. L., and Krasheninnikova, N. L.
Tables of flow parameters for power law bodies of revolution at hypersonic speeds, *TsAGI Rep.*, (1956).

Chapter IV

1. Kochin, N. E., Kibel', I. A., and Roze, N. V.
Theoretical Hydromechanics, Part 2. Gostekhizdat, Moscow and Leningrad, 3rd edition, 1948. Transl. in German as *Theoretische Hydromechanik*, Akademie Verlag, Berlin, 1954.
2. Lighthill, M. J.
Higher approximations, in *General Theory of High Speed Aerodynamics* (W. R. Sears, ed.), Sect. E, pp. 345–489 (Vol. VI of *High Speed Aerodynamics and Jet Propulsion*). Princeton Univ. Press, Princeton, 1954.
3. Epstein, P. S.
On the air resistance of projectiles, *Proc. Nat. Acad. Sci. U.S.A.* **17**, 532–547 (1931).
4. Eggers, A. J., Jr., Syvertson, C. A., and Kraus, S.
A study of inviscid flow about airfoils at high supersonic speeds, *NACA Rep.* no. 1123 (1953).

5. Linnell, R. D.
Two-dimensional airfoils in hypersonic flows, *J. Aero. Sci.* **16**, 22–30 (1949).
6. Lighthill, M. J.
The flow behind a stationary shock, *Phil. Mag.* **40**, 214–220 (1939).
7. Eggers, A. J., Jr., and Syvertson, C. A.
Inviscid flow about airfoils at high supersonic speeds, *NACA Tech. Note no. 2646* (1952). Superseded by Eggers, Syvertson, and Kraus [4], above.
8. Chu, B. T.
On weak interaction of strong shock and Mach waves generated downstream of the shock, *J. Aero. Sci.* **19**, 433–446 (1952).
9. Ferri, A.
Elements of Aerodynamics of Supersonic Flows. Macmillan, New York, 1949.
10. Il'yushin, A. A.
The law of plane sections in hypersonic aerodynamics, *Prikl. Mat. Mekh.* **20**, 733–755 (1956). *Pergamon Transl.* (number and title omitted from list).
11. Guiraud, J. P.
Écoulements hypersoniques infiniment voisins de l'écoulement sur un dièdre, *C. R. Acad. Sci. Paris* **244**, 2281–2284 (1957).
12. Dorodnitsyn, A. A.
Relation between shock wave curvature and surface curvature for an annular body of revolution, (originally *TsAGI Rep.*, 1949) in *Sbornik Teoreticheskikh Rabot Po Aerodinamike, TsAGI (Collection of Theoretical Works in Aerodynamics, TsAGI)*, pp. 64–73. Oborongiz, Moscow, 1957.
13. Mahony, J. J.
A critique of shock-expansion theory, *J. Aero. Sci.* **22**, 673–680, 720 (1955).
14. Thomas, T. Y.
The determination of pressure on curved bodies behind shocks, *Comm. Pure Appl. Math.* **3**, 103–132 (1950).
15. Meyer, R. E.
On supersonic flow behind a curved shock, *Quart. Appl. Math.* **14**, 433–436 (1957).
16. Eggers, A. J., Jr., Savin, R. C., and Syvertson, C. A.
The generalized shock-expansion method and its application to bodies travelling at high supersonic air speeds, *J. Aero. Sci.* **22**, 231–238, 248 (1955).
17. Zienkiewicz, H. K.
A method for calculating pressure distributions on circular arc ogives at zero incidence at supersonic speeds, using the Prandtl-Meyer flow relations, *Curr. Pap.* no. 114, Ministry of Supply, Gt. Brit. Aero. Res. Coun., 1953.

Chapter V

1. Bardsley, O., and Mair, W. A.
Separation of the boundary layer at a slightly blunt edge in supersonic flow, *Phil. Mag.* **43**, 344–352 (1952).

2. Hammitt, A. G., and Bogdonoff, S. M.
Hypersonic studies of the leading edge effect on the flow over a flat plate,
Jet Propulsion **26**, 241–246, 250 (1956).
3. Lighthill, M. J.
Higher approximations, in *General Theory of High Speed Aerodynamics*
(W. R. Sears, ed.), Sect. E, pp. 345–489 (Vol. VI of *High Speed Aerodynamics
and Jet Propulsion*). Princeton Univ. Press, Princeton, 1954.
4. Holder, D. W., and Chinneck, A.
The flow past elliptic-nosed cylinders and bodies of revolution in supersonic
air streams, *Aero. Quart.* **4**, 317–340 (1954).
5. Chernyi, G. G.
Hypersonic flow past an airfoil with a slightly blunted leading edge, *Dokl.
Akad. Nauk SSSR* **114**, 721–724 (1957). *M. D. Friedman Transl.* no. C-112.
6. Lees, L., and Kubota, T.
Inviscid hypersonic flow over blunt-nosed slender bodies, *J. Aero. Sci.* **24**,
195–202 (1957).
7. Chernyi, G. G.
Hypersonic flow around a slender blunt cone, *Dokl. Akad. Nauk SSSR* **115**,
681–683 (1957). *M. D. Friedman Transl.* no. C-113.
8. Chernyi, G. G.
Effect of slight blunting of leading edge of an immersed body on the flow
around it at hypersonic speeds, *Izv. Akad. Nauk SSSR, Otd. Tekhn. Nauk*,
1958, no. 4, 54–66. *Transl. as NASA Tech. Transl.* no. F-35, 1960.
9. Sedov, L. I.
Le mouvement d'air en cas d'une forte explosion, *C. R. (Dokl.) Acad. Sci.
URSS* **52**, 17–20 (1946).
10. Sedov, L. I.
Propagating of strong waves of discontinuity, *Prikl. Mat. Mekh.* **10**,
241–250 (1946). *Pergamon Transl.* no. 1223.
11. Sedov, L. I.
Similarity and Dimensional Methods in Mechanics. Gostekhizdat, Moscow.
Fourth edition 1957. English translation (M. Holt, ed.), Academic Press,
New York and London, 1959.
12. Taylor, G. I.
The formation of a blast wave by a very intense explosion, *Proc. Roy. Soc.
London, Ser. A* **201**, 159–186 (1950).
13. Sakurai, A.
On the propagation and structure of the blast wave, I, *J. Phys. Soc. Japan*
8, 662–669 (1953).
14. Lin, S. C.
Cylindrical shock waves produced by instantaneous energy release, *J. Appl.
Phys.* **25**, 54–57 (1954).

15. Latter, R.
Similarity solution for a spherical shock wave, *J. Appl. Phys.* **26**, 954–960 (1955).
16. Goldstine, H. H., and von Neumann, J.
Blast wave calculation, *Comm. Pure Appl. Math.* **8**, 327–353 (1955).
17. Brode, H. L.
Numerical solutions of spherical blast waves, *J. Appl. Phys.* **26**, 766–775 (1955).
18. Okhotsimskii, D. E., Kondrasheva, I. L., Vlasova, Z. P., and Kazakova, R. K.
Calculation of a point explosion with counterpressure, *Trudy Matemat. Inst. Akad. Nauk SSSR* **50** (1957).
19. Chernyi, G. G.
The problem of a point explosion, *Dokl. Akad. Nauk SSSR* **112**, 213–216 (1957). Transl. as *Rep. no. MOA TIL/T.4871*, Ministry of Aviation (Gt. Brit.), 1959.
20. Sakurai, A.
On the propagation and structure of a blast wave, II, *J. Phys. Soc. Japan* **9**, 256–266 (1954).
21. Brushlinskii, D. N., and Solomakhova, T. S.
Analysis of the strong explosion problem with counterpressure, *Collection of Papers no. 19, Teoretich. Gidromekhanika (Theoretical Hydromechanics)*. Oborongiz, Moscow, 7th edition, 1956.
22. Bertram, M. H., and Baradell, D. L.
A note on the sonic-wedge leading-edge approximation in hypersonic flow, *J. Aero. Sci.* **24**, 627–629 (1957).
23. Cheng, H. K., and Pallone, A. J.
Inviscid leading-edge effect in hypersonic flow, *J. Aero. Sci.* **23**, 700–702 (1956).
24. Bertram, M. H.
Viscous and leading-edge thickness effects on the pressures on the surface of a flat plate in hypersonic flow, *J. Aero. Sci.* **21**, 430–431 (1954).
25. Cox, R. N.
Recent hyperballistics research at ARDE—The ARDE gun tunnels and some experimental studies of hypersonic flow, in *Hypersonic Flow* (A. R. Collar and J. Tinkler, eds.), pp. 111–141. Academic Press, New York, 1960.
26. Bertram, M. H.
Tip-bluntness effects on cone pressures at $M = 6.85$, *J. Aero. Sci.* **23**, 898–900 (1956).
27. Cheng, H. K.
Similitude of hypersonic real-gas flows over slender bodies with blunted noses, *J. Aero/Space Sci.* **26**, 575–585 (1959).
28. Hayes, W. D., and Probstein, R. F.
Hypersonic Flow Theory, pp. 61–65. Academic Press, New York, 1959.

29. Sychev, V. V.
On the theory of hypersonic gas flow with a power-law shock wave, *Prikl. Mat. Mekh.* **24**, 518–523 (1960). Transl. in *J. Appl. Math. Mech.* **24**, 756–764 (1960).
30. Guiraud, J. P.
Possibilité et limites actuelles de la théorie des écoulements hypersoniques, in *Advances in Aeronautical Sciences*, Vol. III, 41–58. Pergamon Press, London and New York, 1961.
31. Cheng, H. K., Hall, J. G., Golian, T. C., and Hertzberg, A.
Boundary-layer displacement and leading-edge bluntness effects in high-temperature hypersonic flow, *J. Aerospace Sci.* **28**, 353–381, 410 (1961).

Author Index

Numbers in brackets are reference numbers and are included to assist in locating references in which the authors' names are not mentioned in the text. Italicized numbers indicate the page on which the reference is listed, and when in parenthesis the number of times it appears on that page.

- Ackeret, J. 1[1,2,3], 2[28], *236*(3), *238*
Andriankin, E. I. 138[37], *247*
- Bam-Zelikovich, G. M. 4[57], 57[7], 80[7],
82[7], *240*, *243*
Baradell, D. L. 211[22], *251*
Bardsley, O. 201[1], *249*
Barenblatt, G. I. 92[25], *244*
Belotserkovskii, O. M. 95[2], 105[2], *245*
Bertram, M. H. 211[22,24], 230[26], *251*(3)
Bethe, H. A. 13[64], *241*
Bogdonoff, S. M. 201[2], 204[2], 211[2], *250*
Brainerd, J. G. 3[46], *239*
Bray, K. N. C. 118[23], *246*
Bredt, I. 8[59], *240*
Brode, H. L. 206[17], *251*
Brown, C. E. 3[42], *239*
Brushlinskii, D. N. 210[21], 216–217[21],
251
Bunimovich, A. I. 4[57], 57[7], 80[7], 82[7],
240, *243*
Busemann, A. 1[6], 2[13,14,18,22], 3[31,53],
121[24], 123[24], 165, *236*, *237*(3),
238(2), *240*, *246*
- Carter, W. J. 111[18], *246*
Charters, A. C. 49[15], *242*
Cheng, H. K. 206[31], 211[23], 231, *251*(2),
252
Chernyi, G. G. 48, 129[31], 138[32–36,38],
147[34,36], 152[36], 155[38], 204[5,7,8],
206[19], 210[19], *247*(6), *248*, *250*(3),
251
Chester, W. 138[42], *248*
Chinneck, A. 203[4], *250*
Chu, B. T. 171[8], 180[8], *249*
Cole, J. D. 138[39], 147[39], 155[39], *248*
Courant, R. 30[3], 32[3], *242*
Cox, R. N. 222[25], *251*
- Crocco, L. 2[20,25], 3[50], *237*, *238*, *240*
- Dennis, D. H. 112[30], 129[30], *247*
Donov, A. E. 2[19], *237*
Dorodnitsyn, A. A. 3[47,48], 186, 191[12],
240(2), *249*
- Eggers, A. J., Jr. 6[58], 112[30], 127[29],
129[30], 168[4], 171[4,7], 192[4], 195[4,
16], *240*, *247*(2), *248*, *249*(2)
- Ehret, D. M. 66[12], *244*
Emmons, H. W. 3[46], *239*
Epstein, P. S. 1[7], 3, 98[6], 166[3], *236*,
245, *248*
- Fal'kovich, S. V. 3[38], 4[55], 56[5], *239*,
240, *243*
Feldman, S. 13[65], 22[65], *241*
Ferrari, C. 3[44], *239*
Ferri, A. 2[27], 109[13], 114[21], 187[9],
238, *246*(2), *249*
Frankl', F. I. 2[15,16,21,26], 3[33], 56[1],
237(2), *238*(3), *243*
Freeman, N. C. 138[43], *248*
Friedrichs, K. O. 30[3], 32[3,4], *242*(2)
- Galin, L. A. 3[35], *239*
Godunov, S. K. 35, *242*
Goldstine, H. H. 206[16], *251*
Goldsworthy, F. A. 57[8], *243*
Golian, T. C. 206[31], *252*
Gonor, A. L. 129[31], 133, 138[40,41], *247*,
248(2)
Grigoryan, S. S. 83[22], 94, *244*
Grimminger, G. 122[25], 124[25], *246*
Grodzovskii, G. L. 83[20], 85[20], 94,
112[19], 154[46], *244*, *246*, *248*
Guderley, G. 2[17], *237*
Guiraud, J. P. 190[11], 206[30], *249*, *252*

- Gunn, J. C. 13[63], 241
 Gurevich, M. I. 3[32], 238
 Gusev, V. N. 92[26], 245
- Hall, J. G. 206[31], 252
 Hammitt, A. G. 201[2], 204[2], 211[2], 250
 Hantzsch, W. 3[45], 239
 Hayes, W. D. 4[56], 48, 56, 72[6], 113,
 122–123[26], 128, 129[26], 206[28],
 240, 243, 247(2), 251
 Heaslet, M. A. 56[3], 110[15], 243, 246
 Hertzberg, A. 206[31], 252
 Hodges, A. J. 49[16], 243
 Holder, D. W. 203[4], 250
 Hopf, E. 36[10], 242
 Howarth, L. 3[49], 240
 Hugoniot, H. 1[9], 237
- Il'yushin, A. A. 57[11], 190[10], 243, 249
- Jones, R. T. 3[43], 239
- Kalikhman, L. E. 3[51], 240
 Kantrowitz, A. 11[60], 15[60], 22[60], 241
 Kármán, T. von, *see* von Kármán
 Karpovich, E. A. 3[33], 56[1], 238, 243
 Kazakova, R. K. 206[18], 251
 Kibel', I. A. 2[24], 27[1], 31[1], 38[1], 46[1],
 114[22], 140, 161–164[1], 166[1], 238,
 241, 246, 248
 Kim, C. S. 105[11], 245
 Kochin, N. E. 27[1], 31[1], 38[1], 46[1],
 114[22], 140[22], 161–164[1], 166[1],
 241, 246, 248
 Kogan, M. N. 110[17], 246
 Kondrasheva, I. L. 206[18], 251
 Kopal, Z. 66[13], 82[13], 99[8], 116–118[8],
 136[8], 244, 245
 Krasheninnikova, N. L. 82[19], 83[19,20],
 85[20], 154[46], 244(2), 248
 Krasil'shchikova, E. A. 3[34,39], 56[2],
 239(2), 243
 Kraus, S. 127[29], 168[4], 171[4], 192[4],
 195[4], 247, 248
 Kubota, T. 83[21], 204[6], 216[6], 244, 250
 Kulikovskii, A. G. 16[66], 241
 Kurzweg, H. H. 22–23[67], 241
- Latter, R. 205[15], 251
 Lax, P. D. 35, 36[7], 242
 Lees, L. 83[21], 89[23], 99, 114[20], 204[6],
 216[6], 244(2), 246, 250
 Lighthill, M. J. 123[28], 138[28], 162[2],
 171[6], 180[6], 202[3], 247–250
 Lin, S. C. 205[14], 250
 Linnell, R. D. 45[13], 171[5], 242, 249
 Logan, J. G. 11[61], 22[68], 241(2)
 Loitsyanskii, L. G. 3[48], 240
 Lomax, H. 56[3], 110[15], 243, 246
- Maccoll, J. W. 2[12], 237
 Mahony, J. J. 192[13], 249
 Maikapar, G. I. 122[27], 247
 Mair, W. A. 201[1], 249
 McLellan, C. H. 99[9], 245
 Mel'nikov, N. S. 210
 Meyer, R. E. 195[15], 249
 Meyer, T. 1[11], 237
 Mikhailova, M. P. 4[57], 57[7], 80[7],
 82[7], 240, 243
 Mises, R. von, *see* von Mises
 Moore, N. B. 1[4], 236
- Neice, S. E. 66[12], 244
 Neumann, J. von, *see* von Neumann
 Newton, I. 3, 44, 97, 98, 110, 240, 245
 Nikol'skii, A. A. 110[16], 246
- Okhotsimskii, D. E. 206[18], 251
 Oleinik, O. A. 36, 242
 Oliver, R. E. 99[10], 103[10], 105[10], 245
 Oswatitsch, K. 48, 50[14], 242
- Pallone, A. J. 211[23], 251
 Prandtl, L. 1[10], 2[13], 237(2)
 Probststein, R. F. 48, 113, 118[23], 122–
 123[26], 128–129[26], 136[26], 194,
 206[28], 246, 247, 251
 Puckett, A. E. 3[36], 239
- Rankine, W. J. M. 1[8], 236
 Resnikoff, M. M. 112[30], 129[30], 247
 Richtmyer, R. D. 35, 242
 Roze, N. V. 27[1], 31[1], 38[1], 46[1],
 114[22], 140[22], 161–164[1], 166[1],
 241, 246, 248

- Rusanov, V. V. 95[1], 245
Ryabinkov, G. M. 103
- Sakurai, A. 205[13], 210[20], 250, 251
Samarskii, A. A. 36[11], 242
Sänger, E. 8[59], 109[12], 240, 241, 245
Savin, R. C. 195[16], 249
Schlichting, H. 3[30], 238
Sedov, L. I. 76[16], 81[17], 92[16], 205,
208–210[11], 215[11], 244(2), 250(3)
Shapiro, A. H. 68[15], 244
Shul'gin, V. I. 103
Sobolev, S. L. 35, 242
Solomakhova, T. S. 210[21], 216–217[21],
251
Stanyukovich, K. P. 92[24], 244
Stevens, V. I. 49[17], 243
Stewart, H. J. 3[41], 239
Sychev, V. V. 206[29], 252
Syvertson, C. A. 127[29], 168[4], 171[4,7],
192[4], 195[4,16], 247, 248, 249(2)
Taylor, G. I. 2[12], 81[18], 152[45], 205,
237, 244, 248, 250
Telenin, G. F. 57[10], 243
Teller, E. 13[64], 241
Thomas, R. N. 49[15], 242
Thomas, T. Y. 195[14], 249
Tikhonov, A. N. 36[11], 242
- Tsien, H. S. 2[23], 4[54], 56, 238, 240, 243
Vallander, S. V. 50, 113
Van Dyke, M. D. 57[9], 68[9,14], 95[3],
243–245
Velesko, L. G. 83[20], 85[20], 154[46], 244,
248
Vlasova, Z. P. 206[18], 251
Voishel, V. V. 2[26], 238
von Kármán, T. 1[4,5], 2[5,23], 3[37],
98[5], 109, 236(2), 238, 239, 245, 246
von Mises, R. 140, 248
von Neumann, J. 34[5], 35, 206[16],
242(2), 251
- Walchner, O. 2[18], 237
Waldman, G. D. 194
Ward, G. N. 3[40], 239
Wendt, H. 3[45], 239
Williams, E. P. 122[25], 124[25], 246
Wilson, R. E. 22–23[67], 241
- Young, G. B. W. 122[25], 124[25], 246
- Zahm, A. F. 98[7], 245
Zeldovich, Ya. B. 13[62], 28[2], 241(2)
Zemskii, O. M. 2[29], 238
Zienkiewicz, H. K. 199[17], 249

Subject Index

- Ackeret theory, 107
“Adiabatic tube” (*see* Piston driven tube)
Aerodynamic shadow, 44, 97, 107
Aerodynamically perfect shape, 55, 56
Affinely related bodies, 56, 60, 63–66, 73
Air, properties of (*see* Equilibrium air; Nonequilibrium air)
Airfoil,
 with flat bottom, 168, 170
 with straight leading edge, 1, 166, 167
Angle of attack, 37–48, 64, 107, 168, 181, 182, 195–199
Annular body,
 boundary layer method for, 155–159
 Busemann formula for, 128
 self-similar solution for, 76–78, 94
 shock and simple wave solution for, 190, 191
Arc discharge, 19, 21
Atmosphere (*see* Hypersonic flight in the atmosphere)
Axisymmetric and two-dimensional flow,
 difference between, 173

Ballistic range, 16, 17, 22, 23
Ballistic vehicle, 3–9, 14
 basic aerodynamic problem, 7
Base pressure, 63
Basic hypersonic limiting process, 48
Bernoulli integral, 39, 70, 114, 117, 176
Blunt-ended cylinder, 206, 213–218, 234
Blunted cone, 226–231, 233, 234
Blunted flat plate, 202, 203, 206–214, 224, 234
 with semicircular leading edge, 211
 with sonic-wedge leading edge, 211
Blunted slender body, 8, 9, 91, 201–234
 center of pressure on, 225, 226
 effect of γ on solution for, 213
 equivalent problem for, 205–207, 211, 218, 231, 232
semi-empirical method for, 202
viscous effects in nose region of, 201, 204, 205, 207, 212–215

Blunted wedge, 218–226, 233, 234
Blunted wing, 9
Body forces, 27
Boundary layer, 2, 3
Boundary layer coordinates,
 physical, 138, 139
 transformed, 140
Boundary layer method, 96, 136–159
 basic assumption, 138, 146, 154
 examples, 151–159
Bow wave, 25, 26, 51, 52
 attached, 25, 26, 38
 detached, 25, 26, 37
 (*see also* Shock wave; Expansion flow; Mach wave)
Bow wave relations, 29, 30
Busemann (pressure) formula, 120–128
 accuracy of, 125, 127
 comparison with self-similar solutions of, 125–127
Busemann (pressure) formula, modified, 123, 124
 accuracy of, 125
 comparison with other solutions and experiment of, 103–105, 124–127
Busemann second-order theory for pressure, 165, 166
 comparison with other solutions of, 165, 193, 194

Centrifugal forces in shock layer, 121, 122, 145, 146
Characteristic surface, 27, 59 (*see also* Mach wave)
Characteristics, 192
 disturbances along, 176, 178, 202
 limiting (*see* Limiting characteristic)
 method of (*see* Method of characteristics)
 outgoing, 192
Chemical reaction, 5
Combustion heating, 19, 21
Concentrated forces due to blunt nose, 204, 205

- Condensation of air (*see* Wind tunnel)
 Condensed layer, 43, 60, 123, 137
 Cone,
 applicability of hypersonic similarity
 for, 67
 approximate hypersonic solution for,
 114-118
 boundary layer method solution for,
 151, 152
 exact solution for, 66, 67, 82, 83
 Newtonian solution for, 99, 108, 109
 self-similar solution for, 77, 79-83
 Cone-cylinder, 31, 32
 with spike, 32, 34
 Conical shock and expansion wave method,
 197-199
 (*see also* Shock-expansion method, generalized)
 Contact surface (*see* Vortex surface)
 Continuation of self-similar solution, 94
 Continuity equation (*see* Equations of motion)
 Continuous solution for supersonic flow, 30
 Corresponding points,
 in hypersonic slender body flow, 41, 63,
 66
 in limiting hypersonic flow, 53
 Counterpressure, 209, 218, 219, 227, 231,
 233
 (*see also* Initial pressure)
 Cylinder, numerical solution for, 105

 Deflecting shield, 128
 Density ratio across shock, 115, 137, 138,
 178
 Detached flow, 41
 Detached shock wave,
 calculation of, 95
 on blunted slender body, 205
 Diamond airfoil, 106-109, 170, 171
 Diffusion, 5, 12, 13
 Discontinuity surfaces, 25, 30-35
 Discontinuous solution in integral form
 (*see* Generalized solution)
 Dissociation, 5, 9-14, 22, 23
 Disturbance,
 incident on shock, 178
 in free stream, 173
 in subsonic nose region, 203
 (*see also* Reflected disturbance)
 Disturbance velocity, 27, 58, 59
 Donov theory for pressure, 166
 Drag,
 as affected by shape, 55
 of blunted slender body, 203
 due to bluntness, 203, 224
 from equivalence principle, 73, 74
 in Newtonian flow, 110, 203
 Drag coefficient,
 from Busemann formula, 128
 for Busemann minimum-drag shapes,
 131, 135, 136
 in hypersonic similarity, 63, 64
 Drag coefficient on,
 annular conical body, 157, 158
 blunted cone, 230
 blunted slender body, 233
 blunted wedge, 224, 225
 circular arc airfoil, 109
 cone, 108, 109, 136, 155, 158, 159
 cone-cylinder, 49
 diamond airfoil, 106, 109, 170
 flat-bottomed airfoil, 170
 flat plate, 45, 106, 161
 half-cone, 108, 109
 nose or leading edge, 208, 211, 212
 ogive of revolution, 109
 parabolic ogive of revolution, 119, 120
 power law body, 83, 85, 90, 91, 154, 155
 sphere, 49
 triangular airfoil, 106, 170
 wedge, 155, 157, 158, 187, 224
 wedgelike airfoil, 187, 188
 Ducted body, 33, 34

 Earth satellite, 4, 7
 Electric and magnetic fields in hypersonic flow, 16
 Electrical conductivity of air, 15, 22
 Energy conservation in explosion, 206, 218
 Ensemble of flows, 48, 49
 Entropy equation (*see* Equations of motion)
 Equation of state, 36

- Equations of motion,
in boundary layer coordinates, 139, 172,
173
in cartesian coordinates, 27
in dimensionless variables, 50
in Lagrangian coordinates, 75, 147
for slender body theory, 61
for slender wing theory, 71
- Equilibrium air,
composition of, 11, 12
heat conductivity of, 5
thermodynamic properties of, 5, 6, 9–13,
17, 18
viscosity of, 5
- Equivalence principle, 47, 72–75
in blunted slender body flow, 205–207,
211, 218, 231, 232
with boundary layer method, 146–155
with self-similar solutions, 76–94
- Euler-d'Alembert paradox, 55
- Existence of generalized solution, 34
- Existence of self-similar solution for power
law bodies, 82, 83, 85
- Existence of solution for supersonic flow,
30
- Expansion flow, 38–42, 165
(*see also* Simple wave flow)
- Explosion analogy for blunted slender
body, 205–208, 219, 231
(*see also* Violent explosion)
- Exponential body, self-similar solution for,
92, 93
- Fineness ratio, 103, 196
- Finite difference method (*see* Method of
finite differences)
- First integral for extremals, 129
- Flat plate at angle of attack, 37–48
in Newtonian flow, 99, 106
- Force coefficient,
in limiting hypersonic flow, 53, 54
- Free electrons, 10, 15
- Free layer, 123
- Frictional drag (*see* Skin friction)
- Gas constant, 36
- Generalized solution, 31–36
- Geodesic lines, 122
- Glide vehicle, 6–9, 14
basic aerodynamic problem, 8
- Half-cone, 108, 109
- Heat transfer to body, 2, 17
in dissociating gas, 12, 13, 19
- High entropy layer, 206
for blunted wedge, 221
- High supersonic flow, 48
- "Hot core," 206
- Hypersonic flight in the atmosphere, 4–9,
13, 14
- Hypersonic flow, 5, 36, 37, 48, 95
aerodynamics of, 1, 4, 13
- Hypersonic similarity, 41, 45, 56, 57,
60–69, 73, 107
for blunted slender body, 231–234
- Hypersonic similarity parameter, 45,
63–68, 226, 233
for blunted slender body, 233
- Hysteresis in supersonic flow past a body,
33
- Initial pressure, 77, 78, 205, 207, 218, 226
(*see also* Counterpressure)
- Internal degrees of freedom, 5, 10, 19
- Internal energy, 28, 29
- Ionization, 5, 10
- Irrationality condition in conical flow,
114
- Kinematic constant, 77, 231
- Lagrangian coordinate, 75, 147, 149, 151
- Law of plane sections, 72
- Legendre condition, 112
- Lift,
from equivalence principle, 74, 75
in shock and simple wave method, 168
- Lift coefficient in hypersonic similarity,
63, 64
- Lift coefficient on,
cone, 108, 109
diamond airfoil, 106, 107, 170
flat-bottomed airfoil, 170
flat plate, 46, 47, 106, 161
half-cone, 108, 109
triangular airfoil, 106, 170

- Lift-drag ratio, 8, 9, 107–109, 171
Lifting vehicles, 4, 8, 9
Light gas gun, 23
Limit line in self-similar solution, 94
Limit state for given initial conditions, 31–34
Limiting characteristic, 202
Limiting flow deflection angle, 137, 138
Limiting hypersonic flow, 48–54, 64
 with blunted slender body, 215, 225, 231, 233, 234
 with power law body, 152–155
 similarity law for, 53, 54
Limiting perfect gas model, 48
Linearized flow, 1–4, 56, 59, 161
 comparison with other solutions of, 193, 194
 validity of, 1, 2, 60, 70, 95
Linearized solution about shock, 171–180
- Mach angle, 38, 39, 60
Mach number,
 relation of with energy change, 36, 37
 free stream, 40, 61
 in modeling, 6, 12, 16–19, 22
 behind shock, 48
Mach number independence, 43, 53
Mach wave, 25, 28, 52, 53, 59
Maximum lift airfoil, 168
Method of characteristics, 2, 68, 95, 96, 161, 195
Method of finite differences, 35, 96
Meteorite, 3, 5, 7
Minimum-drag shapes,
 from Busemann formula, 128–136
 in linearized flow, 109, 110
 from Newtonian formula, 105, 106, 109–112
 for nonnegative pressure condition, 136
 power law, 90, 91, 155
 from wedgelike body solution, 187
Modeling, 16–19
Moment coefficient in limiting hypersonic flow, 53, 54
- Newtonian flow theory, 48, 95–112, 120–136
Newtonian model, 3, 44, 97
- Newtonian (pressure) formula, 3, 98, 99, 120
accuracy of, 105, 125, 127
comparison with exact solutions of, 99, 100
comparison with self-similar solutions of, 125–127
Newtonian (pressure) formula, modified, 101, 103
accuracy of, 125
comparison with other solutions and experiment of, 102–105, 124, 127
Newton's law of resistance, 95, 96
Nitric oxide formation, 5, 10, 22
Nonequilibrium air, 5, 13
 (*see also* Relaxation phenomena)
- Ogive of revolution, applicability of hypersonic similarity for, 67, 68
- Perfect gas, 9, 18, 27, 36
Piston driven tube, 6, 19, 21
Piston in equivalent flow, 72–77
Plane motion, 72–75
Plane parallel flow, 178
Polar diagram,
 airfoils, 106, 107, 170, 171, 195
 slender bodies, 108
Power law body,
 boundary layer method solution for, 152–155
 self-similar solution for, 77, 78, 82–91
Prandtl-Meyer relations, 196
 (*see also* Expansion flow; Simple wave flow)
Pressure in limiting hypersonic flow, 53
Pressure on,
 affinely related bodies, 65, 66
 annular conical body, 157
 blunt-ended cylinder, 213, 215–217
 blunted cone, 234
 blunted flat plate, 208, 211, 212, 214
 blunted wedge, 221, 222, 234
 cone, 117, 120
 ogive-cylinder, 65–69
 parabolic ogive of revolution, 119
 wedge, 120
 wedgelike airfoil, 186

- wedgelike body, 185
- Pressure coefficient,
for Busemann minimum-drag shapes, 130-132
in limiting hypersonic flow, 54, 63
in linearized flow, 161, 186
in shock and simple wave solution, 167, 168
- Pressure coefficient expansion,
across oblique shock, 164, 165
across simple wave, 164, 165, 167
- Pressure coefficient on,
blunt nose, 100-102
blunted cone, 227-229
circular arc airfoil, 127, 195
cone, 66, 67, 99, 100, 118, 152
cone at angle of attack, 99, 102
cone with spherical cap, 103, 104
cylinder, 103, 105
cylinder with ellipsoidal cap, 103, 105
flat plate, 41, 45, 98, 99
leading edge of airfoil, 163, 167
nose of annular body of revolution, 191
ogive of revolution, 124, 196-198
parabolic arc airfoil, 192, 193
power law body, 85-89
slender body, 60
slightly curved wall, 186
wedge, 80, 82, 99, 100, 102, 103, 152
wedgelike airfoil, 188
- Pressure gradient at nose of annular body, 190
- Pressure ratio across shock, 52, 117
- Radiation, 16
- Radio communication in hypersonic flow, 16
- Range for hypervelocity vehicles, 7, 8
- Ratio of specific heats, 27
in modeling, 16, 17
- Rayleigh formula, 101
- Recombination, 13
- Re-entry (*see* Hypersonic flight in the atmosphere)
- Reflected disturbance,
from body, 186
from shock, 171, 176-180, 186-190, 192,
- 194 (*see also* Reflection coefficient from shock)
from vorticity layers, 192, 194
- Reflection coefficient from shock, 178-181, 187-190, 194, 195
- Relative velocity, 42, 47
- Relaxation phenomena, 13, 14, 22, 23
- Relaxation time, 13, 14
- Reynolds number,
based on bluntness dimension, 201, 211-213, 215, 222
effect on flow, 196
in modeling, 6, 16-19, 22
- Rocket propulsion, 4
- Rotational energy transfer, 10, 13
- Satellite (*see* Earth satellite)
- Scale in boundary layer method, 141
- Second law of thermodynamics, 28, 31
- Self-similar solutions, 76-94, 96
effect of γ in, 88, 89
for violent explosion, 206, 210, 216
- Series-expansion about shock, 171-179
- Series-expansion in boundary layer method, 138, 142-151, 206, 207, 210, 218, 219
- Shock and simple wave method, 166-171
- Shock and simple wave approximate method (*see* Shock-expansion method)
- Shock curvature on annular conical body, 159
- Shock-expansion method, 192-199
analytic formulation of, 195
effect of γ in, 195
generalized (to bodies of revolution), 195-199
- Shock layer, 128
- Shock shape,
on blunt-ended cylinder, 215-217
on blunted cone, 227, 228, 234
on blunted flat plate, 208, 213
on blunted wedge, 220-222, 234
on body of revolution, 196, 199
effect on flow, 51-53
at nose of annular body, 191
- Shock tube, 6, 19-23
- Shock wave, 25-30, 34, 35, 50-63

- oblique (attached to flat plate), 42-48
in slender body hypersonic flow, 58-60
- Shock wave propagation velocity, 58, 72
- Shock wave relations, 1, 28-30, 136
in boundary layer coordinates, 141
in dimensionless variables, 50, 51
in Lagrangian coordinates, 76, 149
in limiting hypersonic flow, 52, 137, 138
oblique, 174
oblique (attached to flat plate), 42-48
in slender body hypersonic flow, 60-62
- Similarity and dimensional analysis, 76, 77, 208
- Simple wave flow, 1, 162-165, 171
feedback effect on, 171
- Simulation (*see* Modeling)
- Singular point in boundary layer method, 146
- Skin friction, 2, 5
in dissociating gas, 12, 13
- Skip vehicle, 6, 8
basic aerodynamic problem, 8
- Slender airfoil flows (*see* Slender body flows)
- Slender body flows,
assumptions, 1, 4
hypersonic, 47, 55-94
supersonic, 1, 2, 4, 59
- Slender wing hypersonic flows, 71, 72
- Slightly blunted body (*see* Blunted slender body)
- Small velocity perturbations,
in hypersonic flow, 1, 4, 37, 41, 56, 59, 70
in subsonic flow, 37
in supersonic flow, 1, 56
- Sonic line, 202
- Sound wave, 38, 39, 52
- Specific heat at constant pressure, 10, 11
- Specific heat at constant volume, 27
- Speed of sound, 36, 38
- Stability of generalized solution, 34
- Standard conditions, 10, 11
- Stream function, 140, 156
- Stream surface, 28
- Streamline, relations along, 36
- Strong discontinuity (*see* Shock wave)
- Supersonic flow, 25-36, 51, 55, 161-163, 166
aerodynamics of, 1, 4, 13
- Surface temperature of body, 2, 5, 19
in dissociating gas, 12
- Tangent-cone method, 96, 113, 118-120
- Tangent-wedge method, 96, 113
- Temperature behind shock, 9, 138
- Thickness ratio, 57, 64-67, 90, 106, 118, 133, 135, 232
- Thrust cowl, 128
- Trajectories,
ballistic, 6-8
glide, 6, 8
skip, 8
- Translational energy transfer, 10, 13
- Transport phenomena, 5, 12
- Triangular airfoil, 38, 106, 107, 170, 171
- Turning cowl, 128, 132
- Uniqueness of generalized solution, 34
- Uniqueness of solution to supersonic flow problem, 30, 31
- "Vanishing viscosity" theory, 34, 35
- Velocity of sound, 30
- Very high supersonic flow, 3, 43, 48
(*see also* Limiting hypersonic flow)
- Vibrational degrees of freedom, 9
- Vibrational energy transfer, 10, 13
- Violent explosion, 95, 205, 206
cylindrical, 205, 215, 216, 227
planar, 205, 209, 210
spherical, 205, 209
- Vortex surface, 25, 28, 29, 34
- Vortex surface relations, 28
in slender body hypersonic flow, 62
- Vorticity in flow, 174
for annular body, 158, 159
- Weak discontinuity relations (*see* Expansion flow)
- Weak discontinuity surface (*see* Mach wave)
- Wedge,
boundary layer method solution for, 151, 152

- exact solution for, 81, 82
limit of blunted wedge solution for, 226
as minimum-drag shape, 111
self-similar solution for, 77, 79-82
- Wedge-like bodies, perturbation solution
for, 181-191
- Wind tunnel, 16, 17
- condensation of air in, 6, 17-19
helium, 18
hypersonic, 5, 15, 17-19
supersonic, 2-4, 16
- Zero pressure region, 41, 107, 123, 168